SEDIMENTARY GEOLOGY AND GEOSCIENCE EDUCATION: A COMBINED STUDY OF SEQUENCE STRATIGRAPHY AND SPATIAL VISUALIZATION USING OUTCROP EXAMPLES FROM THE CRETACEOUS TERTIARY OF UTAH

by

Ian Laird Semple

A thesis submitted to the faculty of
The University of Utah
in partial fulfillment of the requirements for the degree of

Master of Science

in

Geology

Department of Geology and Geophysics

The University of Utah

August 2011

The University of Utah Graduate School

STATEMENT OF THESIS APPROVAL

The thesis of **Ian Laird Semple**

has been approved by the following supervisory committee members:

Cari Johnson	, Chair	**6/5/2011** Date Approved
David Chapman	, Member	**6/7/2011** Date Approved
Sarah Creem-Regehr	, Member	**6/7/2011** Date Approved
Jessica Allen	, Member	**6/7/2011** Date Approved

and by **Kip Solomon** , Chair of

the Department of **Geology and Geophysics**

and by Charles A. Wight, Dean of The Graduate School.

ABSTRACT

Chapter 1 examines the stratigraphic architecture of the lower Straight Cliffs Formation across the southwestern portion of the Kaiparowits Plateau in southern Utah. To determine the controls affecting deposition of marginal marine deposits, seven stratigraphic sections (each ~90-100 m) and 729 paleocurrents were measured along a 20 km transect (A-A'). This study divides the lower Straight Cliffs Formation into four depositional units (DU), representing distinct and genetically-related depositional environments: prograding shoreface parasequences (DU-1), tidally influenced fluvial channels and estuaries (DU-2), a transitional sequence of shoreface deposits through fluvial deposits (DU-3), and downstream accreting fluvial deposits (DU-4). This interpretation represents both minor and more significant revisions to previous interpretations of this succession, and highlights the need for high-resolution stratigraphic studies to fully understand depositional complexity in this and similar settings.

Earth scientists often use images to communicate scientific concepts, and they commonly provide cues establishing the scale of features shown ('hammer for scale,' etc.). How effective are these kinds of scaling cues? Chapter 2 examines the effect of scaling cues and interactivity on the ability of earth scientists to extract information from a 2D image. To evaluate both scaling cues and interactivity, a visualization test was created in which participants were asked to estimate the size of several boxes shown in outcrop photos. All test subjects first viewed a static image, followed by an interactive

(gigapan) image of the same outcrop; two different outcrops of different sizes were used. Participants (test group n=63, further testing in progress) represent a range of experience and education levels. Results show that scaling estimates are more difficult for larger/more distant outcrops. Scaling cues can also become a distractor for viewers of any experience level or background. It is important to realize that viewers internalize scaling cues differently, so different types of cues may help some viewers more than others. Also it appears that incorporating interactivity can increase accuracy, due to the ability to customize views that best fits an individual's learning style and internal sense of problem solving. The results of this study contain numerous educational implications for the application of scale and interactivity.

TABLE OF CONTENTS

ACKNOWLEDGEMENTS

First and foremost, I would like to thank my advisor Dr. Cari Johnson for her guidance and support over the past three years. I would also like to thank my committee members, David Chapman, Sarah Creem-Regher, and Jessica Allen for their guidance and input. A great thanks to the National Science Foundation and the Water Earth Science and Teaching Program for their financial support. Thank you to the Bureau of Land Management for permission to conduct research on federal land as well as the GSENM Big Water and Paria BLM centers for their weather and road reports. Thank you to Jared Gooley for endless field hours, Mathew Heumann and Will Gallin for graduate leadership, and Jim Lehane and Megan Crocker for their knowledge and distractions in and out of the office. A special thanks to Ashley Powell for her reassurance and praise during long hours in the office. Last but not least, thank you to my family for their encouragement, support, and inspiration to accomplish my goals.

CHAPTER 1

HIGH RESOLUTION SEQUENCE STRATIGRAPHY OF MARGINAL MARINE DEPOSITS OF THE TIBBET CANYON AND SMOKY HOLLOW MEMBERS, STRAIGHT CLIFFS FORMATION, SOUTHERN UTAH

Abstract

The stratigraphic architecture of the lower Straight Cliffs Formation was examined at four canyons across the southwestern Kaiparowits Plateau in southern Utah to determine the controls affecting deposition of marginal marine deposits. Seven stratigraphic sections (each ~90-100 m) and 729 paleocurrents were measured along a 20 km transect at four locations arranged roughly down depositional dip: Rock House Cove, Coyote Springs, Blue Cove, and Ty Hatch Canyon, west to east, respectively. This study divides the lower Straight Cliffs Formation into four depositional units (DU), defined by facies assemblages representing distinct and genetically-related depositional environments: prograding shoreface parasequences (DU-1) tidally influenced fluvial channels and estuaries (DU-2), a transitional sequence of shoreface deposits through fluvial deposits (DU-3), and downstream accreting fluvial deposits (DU-4). This study

also interpreted five surfaces: three minor flooding surfaces within DU-1; two sequence boundaries, the first within the lower Tibbet Canyon Member separating DU-1 and DU-2 and the second below the Calico Bed separating DU-3 and DU-4; and finally, another flooding surface separating DU-2 and DU-3. This interpretation represents both minor and more significant revisions to previous interpretations of this succession, and highlights the need for high-resolution stratigraphic studies to fully understand depositional complexity in this and similar settings.

Introduction

The Upper Cretaceous Straight Cliffs Formation exposed in the Kaiparowits Plateau of southern Utah comprises nonmarine, coastal, and shallow marine sediments that were deposited in an active foreland basin (Peterson, 1969 a,b; Doelling and Graham, 1972; Vaninetti, 1979; Bobb, 1991; Hettinger et al., 1993; Nummedal and Pang, 1995; Shanley and McCabe, 1995; Liu et al., 2005; Figures 1.1 and 1.2). Excellent exposures of the Straight Cliffs Formation and the general lack of structural complexity facilitate detailed sedimentologic investigations, with broad implications for basin evolution and sequence stratigraphy. Regional stratigraphic equivalents, including the Ferron and Emery Sandstones of central Utah (Gardner, 1995; Shanley and McCabe, 1995; Ryer and Anderson, 2004), can be compared to the Straight Cliffs Formation to interpret paleogeographic and stratigraphic trends at both local and regional scales. These comparisons aid the understanding of local and regional depositional controls, and their stratigraphic expressions. Such investigations bear on fundamental questions in basin analysis, sequence stratigraphy, and petroleum geology.

Relatively few studies focus on the lowermost Smoky Hollow and Tibbet Canyon Members (Shanley and McCabe, 1991 a,b,c, 1992, 1993, 1995; Bobb, 1991), compared to the thickest part of the Straight Cliffs Formation, the coal-bearing John Henry Member (Ryer, 1983; Hettinger et al., 1996, 2000; Shanley and McCabe, 1991 a). Nevertheless, these two older members are important because they represent a time period that is poorly known due to lack of exposures throughout the western US (Coniacian; Eaton et al., 1999), and because previous studies suggest they record multiple changes in base level and thus have interesting implications for sequence stratigraphy.

A sequence boundary is commonly described as a chronostratigraphic surface that represents a regional basinward shift in depositional environments (van Wagoner et al., 1990; Miall, 1996; Boggs, 2006), which separates genetically related sequences. These surfaces are typically expressed in nonmarine and shallow marine deposits as unconformities, indicated by abrupt changes in grain size, sedimentary structures, and bedding architecture (e.g., fluvial incision into shoreface deposits; Posamentier et al., 1992). However, modifications of the original sequence stratigraphic paradigm highlight many different expressions of sequence boundaries (Vail et al., 1977; Posamentier et al., 1988; van Wagoner et al., 1990; Reynolds, 1999; Cattaneo and Steel, 2003). For example, variations in how sequence stratigraphic surfaces are expressed may reflect various depositional controls such as low accommodation within shallow coastal margins or "ramps" (Posamentier and Allen, 1993; Zecchin, 2007); limited accommodation space within incised valleys (Heap and Nichol, 1997; Zaitlin et al., 2002); shoreline evolution and sea-level change (Nummedal and Swift, 1987); and the influence of tectonics on stratigraphy (Emery et al., 1996; Catuneanu and Elango, 2001).

The Tibbet Canyon and Smoky Hollow Members of the Straight Cliffs Formation preserve two possible basinward shifts in facies based on previous studies (Figure 1.2; Shanley and McCabe 1993, 1995): the Tibbet sequence boundary, near the top of the Tibbet Canyon Member, and the Calico sequence boundary, near the top of the Smoky Hollow Member (at the base of the informally named Calico sandstone or Calico bed; Peterson, 1969a). However, contrasting interpretations exist regarding how significant these shifts are and what was primarily driving them (e.g., tectonics vs. eustasy; Bobb, 1991; Shanley and McCabe, 1995). For example, a regional, unconformable basinward shift in facies that correlates with a global sea level fall may reflect a primary eustatic control on accommodation (Haq et al., 1988; Shanley and McCabe, 1995). However, a more complex or transitional (conformable) shift may be associated with tectonism, such as thrusting in the fold and thrust belt resulting in changes in accommodation and sediment supply (Bobb, 1991; Little, 1995; Heller and Paola, 1996). These questions also relate to current debates in recent literature regarding the manifestation and interpretation of sequence stratigraphic surfaces in different basin settings (van Wagoner, 1988; Posamentier and Allen, 1993; Dalrymple et al., 1992; Arnott, 1995; Little, 1995; Howell and Flint, 1996; Heap and Nichol, 1997; Bridge, 2003; Miall, 2006; Catuneanu, 2006).

The lack of research on the lower Straight Cliffs Formation and the different existing interpretations make it important to document and interpret the stratigraphy of the area in high resolution. This study presents research on the Tibbet Canyon and Smoky Hollow Members, focusing on four canyons spanning 20 km, west to east, across the southwestern Kaiparowits Plateau (Figure 1.3). The purpose of this study is to document the stratigraphic relationships, interpret primary controls on depositional patterns,

establish regional correlations, and compare these results to previous studies, in order to investigate implications for sequence stratigraphy and basin reconstructions.

Geologic Background

The Kaiparowits Plateau is located in southern Utah and encompasses an area of approximately 4225 km^2 (Figure 1.1). The boundaries of this plateau provide excellent exposures of Straight Cliffs Formation strata. The Straight Cliffs Formation was deposited within a foreland basin adjacent to the eastward advancing Sevier fold and thrust belt. Regional paleotransport was generally to the east and northeast (Peterson, 1969a; Bobb, 1991; Shanley and McCabe, 1995). Recent studies suggest that basin subsidence reflects not just crustal loading adjacent to the orogenic belt, but also possibly segmented shallow subduction of the Farallon Plate to the west (Nummedal and Pang, 1995; Liu et al., 2005, 2008)

The Straight Cliffs Sandstone was first identified in 1931, and was named after the Straight Cliffs Escarpment, an unusually linear exposure of shoreface sandstones along the eastern edge of the Kaiparowits Plateau (Gregory and Moore, 1931). The name was later revised to the Straight Cliffs Formation (Peterson and Waldrop, 1965), comprising four distinct lithostratigraphic members: the Tibbet Canyon, Smoky Hollow, John Henry, and Drip Tank (Peterson 1969a; Figure 1.2). Deposition of the entire Straight Cliffs Formation spanned from the middle Turonian through the late Santonian but is poorly constrained by radioisotopic dates (Eaton et al., 2001). The Tibbet Canyon and Smoky Hollow Members are the main focus of this study.

The biostratigraphy of the lower Straight Cliffs Formation is summarized by Eaton (1991, 1995; Eaton et al., 1997, 2001; Figure 1.4). The base of the Tibbet Canyon Member contains abundant brackishwater taxa (*Crassostrea soleniscus*, *Craginia whitefieldi*, and *Brachiodonte*) as well as open water taxa (*Mytiloides mytiloides* and *Mytiloides subhercynicus*) indicative of the end of the early Turonian. Within the upper Tibbet Canyon Member, *Inoceramus cuvieri* and *Collignoniceras woollgari* were identified, indicating a middle Turonian age. Within brackish deposits near the base of the Smoky Hollow Member, abundant middle Turonian mollusks, benthic formanifera, and ostracodes are present, representing an age of middle Turonian. Within the lower John Henry Member, the inoceramid *Volviceramus involutus* represents an early Coniacian time period. Based on correlation to the Geological Society of America 2009 time scale (Walker and Geissman, 2009), the fossil assemblage implies that deposition of the lower Straight Cliffs Formation occurred from ~93 to 89 Ma (Figure 1.4).

Existing radiogenic dates from the lower Straight Cliffs Formation include two $^{40}Ar/^{39}Ar$ dates on sanidine collected from bentonites in the Tropic Shale near the base of the Tibbet Canyon Member, measured to be 93.25 +/- 0.55 Ma and 93.40 +/- 0.63 Ma (Figure 1.4; Obradovich, 1993). In addition, to these dates an age of 91.9 +/- 0.3 Ma has been recorded for the upper Smoky Hollow Member based on U/Pb analysis of a detrital zircon (Titus et al., in press). A single $^{40}Ar/^{39}Ar$ date was collected from a euhedral biotite bed, indicating an age of 86.72 +/- 0.58 Ma for John Henry Member equivalent deposits within Cedar Canyon (Eaton et al., 1999). In summary, available radiometric data suggest an age range from ~93 Ma through ~89 Ma (Early Turonian through the

beginning of the Coniacian) for the Tibbet Canyon and Smoky Hollow Members, in broad agreement with the paleontologic data.

Peterson (1969a) presented the first stratigraphic framework for the Straight Cliffs Formation, based on 31 measured sections, most which are located within the south central to north eastern portions of the plateau (Figure 1.1). Peterson identified the Tibbet Canyon Member as the first cliff forming sandstone above the Tropic Shale (Figure 1.4). The basal contact of this member is at the base of the first extensive fine-grained sandstone; the upper contact with the Smoky Hollow Member is easily placed where coals are present; otherwise, it can be difficult to identify in continuous, sandy intervals (Figure 1.4). Based on the lithologies, stratigraphy, and fossil assemblages, Peterson interpreted the Tibbet Canyon Member in this area as shallow marine to beach deposits. Shanley and McCabe (1991) later described the lower Tibbet Canyon member as a prograding shoreface overlain by an abrupt change to fluvial facies at the top. This interpretation implies the presence of an unconformable shift in facies that may represent a sequence boundary (Figure 1.2).

Peterson (1969a) divided the overlying Smoky Hollow Member into three zones based on lithology: the coal zone, the barren zone, and the Calico bed (Figure 1.2). The coal zone was named for the abundance of coal and carbonaceous mudstone present. The barren zone is defined by the absence of coal and the introduction of bentonitic mudstones interbedded with very fine-grained sandstones. The Calico bed corresponds to the white to very light gray and orange, coarse grained, poorly sorted, cross-stratified sandstone capping the Smoky Hollow Member (Peterson, 1969a; Bobb, 1991). Peterson (1969a) identified a regional unconformity separating the Calico bed and the overlying

John Henry Member based on multiple criteria. First, it was noted that bedding planes at the top of the Smoky Hollow Member are erosionally truncated by fluvial channel sandstones of the lower John Henry Member, across a single continuous erosional surface. Furthermore, the same channel sandstones contain distinctive lithologies, bleached coarse sand and pebbles, derived from the underlying Calico bed.

Shanley and McCabe (1991, 1993, 1995) interpreted the lower Smoky Hollow Member as low energy fluvial deposits with increasing frequency of interdistributary deposits towards the middle of the member (i.e., fining upwards). The upper Smoky Hollow Member is truncated by the base of the Calico bed. Shanley and McCabe (1995) correlate this surface to a global eustatic fall (e.g., the 89 Ma sequence boundary of Haq et al., 1988), followed by a slow base level rise that produced a fining upward sequence. Shanley and McCabe (1991) also noted that in Left Hand Collett (Figure 1.1), the "Calico sequence boundary" separates the Calico bed from underlying shoreface deposits, implying the presence of a sequence boundary. In contrast, Bobb (1991) identified a transitional upward coarsening facies between the barren zone and the Calico bed in the northern portion of the plateau. This work suggests that the Smoky Hollow Member may represent a conformable gradual basinward shift in facies from meandering rivers in the coal zone to coarse braided rivers at the base of the Calico bed, at least in some areas of the Kaiparowits Plateau (Figure 1.5).

Above the Calico bed, Eaton et al. (2001) observed an abrupt transition within the fossil assemblage, marking the boundary between the Turonian and Coniacian ages, and placed a major unconformity between the Calico bed and the lower John Henry Member. The combination of radioisotopic dates, biostratigraphic correlation, and regional

relations suggest that there is an unconformity, placing the early Coniacian John Henry Member directly on top of the middle Turonian Smoky Hollow Member represented by either the base of the Calico bed or the transgressive surface identified by Shanley and McCabe (1991). Thus, the amount of time lost across the Calico sequence boundary is still unknown. Finally, although not the focus of this study, two other major sequence boundaries have been interpreted in the upper Straight Cliffs Formation: below the A sandstone (Shanley and McCabe, 1995; cf., Allen and Johnson, 2010) and at the base of the Drip Tank Member (Shanley and McCabe, 1995; Christensen, 2005; Figure 1.2).

Outstanding Questions

Varying interpretations exist regarding facies relationships, regional correlation, and sequence stratigraphy, particularly in the lower members of the Straight Cliffs Formation. How accurately do these interpretations describe the complexities within coastal margin deposits in tectonically active basins? Does the Calico bed represent an unconformable or conformable facies shift? What are the controls on deposition through time and how can these be used to justify important facies shifts? How do these relationships change across the exposures of the southwestern Kaiparowits Plateau? The answers to these questions have major implications for the interpretation of paleogeographic trends and sequence stratigraphy in similar basin and depositional settings. High resolution interpretations of these rocks will provide a more detailed understanding of down dip trends related to deposition and erosion through time.

Methods

A total of seven sections (~ 90 – 100 m) of the Tibbet Canyon and Smoky Hollow Members were measured through three strike canyons and one dip canyon covering 20 km east to west (Figure 1.6). Each section was recorded with centimeter to decimeter scale resolution. The sections were measured in four canyons: Rock House Cove, Coyote Springs Canyon, Blue Cove, and Ty Hatch Canyon, moving west to east, respectively (Figure 1.3). Descriptions include the vertical and lateral extent of each sandstone bed, sedimentary structures, paleocurrents, and both body and trace fossils. Seven hundred and seventy-six paleocurrents were measured across the study area to determine paleoflow and accretion direction (Figure 1.7). Measurements were taken on trough cross and planar bedded stratification, as well as major accretion surfaces where possible.

Between stratigraphic sections, extensive surfaces and beds were mapped utilizing gigapans. Gigapans are high resolution photomosaics that enable the user to zoom and pan around the image. Facies and surfaces can be mapped directly onto the image for comparison between outcrops.

Results

Lithofacies and Facies Associations

From the base of Tibbet Canyon Member through the Calico bed, there are four distinct facies associations (FA 1-4) preserved in the study area. The term "facies association" refers to "a collection of commonly associated sedimentary attributes" (Potter, 1959). In this study, the associations are defined using grain size, the 11 lithofacies relationships (Table 1.1), bedding style, architectural elements, sedimentary

structures, and characteristic trace fossil and body fossil assemblages (Table 1.2). Depositional environments represented by these facies associations include shoreface (FA-1), meandering fluvial channel fill and interdistributary deposits (FA-2), tidally influenced, meandering channel fill and interdistributary deposits (FA-3), and braided fluvial channels with interdistributary deposits (FA-4), as described below.

FA-1 Description

FA-1 consists of interbedded planar laminated siltstone (F-S), hummocky cross stratified sandstone (F-HCS), trough cross bedded sandstone (F-TCS), planar bedded sandstone (F-PBS), and wavy bedded sandstone (F-WS) with minor bioturbated sandstone (F-BS), all occurring in coarsening and thickening upward sequences (Figure 1.6). The base of FA-1 is dominated by siltstone (up to 80%) containing abundant plant material and coal fragments (Figure 1.8 E). Sandstone beds range from 10 cm – 2 m thick, and are very fine to fine grained and tabular. Most sandstone beds are laterally extensive up to 100-500 m, with minor rippled surfaces on the top of the more extensive sandstones. Above these rippled sandstones, thin (less than 10 cm) wavy bedded and hummocky cross stratified sandstones commonly occur (Figure 1.6, Figure 1.9). Hummock sets measured from the base of the swale to the tip of the hummock are on average approximately 50 cm wide by 20 cm thick. The hummocky cross stratified beds transition to finer grained equivalents moving east over the study area. Numerous lag deposits containing shell fragments, pebbles, mud clasts, and teeth are present (Figure 1.8 I). Pebbles are mainly well rounded to subrounded carbonate and quartzite, and less than

2 cm in diameter. These lag deposits occur stratigraphically above thick (greater than 50 cm) hummocky cross stratified beds.

Both bladed and spine shaped teeth are present in discrete zones. Blue Cove contains the only specimens of ammonites identified in this study, within two sandstone beds. The first was found at the base of the section on the top of a thin (<30 cm) bed. The second was found 25 m into the section along with casts of other ammonites. Neither could be diagnostically identified.

Above these coarsening upward packages, FA-1 abruptly transitions to medium grained sandstones that are 5 m to 10 m thick containing hummocky cross stratified sandstone at the base, trough cross stratification in the middle, and planar bedded stratification at the top (Figure 1.6, Figure 1.8 B). The height of hummock sets reach 1 m to 3 m and trough cross bed heights range from 0.5 to 2 m (Figure 1.8 F). One hundred paleocurrents measured from trough cross bedding within Rock House Cove exhibit random orientations of flow with a slightly dominant east-northeast component (Figure 1.7). Beds are laterally extensive (>10 km), tabular, and fine upwards from medium to fine grained sandstone. Thicknesses vary from 2 m up to 15 m over this distance, controlled by surfaces that erode through the association (Figure 1.6). Convolute-bedded sandstone is common in close proximity to these erosional surfaces and where present, the soft sediment deformation completely disrupts the top 2 m of bedding. Mud rip-up clasts and wood fragments are abundant within 1 m of the abrupt contact between the lower and upper halves of FA-1. The clasts are a distinct green-brown mudstone and are less than 3 cm in diameter. Minor wood fragments occur throughout the rest of the bed in variable orientations and on average do not exceed 20 cm in length. Root casts, which

commonly penetrate bedding, and abundant leaf material can be found towards the top of the sequence (Figure 1.8 A).

Trace fossils *Planolites, Ophiomorpha*, *Thalassinoides*, and *Skolithos* are present in sandstones throughout the association. *Planolites* is the most abundant trace fossil in this assemblage occurring as a single vertical or horizontal meandering tube not exceeding 0.5 cm in diameter. *Ophiomorpha* occur as a pelleted branching burrow with diameters less than 1 cm. Commonly, the fill of this trace is weathered out or is a different color from its surrounding matrix (Figure 1.8 G). *Thalassinoides* also occurs as a branching burrow with consistent three-way intersections but lacks pelleted walls. Diameters of this trace do not exceed 0.5 cm. *Lockeia* occurs as an almond shaped mound with an average length of 0.5 cm. One example found reaches 1 cm in length. *Protovirgularia* are found with *lockeia* as a single tube leading to a single mound and always occur with smaller diameters than their associated mound. *Lockeia* and *protovirgularia* are only found in positive hyporelief in sandstone beds thicker than 20 cm (Figure 1.8 D). All other traces are found in variable exposures and may occur in dense clusters (> 20 burrows per square meter). Within the upper half of FA-1, *planolites* can be found in groups of no more than 10 traces in hyporelief on the base of sandstone beds and occasionally in subvertical cross section. Within the planar bedded sandstone, abundant *skolithos*, *planolites*, as well as *thallasinoides* are present with diameters ranging from .5 to 2 cm. *Thallassinoides* are commonly found in groups of 50 to 100 on the top of sandstone beds.

FA-1 Interpretation

FA-1 represents a sharp-based shoreface succession transitioning from distal lower shoreface deposits at it base through storm and fair-weather wave base in the middle with swash zone and foreshore at the top containing minor deltaic influence (Figure 1.10). The presence of hummocky cross stratified sandstone is interpreted as deposition within oscillatory currents formed by storm event waves (Hunter et al., 1979; Dott and Burgeois, 1982; Cheel and Leckie, 1993). The abundance of siltstone indicates that most deposition occurred under low energy conditions with sandstones representing discrete events of high energy strong enough to suspend sand, pebbles, teeth, and shells in the water column. Moving east from Rock House Cove to Ty Hatch (i.e., basinward), the overall thickness of sandstone beds decreases from ~ 8 m to ~6 m (Figure 1.6). These characteristics are a function of both water depth and storm energy. As water depth increases, fewer storms are strong enough to create wave energy that will reach the seafloor and suspend sand (Cheel and Leckie, 1993; Figure 1.6). The abundance of trace fossils and their diversity represent an assemblage of the Skolithos-Cruiziana ichnofacies and represent a low energy environment with high biotic productivity (Frey, 1990), supporting the lower shoreface interpretation.

Within the upper half of FA-1, the thick extensive medium grained sandstones contain hummocky cross stratification transitioning into trough cross bedded stratification before transitioning to planar bedded stratification by the top. The abrupt transition from siltstone and very fine sandstone from the first half of FA-1 to the medium grained sandstones of the upper half indicates an increase in wave energy (Howard and Reineck, 1981). The decrease in trace fossil abundance and size also

supports an increase in wave energy restricting all but the most robust trace makers (Ekdale, 1985; Frey and Howard, 1990). The transition to low angle planar bedding with tabular geometry, the presence of increasing organic material, and root marks indicates exposure and is interpreted as the foreshore swash zone (Kumar and Sanders, 1976). Organic drapes form on the tops of individual beds during waning flow (Massari, 1996). Convolute bedded sandstone could be indicative of chaotic deposition as well as disruption or dewatering from deposition of the overlying bed (Owen, 1996). The presence of wood fragments and coarse pebbles indicate influence from a high energy terrestrial system into the marine realm (i.e., deltaic influence from a river (Bhattacharya et al., 2001). Additionally, the distinct sharp bases of the shoreface deposits are attributed to a net sea-level fall with constant sediment supply rates, again implying deltaic influence from a river (Posamentier et al., 1992; Plint and Nummedal, 2000), and these bases are also exacerbated by shallow basin geometry (Walker and Eyles, 1988).

FA-2 Description

FA-2 consists of medium grained single story trough cross bedded sandstones (F-TCS), convoluted bedded sandstone (F-CBS), and minor sigmoidal bedded sandstone (SBS) interbedded with planar laminated very fine sandstone, siltstone, mudstone, and coal (F- PS, F-S, F-Cl, F-C)(Table 1.1, Figure 1.11 A, F, G, H). The lateral extent of sandstone bodies in this association reaches up to 300 m wide and 15 m thick although commonly dimensions are no more than 100 m wide and 10 m thick (n=10, Table 1.3, Figure 1.12). Sandstones in this association are typically channelized with up to 10 m of erosional relief: they occur as isolated concave-up deposits, with erosional bases,

separated by laterally continuous deposits of planar laminated siltstone (F-S) (interdistributary deposits, Figure 1.12). Internally, sandstones contain accretion sets and trough cross beds. Commonly, fine grained deposits are lobate in cross section, ranging in size from 5 m to 20 m wide and 10 m thick, with abundant organic material and root casts.

The height of trough cross beds in this association commonly range from 0.5 m to 2 m, increasing up to 4 m towards the top of the unit (Figure 1.11 H). One hundred paleocurrent measurements were taken from the lower exposures of FA-2 within Coyote Springs Canyon and exhibit a dominant flow to the north. Accretion sets containing thin (<20 cm) layers of planar laminated siltstone are present with accretion direction to the east and west perpendicular to paleoflow (Figure 1.7). One hundred and seventy six paleocurrents were measured in the upper exposure of FA-2 within Coyote Spring Canyon and Blue Cove. These measurements exhibit dominant flow to the east-southeast in Coyote Springs and transitions to north-northeast flow within Blue Cove (Figure 1.7). Convolute bedded sandstone (F-CBS) contains randomly oriented bedding planes, and is present intermittently near the top of this association.

At the base of sandstone beds, abundant leaf material is present, and coal-rip up clasts and shells are also common (Figure 1.11 C, E). Large wood fragments are present with the largest specimen reaching 50 cm in length (Figure 1.11 C). Where sandstone is not the dominant lithology, 3 m thick fining upward sequences of very fine sandstone to claystone to coal occur, with abundant leaf matter and root horizons within the top 1 m (Figure 1.11 A, B). Mudstone layers that contain roots commonly appear to contain vesicles and erode into two types of pedogenic structures, granular and blocky. Granular

structures contain spherical aggregates which break apart easily into fine granules (Birkeland, 1999). Blocky structures are present as asymmetric blocks with irregular faces intersecting at sharp angles (Mack et al., 1993). Interbedded planar siltstone and very fine sandstone commonly appear as lobe or channel shaped deposits, but these are rare to find due to poor exposure. Coal occurs as sub-bituminous grade only once in a 1m thick accumulation, with all other instances occurring as thinner lignite grade intervals.

Teredolites can be found on wood fragments in each canyon. Individual burrows of *teredolites* do not exceed 0.25 cm in diameter commonly occur in bundles of ten although bundles of over 100 burrows are present. These exhibit the classic club shape distinguishing them from *asthenopodichnium* which has been previously recorded by Moran et al. (2010). *Ophiomorpha*, *thalassinoides*, and *planolites* are preserved in positive hyporelief on the base of sandstone beds. Burrow diameter commonly does not exceed 0.25 cm in Rock House Cove, but by Ty Hatch Canyon, examples of *ophiomorpha* are more abundant and can be found with up to 1 cm diameters. One example of a single *planolites* escape trace was found in Ty Hatch Canyon.

FA-2 Interpretation

FA-2 represents highly sinuous, laterally accreting meandering fluvial channels with interbedded overbank fines deposited in crevasse splays and as paleosols. The suborthogonal relationship between accretion direction and flow direction (Figure 1.7) and the isolated channel belt geometries, with sloping linear accretion sets, indicate a moderate to high sinuosity system (Reesink and Bridge, 2007). This system had approximate channel sizes of 5 m deep by 40 m across (n= 10, Table 1.3). The transition

to larger trough sets at the top of this association indicates higher energy flow and larger channel size. The presence of *teredolites* would suggest these river systems had open connection to the ocean and commonly experienced minor influence from tidal surges (Carmona et al., 2009).

The abundance of leaf material and mud clasts at the base suggest this system was incising through a fine grained floodplain (Kraus, 1999). Logs and escape traces indicate events of extremely high energy flow with increased productivity to the east due to the increased abundance and size of trace fossils (Ekdale, 1985). These high energy events may be produced by large storms creating storm surges which inundate rivers with sediment and debris.

The upward fining sequences containing plant matter, soil horizons, and root casts were deposited as poorly drained peat bogs and exposed paleosols within raised mires between fluvial channels (Birkeland, 1999). Blocky pedogenic structures are inferred to represent the upper layers of the B soil horizon while granular textures indicate deposition within the A soil horizon (Mack et al., 1993). The irregular form of the blocky structures indicates swelling caused by fluctuating water saturation within the clay-rich soils (Kraus, 1999). These processes occur when soils form close to the top of the water table. The isolated sandstone lenses infer minor fluvial systems incising though the mires (Miall, 1996).

FA-3 Description

FA-3 consists of inclined heterolithic strata, planar laminated heterolithic strata, planar laminated silt, trough cross bedded sandstone, sigmoidal bedded sandstone, and

minor wavy bedded sandstone (F-IHS, F-PHS, F-TCS, F-SB, F-WS)(Table 1.1, Figure 1.13 A, C, D, E, F, G). It is only found within Blue Cove and Ty Hatch Canyons (Figure 1.6).

Within Blue Cove, inclined heterolithic strata occur as alternating organic mudstone and siltstone within isolated channels, i.e., concave up deposits with erosional bases and dimensions ranging from 50 m to 60 m wide and 3 to 5 m thick (n=5, Table 1.3; Figure 1.14). Erosional relief can reach up to 1 m. Beds within the deposits do not exceed 20 cm thick and gradually shallow to more planar features by the top of the deposit. Some of these channelized bodies exhibit minor lateral amalgamation but the majority are isolated by planar laminated siltstone and channelized sigmoidal bedded sandstone (Figure 1.14).

Moving east to Ty Hatch Canyon, this interval triples in thickness, to 30 m thick, and contains concave-up planar laminated heterolithic features, similar to those found within Blue Cove, nested between packages of vertically amalgamated sandstone bodies with erosional bases (Figure 1.15). Packages of heterolithic strata, 60 m to 70 m wide and 5 m thick, occur as alternating organic mudstones and siltstones interbedded with thin (0.5 m to 1 m) trough cross bedded and wavy bedded sandstones (Figure 1.15). Within the heterolithic deposits, abundant organic material drapes individual siltstone and sandstone beds (Figure 1.13 G). Minor wood fragments, coal rip-up clasts, and shell material can be found at the base of these beds (Figure 1.13 I).

Between heterolithic packages, there are abundant sandstone packages (>70% sandstone) with similar dimensions (60 m wide, 5 m thick) and concave-up geometry (Figure 1.15). Individual sandstone beds do not exceed 1 m thick and terminate at

adjacent heterolithic deposits. These packages exhibit a fining upward trend. Throughout Ty Hatch Canyon across any horizon, an alternating pattern of heterolithic packages and sandstone dominated packages is present (Figure 1.15).

Trace fossils are present in both the heterolithic and sandstone dominated packages with groups of up to 100 found within the heterolithic deposits, completely disrupting bedding, while groupings within sand-dominated deposits do not exceed 10 traces. *Planolites* is present in hyporelief on the base of individual sandstones as a single meandering horizontal tube (< 0.5 cm diameter) (Figure 1.13 B). *Ophiomorpha* is also present as single traces (<1 cm diameter) in cross section, as a vertical meandering tube containing pelleted walls. *Thalassinoides* is present exclusively within heterolithic deposits in hyporelief on the base of beds as horizontally branching tubes, (in groups of 10 or more) with diameters less than 0.5 cm. *Teredolites* is present within wood fragments and logs with the largest grouping reaching well over 100 individual traces with diameters less than 0.5 cm (Figure 1.13 H)

FA-3 Interpretation

FA-3 is interpreted as tidally influenced channels in Blue Cove transitioning to estuaries and small distributary channels within Ty Hatch. At Blue Cove, the presence of inclined heterolithic strata indicate varying flow regimes (Dalrymple & Choi, 2007). The abundant organic material suggests a rich sediment source like those found along coastal margins. Moving east to Ty Hatch, repeated successions of alternating heterolithic packages and sandstone units that migrate laterally indicate rapidly evolving systems of high energy deposition between protected low energy sediment suspension and fallout

regimes (Figure 1.15; Figure 1.16). Within the sandy intervals, the transition to finer grained heterolithic deposits at the top of the unit is interpreted as waning flow within a river choked with sediment (Miall, 1996; Reesink and Bridge, 2007). During times of low energy, flow deposition is dominated by fine grained siltstones and mudstones, but at higher energies, deposition is dominated by sandstone until the channel becomes completely choked with sediment and is forced to avulse elsewhere (Reesink and Bridge, 2007). As the river avulses to feed another area of the shoreline, the zone of previous fluvial deposition exhibits only low energy flow and minor tidal fluctuation, allowing for thick successions of heterolithic deposits to accumulate.

FA-4 Description

FA-4 (the Calico bed) consists of poorly sorted trough cross bedded sandstone, trough cross bedded pebbly sandstone and convoluted bedded sandstone (F-TCS, F-TCPS, F-CBS) with interbedded planar laminated siltstone (F-S) (Figure 1.17 C, F, G). This association is easily recognizable across most of the plateau as a bleached-white sandstone bench, making it ideal for correlation purposes (Figure 1.18). The Calico bed is actually a misnomer because it represents numerous amalgamated beds and in some cases, these beds are separated by fine grained material (Figure 1.18). Individual sandstone beds do not exceed 8 m thick but can be as thin as 1 m due to scouring of overlying units.

In the western portion of the plateau, the Calico bed comprises isolated lenticular sandstone bodies with concave up geometries (i.e., channels) and moving east, it begins to coalesce into thicker successions of vertically aggrading sandstones (Figure 1.6).

Within this association, individual bar forms are much less distinct and in many cases, sandstone beds are amalgamated. Another distinction separating this association from the other facies associations described here is the general lack of fine grained deposits. Commonly separating individual coarse grained sandstones are thin (less than 15 cm) medium grained sandstones and little or no fine grained material. Bed thickness, grain size, as well as vertical and lateral extent all increase to the top. Grain sizes vary from upper fine sandstone to lower medium sandstone at the base, to upper medium to coarse sandstone at the top of FA-4. Pebble lags are common at the base of beds with clasts that range from subangular to rounded; diameters range from 0.5-0.25 cm. Single sandstone bodies do not exceed 100 m in length and increase in lateral accretion to the east (n=8, Table 1.3). Overall thickness of FA-4 reaches up to 10 m due to vertical aggradation, whereas overall regional extent is greater than 20 km due to high lateral accretion. Relief along the basal scour of the association can reach up to 15 m.

Plant material, wood fragments and coal rip-up clasts are abundant throughout this association (Figure 1.17 D). Wood fragments commonly do not exceed 20 cm and are most abundant along the basal sours of sandstones. No body or trace fossils are present.

Within this association, 279 paleocurrent and 44 accretion measurements were taken at Coyote Springs, Blue Cove, and Ty Hatch (Figure 1.7). Paleocurrents from Coyote Springs have bidirectional dominant flows to the north and northeast. Moving west, within Blue Cove, paleocurrent direction transitions to the north and southeast with parallel accretion directions. Within Ty Hatch Canyon, the paleocurrent direction is

strongly bidirectional to the northeast and southwest and also exhibits parallel accretion sets.

FA-4 Interpretation

FA-4 represents downstream accreting, coarse braided rivers with minor accumulations of overbank siltstones. The high amounts of vertical aggradation and lateral accretion indicate a multichanneled system with continuous avulsion and poor channel development (Posamentier et al., 1992). This hypothesis is supported by the general lack of root casts and organic material, indicating that bar forms within the river were unstable and unable to support vegetation. Also noted is the lack of fine grained overbank deposits, indicating high energy deposition, and that any fine grained material that was deposited was quickly removed with subsequent erosion (Miall, 1997). These patterns would be expected within a primarily downstream accreting, braided river system. The parallel relationship between paleocurrent and accretion measurements also supports a downstream accretion interpretation (Figure 1.7). The presence of subangular pebbles indicates a closer proximity to the source and a higher energy system with a suspended bed load (Ressink and Bridge, 2007).

Depositional Units

Depositional Units

In this study, the Tibbet Canyon and Smoky Hollow Members of the lower Straight Cliffs Formation are divided into four depositional units (DU-1 through DU-4). Depositional units are distinct stratigraphic intervals of unique facies associations and

stratigraphic architectures. Interpretation of these intervals provides insight into the paleogeographic and temporal framework for the region.

Lower Tibbet Canyon Member

Depositional Unit One (DU-1: prograding shoreface successions). DU-1 encompasses the lower Tibbet Canyon Member and contains four stacked shoreface parasequences, each individually bounded by flooding surfaces (A-C), and with an overall regressive trend (Figure 1.19). A parasequence is a regressive shoreface succession bounded by a flooding surface (van Wagoner, 1991). The basal portions of each parasequence represent distal lower shoreface deposits just above storm wave base (Figure 1.20). The coarsening upward trends in all four parasequences, along with the decrease in abundance, size, and diversity of trace fossils suggest a major transition to higher energy environments by the top of DU-1 (i.e., wave dominated shoreface). Flooding surfaces A-C correspond to minor transgressive events bounding each parasequence, and these can be traced across the study area (Figure 1.19). These flooding surfaces are typically bedding-parallel and nonerosive (<5 m relief across the study area).

The third and fourth parasequences are capped by medium grained trough cross bedded sandstones with sharp bases containing bidirectional paleocurrents, fragmented organic material, and little to no bioturbation. These facies are interpreted as a wave dominated shoreface within the swash zone. The abrupt basal contact to coarse-grained sandstone at the base of these sandstones suggests influence by three factors: basin geometry, duration of the shift, and erosive processes (Proust et al., 2001). A shallow basin geometry will produce major shoreline shifts with relatively minor fluctuations in

sea-level. The farther the shoreline shifts, the longer its basal surface is subject to processes such as sediment starvation, and wave ravinement or fluvial scouring, all of which produce sharp based shoreface sandstones (Proust et al., 2001).

At the top of the fourth shoreface parasequence, the sandstones transition to planar bedding with organic drapes on bedding planes indicative of waning flow caused by the retreat of crashing waves within the foreshore (Figure 1.19). Root casts within these sandstones provide evidence of direct contact with terrestrial vegetation and a minor coal seam in the western portion of the plateau (landward) suggests the presence of coastal swamps, oxbow lakes, and interdistibutary deposits just behind the barrier dunes.

Thus, DU-1 represents an overall transitional basinward shift with higher frequency trangressive shifts (flooding surfaces) throughout. This trend describes a relationship where sediment supply is exceeding accommodation driving the shoreface basinward. Minor flooding events push facies slightly landward before being taken over by sediment supply by the top of the next sequence.

Depositional Unit Two (DU-2: fluvial deposits, with tidal and marine influence to the east). In the western part of the study area, DU-2 consists of isolated single story channel sandstones laterally separated by floodplain siltstones (FA-2) (Figure 1.19). These isolated sandstone bodies transition to multistoried amalgamated channel sandstones (FA-2) interbedded with heterolithic strata (FA-3) in the east (1.19). These deposits are interpreted as river, tidally influenced river, and estuarine deposits (Figure 1.21). Within DU-2, FA-2 (fluvial deposits) is present across the entire study area (>20 km), whereas FA-3 (estuarine and tidal deposits) is restricted to the eastern 10 km of the study area within Blue Cove and Ty Hatch Canyons (i.e., basinward) (Figure 1.19). At Ty

Hatch, both amalgamated fluvial channels and planar heterolithic deposits fill nested concave-up features (Figure 1.16). The presence of heterolithic strata in isolated deposits indicates varying flow regimes found within the ebb and flow of tidal influence. The clusters of sandstones within Ty Hatch Canyon separated by intervals of fine grained deposits are interpreted as distributary channels of a larger river system entering the ocean, with estuaries occurring where accommodation space outpaces sediment supply (Figure 1.16). The presence of trough cross bedding within channelized sandstones and paleocurrents indicating a dominant easterly flow support the presence of an east flowing river system. Trace fossil abundance and diversity increases towards Ty Hatch canyon, indicating more marine influence and environments of high bio-productivity to the east.

The facies of DU-2 represent a basinward shift of coastal plain deposits (fluvial and estuarine) over the older shoreface deposits of DU-1. Thus, separating DU-2 and DU-1 is an unconformable surface, previously undocumented, that marks a basinward shift of facies (e.g., a possible "sequence boundary"). Erosional relief on this surface can reach up to 35 m, as within Ty Hatch Canyon where fluvial channels have removed up to two and a half full shoreface parasequences (Figure 1.19; Figure 1.21).

Upper Tibbet Canyon Member and Lower Smoky Hollow Member

Depositional Unit Three (DU-3: shoreface through fluvial deposits). DU-3 ranges in thickness from 20 m to 30 m (Figure 1.19). It records a conformable transition from cliff forming exposures of shoreface deposits (including upper shoreface) and amalgamated fluvial channels at the base to slope forming exposures of isolated fluvial

channels with abundant interdistributary deposits by the top (Figure 1.19; Figure 1.22). Within Rock House Cove and Coyote Springs Canyon, the lower portion of DU-3, which corresponds to the upper part of the Tibbet Canyon Member, consists of laterally amalgamated medium grained sandstones separated by thin fine grained interdistributary deposits (FA-2). Moving east to Blue Cove and Ty Hatch, the lower portion of DU-3 consists of a single prograding shoreface transitioning from fine grained hummocky cross stratified sandstones at its base through medium grained trough cross bedded and planar bedded sandstones by the top (FA-1) (Figure 1.19). The lower portion of DU-3 is interpreted as a meandering fluvial system (in the west) feeding a prograding shoreline in the east (Figure 1.22). Perhaps due to lack of exposure or preservation, no delta feature was observed. Within Ty Hatch, above the shoreface interval, deposits transition conformably to FA-2 (fluvial deposits) marking the beginning of the Smoky Hollow Member.

Separating DU-3 from DU-2 is the largest transgressive shift (i.e., flooding or sudden deepening; Swift, 1968) within the section. Within Blue Cove and Ty Hatch, this surface (flooding surface D) separates underlying FA-2 (fluvial) and FA-3 (estuarine) deposits of DU-2 from FA-1 (shoreface) deposits of DU-3, making it easily identifiable. However, moving west to Coyote Springs and Rock House Cove, this surface becomes less obvious because it separates similar fluvial sandstones as DU-3 transitions to FA-2 (Figure 1.22). Although this surface corresponds to the largest transgressive shift, almost no erosional relief (due to wave or tidal ravinement) is observed. A rapid base level rise, producing abundant accommodation space, suppresses the erosional energy of waves and

tides, thus increasing the preservation potential of the underlying deposits (Cattaneo and Steel, 2003).

The upper part of DU-3 that corresponds to the lower Smoky Hollow Member is approximately 15 m thick and transitions conformably from the lower section of DU-3 (shoreface and fluvial deposits) to isolated distributary channels and interdistributary deposits, with an overall fining upward trend. Peterson (1969b) defined two zones of the lower Smoky Hollow member: the coal zone and the barren zone. Both of these are present in DU-3. The coal zone is easily identifiable by the abundant coal zones throughout, whereas the barren zone can be identified by repeated sequences of paleosols and interdistributary deposits with fewer channels towards the top. The coal zone contains isolated fluvial channels, interdistibutary deposits, and coal deposits. The coal deposits are discrete (less than 100 m wide) and interpreted as oxbow lakes which filled with organic material and fine grained deposits. Moving upward in the section to the barren zone, coal deposits are replaced by thick paleosols interbedded with isolated fluvial channels and interdistributary deposits. This unit is interpreted to have been deposited within a low-energy meandering river system with very low rates of avulsion due to the extensive buildup of interdistributary deposits and paleosols. Thus, DU-3 represents an overall conformable basinward transition in facies from shoreface through fluvial deposits, or a gradual increase in sediment supply relative to accommodate space.

Upper Smoky Hollow Member/Calico Bed

Depositional Unit Four (DU-4: Calico bed–braided fluvial deposits). DU-4 (Calico bed) ranges in thickness from 3 m to 10 m with thickest exposures to the east, and

consists of coarse grained fluvial channels interbedded with minor fine grained interdistributary deposits (FA-4) (Figure 1.19; Figure 1.23). The Calico bed is a slight misnomer because in many exposures, it is comprised of a series of sandstone bodies, although moving east, they amalgamate into a single bed. The presence of pebbles within a coarse grained matrix indicates closer proximity to the source than any previous sandstone in the section. Increased amalgamation of channels both vertically and laterally to the east across the study area are indicative of a change in migration patterns of the rivers. The sheet geometries exhibit less connectivity in the west and become more amalgamated to the east (Figure 1.23). Overall, DU-4 records mainly downstream accreting; likely, braided river systems formed as sediment supply outpaced accommodation.

The basal surface of this unit corresponds to a basinward transition to coarse grained laterally amalgamated channel deposits of the Calico bed from the underlying fine grained isolated channels of the "barren zone" of the lower Smoky Hollow Member (upper DU-3). Commonly, a transitional facies of fine grained fluvial channels containing minor amounts of coarse clasts is present below this surface. The presence of this bed suggests a gradational transition to the coarse material found within the Calico bed. However, the erosional relief (up to 10 m) and sudden grain size shift found on the basal surface of the coarsest beds justifies the presence of a local unconformity. Bobb (1991) recognized a similar trend in grain sizes and also placed an unconformity at this interval, supporting a more regional shift. The biostratigraphy (Figure 1.4) records a major transition with faunal assemblages, from the base of the Calico bed through the overlying lower John Henry Member, supporting the loss of a significant amount of time.

Discussion

Detailed study of the Tibbet Canyon and Smoky Hollow Members in the southwest Kaiparowits Plateau argues for more complexity in the stratigraphic architecture of these units than has been previously recognized. This research documents numerous surfaces and facies changes, including both major and regionally significant shifts as well as minor transitions. Thus, the stratigraphic evolution of the lower Straight Cliffs Formation as documented here raises questions regarding how sequence boundaries are recognized and defined in similar depositional settings, and the forces controlling the creation and preservation of these facies relationships and key surfaces.

The lower Tibbet Canyon Member, overall, is a progradational shoreface (c.f., Shanley and McCabe, 1995). However, this study identifies three additional small-scale shoreline shifts within this succession. These shifts correlate to three flooding surfaces separating four coarsening upward shoreface parasequences. These surfaces are present in all four canyons, across 20 km, suggesting they are not just local features, but their exposure and geometry change significantly across the study area.

Furthermore, within the lower Tibbet Canyon Member but below what is formally recognized as the Tibbet Canyon Sequence Boundary, there is an additional and apparently significant basinward shift in facies, placing fluvial and estuarine deposits unconformably on top of lower shoreface deposits, unrecognized by earlier studies (Figure 1.19). The unconformable juxtaposition of facies implies a possible new sequence boundary within the lower Tibbet Canyon Member. However, its regional significance needs further study. The basinward shift was identified within Ty Hatch Canyon where it is associated with 35 m of erosional relief (Figure 1.16; Figure 1.19).

However, tracking this surface westward, it becomes much less apparent, with a conformable shift in facies of fluvial systems incising into the foreshore and less than 5 m relief (c.f., Adams and Bhattacharya, 2005). Here a sequence boundary interpretation is preferred, mainly because of the scale of the erosional surface at Ty Hatch Canyon; it is difficult to explain a 35 m erosional surface that cuts out two and a half shoreface parasequences over a kilometer of outcrop without calling on a major base level change relative to sediment input.

Studies from the Ferron Sandstone (age equivalent strata) observe similar large scale erosional surfaces (up to 40 m of erosional relief), with concave up geometry, that exhibit vertical transitions in facies, like those observed within Ty Hatch, from fluvial deposits to tidal or tidally influence fluvial deposits and back to fluvial deposits by the top (Li et al., 2010). The progradation of the Ferron is attributed to small scale climate changes and eustatic fluctuations (Li et al., 2010). Furthermore, additional studies of the Desert, Kenilworth, and Grassy Members within the Blackhawk Formation (younger than the Straight Cliffs Formation) of the Book Cliffs have also observed large amounts of erosional relief (~40 m to ~20 m, respectively), supporting the hypothesis that these deposits are not that uncommon (van Wagoner et al., 1990). However, these incisions are attributed to lack of accommodation space during base level fall as well as stacked sequences of interfluve deposits (O'Byrne and Flint, 1995). The apparently conformable updip expression of this feature underscores regional variability in these deposits and the need for similar high resolution studies. Furthermore, two previously recognized sequence boundaries, the Tibbet Canyon and Calico (Shanley and McCabe, 1995), are shown to have transitional regressive facies below them in the study area. Relationships

like these once again complicate the recognition of a sequence boundary in any given location and these points will be discussed later.

Within the upper Tibbet Canyon Member, but still below the Tibbet Canyon Sequence Boundary (defined by Shanley and McCabe, 1991), is a previously unrecognized and significant flooding event. At Ty Hatch and Blue Cove, this surface represents the largest landward shift in facies observed in the study area, placing offshore transition zone deposits directly on estuarine and fluvial deposits. Moving west (landward) to Coyote Springs and Rock House Cove, this surface places fluvial facies directly onto underlying fluvial facies. Although this surface correlates to the largest flooding event, it contains minimal erosional relief (< 5 m) and can be difficult to differentiate (c.f., Plint et al., 2001) to the west (Figure 1.19). However, moving east (basinward), the increase in finer grained material, as well as increased erosional relief along the underlying sequence boundary, make individual sequences and surfaces much more apparent (c.f., Taylor and Lovell, 1995; van Wagoner, 1991). This once again underscores the need for high resolution regional correlation to identify surfaces correctly as well as determine the along strike and dip variations. These surfaces suggest a much more complex history for the Tibbet Canyon Member than previously interpreted, but similar studies in other parts of the plateau are needed to determine if these features can be recognized regionally or if they represent local variations.

As previously described, the Tibbet Canyon sequence boundary incises into the top of the upper Tibbet Canyon Member, marking a basinward shift from shoreface deposits to fluvial deposits (Shanley and McCabe, 1995). This relationship is observed within Rock House Cove, although the incision is minor and only removes the foreshore.

Moving to the east (basinward), erosional relief does not exceed 10 m and channel incision only removes interdistributary deposits, from fluvial facies, without reaching the shoreface. Shanley and McCabe (1995) correlated this basinward shift further to the east (i.e., Wiregrass Canyon), where fluvial deposits lie directly on the lower shoreface. This interpretation needs to be tested further, but if correct, the relationships observed in this study suggest that the updip expression of the Tibbet Canyon sequence boundary is more conformable, perhaps due to local variations in sediment supply. In any case, the interpretation pitfalls associated with depositional variability are clear.

Similar discrepancies occur within the upper Smoky Hollow Member. Observations from this study recognize numerous deposits of a transitional, coarse-grained fluvial facies separating the barren zone from the overlying Calico bed (Figure 1.17 B, C). Within the barren zone, fluvial deposits appear as isolated sandstone channels separated by abundant interdistributary deposits. Within the upper barren zone, fluvial channels begin to coarsen and incorporate coarse pebbles lags before being removed by the basal surface of the Calico bed. Bobb (1991) observed similar relationships within the northern portion of the plateau. However, Shanley and McCabe (1995) note an abrupt change within the eastern portion of the plateau, from the fine grained facies of the barren zone to a single coarse grained "sheet" sandstone identified as the Calico bed. Fossil assemblage evidence and erosional relief supports the presence of a sequence boundary (Eaton et al., 1999) and the observations from this study do not negate this interpretation. However, the presence of transitional facies may imply some tectonic control on sediment supply and accommodation space. A eustatically-driven base level fall may result in major fluvial incision with abundant sediment bypass (i.e., major base level fall)

rather than regressive pulses. The presence of these pulses suggests tectonic uplift and exposure of the Sevier Fold and Thrust Belt to the west, gradually shifting facies basinward. Additionally, studies of the Ferron sandstone have identified a conformable shift to a coarse grained facies at the top of the association supporting tectonic influence (Li et al., 2009). These inconsistencies demonstrate the complexity of the region and its controlling process, and the need for more regional correlation.

Conclusions

The Tibbet Canyon and Smoky Hollow Members of the Straight Cliffs Formation can be divided into four depositional units; progradational shoreface successions (DU-1), fluvial deposits with tidal and marine influence to the east (DU-2), a transitional sequence from fluvial through shoreface deposits (DU-3), and braided fluvial deposits (DU-4, the Calico bed). The varying exposures and geometries of these units across the study area illustrate the need for high resolution stratigraphic studies to identify and interpret small scale changes within pre-existing frameworks. This caveat largely reflects depositional complexity, or the spatial variation of given successions across a region. Changes in local controls such as sediment supply, accommodation space, drainage geometry, and local base level shifts (Posamentier and Allen, 1993) as well as regional controls such as tectonics, eustatic changes, and climate (Emery et al., 1996; Miall, 1996) give rise to such regional complexity. Two newly recognized surfaces that exemplify regional variation are the major basinward shift within the lower Tibbet Canyon Member and the major flooding surface within the upper Tibbet Canyon Member. Both of these surfaces have radically different expressions across the 20 km from Rock House Cove in the west to Ty

Hatch Canyon in the east. Similarly, two previously-recognized "major" surfaces, the Tibbet Canyon and Calico sequence boundaries (Shanley and McCabe, 1995), can alternatively be interpreted as more transitional shifts (Bobb, 1991; this study), implying a tectonic control on deposition in addition to or instead of eustacy. Thus, this study highlights the variability with surface and depositional expression as well as the need for high resolution regional correlation.

Figure 1.1 – Map of the Kaiparowits Plateau showing measured section locations compared in this study. Green shading indicates exposures of Cretaceous strata. Sections shown in this figure include measured sections from Peterson (1969 a,b), Shanley and McCabe (1991), and Bobb (1991). Transect A-A' correlates to the cross section of this study. (Insert) A map of Utah, with the position of the Kaiparowits Plateau and the orientation of the paleoshoreline, during deposition of the Tibbet Canyon Member approximately 92 million years ago (Decelles et al., 1995).

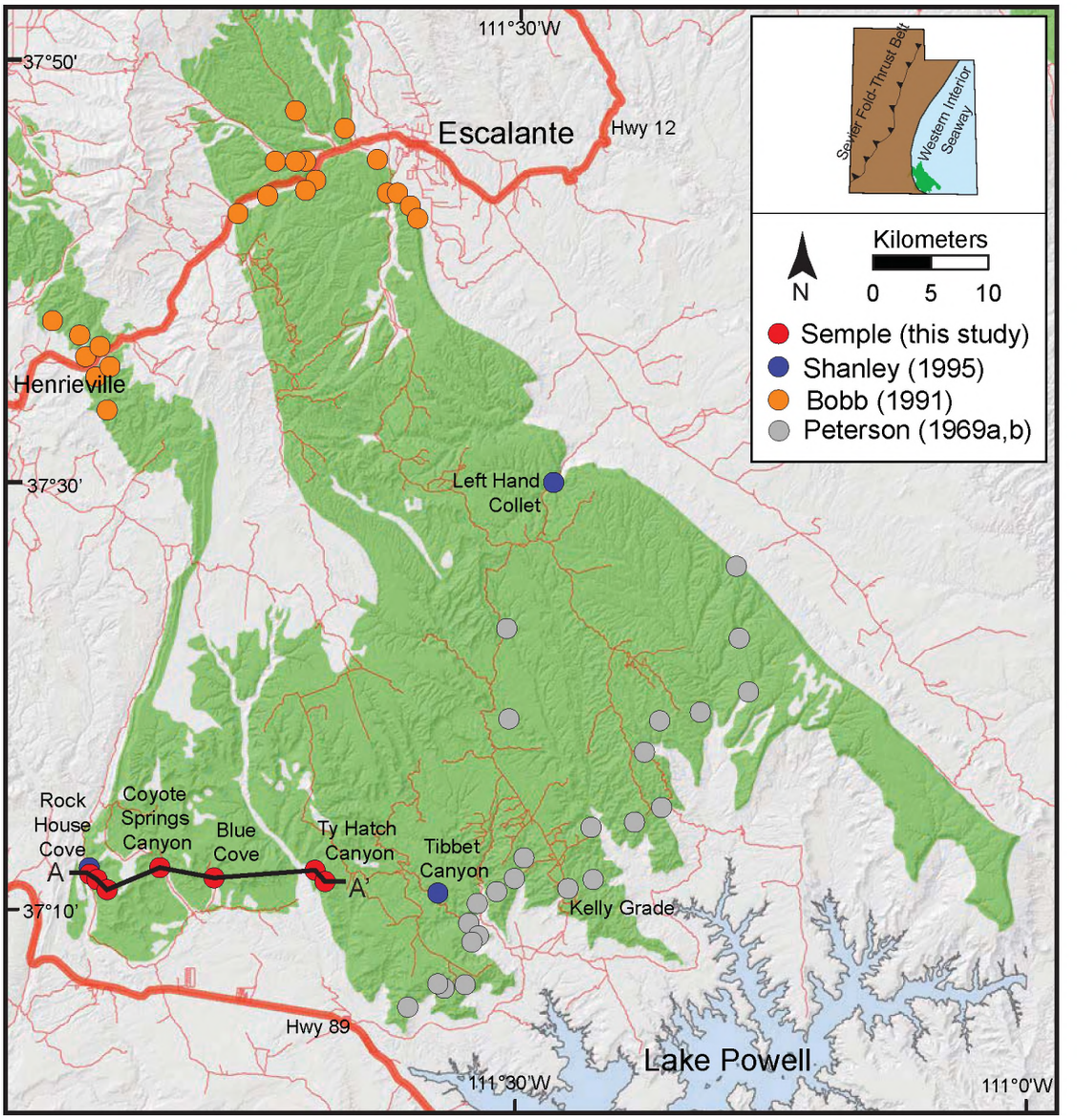
111°30'W
37°50'
Escalante
Hwy 12
Sevier Fold-Thrust Belt
Western Interior Seaway
Kilometers
N
0 5 10
Semple (this study)
Shanley (1995)
Bobb (1991)
Peterson (1969a,b)
Henrieville
37°30'
Left Hand Collet
Rock House Cove
Coyote Springs Canyon
Blue Cove
Ty Hatch Canyon
Tibbet Canyon
A
A'
37°10'
Kelly Grade
Hwy 89
Lake Powell
111°30'W
111°0'W

Figure 1.2 – Late Cretaceous stratigraphy of Kaiparowits Plateau (modified from Gooley, 2010). A) Lithostratigraphy of the Straight Cliffs Formation, marginal marine through fluvial facies are shown for the John Henry Member. Marine transgressive-regressive cycles correlating to documented marine sandstones (A-G) are represented by black triangles (Allen, 2009). The Tibbet Canyon and Smoky Hollow Members are detailed in Figure 1.4. B) Regional stratigraphy of the Kaiparowits Plateau.

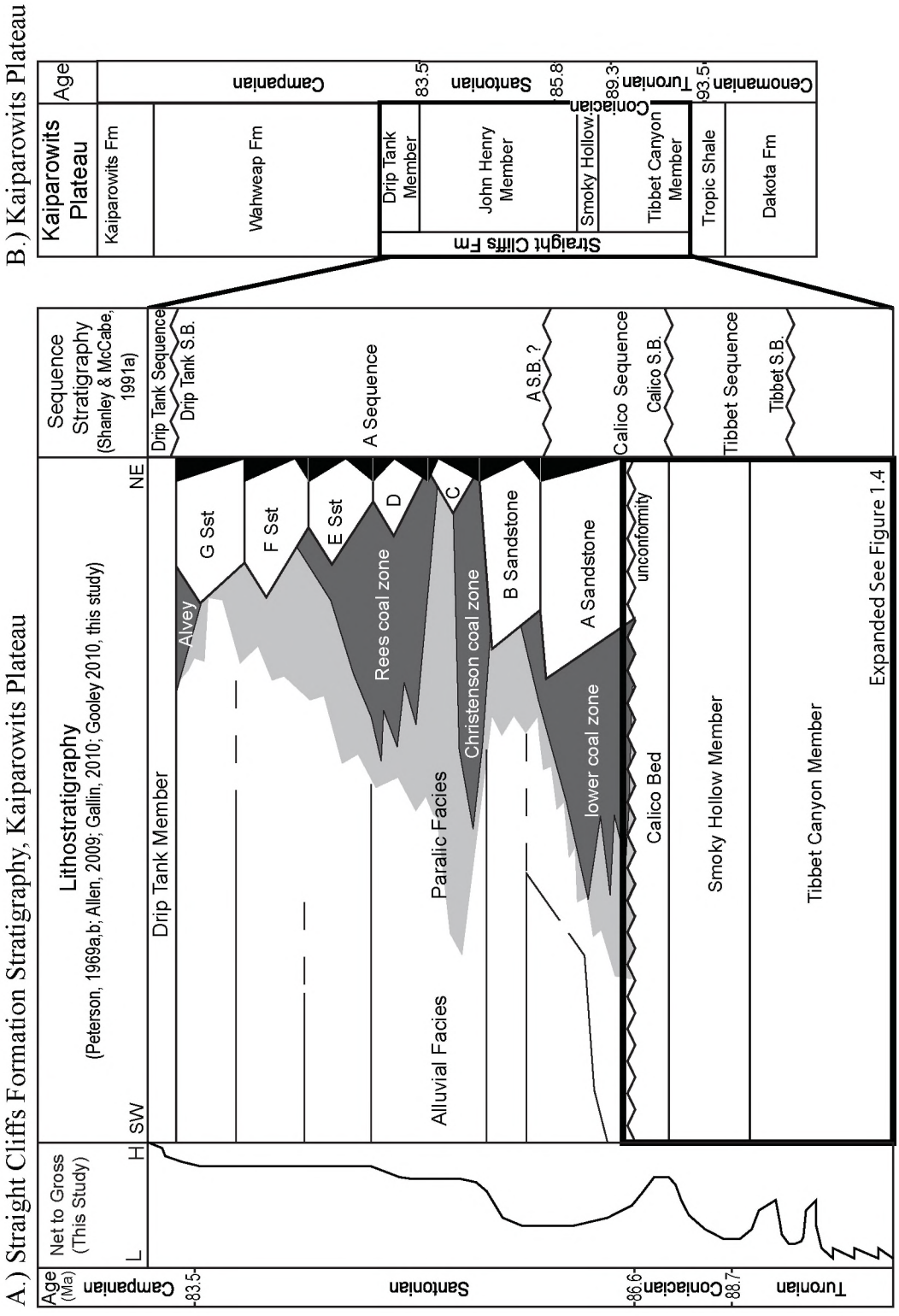
A.) Straight Cliffs Formation Stratigraphy, Kaiparowits Plateau
B.) Kaiparowits Plateau
Age (Ma)
Net to Gross (This Study)
L
H
Lithostratigraphy
(Peterson, 1969a,b; Allen, 2009; Gallin, 2010; Gooley 2010, this study)
SW
NE
Sequence Stratigraphy (Shanley & McCabe, 1991a)
Campanian
Santonian
Coniacian
Turonian
83.5
86.6
88.7
Drip Tank Member
Drip Tank Sequence
Drip Tank S.B.
Alvey
G Sst
F Sst
E Sst
D
C
B Sandstone
A Sandstone
Rees coal zone
Christenson coal zone
lower coal zone
Paralic Facies
Alluvial Facies
A Sequence
A.S.B.?
Calico Sequence
Calico S.B.
unconformity
Calico Bed
Tibbet Sequence
Tibbet S.B.
Smoky Hollow Member
Tibbet Canyon Member
Expanded See Figure 1.4
Kaiparowits Plateau
Age
Kaiparowits Fm
Wahweap Fm
Campanian
83.5
Santonian
85.8
89.3
Turonian
93.5
Cenomanian
Straight Cliffs Fm
Drip Tank Member
John Henry Member
Smoky Hollow
Tibbet Canyon Member
Tropic Shale
Dakota Fm

Figure 1.3 – Detailed hillshade image of the southwestern portion of the Kaiparowits Plateau showing measured sections. Transect A-A' marks the cross section of this study. The DEM for the hillshade was generated with 10 meter NED Maps from the Utah GIS Portal (ARGC, 2011).

Location Map Southwestern Kaiparowits Plateau

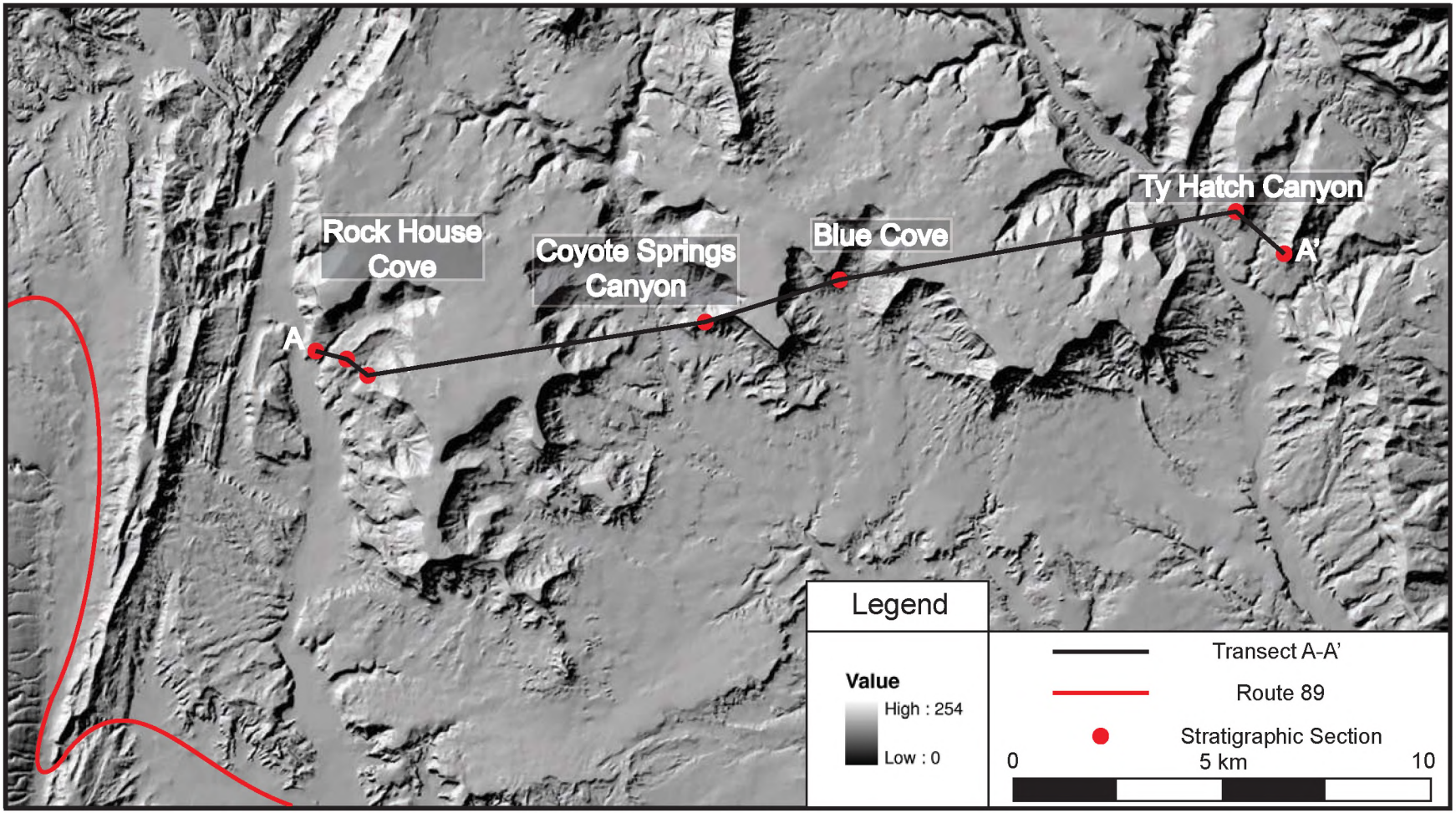

Figure 1.4 - Lithostratigraphic framework for the Tropic Shale through the John Henry Member (94-86 Ma). (From left to right) Sequence Stratigraphy, Eustatic Curves, Biostratigraphy/Radiometric Dates. Previous sequence stratigraphic frameworks have surfaces denoted by dashed lines and the thickness of those lines represent the duration of the unconformity.

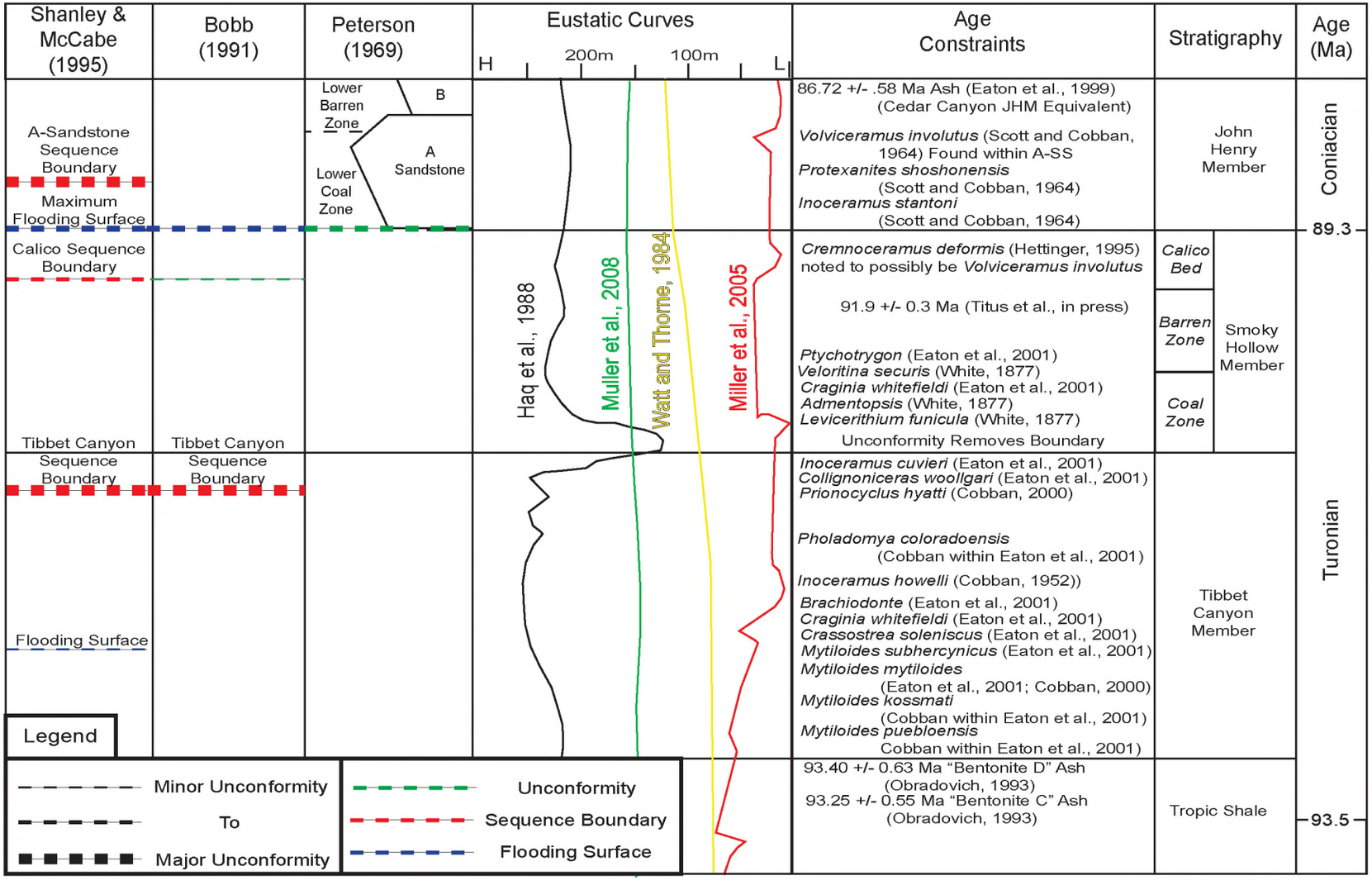
Shanley & McCabe (1995)
Bobb (1991)
Peterson (1969)
Eustatic Curves
H
200m
100m
L
Age Constraints
Stratigraphy
Age (Ma)
Lower Barren Zone
B
A Sandstone
Lower Coal Zone
A-Sandstone Sequence Boundary
Maximum Flooding Surface
86.72 +/- .58 Ma Ash (Eaton et al., 1999)
(Cedar Canyon JHM Equivalent)
Volviceramus involutus (Scott and Cobban, 1964) Found within A-SS
Protexanites shoshonensis
(Scott and Cobban, 1964)
Inoceramus stantoni
(Scott and Cobban, 1964)
John Henry Member
Coniacian
89.3
Calico Sequence Boundary
Haq et al., 1988
Muller et al., 2008
Watt and Thorne, 1984
Miller et al., 2005
Cremnoceramus deformis (Hettinger, 1995)
noted to possibly be Volviceramus involutus
91.9 +/- 0.3 Ma (Titus et al., in press)
Ptychotrygon (Eaton et al., 2001)
Veloritina securis (White, 1877)
Craginia whitefieldi (Eaton et al., 2001)
Admentopsis (White, 1877)
Levicerithium funicula (White, 1877)
Unconformity Removes Boundary
Calico Bed
Barren Zone
Coal Zone
Smoky Hollow Member
Tibbet Canyon Sequence Boundary
Tibbet Canyon Sequence Boundary
Inoceramus cuvieri (Eaton et al., 2001)
Collignoniceras woollgari (Eaton et al., 2001)
Prionocyclus hyatti (Cobban, 2000)
Pholadomya coloradoensis
(Cobban within Eaton et al., 2001)
Inoceramus howelli (Cobban, 1952))
Brachiodonte (Eaton et al., 2001)
Craginia whitefieldi (Eaton et al., 2001)
Crassostrea soleniscus (Eaton et al., 2001)
Mytiloides subhercynicus (Eaton et al., 2001)
Mytiloides mytiloides
(Eaton et al., 2001; Cobban, 2000)
Mytiloides kossmati
(Cobban within Eaton et al., 2001)
Mytiloides puebloensis
Cobban within Eaton et al., 2001)
Tibbet Canyon Member
Turonian
Flooding Surface
Legend
Minor Unconformity
To
Major Unconformity
Unconformity
Sequence Boundary
Flooding Surface
93.40 +/- 0.63 Ma "Bentonite D" Ash
(Obradovich, 1993)
93.25 +/- 0.55 Ma "Bentonite C" Ash
(Obradovich, 1993)
Tropic Shale
93.5

Figure 1.5 – Comparison of sequence stratigraphic models of the lower Straight Cliffs Formation as proposed by Shanley and McCabe (1995), and Bobb (1991). The model proposed by Shanley and McCabe (1995) describes the Tibbet Canyon Member as a single prograding shoreface erosionally truncated by fluvial channels, marking the Tibbet Canyon Sequence Boundary. The Smoky Hollow Member is described as isolated fluvial channels separated by abundant interdistributary deposits before being erosionally truncated by the Calico bed, marking the Calico Sequence Boundary. The model proposed by Bobb (1991) suggests a similar trend in the Tibbet Canyon Member but argues for the presence of a coarsening upward transitional facies below the Calico bed, marking the shift by a small unconformity rather than a sequence boundary.

Shanley and McCabe (1995)

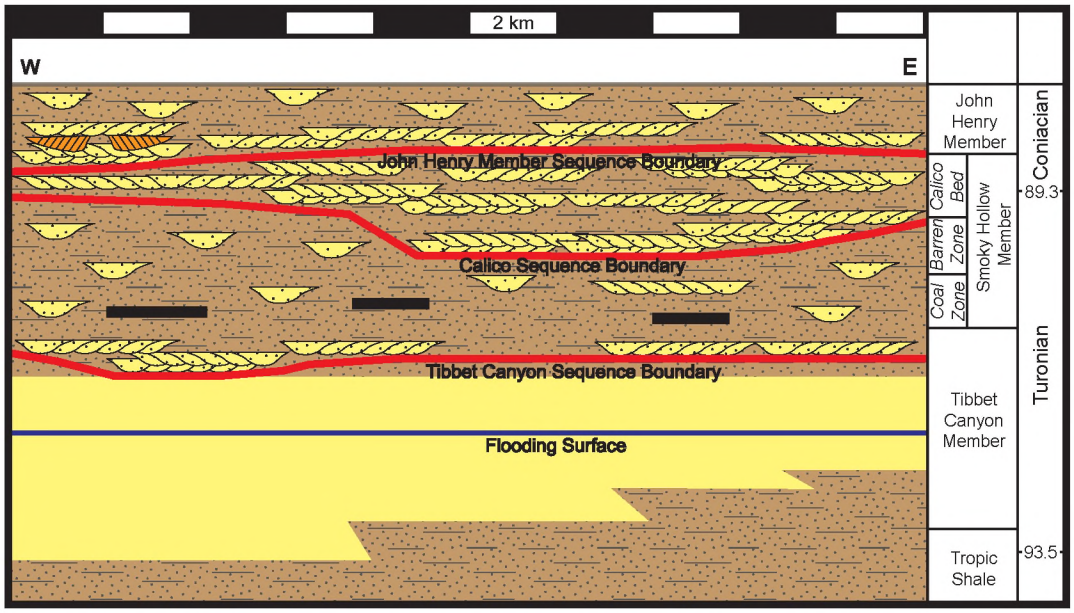

Bobb (1991)

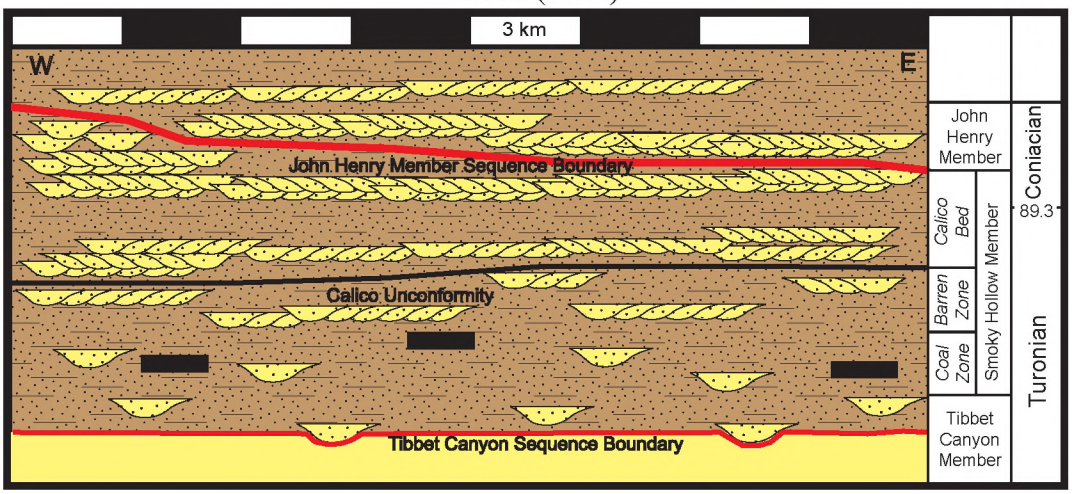

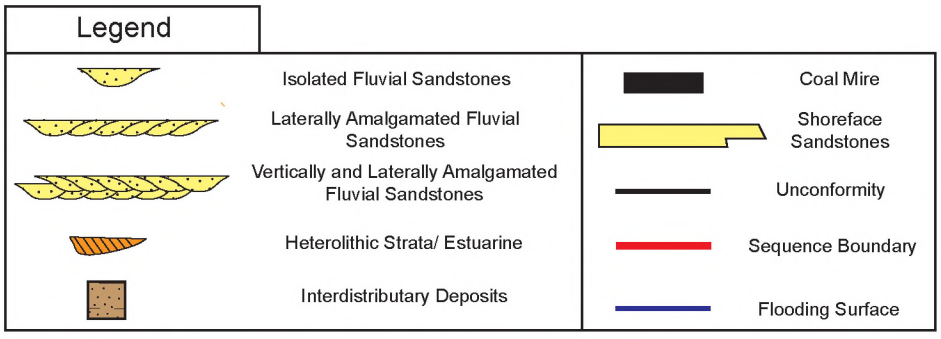

Figure 1.6 – Correlation of stratigraphic sections across transect A-A'. Four facies associations are outlined as well as the bounding members, the Tropic Shale and John Henry Member. Paleocurrents are denoted by arrows within white circles. Vertical scale is 10 meters between tick marks.

Stratigraphic Correlation with Facies Associations

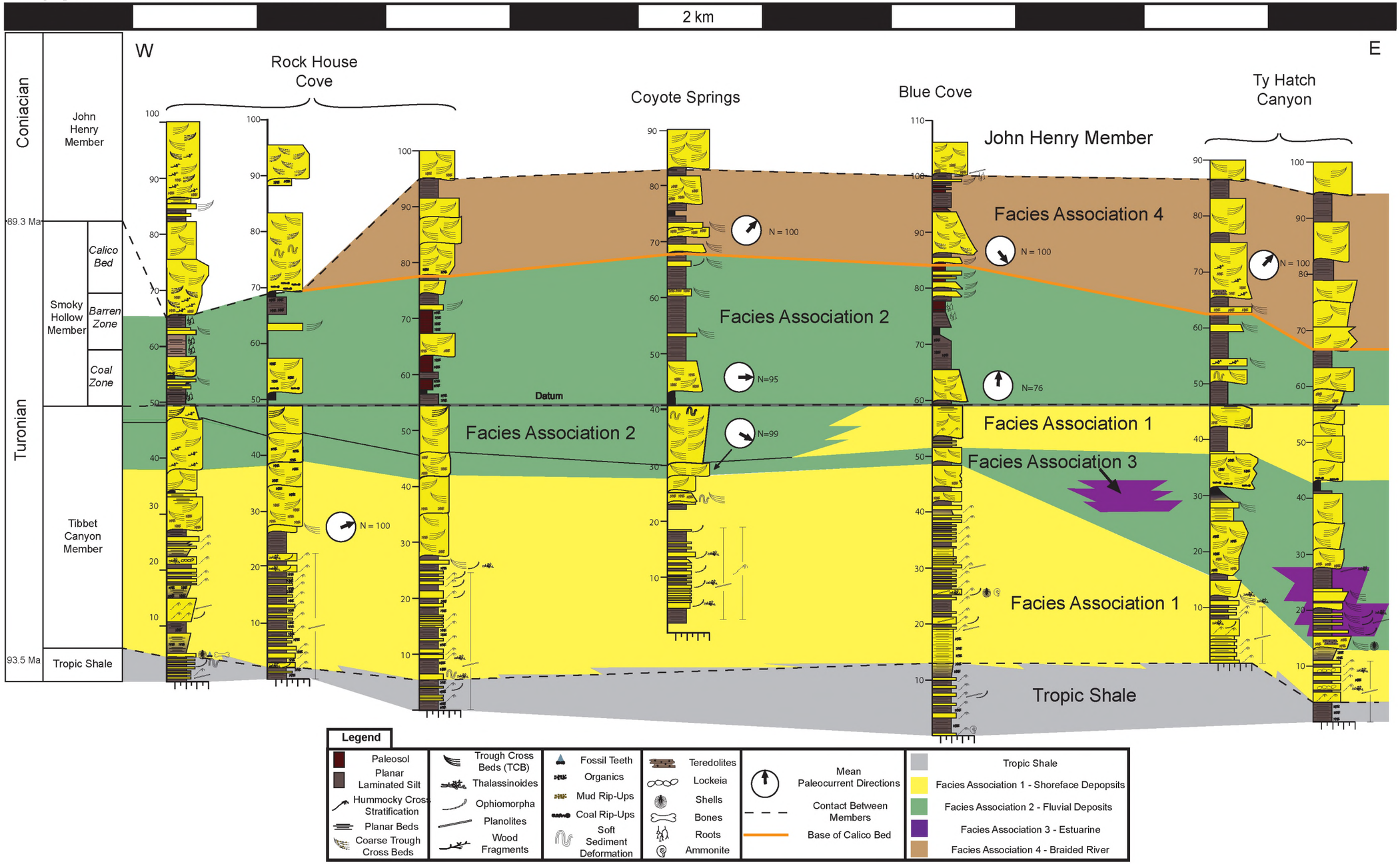

Figure 1.7 – Paired rose diagrams depicting paleocurrent and accretion direction for each of the four canyons from this study. Blue measurements correlate to paleocurrent direction while red measurements correlate to accretion set direction. Black arrows correspond to the mean for each diagram.

Paleocurrents

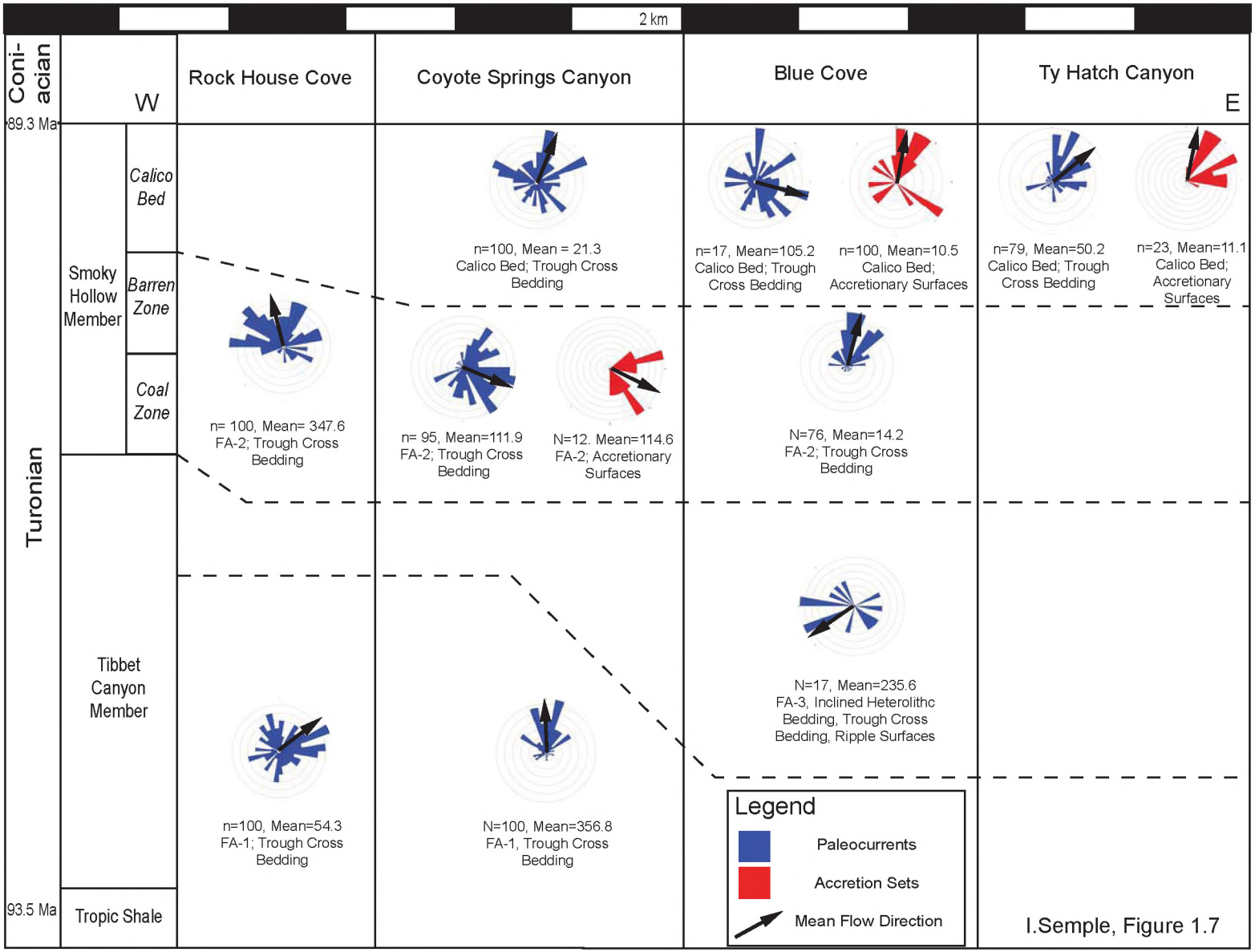

Table 1.1

Lithofacies

Lithofacies Code	Lithofacies	Description
F-C	Coal	Dull to vitreous in color, ranges from lignite to sub-bituminous, low competence, thickest interval was 1.5m. Occurs in fining upward deposits, likely overlying clay, or carbonaceous shales. Almost exclusively below sharp contacts of sandstone.
F-Cl	Clay	Reddish- brown, orange, or blue-black in color, forms in layers, create slope forming intervals within sections, roots commonly present
F-CS	Carbonaceous Shale	Horizontally laminated deposits, laminations 1mm – 5mm, organics throughout, trace fossils present as casts on the bottom of beds.
F-PS	Planar Laminated Siltstone	Gray color, horizontal laminations 2mm – 10mm thick, found throughout section, slope forming
F-HS	Heterolithic Strata	Planar beds of alternating very fine sandstone, siltstone, and mudstone. Beds can reach up to 20 cm thick although commonly are no more than 10 cm. Bedding planes are commonly draped with organic material. Trace fossils include planolites, ophiomorha, lockeia, and protovirgularia.
F-IHS	Inclined Heterolithic Strata	Alternating inclined beds of very fine sandstone, siltstone, and mudstone. Bed are commonly no more than 10 cm thick. Carbonaceous material drapes the bases of troughs and abundant plant material can be found. Trace fossils include planolites, ophiomorpha, lockeia, and protovirgularia.

Table 1.1 Continued

Lithofacies Code	Lithofacies	Description
F-WBS	Wavy Bedded Sandstone	Sanstones containing wave ripples throughout, mior wave ripple surfaces occur on the top of sandstone beds, usaully less than 20 cm thick, grainsizes range from fine to medium sand.
F-HCS	Hummocky Cross Stratified Sandstone	Hummocks and swales present as trough sets ranging from 5cm – 30cm, grainsize ranges from very fine sand to fine sand. Trace fossils common, bed thicknesses range from .1m to 1m
F-TCS	Trough Cross Bedded Sandstone	Trough sets range from .3m to 5m thick, Grainsize variable from very fine sand to very coarse sand.
F-TCPS	Trough Cross Pebbly Sandstone	Trough sets range from 1m to 3m thick, troughs contain minor lag deposits of subangular to rounded pebbles, as well as fossil fragments, matrix grainsize ranges from fine sand to very coarse sand.
F-PBS	Planar Bedded Sandstone	Planar laminated sandstones, laminations range from 5cm to 40 cm thick, grainsize ranges from fine sand to medium sand
F-BS	Bioturbated Sandstone	Bedding plane structures within these sandsotnes have been disturbed by animal activity (such as burrowing). Trace fossils can be found throughout the deposits.
F-CBS	Convoluted Bedded Sandstone	This sandstone can be seen with disturbed layers, individual bedding lines can be truncated, and folded making them hard to trace. This bedding makes paleocurrent measurements impossible.

Table 1.2

Trace Fossils of Tibbet Canyon and Smoky Hollow Members

Trace Fossil	Trace Fossils	Description
TF-P	Planolites	Simple singular tube with circular cross section, can be found horizontal to sub-horizontal and may contain backfill. Probable Tracemaker: Invertebrates, many possible tracemakers
TF-S	Skolithos	A simple vertical burrow that exhibits much greater depth than width. May contain a wall lining. Used for protection and dwelling. Probable Tracemaker: Invertebrates, possibly worms
TF-O	Ophiomorpha	A branching burrow that can be oriented in any direction. The walls of the trace are lined with pellets which vary in size and shape between species. Probable Tracemaker: Decapod, Callianassid Shrimp
TF-Th	Thalassinoides	Small, cylindrical burrows that contain three-way intersections. Tracemakers will line the burrows creating competent open passageways. Infilling is common once the burrow is vacated. Probable Tracemaker: Decapods
TF-Te	Teredolites	Long tubular borings into wood that generally occur in dense clusters. The borings usually begin perpendicular to the wood surface and then abruptly turn parallel to the wood grain. Possible Tracemaker: Pholadid Bivalves (shipworms)
TF-L	Lockeia	Broadly symmetrical almond shaped mound with blunt rounded ends. Size ranges from 1-3cm, Probable Tracemaker: Bivalves

Table 1.2 Cont.

Trace Fossil	Trace Fossils	Description
TF-Pr	Protovirgularia	Horizontal to sub-horizontal trail or tunnel, found on bedding surfaces. The furrow of the trace is lined on both sides with ridges and internal structures consist of chevron or rib-like grooves. Probable Tracemaker: Shelled Mollusks

Table 1.3

Channel Dimensions

Facies Association	Canyon	Width	Height
2	RHC	90	8.5
2	RHC	70	6.0
2	RHC	65	5.5
2	RHC	80	8.5
2	CSC	50	6.0
2	BC	85	5.5
2	THC	75	8.0
2	THC	70	7.0
2	THC	100	10.0
2	THC	95	9.5
3	BC	45	3.0
3	BC	55	5.0
3	BC	50	3.5
3	THC	50	4.0
3	THC	60	6.0
4	CSC	80	5.0
4	CSC	85	6.5
4	BC	65	6.5
4	BC	85	8.0
4	BC	75	4.0
4	THC	95	8.0
4	THC	90	7.5
4	THC	100	8.0
4	THC	95	4.5

Figure 1.8 – Facies Association One lithofacies (see Table 1.1 for description), trace fossils (see Table 1.2 for description), sedimentary features, and generalized stratigraphic section. A) Lignitic Coal Seam (F-C). B) Trough Cross Stratified Sandstone (F-TCS) underlying Planar Stratified Sandstone (F-PSS). C) Mud rip-up clasts. D) *Protovirgularia* and *lockeia* E) Hummocky Cross Stratified Sandstone (F-HCS). F) Hummocky Cross Stratified Sandstone. G) *Ophiomorpha* (TF-O) on bedding surface. H) Ammonite specimen found on bedding surface. I) Fossiliferous Pebble Lag.

Facies Association One Field Photos

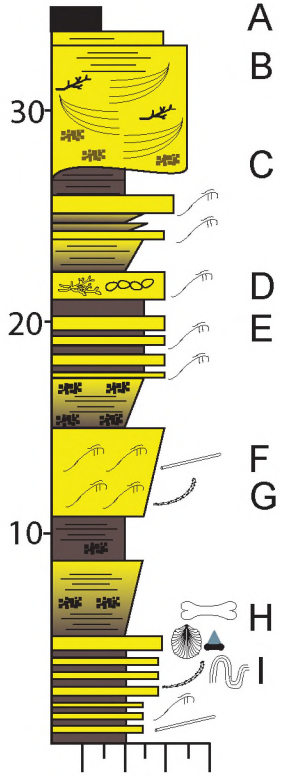

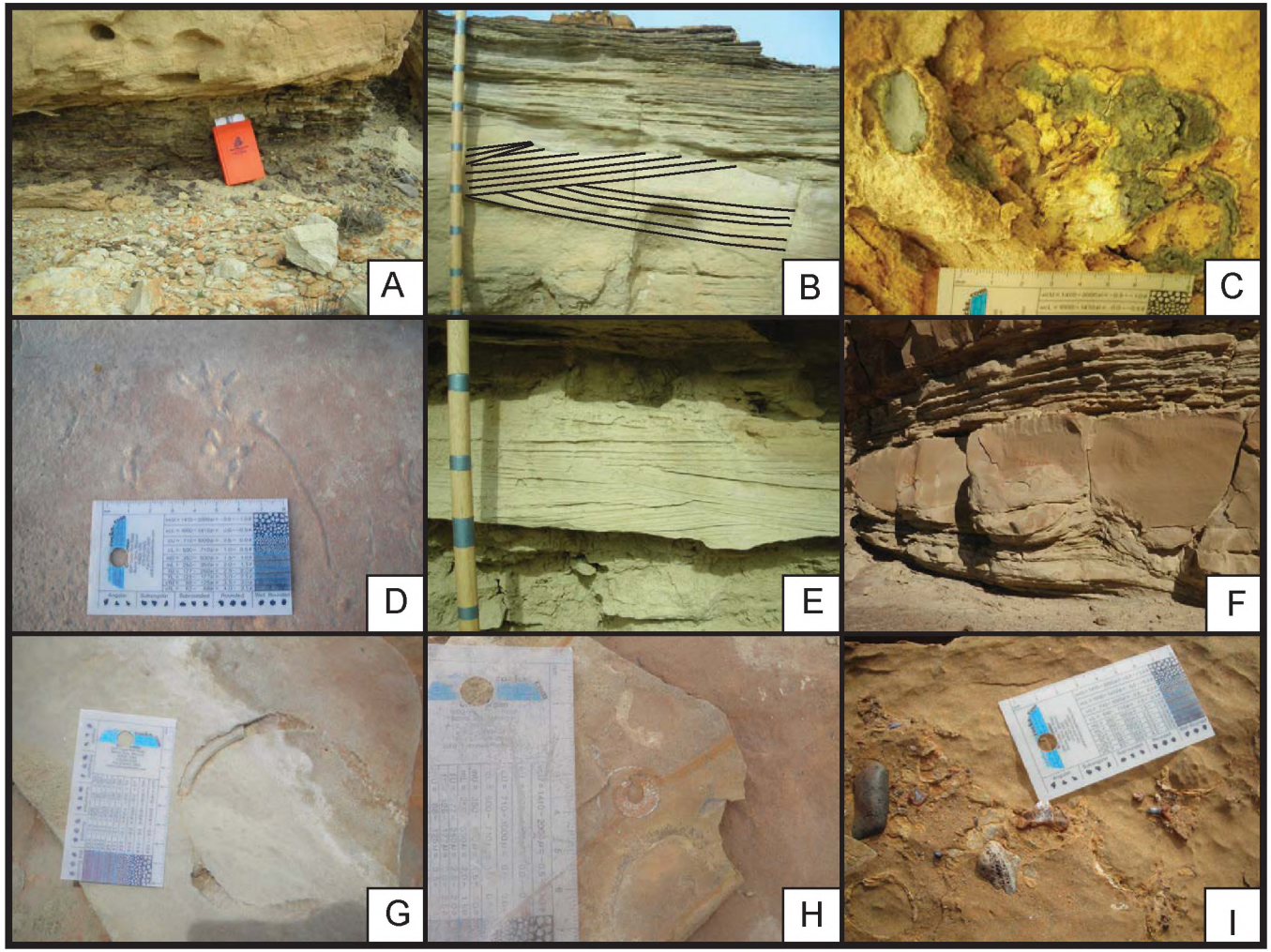

Figure 1.9 – Gigapan interpretation of Facies Association One with generalized stratigraphic section. Blue lines mark flooding events. Gigapan was collected from Ty Hatch Canyon facing east.

Facies Association One Gigapan Interpretation

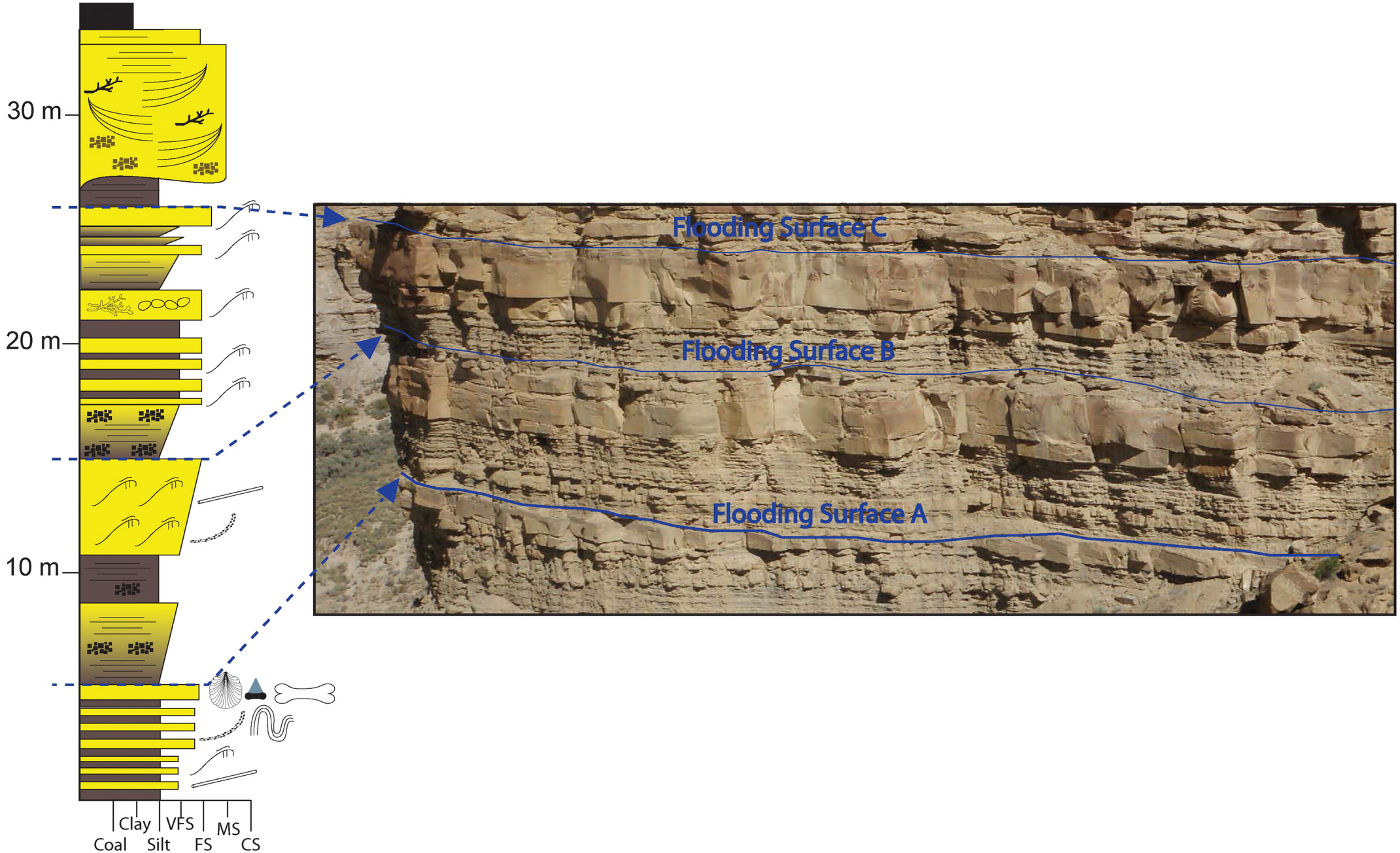

Figure 1.10 – Comparison of a shoreface succession from this study to the model succession described by Coe (2003). Blue lines mark flooding events.

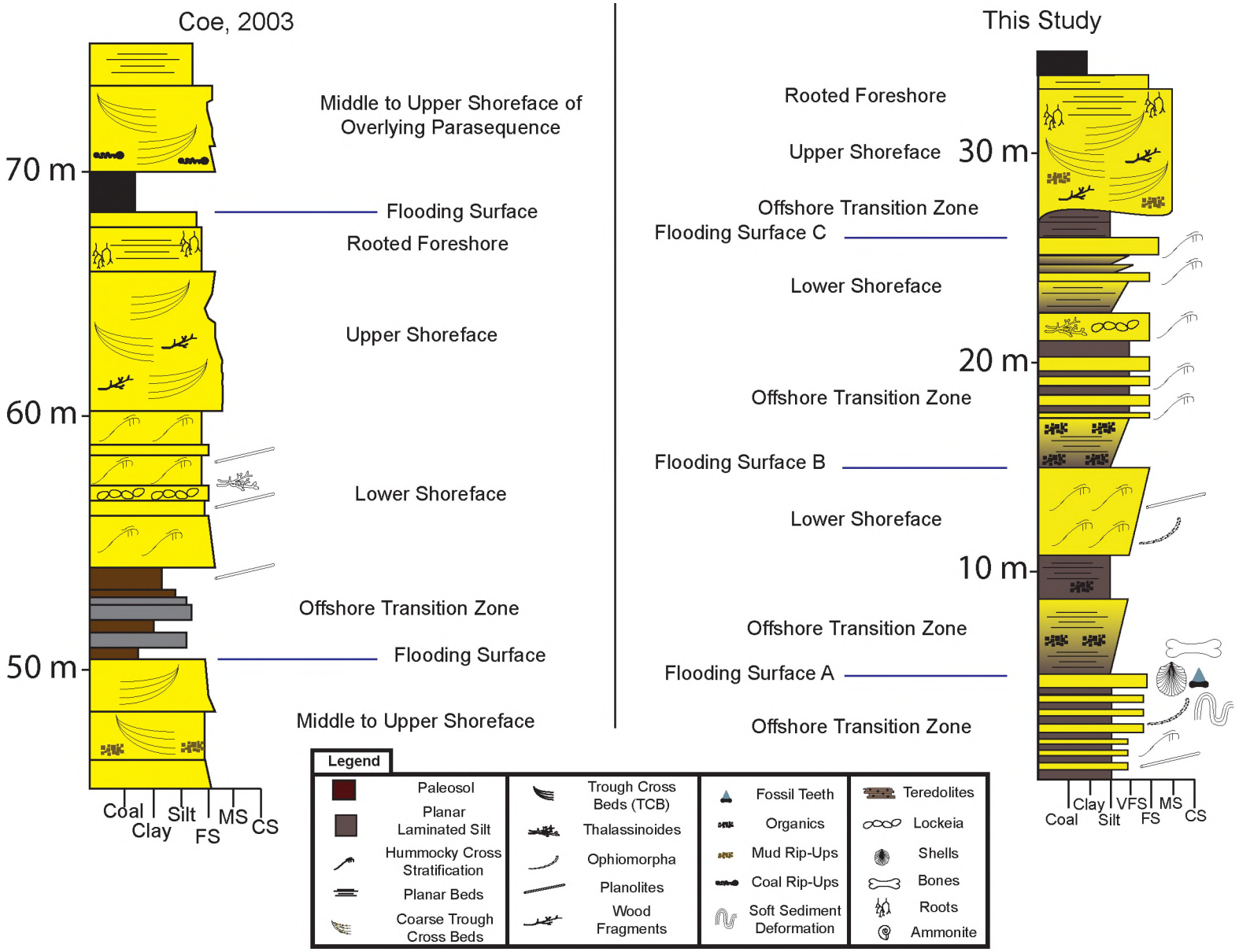
Coe, 2003
70 m
60 m
50 m
Middle to Upper Shoreface of Overlying Parasequence
Flooding Surface
Rooted Foreshore
Upper Shoreface
Lower Shoreface
Offshore Transition Zone
Flooding Surface
Middle to Upper Shoreface
Coal
Clay
Silt
FS
MS
CS
This Study
30 m
20 m
10 m
Rooted Foreshore
Upper Shoreface
Offshore Transition Zone
Flooding Surface C
Lower Shoreface
Offshore Transition Zone
Flooding Surface B
Lower Shoreface
Offshore Transition Zone
Flooding Surface A
Offshore Transition Zone
Coal
Clay
Silt
VFS
FS
MS
CS
Legend
Paleosol
Planar Laminated Silt
Hummocky Cross Stratification
Planar Beds
Coarse Trough Cross Beds
Trough Cross Beds (TCB)
Thalassinoides
Ophiomorpha
Planolites
Wood Fragments
Fossil Teeth
Organics
Mud Rip-Ups
Coal Rip-Ups
Soft Sediment Deformation
Teredolites
Lockeia
Shells
Bones
Roots
Ammonite

Figure 1.11 – Facies Association Two lithofacies (see Table 1.1 for description), trace fossils (see Table 1.2 for description), sedimentary features, and generalized stratigraphic section. A) Interbedded claystone (F-Cl) and mudstone (F-M). B) Root Casts. C) *Teredolites* (TF- T). D) *Ophiomorpha* (TF-O) in vertical cross section. E) Shell Fragment. F) Sigmoidal stratified sandstone (F-SSS). G) Sigmoidal Stratified Sandstone (F-SSS). H) Trough Cross Stratified Sandstone (F-TCS).

Facies Association Two Field Photos

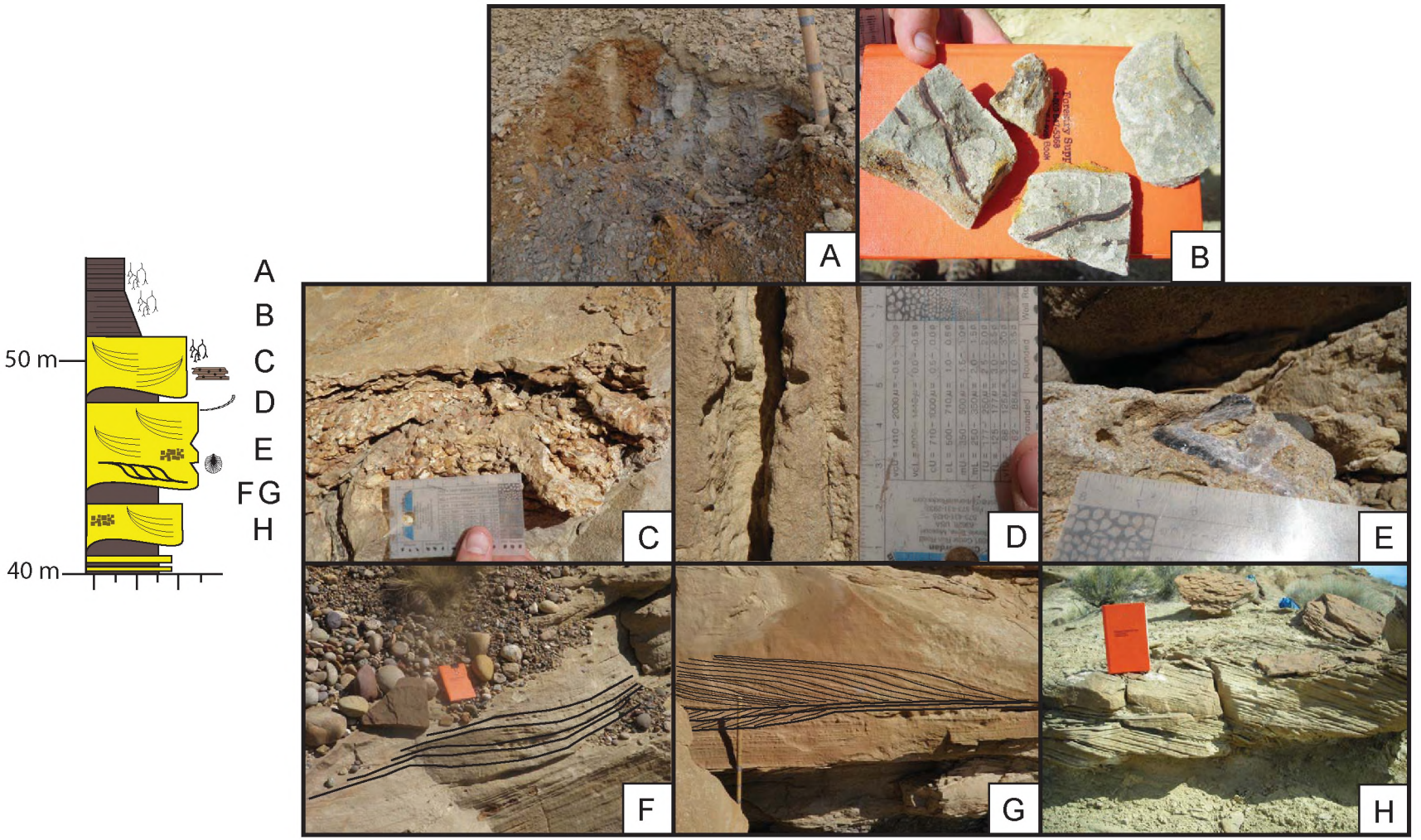

Figure 1.12 – Gigapan interpretation of Facies Association Two and generalized stratigraphic section. Blue lines mark flooding events and red lines mark sequence boundaries. Gigapan was collected from Blue Cove facing north.

Facies Association 2 - Outcrop Scale

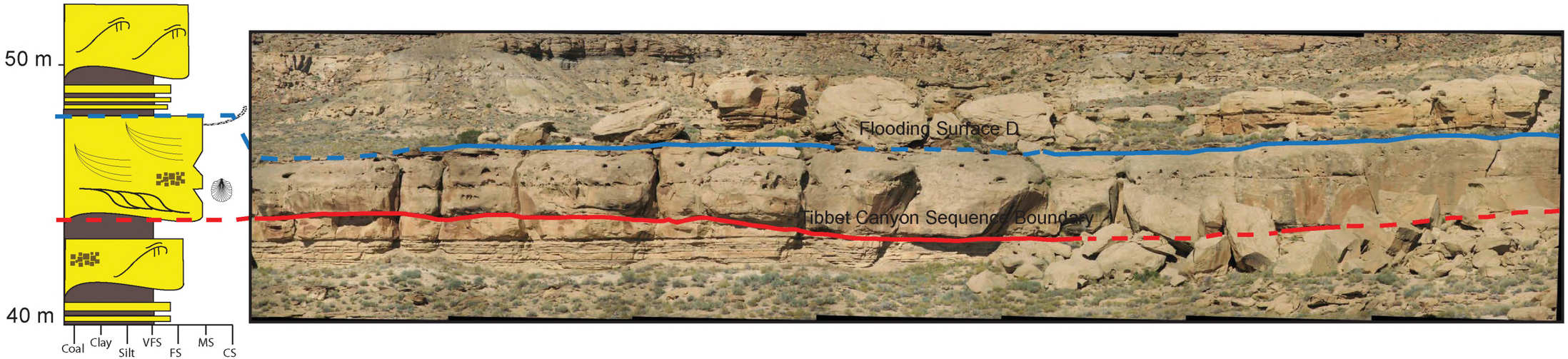

Figure 1.13 – Facies Association Three lithofacies (see Table 1.1 for description), trace fossils (see Table 1.2 for description), sedimentary features, and generalized stratigraphic section. A) Erosion along basal surface of the association. B) *Planolites* (TF-P) and *thalassinoides* (TF-Th). C) Inclined heterolithic strata (F-IHS) below channel incision. D) Highly organic heterolithic strata. E) Channelized inclined heterolithic strata. F) Inclined Heterolithic Strata (F-IHS). G) Alternating beds of wave rippled sandstone (F-WRS) and planar hetrolithic strata (F-PHS). H) Log containing *teredolites* (TF-T). I) Coal rip-up clast.

Facies Association Three (FA-3) Estuarine and Tidally Influenced Channels

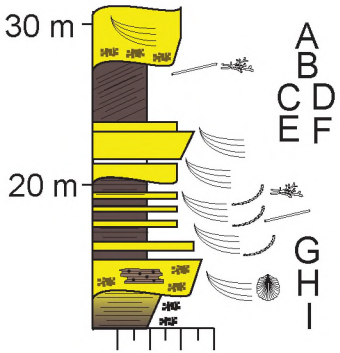

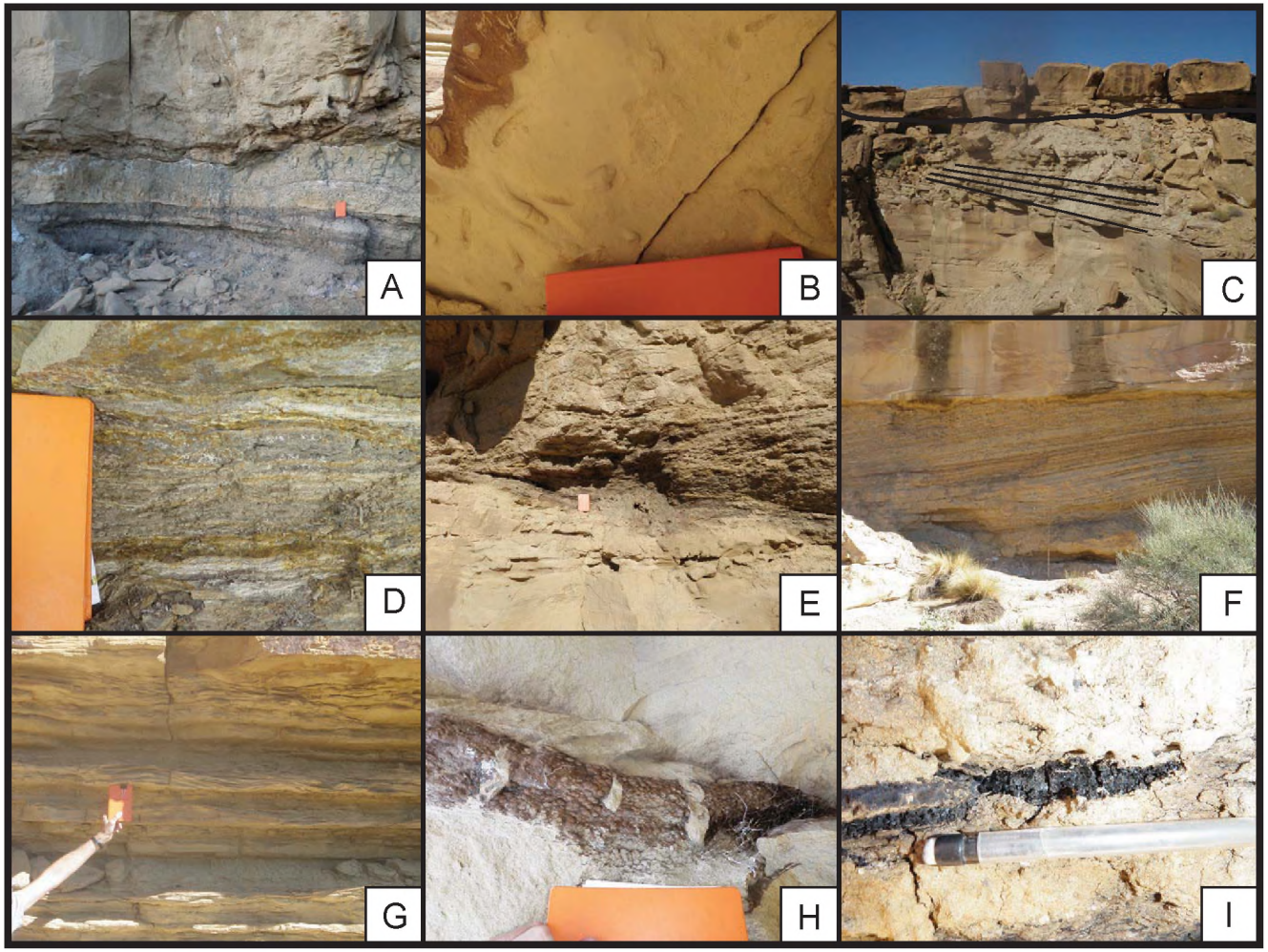

Figure 1.14 – Gigapan interpretation of Facies Association Three within Blue Cove with generalized stratigraphic section. Blue lines mark flooding events and red lines mark sequence boundaries. Gigapan was collected within Blue Cove facing east.

Facies Association 3 - Tidally Influence Channels/Estuaries

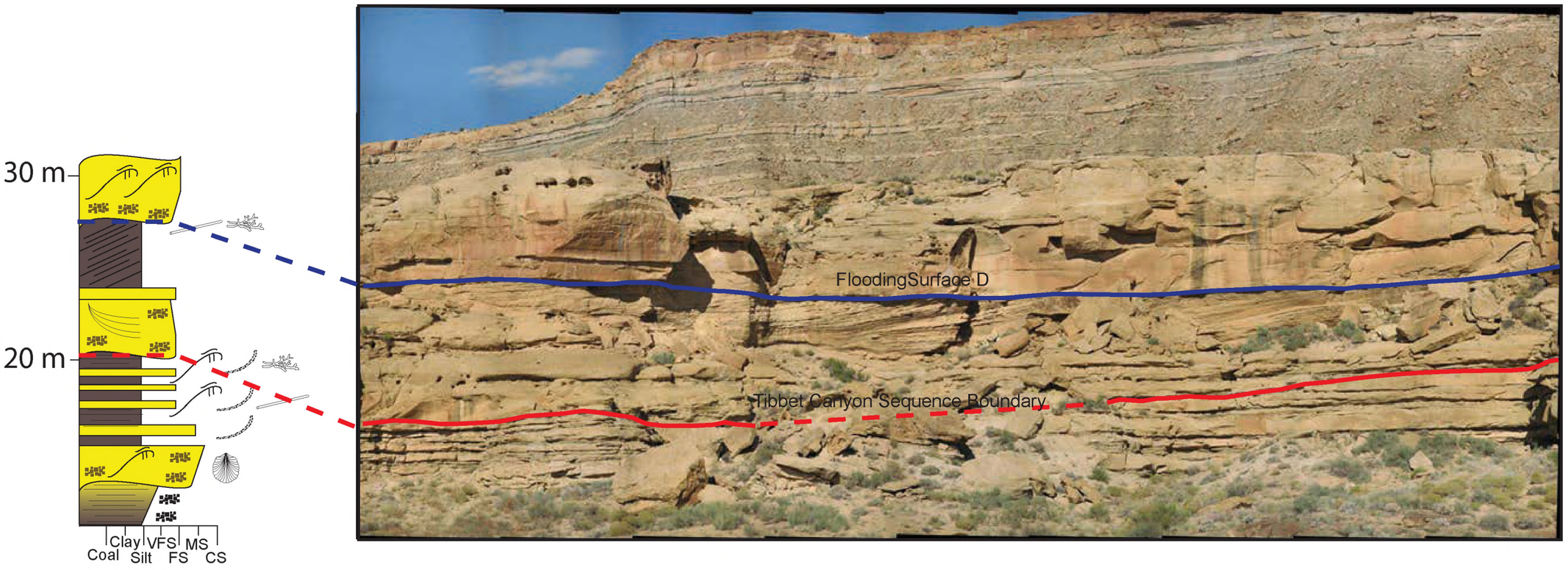

Figure 1.15 – Gigapan interpretation of Facies Association Three within Ty Hatch with generalized stratigraphic section. Blue lines mark flooding events and red lines mark sequence boundaries. Gigapan was collected within Ty Hatch facing north.

Facies Association 3 within Ty Hatch Canyon - Tidally Influence Channels and Estuaries

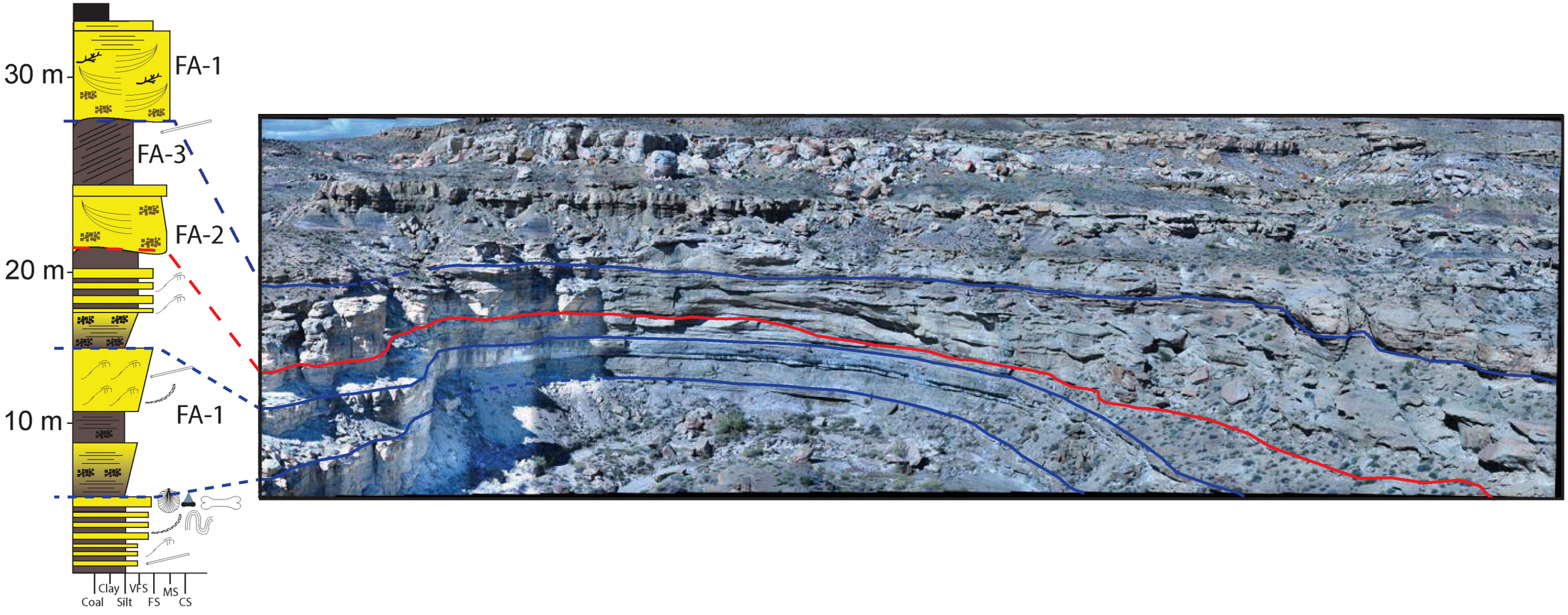

Figure 1.16 – Gigapan interpretation and overlay of Facies Association Three within Ty Hatch with generalized stratigraphic section. Blue lines mark flooding events and red lines mark sequence boundaries. Gigapan was collected within Ty Hatch facing northeast. The overlay denotes depositional environments of the deposits. Up to 20 m of erosional relief is observed on this surface.

Ty Hatch Facies Fluvial and Estuarine Facies

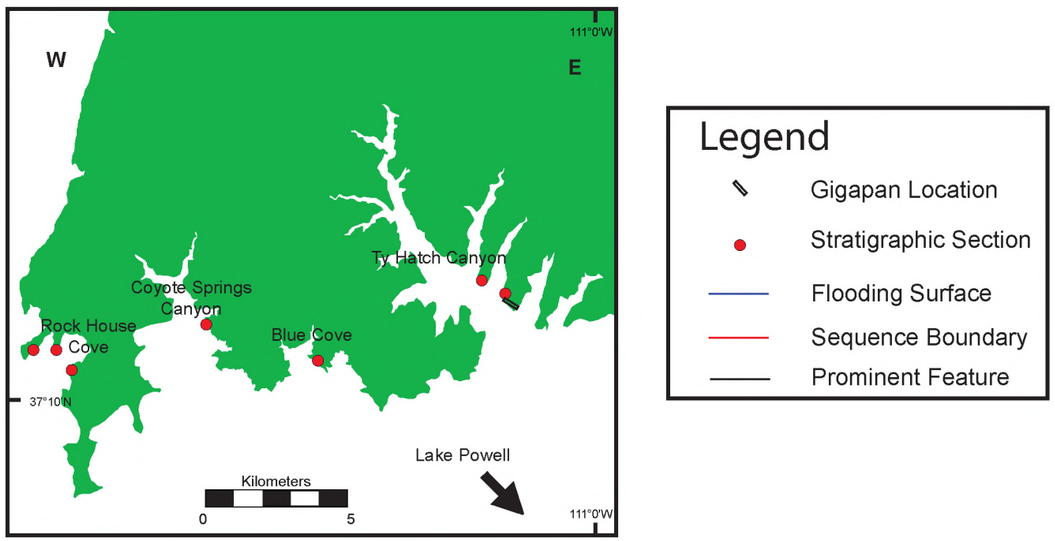

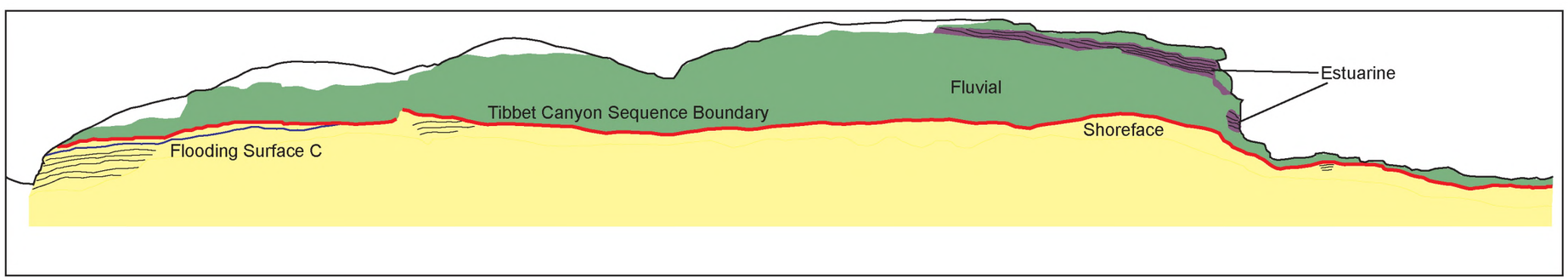

Figure 1.17 – Facies Association Four lithofacies (see Table 1.1 for description), trace fossils (see Table 1.2 for description), sedimentary features, and generalized stratigraphic section. A) Outcrop scale photo of the Calico bed being removed by the John Henry Member. B) Coarse grained sandstone of the Calico Bed. C) Fining upward trend common in the Calico bed. D) Mud rip-up clasts. E) Sub-bituminous coal seam. F) Fine grained interdistributary deposits. G) Trough cross stratified sandstone (F-TCS).

Facies Association 4 (FA-4) Calico bed, braided fluvial deposits

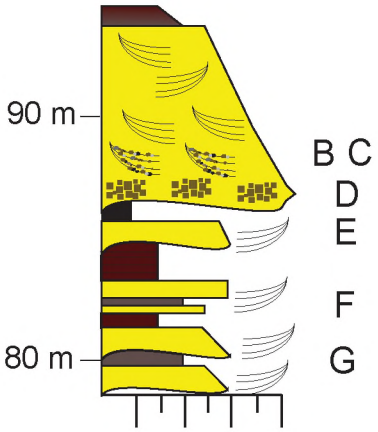

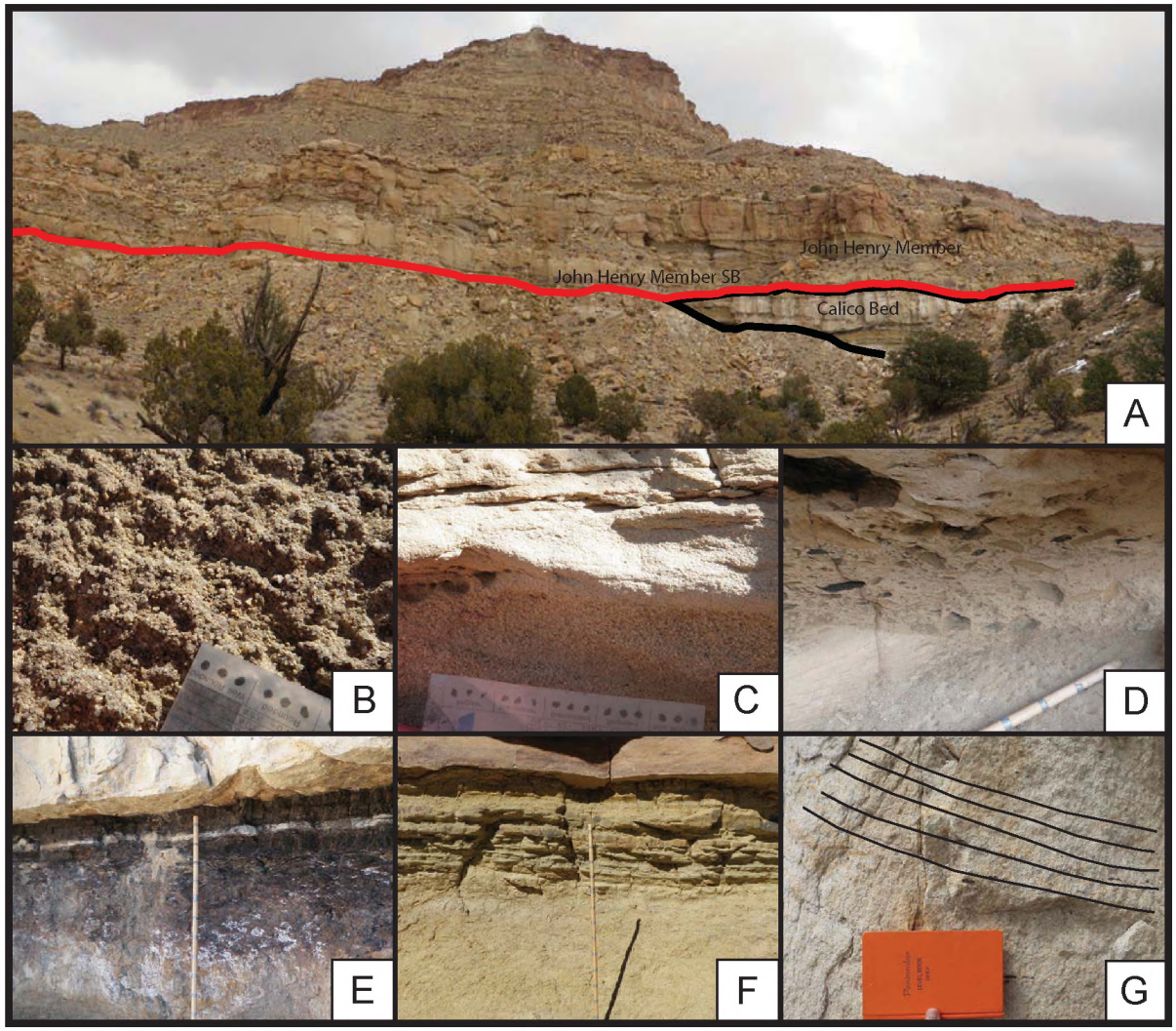

Figure 1.18 – Gigapan interpretation of Facies Association Four (Calico bed) with generalized stratigraphic section. Black lines represent a regional unconformity. Gigapan was taken within Ty Hatch facing North.

Facies Association 4, The Calico Bed

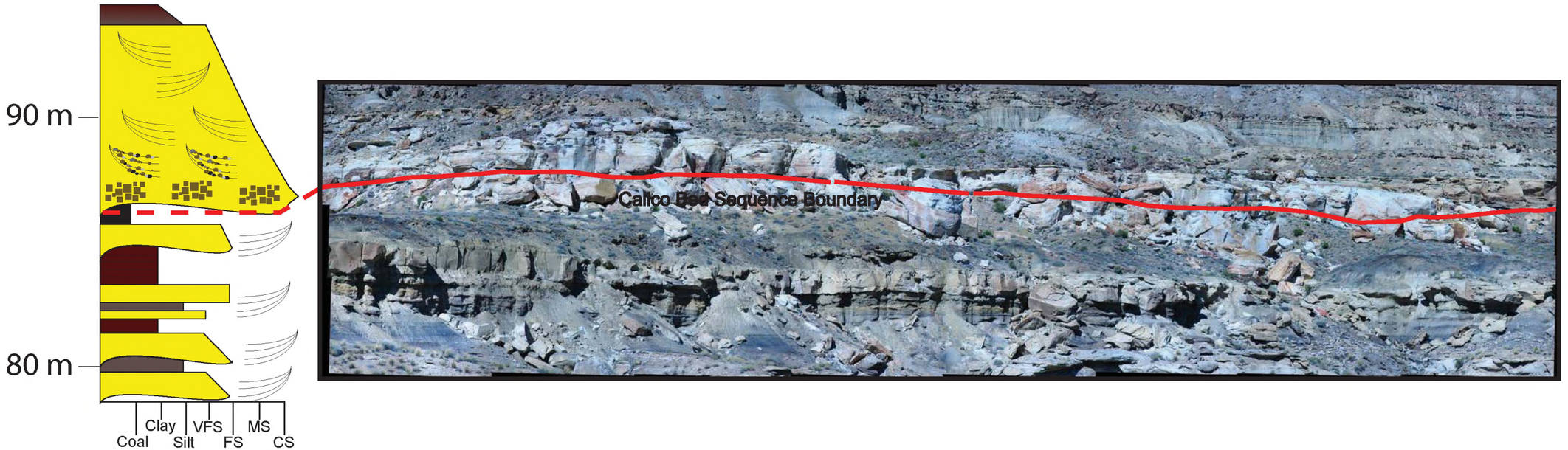

Figure 1.19 – Correlation of stratigraphic sections along transect A-A'. Four depositional units are outlined. Blue lines correlate to flooding surfaces. Red lines correlate to sequence boundaries. Vertical scale is 10 meters between tick marks.

Stratigraphic Sections with Depositional Units

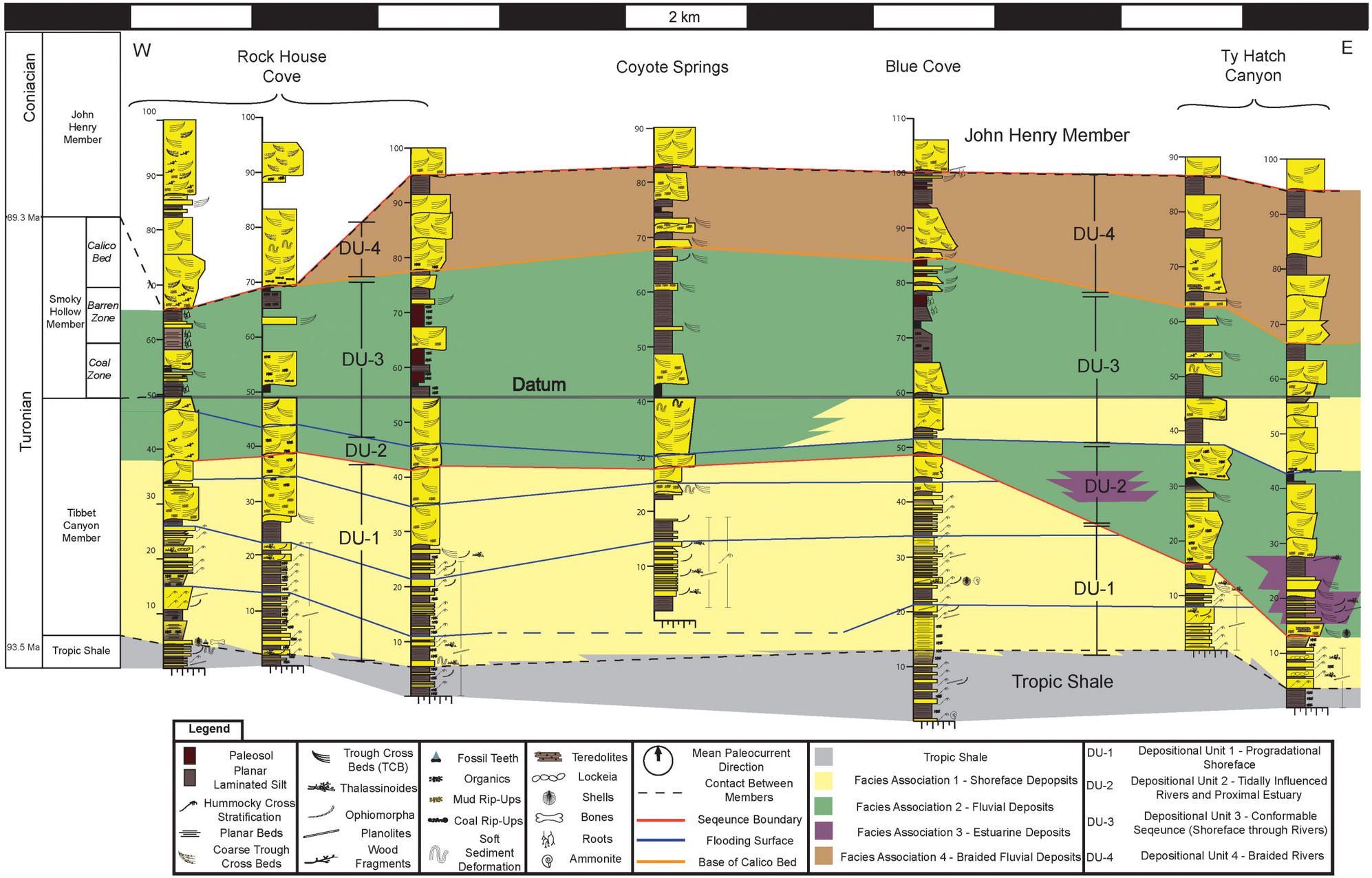

Figure 1.20 – Map view schematic of Depositional Unit One. Vertical panels represent the geology observed along the A-A' transect with measured sections overlaid.

Depostional Unit 1 - Prograding Shoreface

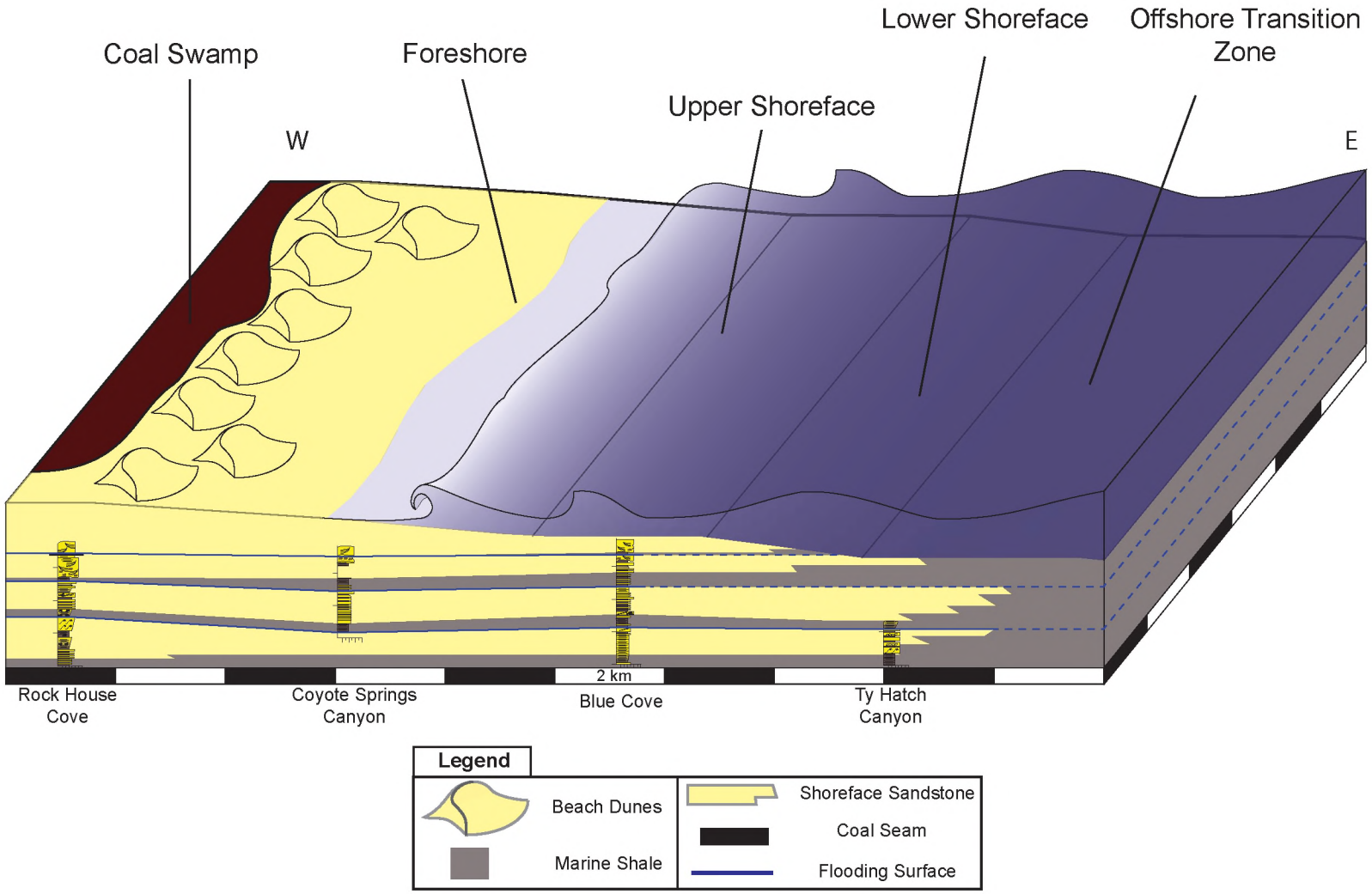

Figure 1.21 – Map view schematic of Depositional Unit Two. Vertical panels represent the geology observed along transect A-A' with measured sections overlaid.

Depositional Unit Two (DU-2) Tidally Influenced Rivers and Proximal Estuary

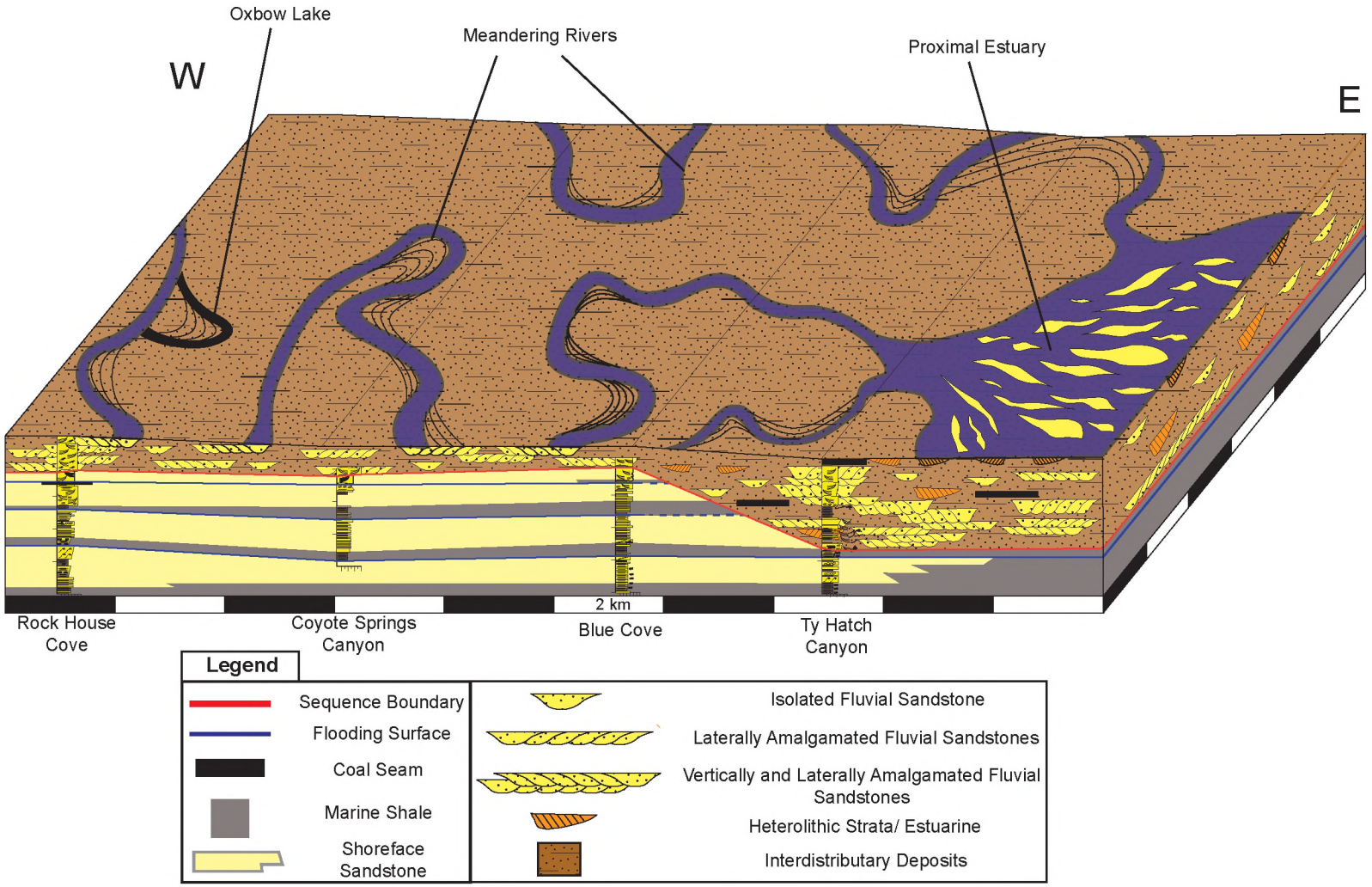

Figure 1.22 – Map view schematic of Depositional Unit Three. Vertical panels represent the geology observed along transect A-A' with measured sections overlaid.

Depositional Unit 3 (DU-3) Conformable Sequence (Shoreface through River)

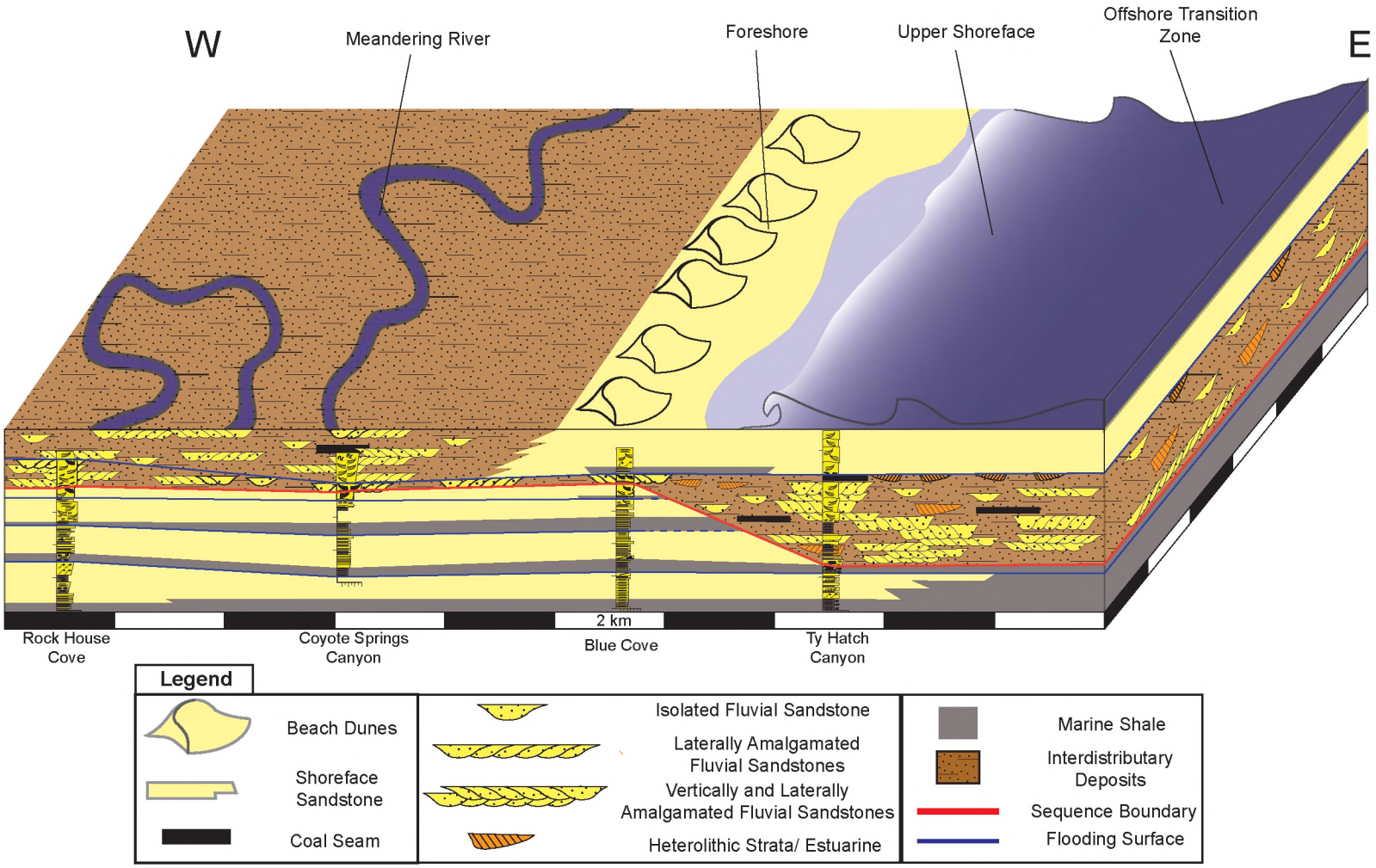

Figure 1.23 – Map view schematic of Depositional Unit Four. Vertical panels represent the geology observed along transect A-A' with measured sections overlaid.

Depostional Unit 4 (DU-4) Braided River

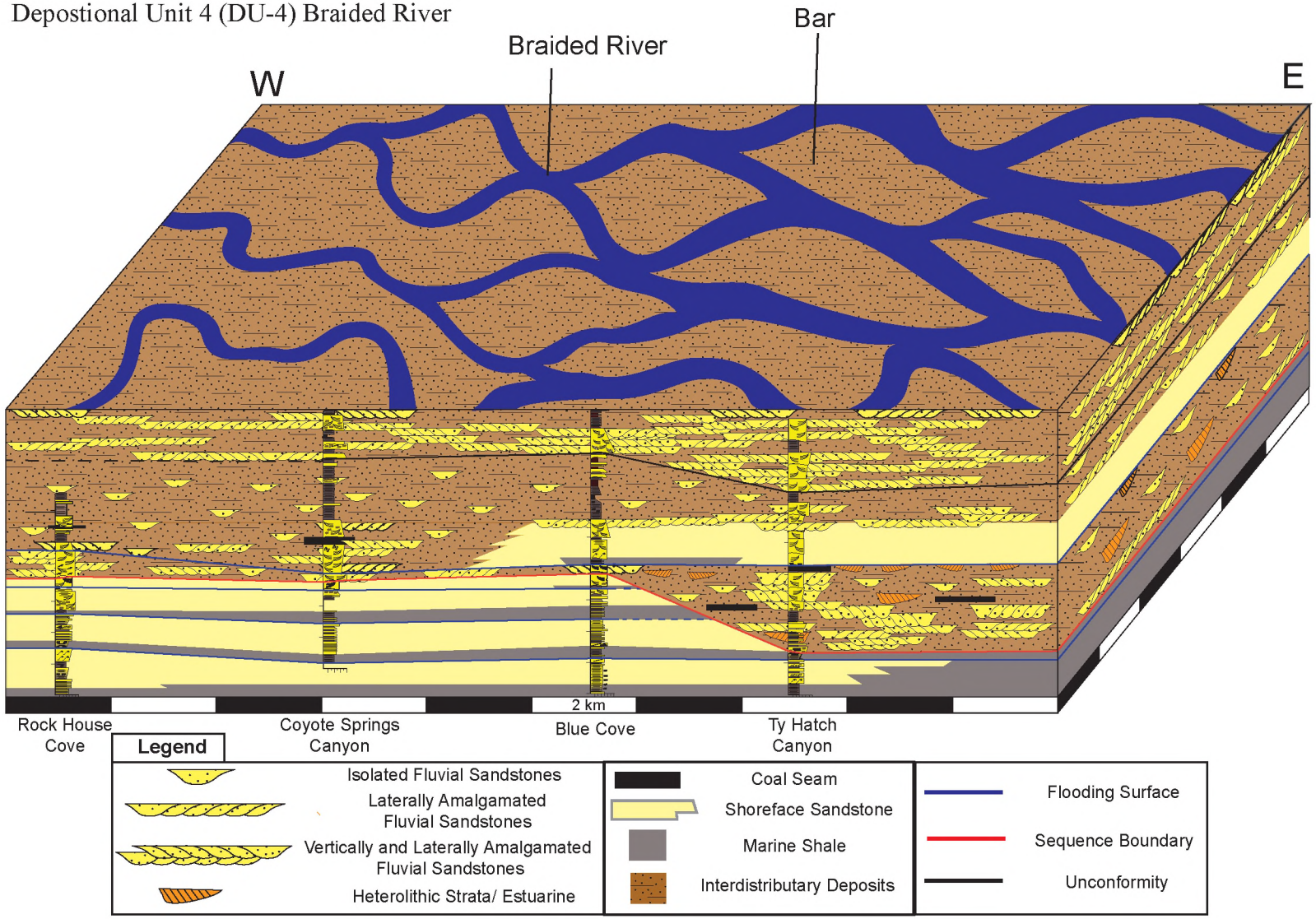

CHAPTER 2

THE EFFECTS OF SCALING CUES AND INTERACTIVITY ON A VIEWER'S ABILITY TO ESTIMATE THE SIZE OF FEATURES SHOWN ON OUTCROP IMAGERY

Abstract

Earth scientists often use images to communicate scientific concepts, and they commonly provide cues establishing the scale of features shown ("hammer for scale," etc.). How effective are these kinds of scaling cues? Do observers translate that information correctly? This study highlights the benefits of interactivity and the possible pitfalls of scaling cues when a viewer is asked to extract information from a 2D image. A visualization test was created in which participants were asked to estimate the size of several boxes shown in outcrop photos. All test subjects first viewed a static image, followed by an interactive (gigapan) image of the same outcrop; two different outcrops of different sizes were used. A control group was asked to estimate the size of features without any scaling information, whereas a second test group was given some general scaling cues, and then asked to perform the same tasks using the same images. Participants (test group n=63, further testing in progress) represent a range of experience

and education levels, including geology, other science, and nonscience majors, and also including undergraduates, graduate students, and faculty. Results show that scaling estimates are more difficult for larger/more distant outcrops. Scaling cues can also become a distractor for viewers of any experience level or background and become even more of factor with images containing significant distortion. It is important to realize that viewers internalize scaling cues differently, so different types of cues may help some viewers more than others. Also it appears that incorporating interactivity can increase accuracy, due to the ability to customize views that best fits an individual's learning style and internal sense of problem solving. The results of this study contain numerous educational implications for the application of scale and interactivity, the representation of information in visualizations, and the extraction of that information by viewers of diverse backgrounds.

Introduction

Spatial cognition and visualization are complex but essential components of earth science education and research. Geologic datasets reveal "deep time" by preserving records of Earth's evolution. Interpreting those records of Earth dynamics commonly requires, among many other skills, an understanding of the absolute and relative scale of geologic features. For example, the relative scales of different "architectural" elements preserved in sedimentary layers relate to the original processes of deposition (Sadler, 1981; Miall, 2000; Boggs, 2006). This study investigates how viewers estimate scale using outcrop imagery, specifically high resolution photopanoramas that cover large swaths (>10 m) of rock exposure.

In geoscience, spatial representations commonly convey complex three-dimensional (3D) data using a two-dimensional (2D) plane (e.g., maps, cross sections, seismic sections). But how accurately do viewers use this information and what processes are they using? To understand, produce, or manipulate any visual representation, individuals use a variety of spatial thinking skills. In the geosciences, these skills include recognizing patterns and shapes, recalling previously observed objects, understanding frames of reference, integrating separate observations into a single image, and mentally manipulating surfaces and perspectives (Ishikawa and Kastens, 2005), just to name a few. Two common problems geoscientists face when using spatial skills are: 1) the ability to generate a 3D mental image using only a minimal amount of observed 2D data (i.e., orientation of objects on a 2D plane); and 2) extrapolation of information from a photograph, specifically distance from the camera, scale, and relationship of objects across the photo (Kastens, 2010).

In images of geologic features such as those used in educational settings, the size of features is often depicted by a familiar object that represents scale (e.g., a person, notebook, or hammer). This is potentially problematic for several reasons, including how well and how quickly viewers can actually process and apply that information. Scale features have also been demonstrated as possible distracters based on eye-tracking studies (Coyan et al., 2010). Such distracters tend to impact novice-level viewers in particular, so there are important implications for education (Coyan et al., 2010).

Interactivity is another major focus of previous studies pertaining to understanding of 3D data. Geowalls are dual projection systems which display stereographic 3D datasets that can be viewed through polarized glasses (Kelly and Riggs,

2006). Geowalls allow viewers to interact with data by rotating and viewing 3D images from different perspectives, manipulating data "layers," etc. Other interactive visualization methods used to improve spatial thinking include shaded topographic displays and block diagrams that can be rotated and turned partially transparent to permit penetrative visualization of the block interior (Piburn et al., 2002; Reynolds et al., 2005). These investigations demonstrate that both the interactivity as well as the presence of 3D data is facilitating interpretation of the imagery. How does interactivity alone improve an individual's understanding?

This study focuses on scaling estimates based on 2D photopanoramas of outcrops, and the potential impact of interactive visualizations on scaling estimates. Interpreting these representations requires knowledge of the perspective and scale. How well do individuals from different backgrounds or skill levels apply their knowledge to these types of images, and what can instructors do to facilitate this transition? Interactive images enable the viewer to focus on the data shown in the image at different scales and from different perspectives. In theory, this interactivity might allow the viewer to continuously customize their perspective of the image to best fit their thought process, perhaps based on their background and spatial capabilities (e.g., comparison of nearby objects that are more familiar).

Many geoscience visualizations represent real-world objects such as rock outcrops, topography, sedimentary layers, etc. Previous connections with real-world objects can produce a training effect called representational correspondence (Ishikawa and Kastens, 2005), which means that previous experience can influence, correctly or not, an individual's understanding of a given visualization. Examples of representational

correspondence include familiarity with the size of common objects such as trees, animals, or people as well as more specific contextual understandings from a given individual's background. In sedimentary geology imagery, these examples may also include geologic features such as erosional surfaces, weathering patterns, as well as observations from a similar depositional environment (e.g., channel depths, shoreface thicknesses, and individual layer thicknesses). Thus, prior experience affects the interpretation of visualizations, as does the display itself.

Distortion in photos can also create confusing misrepresentations. There are two main types of perspective distortion common in geologic images: 1) extension distortion (resulting in a forelengthening effect) and 2) compression distortion (resulting in a foreshortening effect) (Pratt, 1978). Extension distortion (or wide-angle distortion) occurs when a wide angle photograph is taken of a subject close to the camera. This distortion will make objects closer to the camera appear larger in size relative to objects that are farther away (forelengthening). Conversely, compression distortion (telephoto distortion) occurs when a photograph is taken of objects far away from the camera most commonly with panoramic photos. Objects distant from the camera appear large relative to those that are closer (foreshortening). This effect greatly reduces the viewer's ability to judge distance and size. This study uses two panoramas, one with extension distortion and the other with compression distortion, to evaluate relative changes in scaling estimates.

Methods

Photopanoramas

For this study, two high resolution photopanoramas were taken from two canyons, Nelson Canyon (NC) and Stone House Canyon (SHC), in Range Creek Canyon in central Utah (Figure 2.1). This area was chosen because the features within Range Creek Canyon are very typical of many sedimentary geologic formations found in Utah. Both the Flagstaff and Colton Formations (Paleocene-Eocene), featured in the panoramas, are widespread units across much of central Utah and also have many familiar outcrop characteristics to other nonmarine units in the region. The panoramas were produced with a tripod-mounted robot which takes individual photos in vertical columns that are then stitched together to produce a single high resolution image (DeepLocal, 2008). Both panoramas were taken with the camera fully zoomed (12x). The Nelson Canyon (NC) panorama was taken close to the outcrop (30 m away), producing extension distortion, while the Stone House Canyon (SHC) panorama was taken from far away (~1,000 m away), producing compression distortion. The size of features used in the test estimates was checked in the field where possible.

Exercise

The workflow for the test exercise is summarized in Figure 2.2 and presented in Appendix 2.1. Before the exercise began, participants (n=63) were asked basic demographic questions, such as age, gender, degree sought/obtained etc. (see sample survey, Appendix 2.1). This form was turned in before the exercise began. Participants

were also given a short purpose and background for the exercise as well as the location of the images (Appendix 2.1).

The test was conducted using a computer screen or laptop, with screen sizes ranging from 16 to 18 inches diagonally. Data were collected over 6 months between March and August 2010. All test subjects (n=63) first viewed static images, followed by interactive (Gigapan) images; two different outcrops of two different sizes were used. A control group was asked to estimate the size of features without any scaling information (we refer to this as the "NS" or no-scale group, n= 27, 47% of the test population), whereas a test group was given some general scaling cues (the "S" group or scale group, n= 30, 52% of the test population), and then asked to perform the same tasks using the same images. For the NC panorama, the distance to the base of the cliff as well as the height of the cliffs at the highest point in the center were given in both feet and meters. For the Stone House Canyon panorama, the distance and height of the furthest cliff as well as the cliff on the right side of the panorama were given in both feet and meters (Figure 2.2).

Both groups performed the same tasks, the only difference was whether they were given scaling cues or not. For part one of the exercise, static images of each panorama were displayed on a computer and participants were instructed to estimate the height of the three boxes for each (NC1, SHC1; Figure 2.2) using either feet or meters (their choice). Participants were given a time limit of 90 seconds to complete the estimates for each panorama, although most did not need that much time. Each participant was then asked to describe the process they used to estimate the size of the boxes as well as how

close they thought their answer was from the true value. This form was turned in before the next portion of the exercise began.

For part two of the exercise, the participants were given the same images in an interactive format with the ability to zoom and pan. After learning the controls, viewers were asked to estimate the height of three different boxes on each panorama with the same 90-second time limit. Once again, they were asked to describe the process they used to estimate the heights as well as how close they thought they were to the true value.

Results

Dataset

All of the information from the exercise was placed into an Excel spreadsheet to statistically evaluate results as well as to identify patterns (Table 1.1). All estimates are presented in meters, converted from feet if necessary. Any participant who reported at least one estimate exceeding two times the standard deviation was identified as an outlier and removed from the rest of the calculations; six participants were removed in this manner so these are not included in the following statistical analysis. Participants given scaling cues were separated from those without any cues (i.e., S versus NS groups) to determine the effect scale has on their ability to estimate correctly. Participants were also asked to provide an estimate of how close they thought they were to the correct answer (i.e., a "confidence" factor) and also to describe their estimation process. Many participants provided answers in feet or meters and some provided a percentage of their estimate. To normalize these values, all error estimates were converted to percent, which compared their accuracy prediction to the magnitude of their estimate (Table 2.1). In

addition to comparing part one versus two (to investigate effects of static versus interactive images), the data were sorted to investigate various population differences. The following sections focus on the most clear population differences: those between the scale and no scale groups, differences between participants in geoscience versus "other" disciplines, and differences based on experience level.

Participants

The test subjects (n=57 after outliers were removed) were asked to provide background information prior to the beginning of the test (Appendix 2.2). The average age of the group is 27, and 68% are male. Both graduate and undergraduate students as well as a few faculty were included in the test group. Almost half (48%) are undergraduate students (BS, BA), 35% are masters candidates (MS), 14% are doctoral candidates (PhD), and 3% are faculty (PhD). Participants were allowed to answer in either feet or meters (Figure 2.3). More than half (58%) answered in feet, 36% answered in meters, whereas 6% used a combination of both (Figure 2.3). All estimates were converted to meters before being evaluated. There does not appear to be a clear population-based predictor of what measurement system was used.

Scaling Cues Group vs. No Scaling Cues Group: Estimates

With only one exception (NC-1 left box), the scaling cues group (S group) estimated consistently higher than the no scaling cues group (NS group) (Figure 2.4; Table 2.1). The S group exhibited a greater standard deviation in 7 of the 12 boxes than the NS group (Figure 2.4). Both of these groups consistently estimated higher values,

with greater standard deviations, in the Stone House Canyon panorama (the compression distorted panorama) than in Nelson Canyon (the extension distorted panorama). This result is expected because the Stone House Canyon panorama covers a much larger area and estimating the size of an object that is further away is naturally harder to do (Stroebel and Zakia, 1993). Additionally the NS group increased their estimates for Nelson Canyon by 28% for part two (the interactive portion of the test), but decreased their answers by 6% for Stone House Canyon (Figure 2.4). The S group increased their estimates by 10% for Nelson Canyon from part one to two of the test, but also decreased their answers by 30% for Stone House Canyon (Figure 2.4).

Scaling Cues Group vs. No Scaling Cues Group: Difference from Correct

When comparing the difference of estimates from the correct answer, the S group overestimated for 10 of the 12 boxes while the NS group underestimated for a different set of 10 of the 12 boxes (Figure 2.5). The NS group showed greater accuracy than the S group in 7 of the 12 boxes. On the Nelson Canyon panorama, the NS group saw a decrease in accuracy for all three boxes from part one to part two, with the largest decrease being 50% of the correct answer on the left box (Figure 2.6). Conversely, the S group saw an increase in accuracy for all three boxes in Nelson Canyon from part one to part two, with the largest increase being 42% on the right box (Figure 2.6). On the Stone House Canyon panorama, the NS group saw an increase in accuracy for both the left and center boxes (up to 26% increase) and a decrease for the left box (~25%) (Figure 2.6). The S group saw a slight increase in accuracy for the left box (~2%) and a large increase

for the right box (~35%), but a small decrease in accuracy for the center box (~15%) (Figure 2.6). Thus, although the NS group was generally more accurate, the scaling group saw a greater overall increase in accuracy from part one to part two: from 45% to 31% as compared to 13% to 21% for the NS group.

Scaling Cues Group vs. No Scaling Cues Group: Confidence Factors

After each part of the exercise, participants were asked to estimate how close they thought they were to the correct answer (they typically answered in meters or feet). These self-reported "error" estimates (i.e., confidence factors) were converted to percent relative to the size estimate for each box (Figure 2.7; Table 2.1). Both the S and NS groups thought they were closer to correct, relative to their average estimates, in Stone House Canyon (SHC) than in Nelson Canyon (NC) (Figure 2.7). The NS group estimates of self-predicted normalized error decreased from part one to part two of the exercise, from 81% to 44% for Nelson Canyon and 27% to 22% for Stone House Canyon (Figure 2.7). In contrast, the S group estimates of error increased (i.e., became slightly less confident) from part one to part two, from 62% to 72% for Nelson Canyon and 22% to 25% for Stone House Canyon (Figure 2.7). In part one of the exercise (static images), the NS group estimated they were less correct than the S group by 20% for the NC panorama and 4% for the SHC panorama (for calculations see Appendix 2.2). This pattern reversed during part two (interactive images) with the NS group estimating they were more accurate than the S group by 28% for the NC panorama and 4% for the SHC panorama. Participants all reported similar "methods" for estimating scale, mainly using trees and other objects as comparisons (see Appendix B.2).

Geoscience vs. Other Discipline: Estimates

Participants were also sorted by focus of study: geoscience discipline (Geology and Geophysics) and "other" discipline (all others, see Figure 2.3). The geoscience group is approximately equally represented in both the S and NS groups, while the other group is slightly more represented by the S group (~65%). With the exception of only one box (SHC-1 Center), the "other" group had consistently higher standard deviations than the geoscience group (Figure 2.8). The "other" group also consistently estimated higher for every box (Figure 2.8). Both the geoscience and "other" groups consistently estimated higher values, with greater standard deviations, in the Stone House Canyon Panorama (the compression distorted panorama) than in Nelson Canyon (the extension distorted panorama). Both groups saw a decrease in estimates and standard deviations for all boxes from part one (static images) to part two (interactive images), except for the geoscience group on the SHC left box (Figure 2.8).

Geoscience vs. Other Discipline: Difference from Correct

When comparing the difference of estimates from the correct answer, the geoscience group overestimated in 6 of the 12 boxes while the "other" group overestimated in 11 of the 12 boxes (Figure 2.9). Overall, the geoscience group averaged closer to correct by 20%, based on comparing both parts one and two, and both canyons. For the Nelson Canyon panorama, the geoscience group decreased their accuracy for all three boxes with the largest change (~35%) on the left box. In contrast, the "other" group increased their accuracy from part one to two for all three boxes with the largest change (~55%) on the center box (Figure 2.10). For the Stone House Canyon panorama, the

geoscience group increased accuracy for the left (~42%) and center box (~30%) and slightly decreased accuracy for the right box (~1%), while the "other" group slightly decreased accuracy for the left (~5%) and center (~2%) boxes and greatly increased their accuracy on the right box (~110%) (Figure 2.10). Thus, although the geoscience group was more accurate, the "other" group saw a greater overall increase in accuracy from part one to part two.

Geoscience vs. Other Discipline: Confidence

Overall, the "other" group reported higher confidence by about 56% than the geoscience group. For both parts of the exercise, both groups (geoscience and "other") felt more confident in their answers for the Stone House Canyon panorama (Figure 2.11) than Nelson Canyon. In part one (static images) of the exercise, the "other" group reported higher confidence than the geoscience group by 55% for the Nelson Canyon (NC) panorama and 8% for the Stone House Canyon (SHC) panorama. In part two (interactive images) of the exercise, the "other" group felt more confident by 30% for the NC panorama and 6% for the SHC panorama (Figure 2.11). Additionally, the geoscience group saw an increase in confidence from part one to part two by 80% for the NC panorama, and 3% for the SHC panorama (Figure 2.11). The "other" group saw similar trends from part one to part two with an increase in confidence by 15% for the NC panorama and a 4% increase for the SHC panorama.

Undergraduate vs. Graduate Experience Level: Estimates

Finally, the test population was sorted by experience level. Forty-four percent of the undergraduate experience level was represented by the NS group while 50% of the graduate and faculty group was the NS group. However, the graduate and faculty group was heavily represented by geoscientists (~75%). When plotted against experience level (undergraduate vs. graduate and faculty) the undergraduate participants produced higher average estimates and standard deviations in 8 of the 12 boxes (Figure 2.12). Both groups exhibited higher average estimates and standard deviations in Stone House Canyon (SHC) than in Nelson Canyon (NC) (Figure 2.12). The undergraduate group saw a decrease in both their estimates and standard deviations for every box from part one to part two while the graduate group saw a decrease in 9 of the 12 boxes, no change in 2 of the boxes (SHC Left and Center), and an increase in 1 of the boxes (NC Left)(Figure 2.12).

Undergraduate vs. Graduate Experience Level: Difference from Correct

When comparing the difference of estimates from the correct answer, the undergraduate group overestimated in 9 of the 12 boxes while the graduate group overestimated on only 2 of the boxes (Figure 2.13). Overall, the graduate group averaged closer to correct by ~5%, based on comparing both parts one and two, and both canyons. In the Nelson Canyon panorama (NC), both groups increased their accuracy, from part one to part two, on the center box only (Figure 2.14) although the undergraduate group saw a 20% larger change than the graduate group. In the Stone House Canyon panorama (SHC) the undergraduate group increased their accuracy on two boxes with the largest

change (~8%) on the on the right box (Figure 2.14). In the same panorama, the graduate group saw an increase in accuracy on two different boxes with the largest change (~33%) on the left box (Figure 2.14). The graduate group was more accurate and saw a greater overall increase in accuracy from part one to part two: from 18% to 16% as compared to 21% to 20% for the geoscience group.

Undergraduate vs. Graduate Experience Level: Confidence

Overall, the graduate group reported higher confidence by only 5% than the undergraduate group. For both parts of the exercise, both groups (undergraduate and graduate) felt more confident in their answers for the Stone House Canyon panorama (Figure 2.15) than Nelson Canyon. In part one (static images) of the exercise, the undergradute group reported higher confidence than the graduate group by 14% for the Nelson Canyon (NC) panorama. Both groups had equal confidence for the Stone House Canyon (SHC) panorama. In part two (interactive images) of the exercise, the graduate group felt more confident by 14% for the NC panorama and 6% for the SHC panorama (Figure 2.15). Additionally, the undergraduate group saw a decrease in confidence from part one to part two by 6% for the NC panorama, and 3% for the SHC panorama (Figure 2.11). The graduate group saw opposite trends with an increase in confidence by 24% for the NC panorama and a 4% increase for the SHC panorama.

Discussion

Key results are summarized in Table 2.1 and Table 2.2. The following discussion focuses on the impact of scaling cues and interactivity on scaling estimates, accuracy, and confidence among the different groups.

Scaling Cues

The use of scaling cues to aid in size estimates produced mixed results. Somewhat surprisingly, the NS group produced more accurate results by 50% on average than the S group. This may reflect confusion over the type of scaling information that was given (height and distance of cliffs). Scale bars were not used in this exercise in order to test subjects' estimates without a potential "distractor" (c.f., Coyan et al., 2010). Virtually all participants reported using trees and other objects to help with their estimates, so in the case of the NS group (which in general reported more accurate estimates), this approach seems to be effective. In contrast, the S group may have relied too heavily on the scale information they were given, which suggests that such scaling cues are actually less effective than no information.

The fact that the NS group consistently had smaller estimates (Figure 2.5) and underestimated the correct size of the box (Figure 2.6) suggests that viewers will naturally estimate conservatively given no sense of scale. Conversely, it appears that when given scale, the viewer will have a false sense of accuracy tending towards larger overall estimations. This observation is supported by confidence estimates. The S group was more confident overall compared to the NS group but was actually less accurate. The NS group felt as though they were not accurate at all as seen by the Nelson Canyon left

box which exhibits 83% error normalized to their answer (Figure 2.7). This further illustrates the possibility that scaling cues can become distracting and confusing when extracting information from a photograph as well as make the viewer overconfident.

Another trend seen in every group comparison was larger estimates and standard deviations for the Stone House Canyon panorama than the Nelson Canyon panorama. This is expected because it is more difficult to estimate the size of an object that is further away (Stroebel and Zakia, 1993). There is also a greater room for error because the boxes themselves are larger. The variable answers given, specifically for the center box in Stone House Canyon (the furthest box away), produced a greater standard deviation.

Experience

Personal experience and familiarity with the geoscience appears to play a role in scale estimates. Nongeoscientists ("other" group) were less accurate in the majority of boxes (10 of 12) than geoscientists (Figure 2.13). The nongeoscientists overestimated in 11 of the 12 boxes while the geoscientists overestimated in only 6 of the 12 boxes (Figure 2.13). This suggests that viewers with less geoscience experience tend to overestimate while those with more geoscience experience tend to be more conservative with their estimates. Geoscientists may have a better understanding of the size of naturally occuring scale indicators (i.e., trees and geologic features), and/or may be able to apply those scales more correctly. Many viewers reported that they used trees as a scaling indicator for both panoramas. However, although the geoscience group was more accurate, they were less confident (Figure 2.11); perhaps experience level also brings some awareness of how difficult it is to estimate scale.

These trends can also be seen when comparing experience level, i.e., undergraduate (currently seeking B.S. and B.A. degrees) versus the graduate students and faculty (M.S. and Ph.D.), although it should be noted that the graduate group was also 75% geoscientists. The undergraduate participants were less accurate in 8 of the 12 boxes compared to the graduate students (Figure 2.13). Additionally, the undergraduate participants overestimated in 9 of the 12 boxes while the graduate students overestimated in only 2 of the 12 boxes (Figure 2.13). The graduate group was also more confident for both panoramas in both parts one and two. Again, this highlights the trend that less experience (in this case, fewer years in geoscience degree programs) causes participants to overestimate and be less accurate as well as less confident.

Interactivity

The impact of interactivity (i.e., part one versus part two answers) appears to show mixed results but overall, the data imply that interactivity improves scale estimates. It should be noted that the improved estimates in part two may also partially reflect a training effect due to second exposure to the same images. However, different boxes were used in part two to reduce this possible effect, and there were enough population-based differences that the interactivity seems to play a greater role than the second exposure.

Accuracy increased on 2 of the 6 boxes for the NS group and 5 of the 6 boxes for the S group (Figure 2.6). The S group seemed to benefit more from interactivity than the NS group, and both groups improved more consistently in the more distant Stone House Canyon panorama than in Nelson Canyon. Similar trends are evident based on experience type and level (e.g., geoscience vs. "other" (Figure 2.9) and undergraduate versus

graduate level (Figure 2.13)). Overall accuracy among these groups tends to increase from part one to part two (with some exceptions), and in general, the effect is more dramatic for the Stone House Canyon panorama than Nelson Canyon. There is also a possible correlation with experience type and level, where participants with more experience in geoscience appear to benefit more from the interactivity.

Conclusions

This study suggests that scaling cues of the type we provided do not necessarily result in more accurate scale estimates. Interactivity, such as zooming in and out of a panorama, does seem to improve estimates, particularly for a more distant and larger panorama. It also appears that experience type and level impact scaling estimates, with more experience, particularly in geoscience resulting in slightly more accurate estimates. Self-reported confidence estimates do not necessarily reflect accuracy.

Figure 2.1 - Hillshade map of Range Creek Canyon, central Utah. The DEM for this hillshade was generated using 10 m NED maps for the Utah GIS portal (ARGC, 2011).

Range Creek Location Map

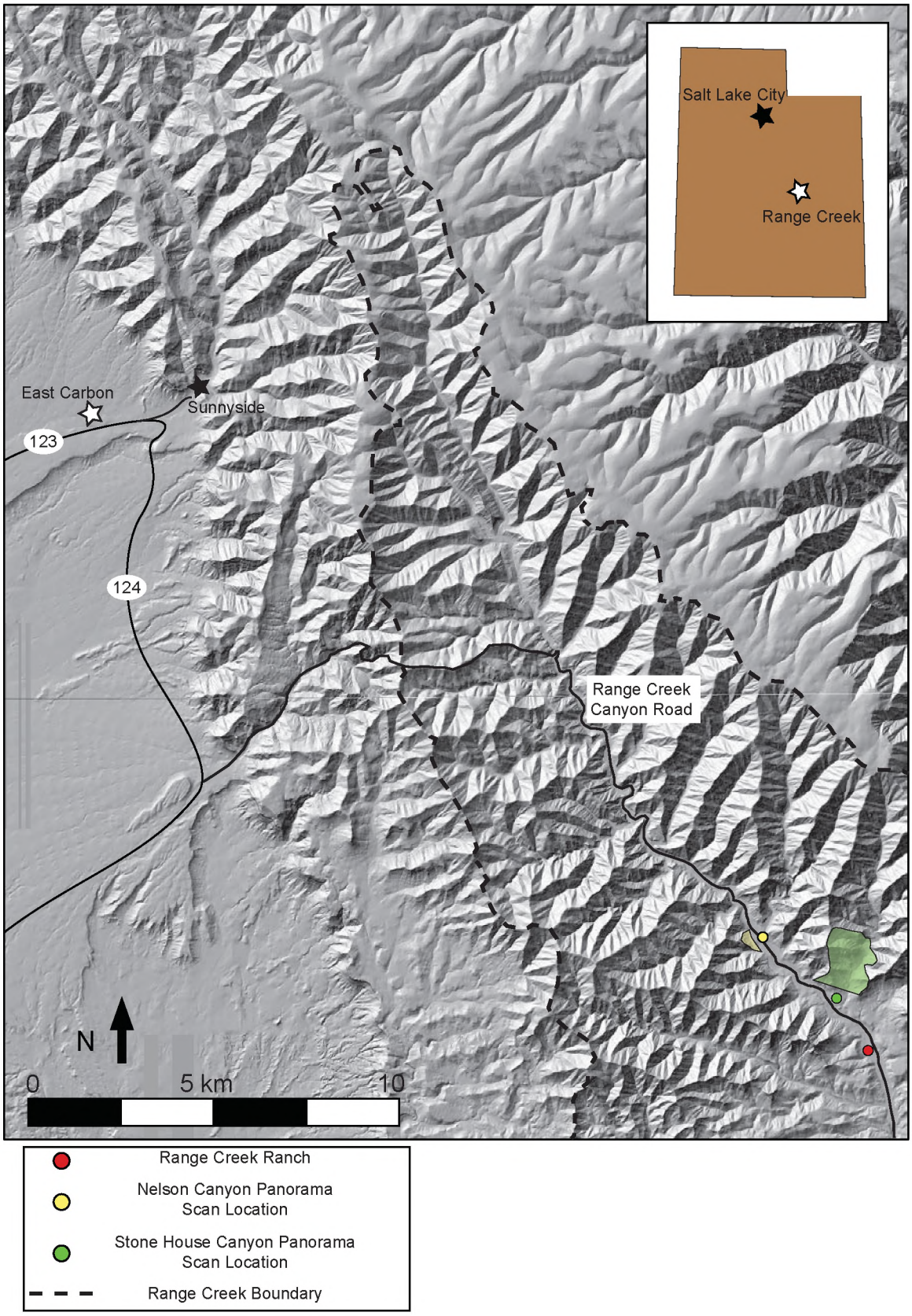

Figure 2.2 – Flow chart of the exercise. A) Nelson Canyon static photopanorama used for part one of the exercise. B) Stone House Canyon static photopanorama used for part one of the exercise. C) Nelson Canyon interactive photopanorama used in part two of the exercise with close up images of each box. D) Stone House Canyon interactive panorama used in part two of the exercise with close up images of each box. Under each of the panoramas are the correct answers determined for every box. In Nelson Canyon, the scaling cues that were given are the height from the base of the cliffs to the top of the boulder (~90 m) in the center of the panorama as well as the distance from the camera (30 m) to the base of the cliff. In Stone House Canyon, two sets of scaling cues were given: 1) The height of the distant cliffs in the center (~3600 m) and their approximate distance to the camera (~950 m)(yellow dot); and 2) The height of the cliffs on the right (~400 m) and their approximate distance from the camera (~1000 m) (green dot).

Experiment Flow Chart

Part I Static Images

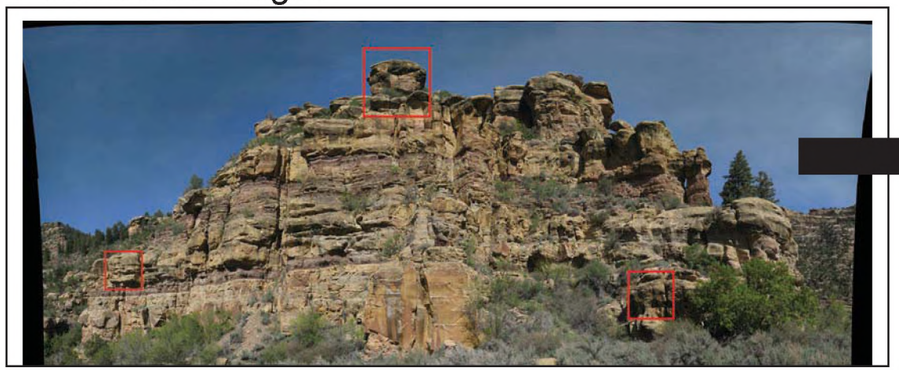

A Correct Dimensions: Left: 5.5 m, Center: 8.0 m, Right: 4.5 m

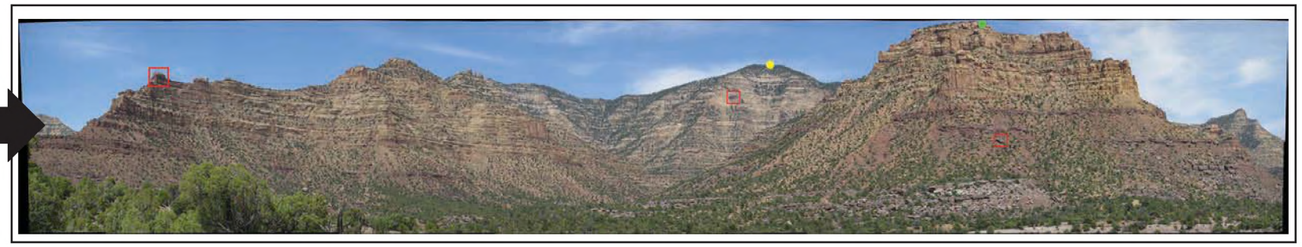

B Correct Dimensions: Left: 35 m, Center: 60 m, Right: 20 m

Part One: Estimate the size of red boxes shown on these static images. Group B is given scaling cues, i.e., distance to and height of green and yellow circles shown above. Group NS is not provided scale information.

Part II Interactive Images

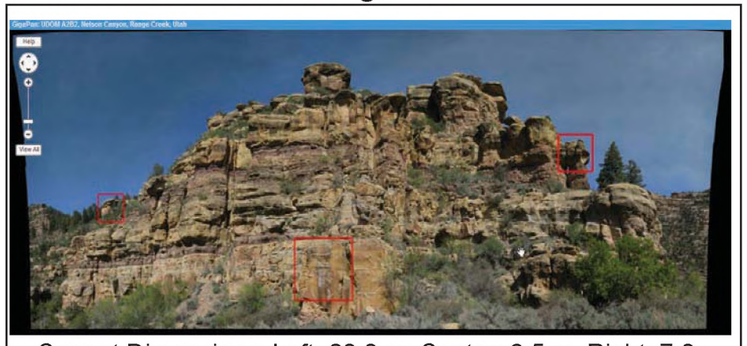

Correct Dimensions: Left: 20.0 m, Center: 6.5 m, Right: 7.0

C

Correct Dimensions: Left: 25 m, Center: 35 m, Right: 25 m

D Part Two: New estimates obtained using interactive Gigapan images of the same outcrops. Participants could zoom in and out and pan across the images. Different boxes were used.

Figure 2.3 – Pie charts of demographic information. For education level, demographic participants seeking either a B.A. or B.S. degree were placed into the undergraduate level while those seeking a M.S. or Ph.D. as well as faculty (post-Ph.D.) were grouped into the graduate level.

Demographic Information

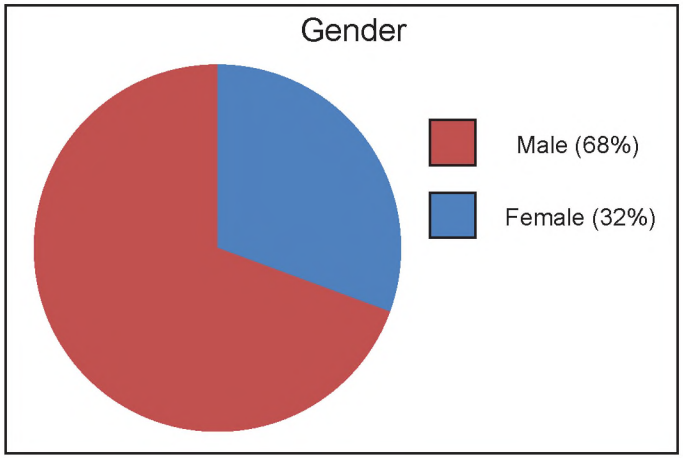

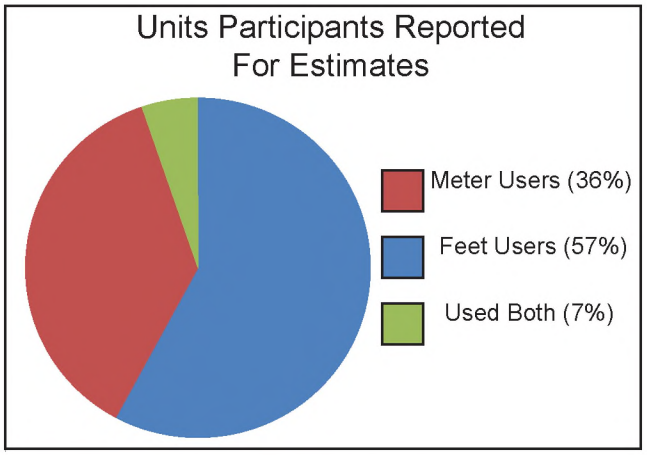

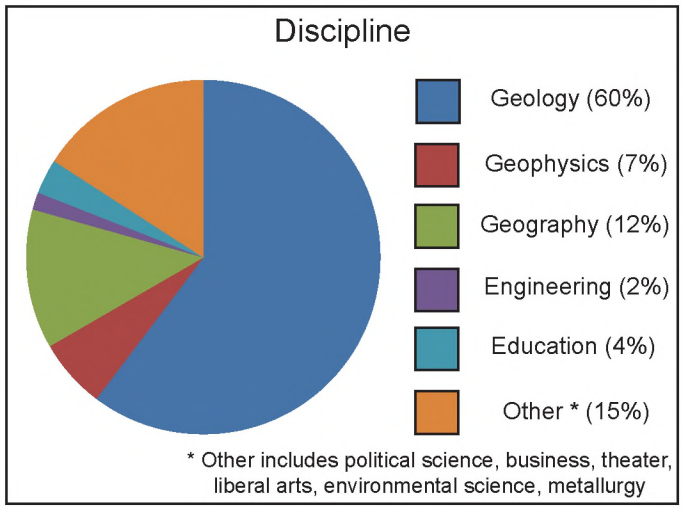

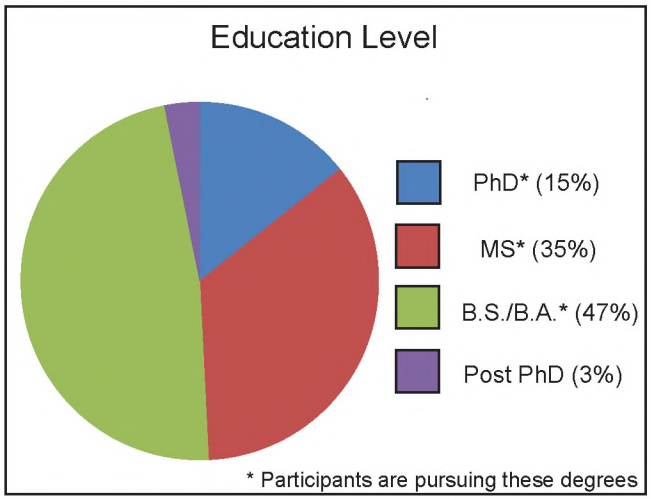

Figure 2.4 – This graph illustrates the average estimates (triangles) and standard deviations (columns) of the no scaling and scaling groups for every box. The x-axis corresponds to the left, center, or right boxes on each panorama with part one (static) of the exercise on the left half and part two (interactive) of the exercise on the right half. The y-axis corresponds to their estimate value in meters. The insert exhibits the panorama averages for both groups from part one to part two of the exercise plotted with the same axes.

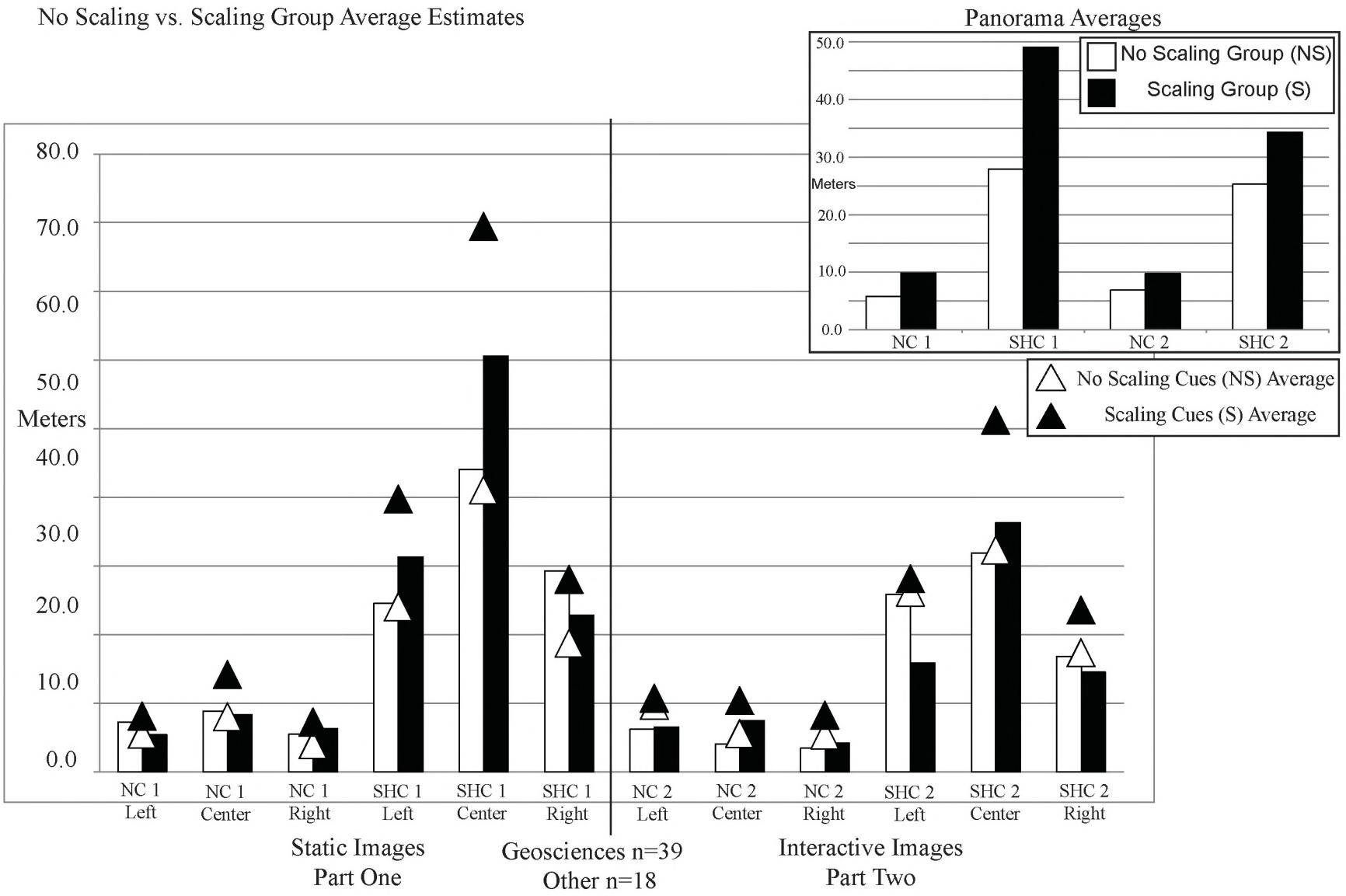
No Scaling vs. Scaling Group Average Estimates
Panorama Averages
No Scaling Group (NS)
Scaling Group (S)
50.0
40.0
30.0
Meters
20.0
10.0
0.0
NC 1
SHC 1
NC 2
SHC 2
No Scaling Cues (NS) Average
Scaling Cues (S) Average
80.0
70.0
60.0
50.0
Meters
40.0
30.0
20.0
10.0
0.0
NC 1 Left
NC 1 Center
NC 1 Right
SHC 1 Left
SHC 1 Center
SHC 1 Right
NC 2 Left
NC 2 Center
NC 2 Right
SHC 2 Left
SHC 2 Center
SHC 2 Right
Static Images Part One
Geosciences n=39
Other n=18
Interactive Images Part Two

Figure 2.5 – These graphs illustrate the average percent difference of estimates, normalized to the correct answer, for the no scaling (NS Group) and scaling cues group (S Group). The x-axis represents the left, center, and right box of each panorama and the y-axis illustrates percent from correct. The top two graphs correspond to the estimates made for the Nelson Canyon panorama while the bottom two graphs correspond to Stone House Canyon. The left two graphs represent part one of the exercise (static images) while the two graphs on the right represent part two of the exercise (interactive images).

To normalize the estimates, the correct answer (A) for the box in question was subtracted from the average estimates of each participant (B) and then divided by the correct value ({B-A}/A). These answers were then averaged for each box and each group (NS or S) (Table 2.1). For example, estimates for the Nelson Canyon left box in part one were almost exactly correct for the NS group, and about 45% overestimated by the S group.

No Scale vs. Scale: Average Normalized Percent Difference From Correct From Correct

Nelson Canyon Part 1 (Static Image)

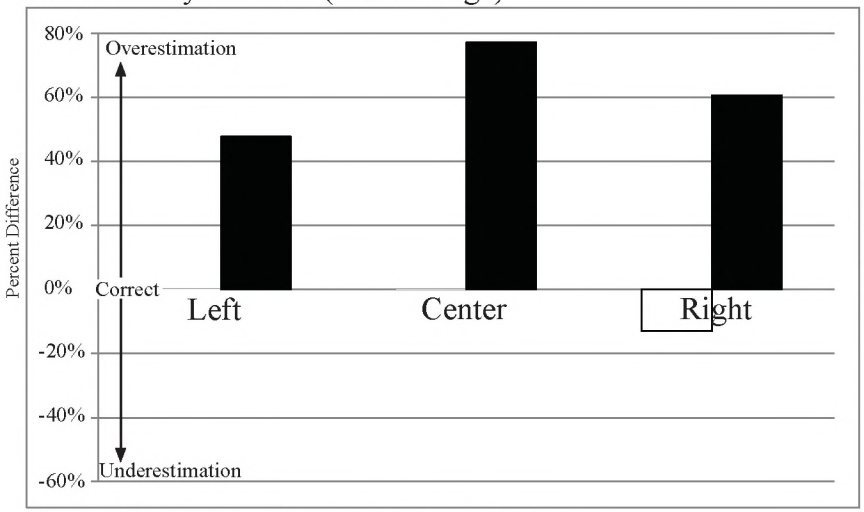

Nelson Canyon Part 2 (Interactive Image)

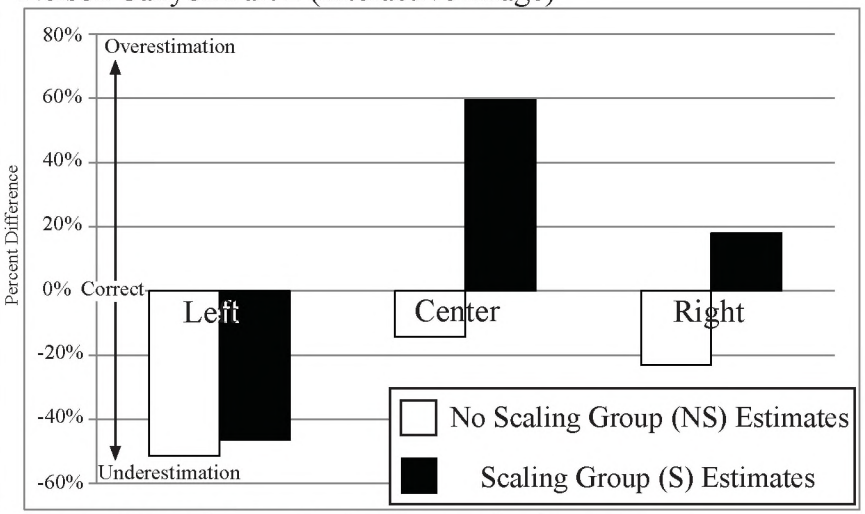

Stone House Canyon Part 1 (Static Image)

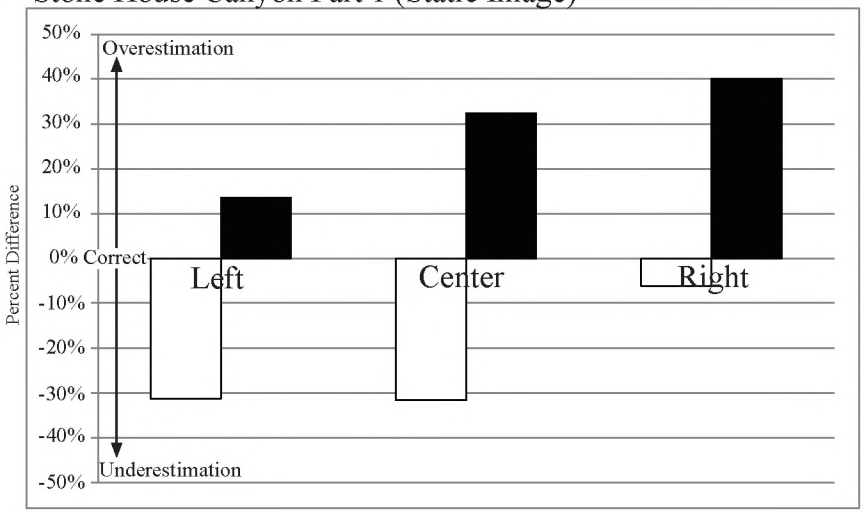

Stone House Canyon Part 2 (Interactive Image)

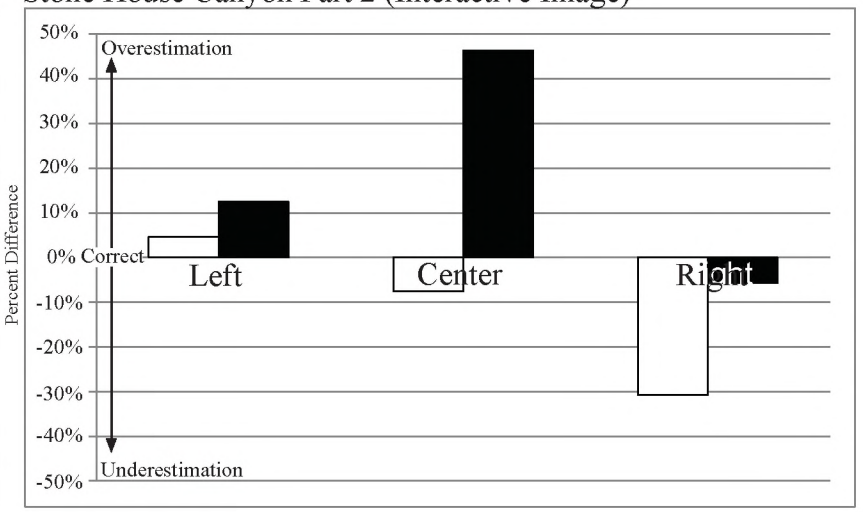

Figure 2.6 – These graphs illustrate the no scaling and scaling groups' percent change in accuracy from part one (static) to part two (interactive) of the exercise. This was calculated by subtracting the part two normalized values of the difference from correct, plotted in Figure 2.5, from the part one normalized values. [(Part one) – (Part two) = Percent Change] (Table 2.1). A positive value indicates a decrease in accuracy (i.e., part two was further off from correct than part one), and a negative value indicates an increase in accuracy. The x-axis corresponds to the left, center, and right box of each panorama and the y-axis corresponds to the percent change as a percent. The top graph represents the change for Nelson Canyon from part one to part two and the bottom graph corresponds to Stone House Canyon from part one to part two.

No Scale vs. Scale: Percent Change Accuracy Part 1 to Part 2

Nelson Canyon

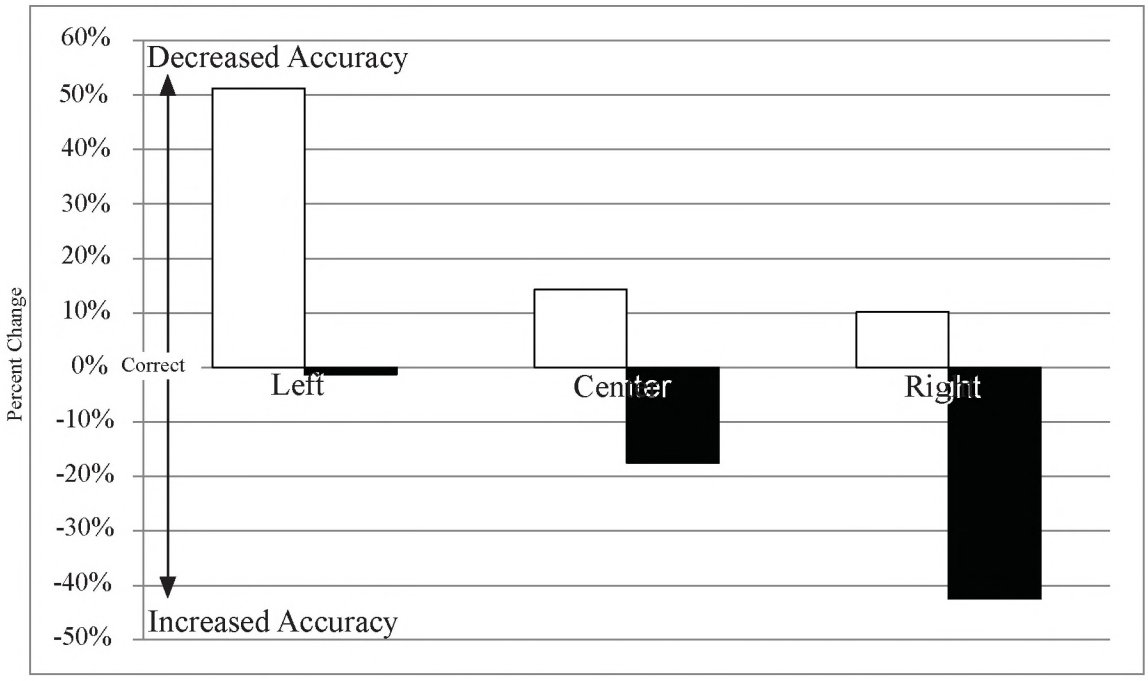

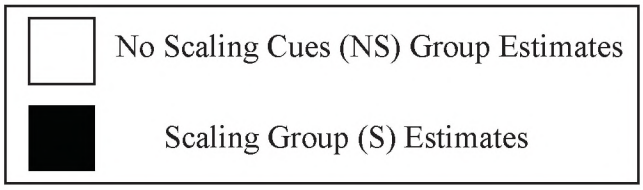

Stone House Canyon

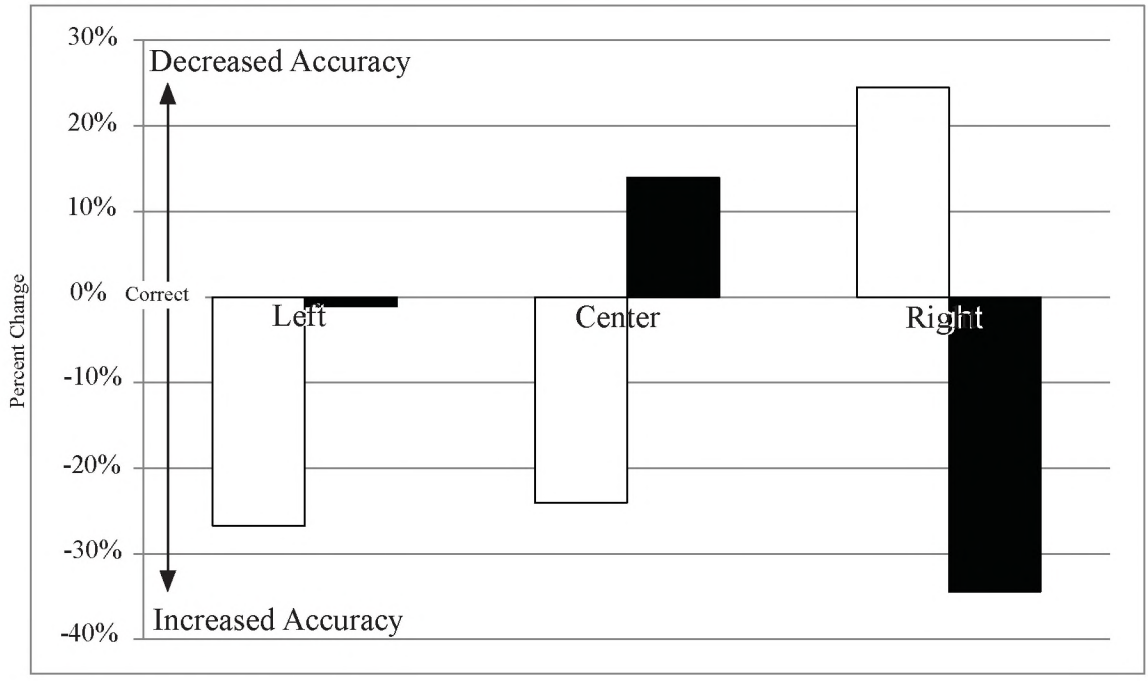

Figure 2.7 – Graph of the confidence expressed by the no scaling and scaling groups. The x-axis corresponds to each box (left, right, or center) within each panorama, Nelson Canyon (NC), and Stone House Canyon (SHC). The left half corresponds to part one (static images) of the exercise while the right half corresponds to part two (interactive images) of the exercise. The y-axis corresponds to their confidence estimate as a percentage of their height estimate.

Confidence estimates were normalized to the individual's estimate, averaged by group, and plotted as percent. To normalize the confidence values, the participant's estimate (B) for the box height in question was subtracted from the confidence estimate provided (C) and then divided by their estimate ({C-B}/B). In other words, a higher percentage reflects a higher estimate of error and thus less "confidence."

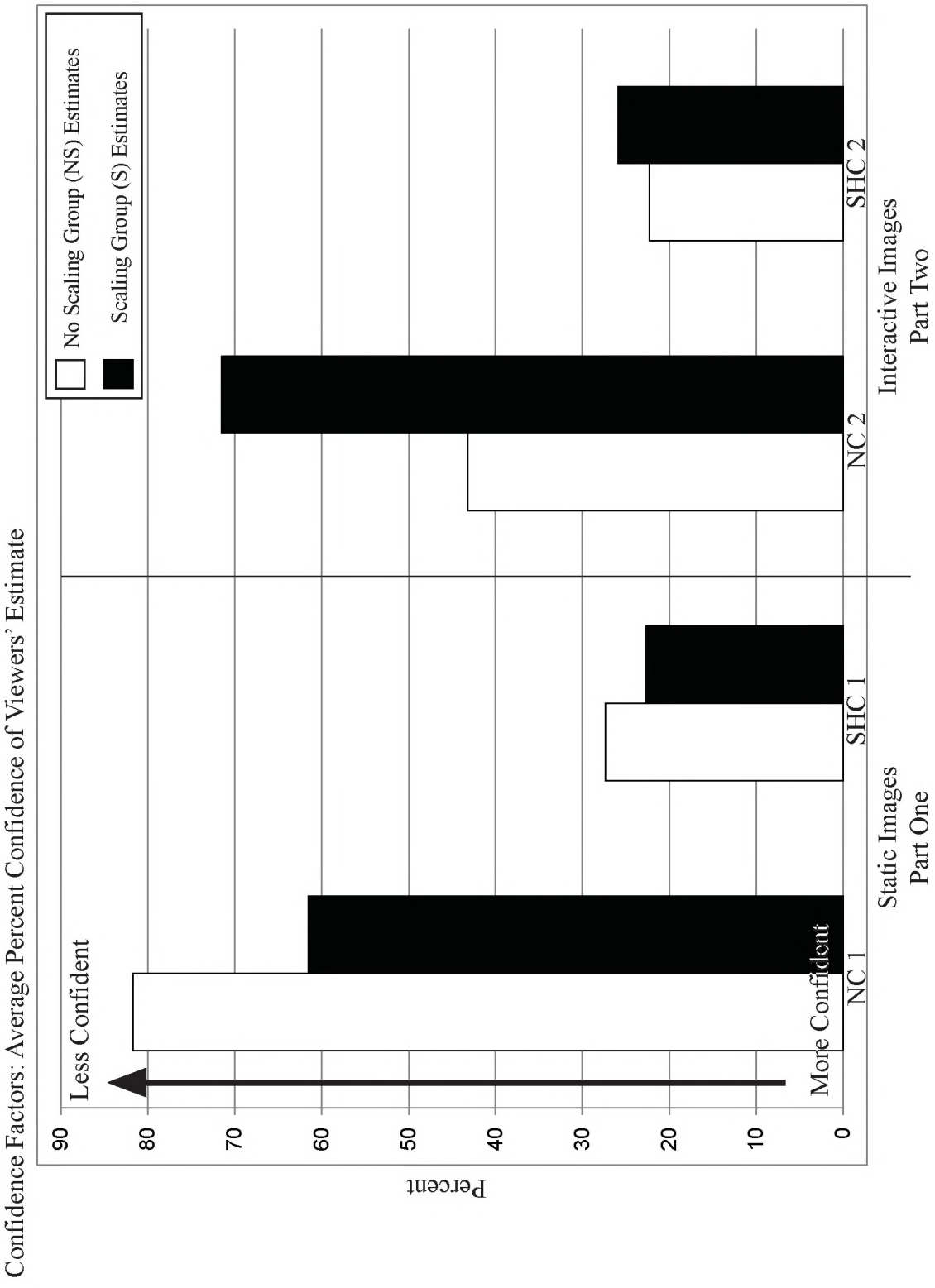
Confidence Factors: Average Percent Confidence of Viewers' Estimate
No Scaling Group (NS) Estimates
Scaling Group (S) Estimates
Less Confident
More Confident
Percent
90
80
70
60
50
40
30
20
10
0
NC 1
SHC 1
NC 2
SHC 2
Static Images
Part One
Interactive Images
Part Two

Figure 2.8 – This graph illustrates the average estimates (triangles) and standard deviations (columns) of the geoscience and "other" groups for every box. The x-axis corresponds to the left, center, or right boxes on each panorama with part one (static) of the exercise on the left half and part two (interactive) of the exercise on the right half. The y-axis corresponds to their estimate value in meters. The insert shows the panorama averages for both groups from part one to part two of the exercise plotted with the same axes.

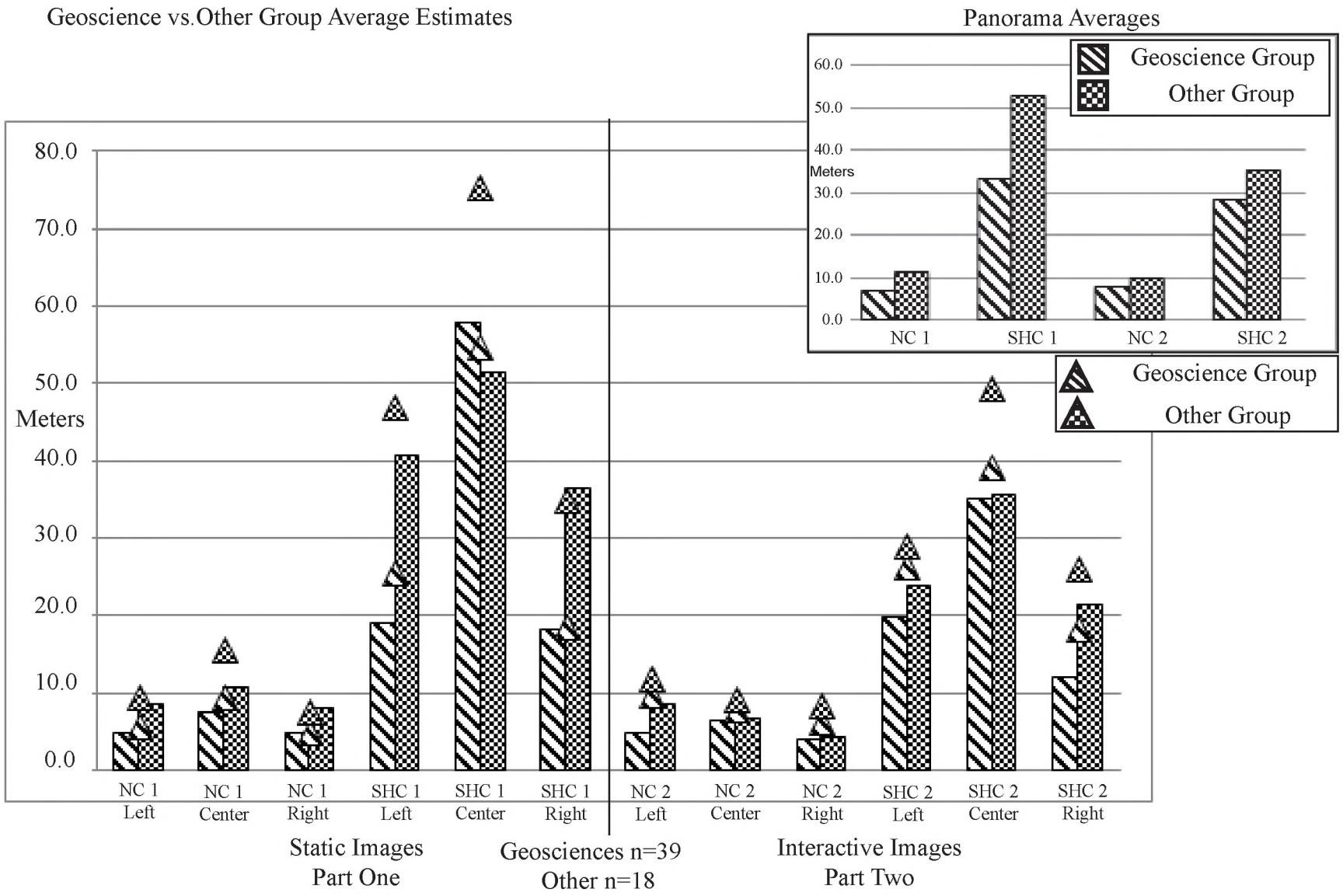
Geoscience vs.Other Group Average Estimates
Panorama Averages
Geoscience Group
Other Group
60.0
50.0
40.0
Meters
30.0
20.0
10.0
0.0
NC 1
SHC 1
NC 2
SHC 2
Geoscience Group
Other Group
80.0
70.0
60.0
50.0
Meters
40.0
30.0
20.0
10.0
0.0
NC 1 Left
NC 1 Center
NC 1 Right
SHC 1 Left
SHC 1 Center
SHC 1 Right
NC 2 Left
NC 2 Center
NC 2 Right
SHC 2 Left
SHC 2 Center
SHC 2 Right
Static Images Part One
Geosciences n=39
Other n=18
Interactive Images Part Two

Figure 2.9 – These graphs illustrate the average percent difference of estimates, normalized to the correct answer, for the geoscience and other disciplines. The x-axis represents the left, center, and right box of each panorama and the y-axis illustrates percent. The top two graphs correspond to the estimates made for the Nelson Canyon panorama while the bottom two graphs correspond to Stone House Canyon. The left two graphs represent part one of the exercise (static images) while the two graphs on the right represent part two of the exercise (interactive images).

To normalize the estimates, the correct answer (A) for the box in question was subtracted from the average estimates of each participant (B) and then divided by the correct estimate ({B-A}/A) (Table 2.1). These answers were then averaged for each box and each group (Geoscience or "Other"). For example, estimates for the Nelson Canyon left box in part one were almost exactly correct for the Geoscience group, and about 72% overestimated by the "Other" group.

No Scale vs. Scale: Average Normalized Percent Difference From Correct From Correct

Nelson Canyon Part 1 (Static Image)

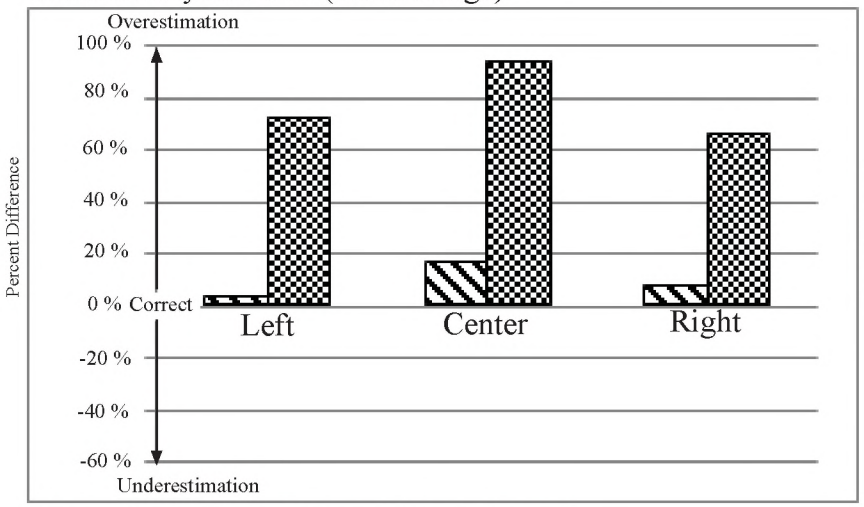

Nelson Canyon Part 2 (Interactive Image)

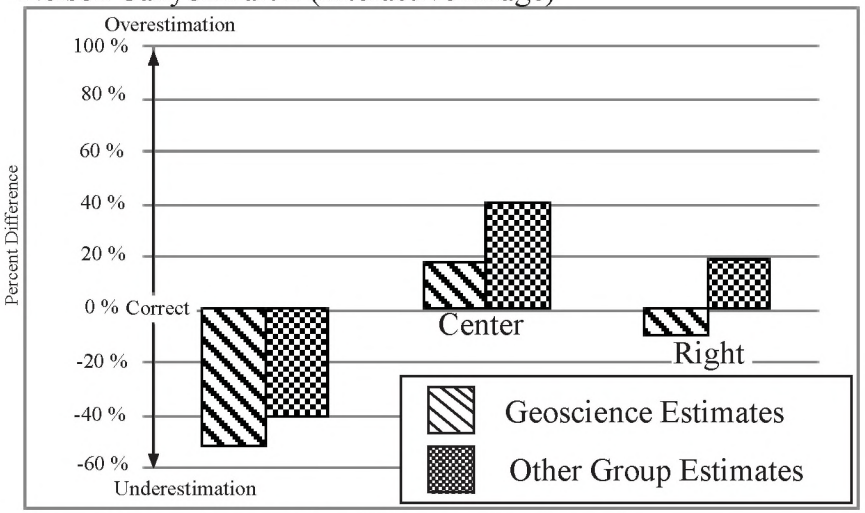

Stone House Canyon Part 1 (Static Image)

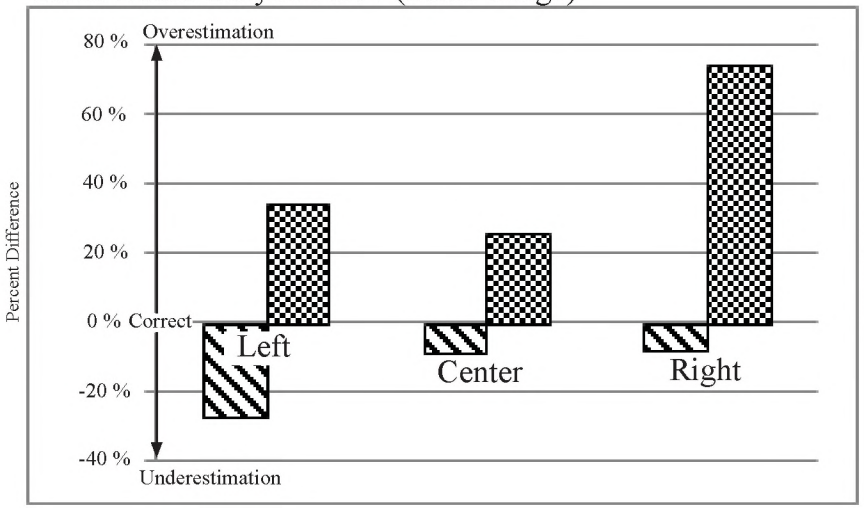

Stone House Canyon Part 2 (Interactive Image)

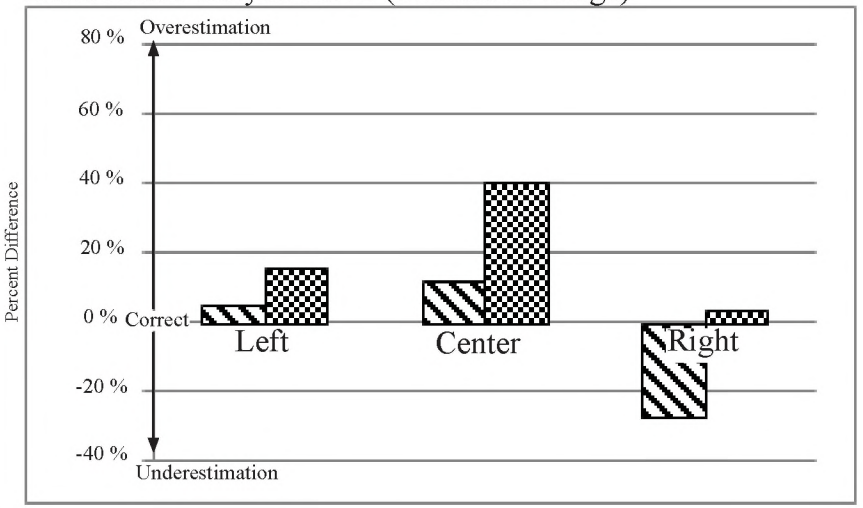

Figure 2.10 – These graphs illustrate geoscience and "other" groups' percent change in accuracy from part one (static) to part two (interactive) of the exercise. The x-axis corresponds to the left, center, and right box while the y-axis corresponds to the percent change as a decimal. The top graph represents the change for Nelson Canyon from part one to part two and the bottom graph corresponds to Stone House Canyon from part one to part two.

This was calculated by subtracting the part two normalized values of the difference from correct, plotted in Figure 2.9, from the part one normalized values. [(Part one) – (Part two) = Percent Change] (Table 2.1). A positive value indicates a decrease in accuracy (i.e., part two was further from correct than part one), whereas a negative value indicates an increase in accuracy.

Geoscience vs. Other: Percent Change Part 1 to Part 2

Nelson Canyon

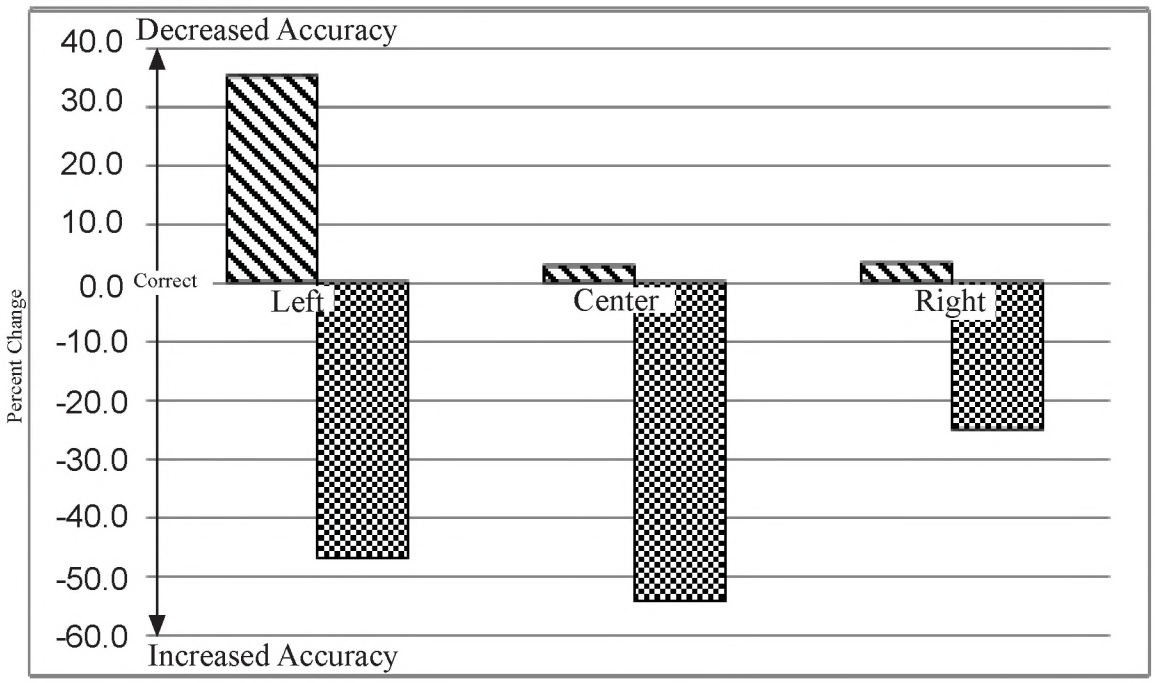

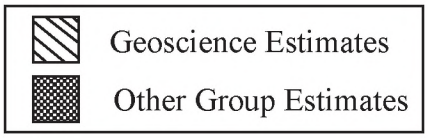

Stone House Canyon

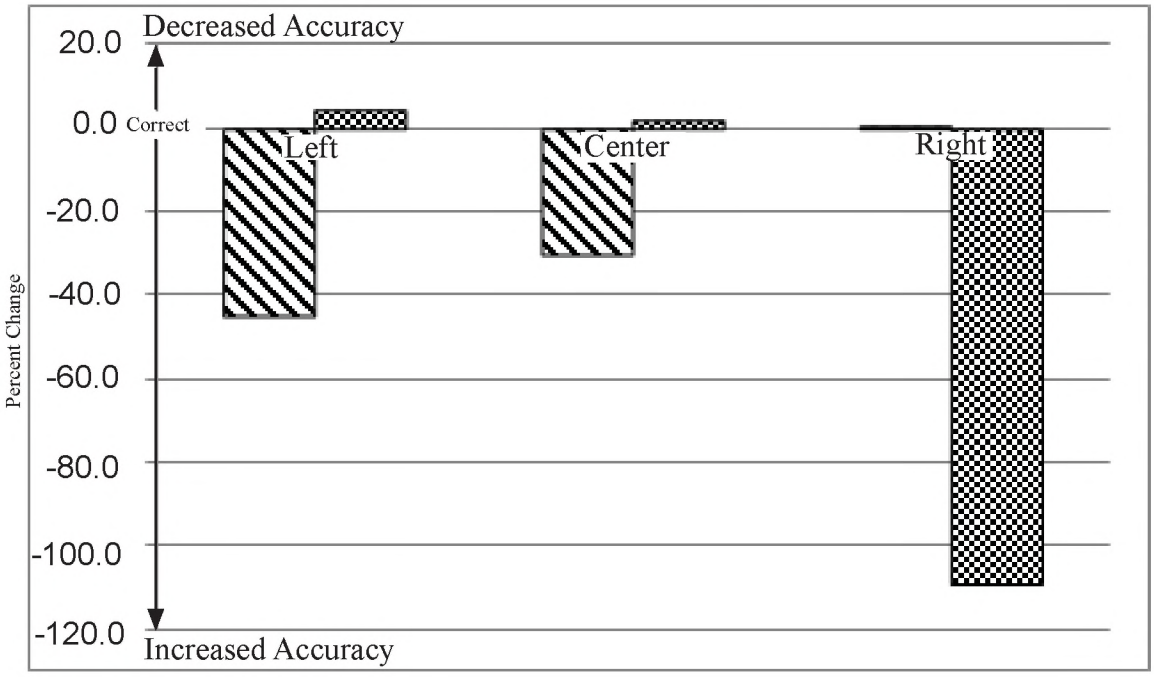

Figure 2.11 – Graph of the confidence expressed by the geoscience and "other" groups about the accuracy of their own estimates. Answers were normalized to their answer and plotted as percent. The X-axis corresponds to each box (left, right, or center) within each panorama, Nelson Canyon (NC), and Stone House Canyon (SHC). The left half corresponds to part one (static images) of the exercise while the right half corresponds to part two (interactive images) of the exercise. The Y-axis corresponds to their confidence estimate as a percentage of their height estimate.

To normalize the confidence values, the participant's estimate (B) for the box height in question was subtracted from the confidence estimate provided (C) and then divided by their estimate ({C-B}/B) (Table 2.1). In other words a higher percentage reflects a higher estimate of error and thus less "confidence."

Geoscience vs. "Other" Confidence Factors: Average Percent of Viewers' Estimate

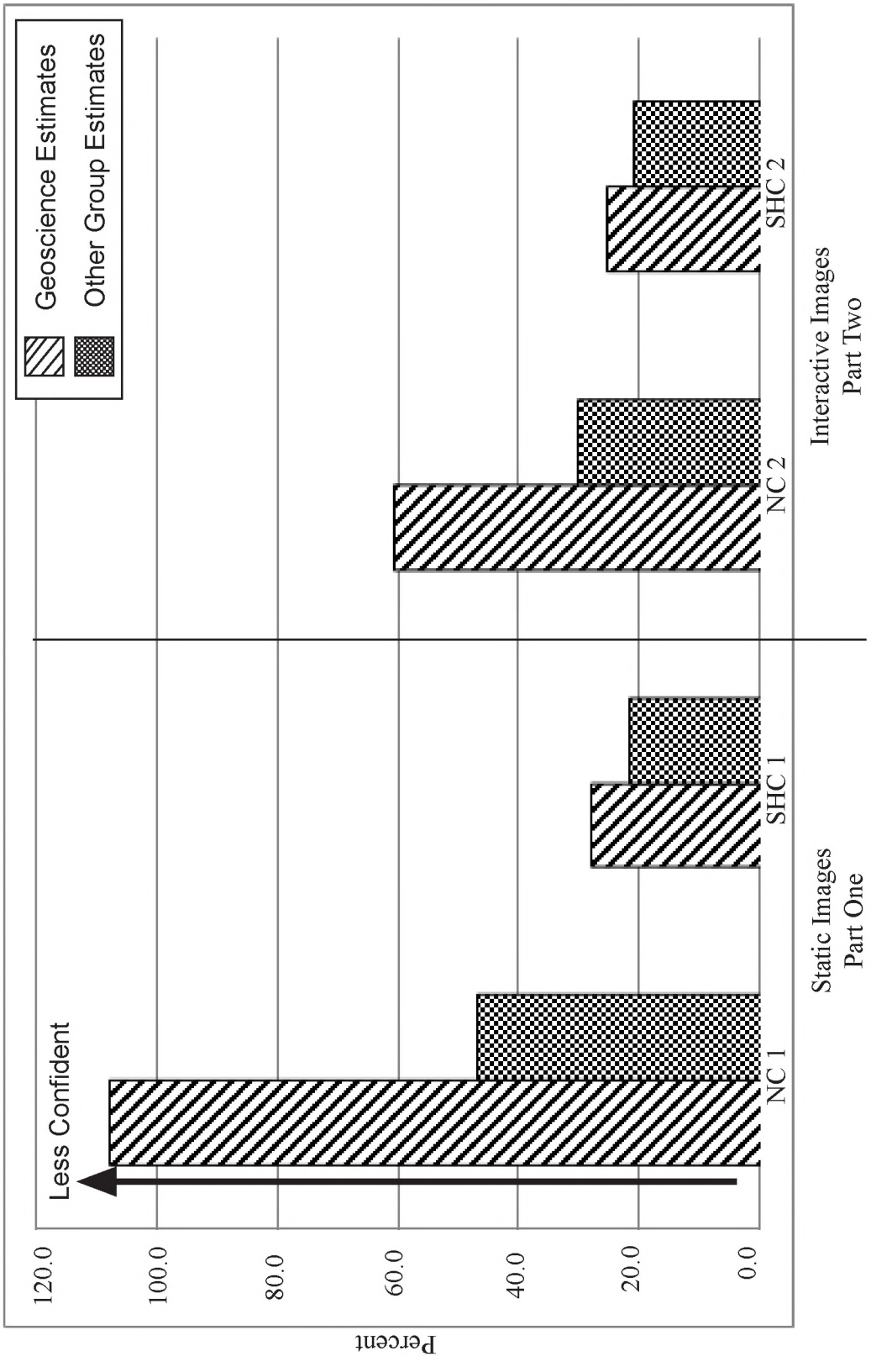

Figure 2.12 – This graph illustrates the average estimates (triangles) and standard deviations (columns) of the undergraduate and graduate groups for every box. The x-axis corresponds to the left, center, or right boxes on each panorama with part one (static) of the exercise on the left half and part two (interactive) of the exercise on the right half. The y-axis corresponds to their estimate value in meters. The insert exhibits the panorama averages for both groups from part one to part two of the exercise plotted with the same axes.

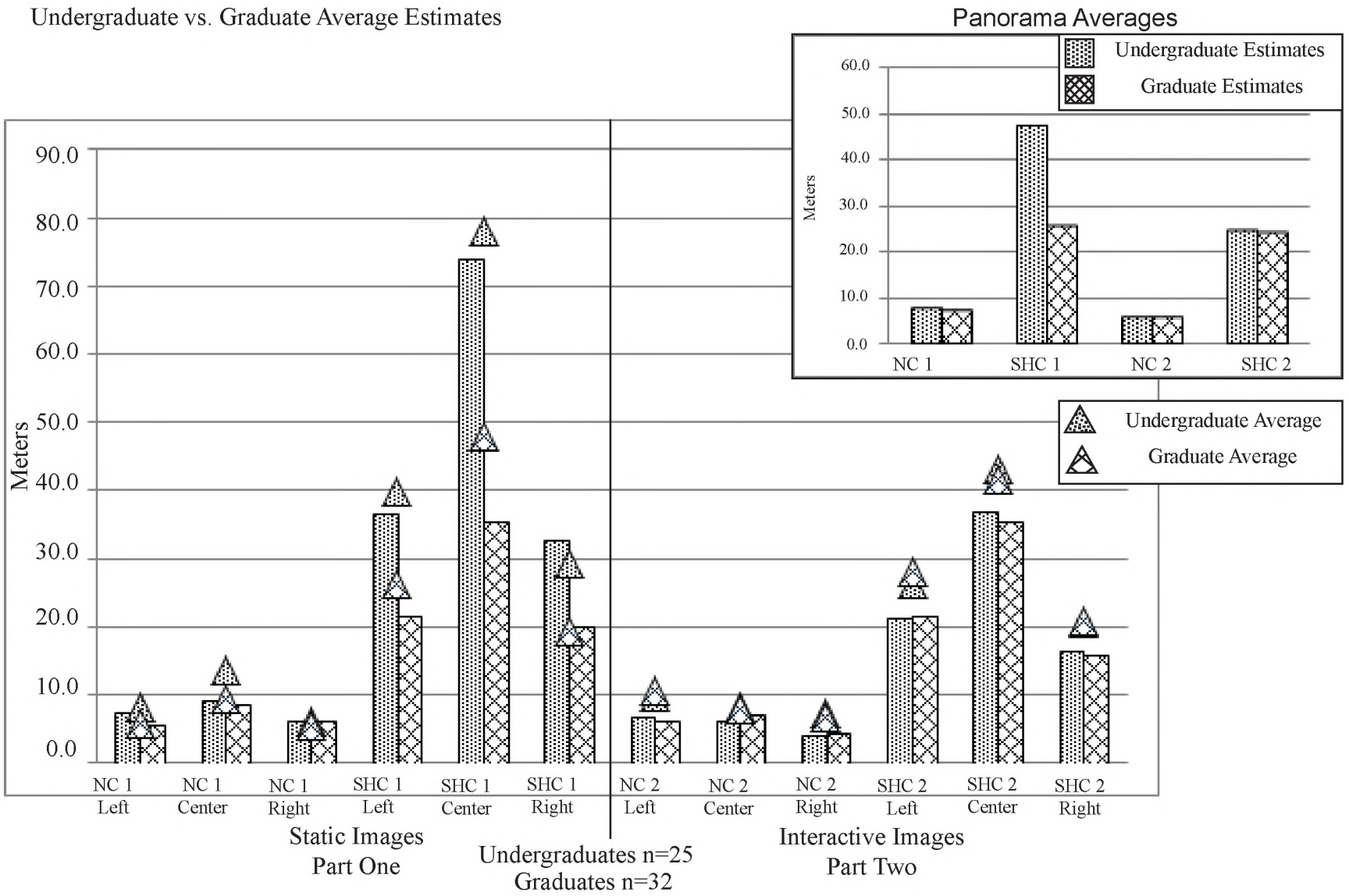
Undergraduate vs. Graduate Average Estimates
Panorama Averages
Undergraduate Estimates
Graduate Estimates
Undergraduate Average
Graduate Average
Meters
90.0
80.0
70.0
60.0
50.0
40.0
30.0
20.0
10.0
0.0
NC 1 Left
NC 1 Center
NC 1 Right
SHC 1 Left
SHC 1 Center
SHC 1 Right
NC 2 Left
NC 2 Center
NC 2 Right
SHC 2 Left
SHC 2 Center
SHC 2 Right
Static Images
Part One
Undergraduates n=25
Graduates n=32
Interactive Images
Part Two

Figure 2.13 – These graphs illustrate the average percent difference of estimates, normalized to the correct answer, for the undergraduate and graduate experience levels. The x-axis represents the left, center, and right box of each panorama and the y-axis illustrates percent. The top two graphs correspond to the estimates made for the Nelson Canyon panorama while the bottom two graphs correspond to Stone House Canyon. The left two graphs represent part one of the exercise (static images) while the two graphs on the right represent part two of the exercise (interactive images).

To normalize the estimates, the correct answer (A) for the box in question was subtracted from the average estimates of each participant (B) and then divided by the correct estimate ({B-A}/A) (Table 2.1). These answers were then averaged for each box and each group (Undergraduate or Graduate). For example, estimates for the Nelson Canyon left box in part one were overestimated by 24% by the undergraduate group, and about 12% underestimated by the graduate group.

Experience Level: Average Normalized Percent Difference From Correct

Nelson Canyon Part 1 (Static Image)

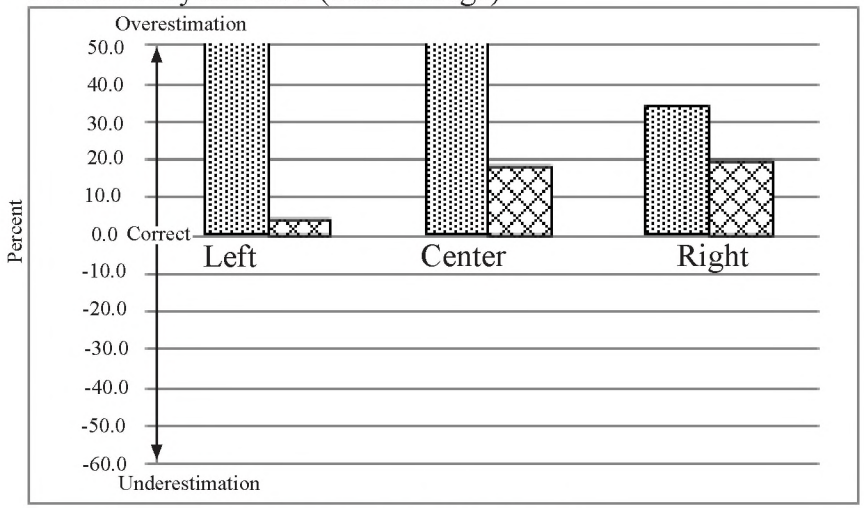

Nelson Canyon Part 2 (Interactive Image)

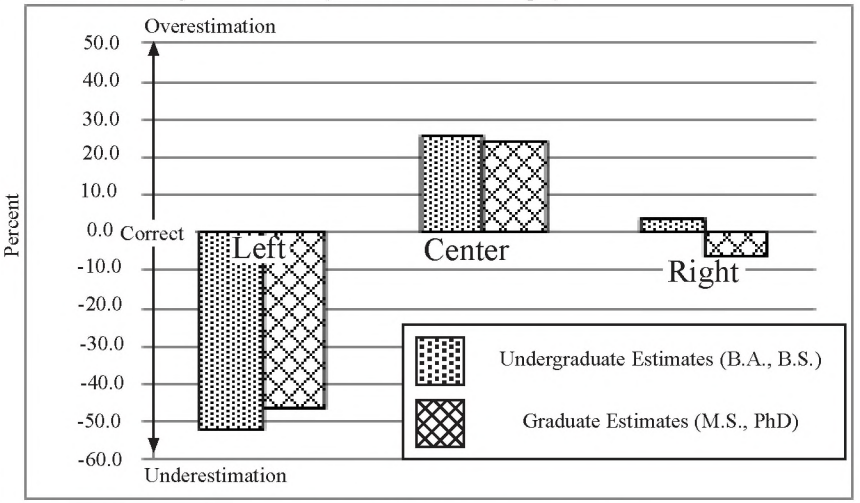

Stone House Canyon Part 1 (Static Image)

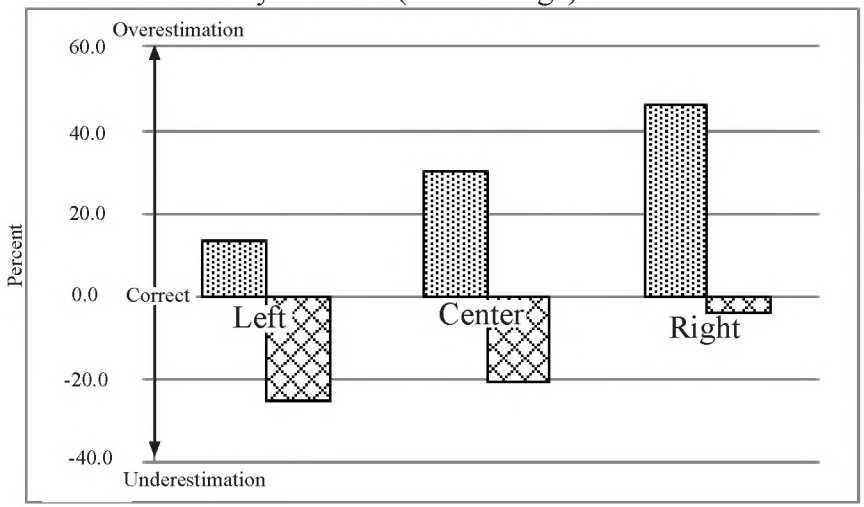

Stone House Canyon Part 2 (Interactive Image)

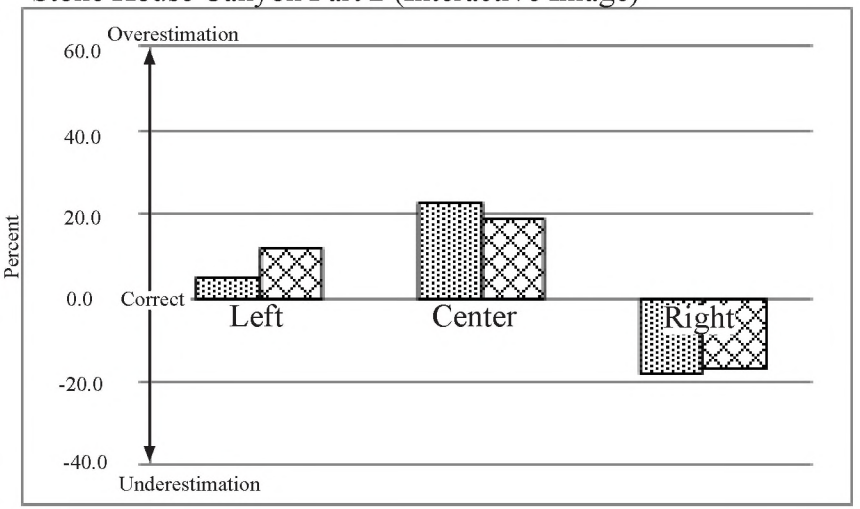

Figure 2.14 – These graphs illustrate the graduate and undergraduate groups' percent change in accuracy from part one (static) to part two (interactive) of the exercise. The x-axis corresponds to the left, center, and right box while the y-axis corresponds to the percent change as a decimal. The top graph represents the change for Nelson Canyon from part one to part two and the bottom graph corresponds to Stone House Canyon from part one to part two.

The percent change was calculated by subtracting the part two normalized values of the difference from correct, plotted in Figure 2.13, from the part one normalized values [(Part one) – (Part two) = Percent Change] (Table 2.1). A positive value indicates a decrease in accuracy (i.e., part two was further from correct than part one), while a negative value indicates an increase in accuracy.

Experience Level: Decimal Percent Change Part 1 to Part 2

Nelson Canyon

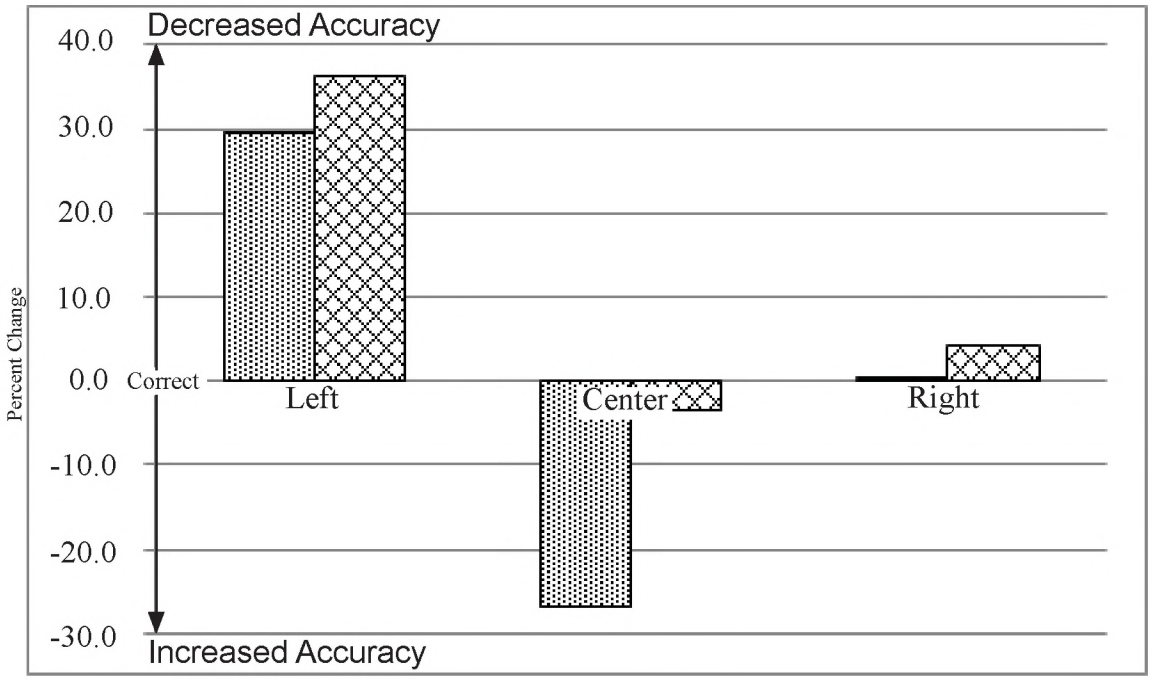

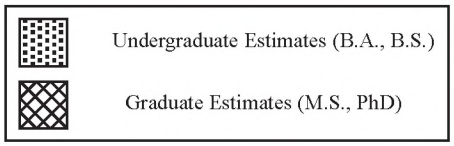

Stone House Canyon

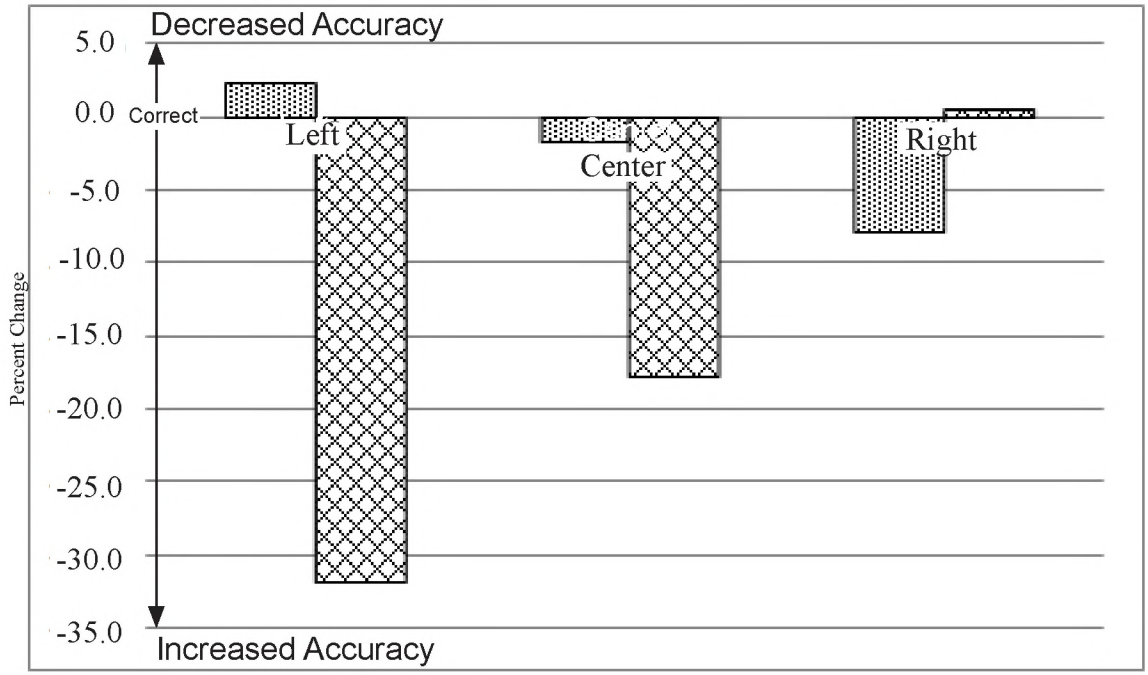

Figure 2.15 – Graph of the confidence expressed by the graduate and undergraduate groups about the accuracy of their own estimates. Answers were normalized to their answer and plotted as percent. The X-axis corresponds to each box (left, right, or center) within each panorama, Nelson Canyon (NC), and Stone House Canyon (SHC). The left half corresponds to part one (static images) of the exercise while the right half corresponds to part two (interactive images) of the exercise. The Y-axis corresponds to their confidence estimate as a percentage of their height estimate.

To normalize the confidence values, the participant's estimate (B) for the box height in question was subtracted from the confidence estimate provided (C) and then divided by their estimate ({C-B}/B) (Table 2.1). For example, for the Nelson Canyon panorama in part one of the exercise, the undergraduate group estimated error, on average, to be ~ 10% of their estimate. So if they estimated the box to be 10 m, their error would be 1 m. In other words, a higher percentage reflects a higher estimate of error and thus less "confidence."

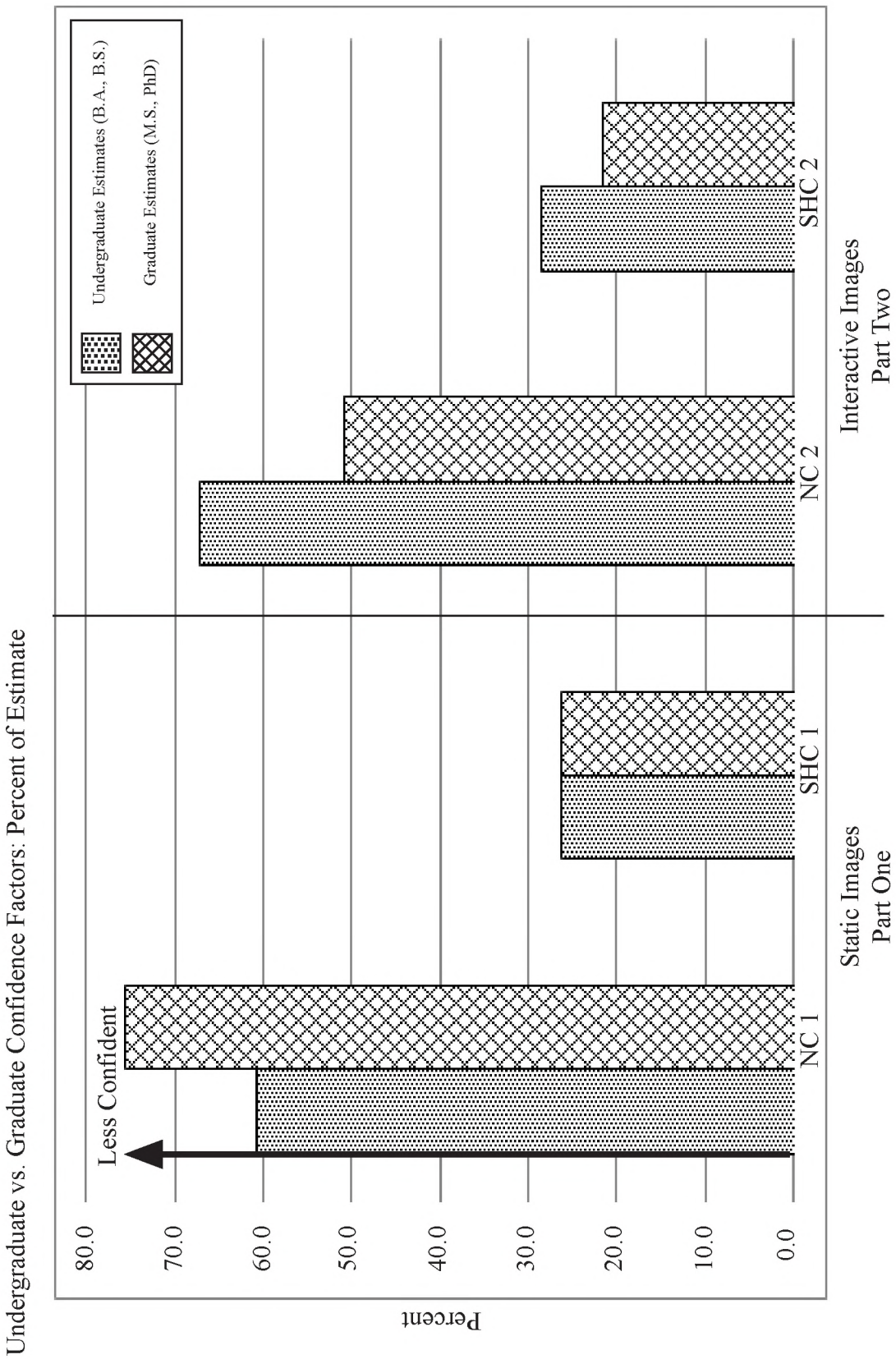
Undergraduate vs. Graduate Confidence Factors: Percent of Estimate
Undergraduate Estimates (B.A., B.S.)
Graduate Estimates (M.S., PhD)
Less Confident
Percent
80.0
70.0
60.0
50.0
40.0
30.0
20.0
10.0
0.0
NC 1
SHC 1
NC 2
SHC 2
Static Images
Part One
Interactive Images
Part Two

Table 2.1

Summary of Data Averaged and Sorted by Group

	Estimates (m);{Standard Deviation}											
	NC-1			SHC-1			NC-2			SHC-2		
	Left	Center	Right	Left	Center	Right	Left	Center	Right	Left	Center	Right
Correct	5.5	8	4.5	35	60	20	20	6.5	7	25	35	25
No Scaling (N=27)	(5.5);{7.3}	(8.0);{8.8}	(3.9);{5.5}	(24.0);{24.5}	(41.0);{44.1}	(18.8);{29.2}	(9.7);{6.2}	(5.6);{4.1}	(5.4);{3.5}	(26.2);{25.9}	(32.3);{31.9}	(17.3);{16.8}
Scaling (N=30)	(8.1);{5.5}	(14.2);{8.3}	(7.2);{6.3}	(39.7);{31.3}	(79.4);{60.6}	(28.0);{22.8}	(10.7);{6.5}	(10.4);{7.5}	(8.3);{4.3}	(28.1);{15.9}	(51.2);{36.3}	(23.6);{14.5}
Geoscience (N=39)	(5.7);{4.9}	(9.2);{7.6}	(4.8);{4.9}	(25.6);{19.2}	(54.7);{57.9}	(18.4);{18.3}	(9.5);{4.9}	(7.6);{6.4}	(6.3);{4.0}	(26.3);{19.9}	(39.0);{35.0}	(18.2);{12.0}
Other (N=18)	(9.5);{8.6}	(15.5);{10.6}	(7.5);{8.0}	(46.9);{40.6}	(75.3);{51.6)	(34.8);{36.4}	(11.8);{8.6}	(9.1);{6.8}	(8.3);{4.3}	(29.0);{23.8}	(49.2);{35.8}	(26.0);{21.4}
Graduate (N=25)	(8.3);{7.4}	(13.5);{9.2}	(6.0);{6.1}	(39.8);{36.4}	(78.2);{74.0}	(29.3);{32.7}	(9.6);{6.8}	(8.2);{6.1}	(7.3);{4.1}	(26.2);{21.3}	(43.0);{36,9}	(20.4);{16.4}
Undergrad (N=32)	(5.7);{5.5}	(9.5);{8.7}	(5.4);{6.3}	(26.4);{21.6}	(47.9);{35.4}	(19.2);{20.0}	(10.7);{6.0}	(8.1);{7.0}	(6.6);{4.3}	(28.0);{21.4}	(41.7);{35.2}	(20.7);{15.8}
	Difference From Correct (m);{Standard Deviation}											
	NC-1			SHC-1			NC-2			SHC-2		
	Left	Center	Right	Left	Center	Right	Left	Center	Right	Left	Center	Right
Correct	5.5	8	4.5	35	60	20	20	6.5	7	25	35	25
No Scaling (N=27)	(0.0);{7.3}	(0.0);{8.8}	(-0.1);{5.5}	(-0.3);{24.5}	(-0.3);{44.1)	(-0.1);{29.2}	(-0.5);{6.2}	(-0.1);{4.1}	(-0.2);{3.5}	(0.0);{25.9}	(-0.1);{31.9}	(-0.3);{16.8}
Scaling (N=30)	(8.1);{5.5}	(14.2);{8.3}	(7.2);{6.3}	(39.7);{31.3}	(79.4);{60.6}	(28.0);{22.8}	(10.7);{6.5}	(10.4);{7.5}	(8.3);{4.3}	(28.1);{15.9}	(51.2);{36.3}	(23.6);{14.5}
Geoscience (N=39)	(0.2);{4.9}	(1.3);{7.6}	(0,3);{4.9}	(-9.4);{19.2}	(-5.3);{57.9}	(-1.6);{18.3}	(-10.5);{4.9}	(1.1);{6.4}	(-0.7);{4.0}	(1.3);{19.9}	(4.1);{35.0}	(-6.8);{12.0}
Other (N=18)	(0.7);{1.6}	(0.9);{1.3}	(0.7);{1.8}	(0.3);{1.2}	(0.3);{0.9}	(0.7);{1.8}	(-0.4);{0.43}	(0.4);{1.0}	(0.2);{0.6}	(0.2);{1.0}	(0.4);{1.0}	(0.0);{0.9}
Graduate (N=25)	(0.5);{1.3}	(0.7);{1.2}	(0.3);{1.3}	(0.1);{1.0}	(0.3);{1.2}	(0.5);{1.6}	(-0.5);{0.3}	(0.3);{0.9}	(0.0);{0.6}	(0.0);{0.8}	(0.2);{1.0}	(-0.2);{0.6}
Undergrad (N=32)	(0.0);{1.0}	(0.2);{1.1}	(0.2);{1.4}	(-0.3);{0.6}	(-0.2);{0.6}	(-0.0);{1.0}	(-0.5);{0.3}	(0.2);{1.1}	(-0.1);{0.6}	(0.1);{1.0}	(0.2);{1.0}	(-0.2);{0.6}

	Confidence (Percent);{Standard Deviation}			
	NC-1	SHC-1	NC-2	SHC-2
Correct				
No Scaling (N=27)	(71.3);{66.6 (27.0);{10.8}	(36.6);{20.9}	(21.6);{8.9}	
Scaling (N=30)	(68.5);{50.3 (25.7);{20.5}	(76.1);{58.3}	(26.8);{11.0}	
Geoscience (N=39)	(107);{2.1}	(28.0);{0.2}	(60.5);{0.45}	(25.3);{0.12}
Other (N=18)	(46.8);{0.6}	(21.5);{0.3}	(30.0);{0.3}	(21.0);{0.3}
Graduate (N=25)	(60.8);{0.5}	(26.2);{0.3}	(67.2);{0.6}	(28.4);{0.1}
Undergrad (N=32)	(75.6);{0.6}	(26.3);{0.2}	(51.0);{0.4}	(21.7);{0.1}

Table 2.2

Summary of key results

No Scaling vs. Scaling: Estimates

- Both groups exhibited higher estimates and standard deviations in the SHC panorama than the NC panorama.
- The NS group had lower average estimates and standard deviations than the S group.
- From part one to part two (static to interactive) the NS group decreased estimates for all boxes in the NC panorama and decreased estimates in 2 of 3 boxes in the SHC panorama.
- From part one to part two the S group decreased estimates in 2 of 3 boxes within the NC panorama and all boxes within the SHC panorama.

No Scaling vs. Scaling: Difference From Correct

- The NS group underestimated for 10 of the 12 boxes in the exercise
- The NS group increased accuracy for only two of the 6 boxes from part one (static) to part two (interactive)
- The S group overestimated for 10 of the 12 boxes in the exercise
- The S group increased accuracy for 5 of the 6 boxes from part one to part two.

No Scaling vs. Scaling: Confidence

- The NS group was less confident in their estimates than the S group in part 1 of the exercise, but more confident than the S group in their estimates in part 2.
- The NS group increased their confidence from part one to part two.
- The S group decreased their confidence from part one to part two.

Geoscience Discipline vs. "Other" Discipline: Estimates

- Except for one box the “other” group produced consistently higher estimates and standard deviations than the geoscience group.
- Both groups exhibited higher estimates within the SHC panorama than in the NC panorama.
- Both groups saw a decrease in estimates and standard deviations from part one to part two with the exception of the geosciences group for one box.

Geoscience Discipline vs. "Other" Discipline: Difference From Correct

- The geoscience group overestimated in 6 of the 12 boxes while the “other” group overestimated in 11 of the 12 boxes.
- From part one to part two, in the NC panorama, the geoscience group saw a decrease in accuracy for all 3 boxes, while “other” group exhibited an increase in accuracy for all 3 boxes.
- From part one to part two in the, SHC panorama, the geoscience group saw an increase in accuracy for 2 of the 3 boxes, while the “other” group saw an increase in accuracy for 1 of the 3 boxes.

Geoscience Discipline vs. "Other" Discipline: Confidence

- Both groups were more confident within the SHC panorama than the NC panorama.
- The “other” group was more confident than the geoscience group in both panoramas.
- From part one to part two both groups saw an increase in confidence for both panoramas.

Undergraduate vs. Graduate Experience Level: Estimates

- Both groups exhibited higher estimates and standard deviations in the SHC panorama than the NC panorama.
- The undergraduate group had higher average estimates and standard deviations in 8 of the 12 boxes.
- From part one to part two the undergraduate group decreased both average estimates and standard deviations for every box
- From part one to part two the gradaute group decreased their estimates in 9 of the 12 boxes

Undergraduate vs. Graduate Experience Level: Difference From Correct

- The undergraduate group overestimated in 9 of the 12 boxes while the graduate group overestimated in only 2 of the 12 boxes.
- In the NC panorama both groups increased their accuracy from part one to part two on the center box only.
- In the SHC panorama both groups increased their accuracy from part one to part two on 2 of the 3 boxes (different pairs of boxes for each group).

Undergraduate vs. Graduate Experience Level: Confidence

- Both groups were more confident in the Stone House Canyon (SHC) panorama than the Nelson Canyon (NC) Panorama.
- The undergraduate group was less confident than the graduate group.
- Both groups saw an increase in confidence from part one to part two.

APPENDIX A

MEASURED STRATIGRAPHIC SECTIONS

Appendix A comprises the seven stratigraphic sections detailed in this study across transect A to A': three from Rock House Cove (RHC), one from Coyote Springs Canyon (CSC), one from Blue Cove (BC), and two from Ty Hatch Canyon (THC). A legend of symbols and color schemes is provided. See Figure 1.1 for locations within the Kaiparowits Plateau. See Figure 1.3 for a detailed map of transect A-A'.

Measured Section Legend


Hummocky Cross Stratification


Planar Stratification


Trough Cross Stratification (TCB)


Coarse Trough Cross Stratification


Soft Sediment Deformation


Thalassinoides


Ophiomorpha


Planolites


Lockeia


Teredolites


Wood Fragments


Fossil Teeth


Shell Material


Bone Material


Roots


Ammonite

Organics

Mud Rip-Up Clasts

Coal Rip-Up Clasts


Sandstone


Siltstone


Coal Seam


Paleosols


Mean Paleocurrent Direction

Contact Between Members

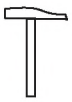
Sandstone Sample

Rock House Cove Section 1

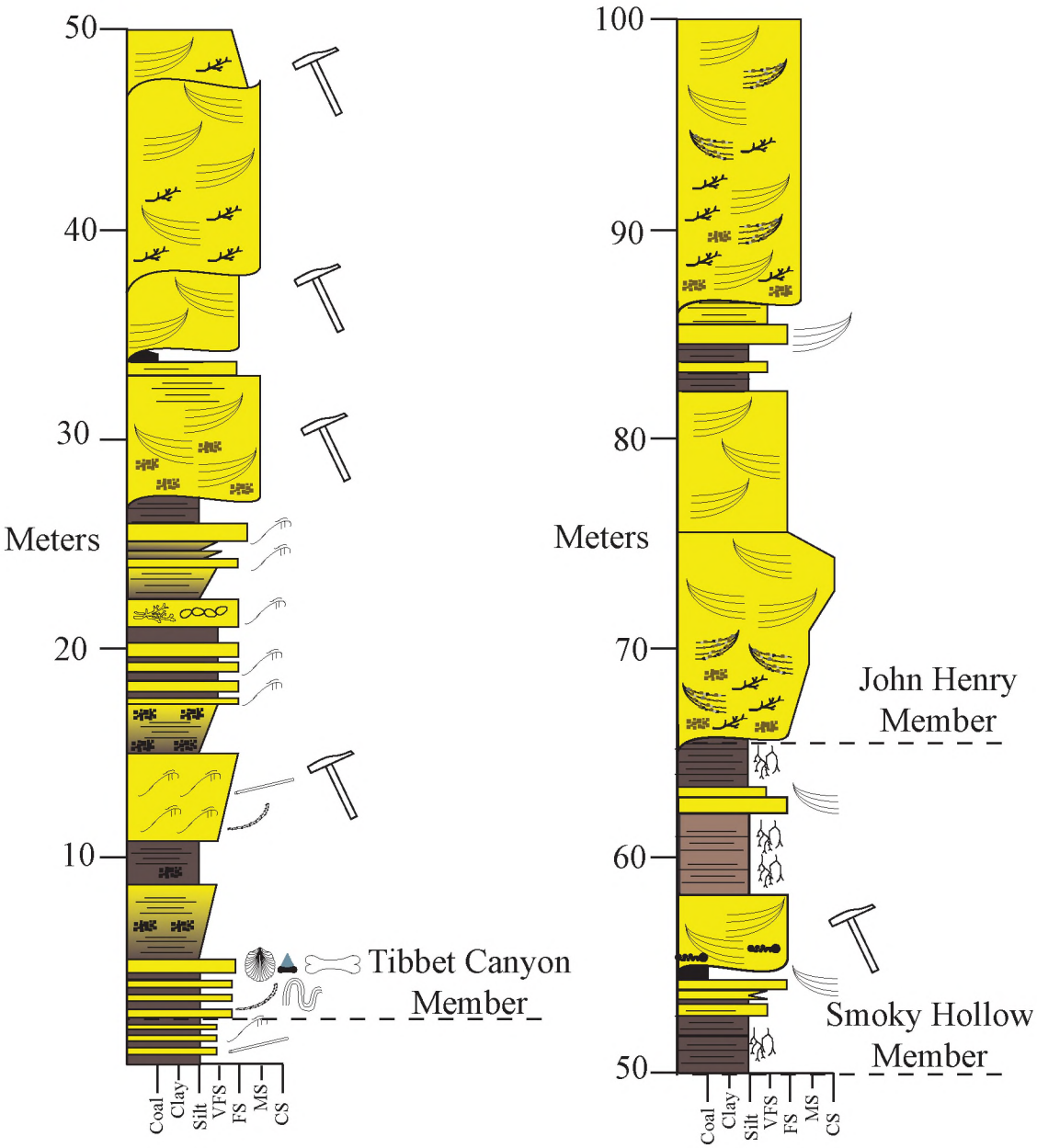

Rock House Cove Section 2

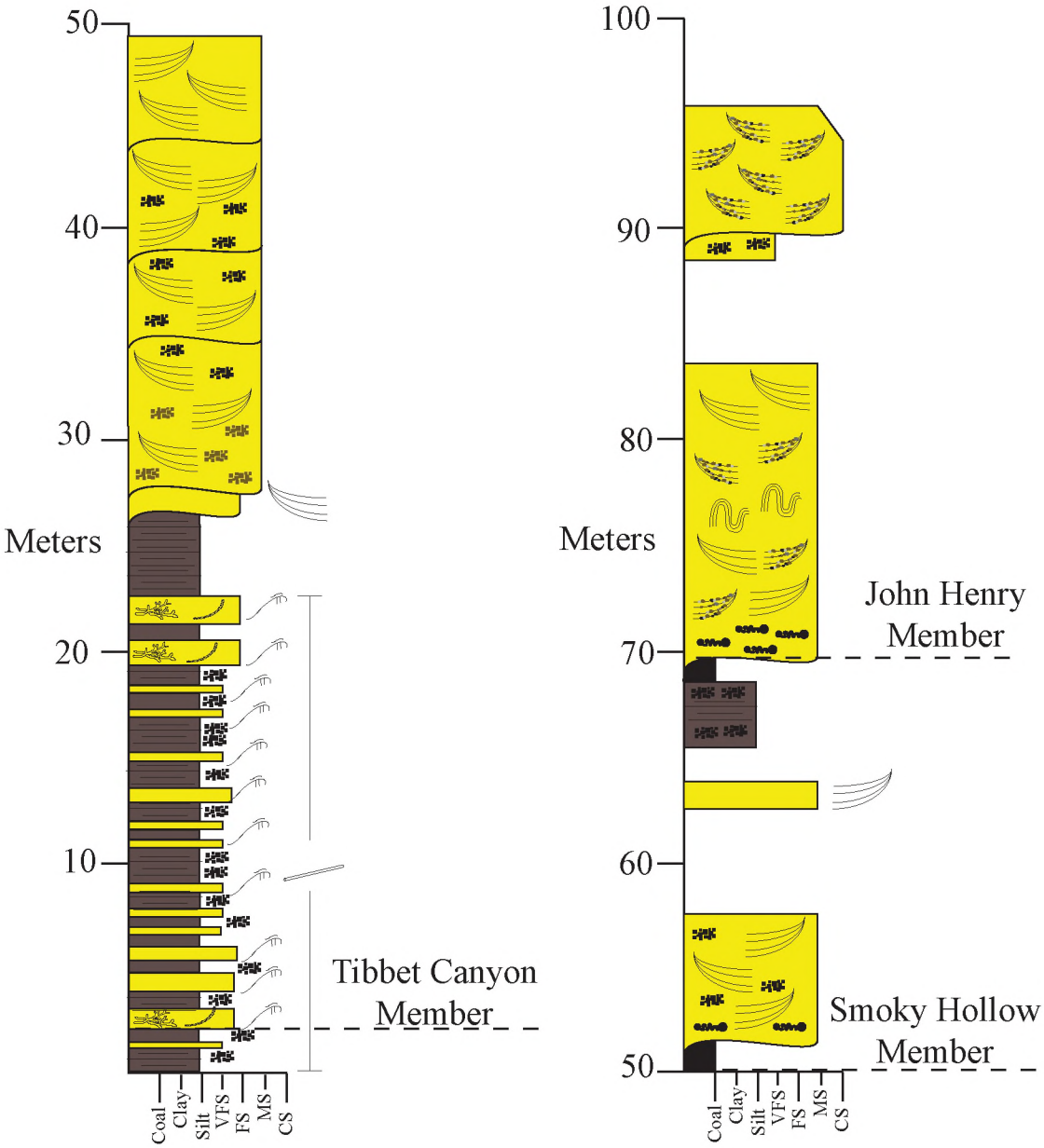

Rock House Cove Section 3

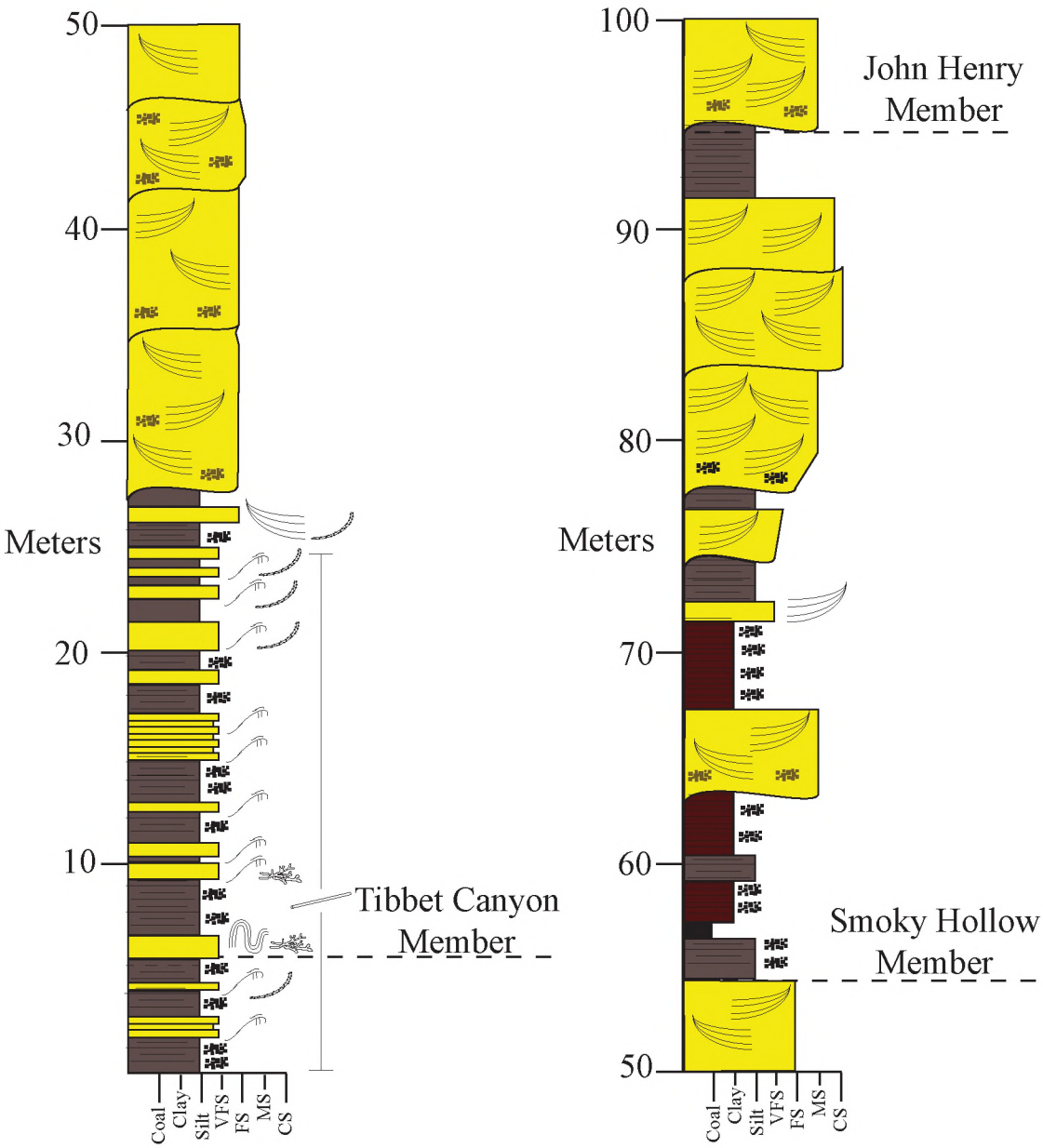

Coyote Springs Canyon Section

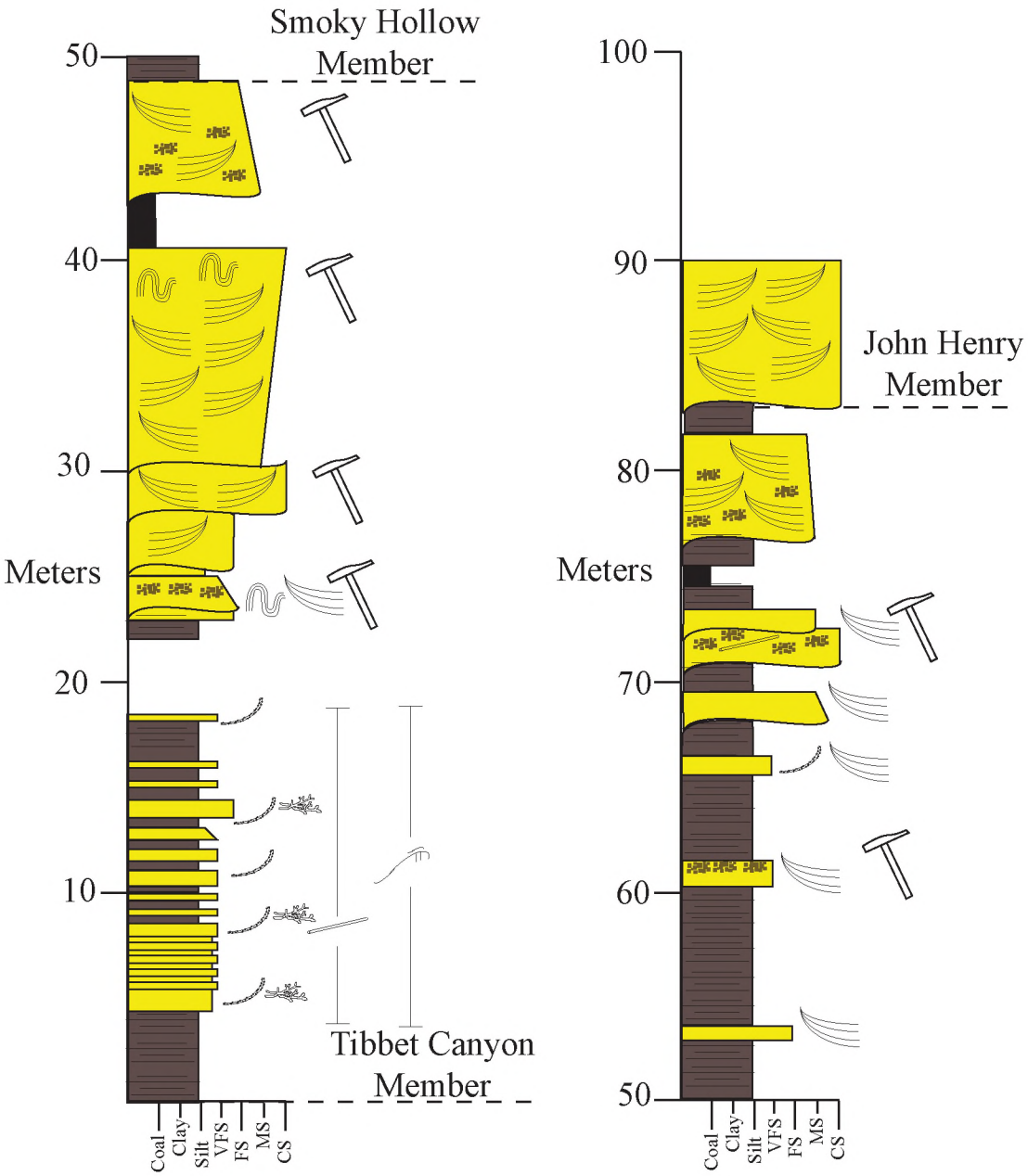

Blue Cove Section

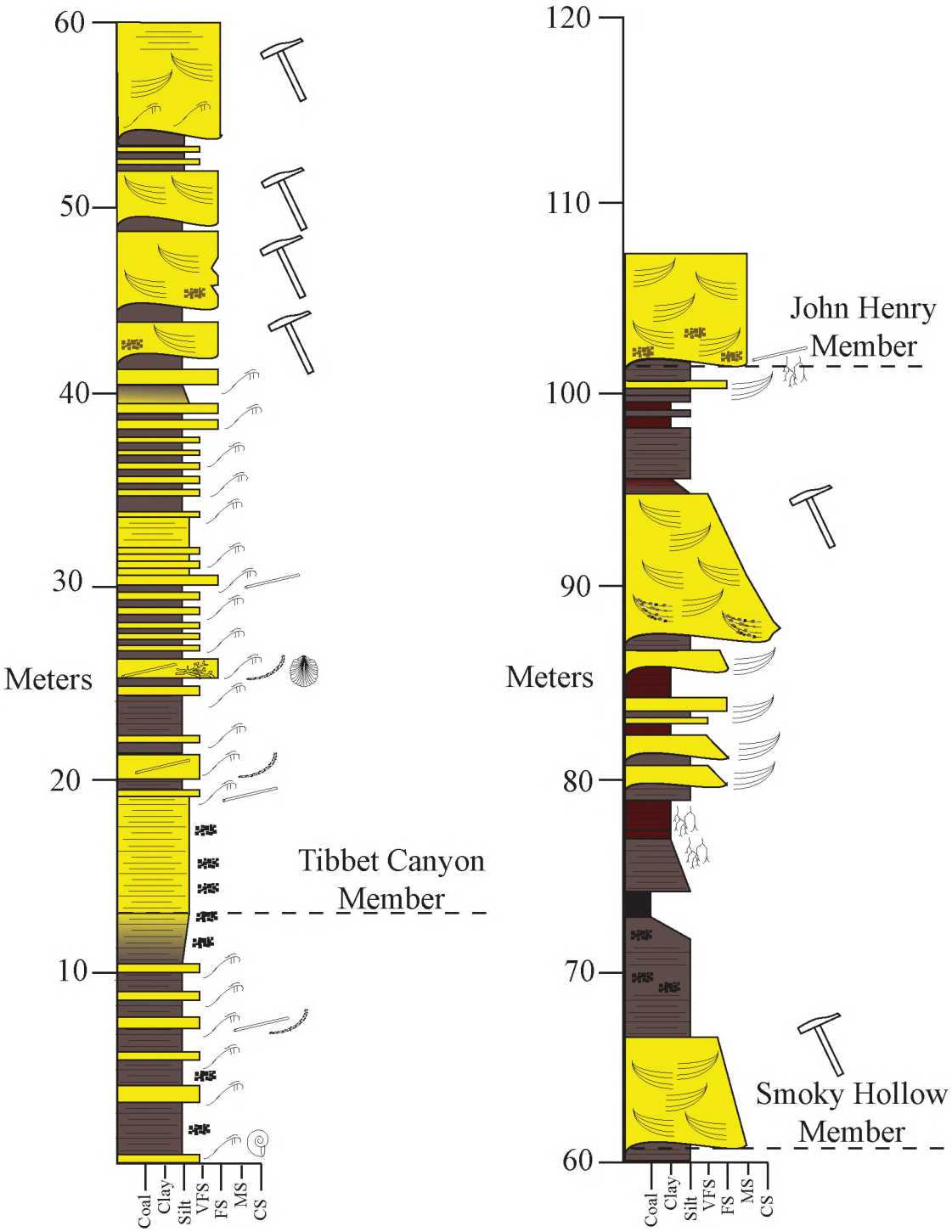

Ty Hatch Canyon Section 1

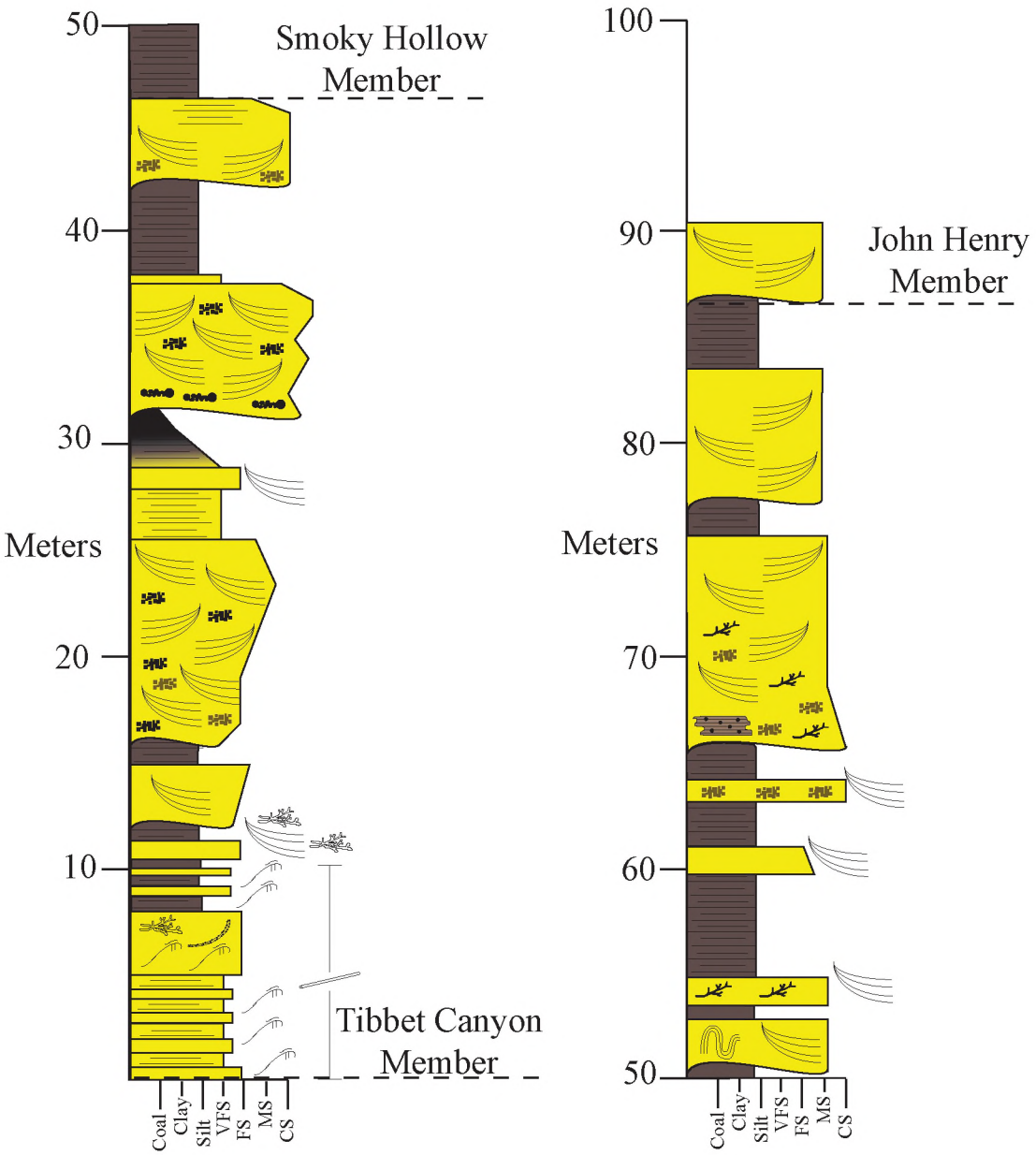

Ty Hatch Canyon Section 2

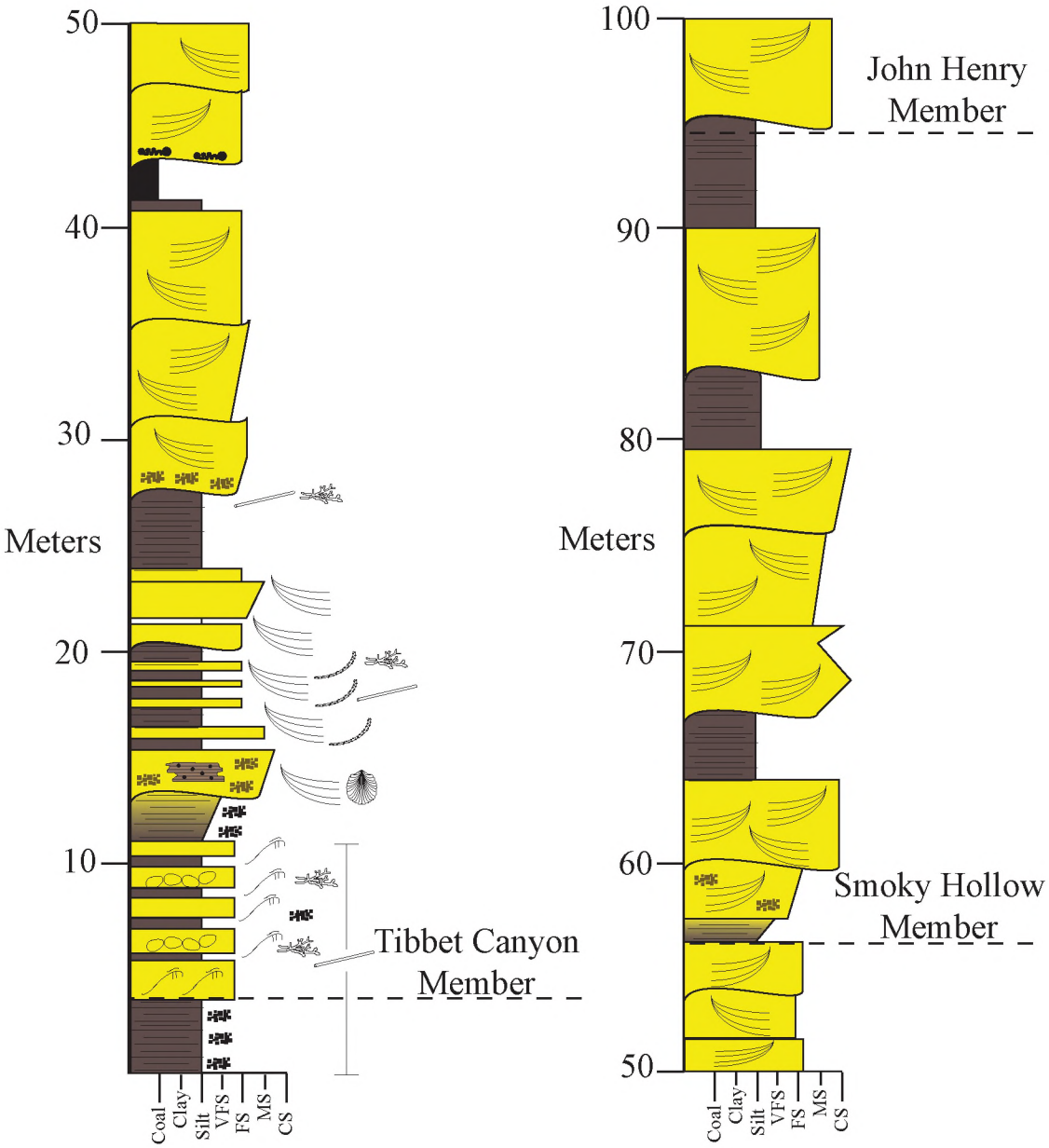

APPENDIX B

VISUALIZATION TEST BLANK SURVEY SHEETS

Appendix B comprises examples of the blank survey sheets provided for the visualization test outlined in Chapter 2. The survey sheet consists of three pages with both the no scaling version and scaling version provided. The first page of the survey contains simple demographic questions as well as a short background of the Gigapan system and Range Creek Canyon where the photopanoramas were taken. The second page pertains to part one of the exercise for both the Nelson Canyon and Stone House Canyon panoramas. Once estimates were given, participants were asked to describe the process they used to determine their estimates as well as how confident they thought their estimates were. For the scaling group, scaling cues (distance to and the height of the cliffs) are provided for each panorama. The third page of the survey pertains to part two of the exercise with the same layout as part one. Once again, the same scaling cues were provided for each panorama.

General Information

Name_____ Date_____

Age_____ Gender_____

Expected Degree (Circle One) BS/MS/PhD Expected Graduation Year_____

Major/Degree Focus (Geology, Geophysics, Geological Engineering, Education, Other)

On average, How many hours do you spend outdoors each week?_____

What types of outdoor activities do you participate in?

This exercise is designed to help us gather information about spatial thinking and visualization skills in geoscience education. You will be asked to estimate the dimensions of rock outcrops from photopanoramas. These special panoramas are created using Gigapan technology (for more info see http://www.gigapansystems.com/). Please note that your responses will be held confidential (all identifying information will be removed before any results are published), and in no way will this impact your grade or progress towards your degree. We would also appreciate it if you did not discuss the details of this exercise with others, as we are always seeking more test participants. Thanks for your time!

The panoramas used in exercise 1 were taken from Range Creek Canyon within the Book Cliffs, Utah. The canyon consists of sandstone, mudstone, and carbonates deposited by rivers flowing into ancient Lake Uinta during the Eocene (~60-45 Ma). Range Creek is also well known for its extensive archaeological sites left behind by the Fremont Indians.

Exercise Size Estimates

Materials
Computer with internet connection
START HERE: http://www.earth.utah.edu/basins/UDOM/

No Scaling Group – Part One
Directions. Size Estimates (3 Minutes to Complete)
Answer the following questions and turn this sheet in. Using the two panoramas provided on the main web page, estimate the height of the three red boxes. You may use feet or meters but please specify what units you are using.

Nelson Canyon (90 seconds)

Left Box	Center Box	Right Box
Height (ft or m)_____	Height (ft or m)_____	Height (ft or m)_____

Stone House Overview (90 seconds)

Left Box	Center Box	Right Box
Height (ft or m)_____	Height (ft or m)_____	Height (ft or m)_____

Part One Response
Describe the process you used to estimate the size of the boxes:

How confident are you in your measurements (i.e., I think I am within __ feet or meters from the true measurement)?

Turn in this sheet before proceeding.

Part Two. Interactive Estimates (5 Minutes to Complete)

Use the computer to bring up the same photopanoramas, now in an interactive format, on the screen following the links below (or from the main web page). There is a navigation bar on the left that allows you to zoom in and out and move around the panorama. You can also navigate with your mouse wheel. Spend 2 minutes to learn the controls and navigation.

You will then be asked to estimate the height of three more boxes on each image. You may use feet or meters but please specify what units you are using.

Nelson Canyon (90 seconds)

http://www.earth.utah.edu/basins/UDOM/Part2_NC.html

Left Box	Center Box	Right Box
Height (ft or m)_____	Height (ft or m)_____	Height (ft or m)_____

Stone House Overview (90 seconds)

http://www.earth.utah.edu/basins/UDOM/Part2_SHC.html

Left Box	Center Box	Right Box
Height (ft or m)_____	Height (ft or m)_____	Height (ft or m)_____

Part Two Response

Describe the process you used to estimate the size of the boxes:

How confident are you in your measurements (i.e., I think I am within __ feet or meters from the true measurement)?

Turn in this sheet before proceeding

General Information

Name_____ Date_____

Age_____ Gender_____

Expected Degree (Circle One) BS/MS/PhD Expected Graduation Year_____

Major/Degree Focus (Geology, Geophysics, Geological Engineering, Education, Other)

On average, How many hours do you spend outdoors each week?_____

What types of outdoor activities do you participate in?

This exercise is designed to help us gather information about spatial thinking and visualization skills in geoscience education. You will be asked to estimate the dimensions of rock outcrops from photopanoramas. These special panoramas are created using Gigapan technology (for more info see http://www.gigapansystems.com/). Please note that your responses will be held confidential (all identifying information will be removed before any results are published), and in no way will this impact your grade or progress towards your degree. We would also appreciate it if you did not discuss the details of this exercise with others, as we are always seeking more test participants. Thanks for your time!

The panoramas used in exercise 1 were taken from Range Creek Canyon within the Book Cliffs, Utah. The canyon consists of sandstone, mudstone, and carbonates deposited by rivers flowing into ancient Lake Uinta during the Eocene (~60-45 Ma). Range Creek is also well known for its extensive archaeological sites left behind by the Fremont Indians.

Exercise Size Estimates

Materials
Computer with internet connection
START HERE: http://www.earth.utah.edu/basins/UDOM/

Scaling Group – Part One
Directions. Size Estimates (3 minutes to complete)
Answer the following questions and turn this sheet in. Using the two panoramas provided on the main web page, estimate the height of the three red boxes. You may use feet or meters but please specify what units you are using.

Nelson Canyon (90 seconds)
The distance to the base of the cliff in the Nelson Canyon panorama is approximately 30 m (100 ft) away. The cliffs are approximately 90m (300ft) tall at the highest point near the center.

Left Box	Center Box	Right Box
Height (ft or m)_____	Height (ft or m)_____	Height (ft or m)_____

Stone House Overview (90 seconds)
The cliffs in the foreground on the right side of the Stone House panorama (**green dot**) are approximately 1000m (3300ft) away and 400 m (1300 ft) tall. The distant cliffs in the center (**yellow dot**) are approximately 3600m (11,800 ft or 2.2 miles) away and 950 m (3100 ft) tall.

Left Box	Center Box	Right Box
Height (ft or m)_____	Height (ft or m)_____	Height (ft or m)_____

Part One Response
Describe the process you used to estimate the size of the boxes:

How confident are you in your measurements (i.e., I think I am within __ feet or meters from the true measurement)?

Turn in this sheet before proceeding

Part Two. Interactive Comparison (5 Minutes to Complete)

Use the computer to bring up the same photopanoramas, now in an interactive format, on the screen following the links below (or from the main web page). There is a navigation bar on the left that allows you to zoom in and out and move around the panorama. You can also navigate with your mouse wheel. Spend 2 minutes to learn the controls and navigation.

You will then be asked to estimate the height of three more boxes on each image. You may use feet or meters but please specify what units you are using.

Nelson Canyon (90 seconds)
http://www.earth.utah.edu/basins/UDOM/Part2_NC.html
The distance to the base of the cliff in the Nelson Canyon panorama is approximately 30 m (100 ft) away. The cliffs are approximately 90m (300ft) tall at the highest point near the center.

Left Box	Center Box	Right Box
Height (ft or m)_____	Height (ft or m)_____	Height (ft or m)_____

Stone House Overview (90 seconds)
http://www.earth.utah.edu/basins/UDOM/Part2_SHC.html
The cliffs in the foreground on the right side of the Stone House panorama (**green dot**) are approximately 1000m (3300ft) away and 400 m (1300 ft) tall. The distant cliffs in the center (**yellow dot**) are approximately 3600m (11,800 ft or 2.2 miles) away and 950 m (3100 ft) tall.

Left Box	Center Box	Right Box
Height (ft or m)_____	Height (ft or m)_____	Height (ft or m)_____

Part Two Response
Describe the process you used to estimate the size of the boxes:

How confident are you in your measurements (i.e., I think I am within __ feet or meters from the true measurement)?

Turn in this sheet

APPENDIX C

DATA TABLES

Paleocurrent Measurements

A total of 807 paleocurrent and accretion set measurements were acquired from Rock House Cove (RHC) (Table C.1), Coyote Springs Canyon (CSC) (Table C.2), Blue Cove (BC) (Table C.3), and Ty Hatch Canyon (THC) (Table C.4) across the transect A-A' outlined in Figure 1.1. Measurements were taken from depositional units 1-4 where present. In Tables C.1 through C.4 abbreviations are as follows: RHC = Rock House Cove, CSC = Coyote Springs Canyon, BC = Blue Cove, and THC = Ty Hatch Canyon, TCS = trough cross stratification, AS = accretion sets, and IHS = inclined heterolithic strata. Data are divided by depositional units and designated sections. Interpretations of paleotransport are discussed in Chapter 1 and summarized in Figure 1.6.

Participant Estimates Data and Calculations

Table C.5 contains the raw data of participant's (n=63) estimates for part one and part two of the visualization test discussed in Chapter 2. Estimates were given in feet or meters or both, and then converted to meters for comparison. Both parts of the exercise contain two panoramas, Nelson Canyon and Stone House Canyon. Each panorama contained three boxes (left, center, and right) for a combined total of 12 estimates per

Table C.1

Rock House Cove Measurements

Canyon	DU	Dip	Dip Direction	Structure
RHC	1	18	007	TCB
RHC	1	10	308	TCB
RHC	1	17	032	TCB
RHC	1	07	008	TCB
RHC	1	13	354	TCB
RHC	1	27	058	TCB
RHC	1	12	182	TCB
RHC	1	16	193	TCB
RHC	1	28	332	TCB
RHC	1	10	054	TCB
RHC	1	13	328	TCB
RHC	1	15	060	TCB
RHC	1	09	050	TCB
RHC	1	12	033	TCB
RHC	1	09	012	TCB
RHC	1	10	030	TCB
RHC	1	07	085	TCB
RHC	1	09	043	TCB
RHC	1	11	345	TCB
RHC	1	12	248	TCB
RHC	1	15	305	TCB
RHC	1	17	334	TCB
RHC	1	09	004	TCB
RHC	1	10	329	TCB
RHC	1	18	063	TCB
RHC	1	10	066	TCB
RHC	1	16	009	TCB
RHC	1	20	032	TCB
RHC	1	16	318	TCB
RHC	1	17	087	TCB
RHC	1	16	022	TCB
RHC	1	17	330	TCB
RHC	1	06	210	TCB
RHC	1	07	351	TCB
RHC	1	09	253	TCB
RHC	1	20	320	TCB
RHC	1	09	344	TCB
RHC	1	10	318	TCB
RHC	1	19	309	TCB
RHC	1	20	279	TCB
RHC	1	08	289	TCB
RHC	1	20	115	TCB
RHC	1	05	175	TCB
RHC	1	24	325	TCB
RHC	1	07	270	TCB
RHC	1	09	357	TCB
RHC	1	11	254	TCB
RHC	1	15	230	TCB
RHC	1	09	072	TCB
RHC	1	10	090	TCB
RHC	1	08	234	TCB
RHC	1	12	104	TCB
RHC	1	22	063	TCB
RHC	1	17	120	TCB
RHC	1	03	212	TCB
RHC	1	15	083	TCB
RHC	1	17	088	TCB
RHC	1	08	018	TCB
RHC	1	12	110	TCB
RHC	1	15	163	TCB
RHC	1	27	156	TCB
RHC	1	13	089	TCB
RHC	1	16	097	TCB
RHC	1	10	060	TCB
RHC	1	23	094	TCB
RHC	1	28	099	TCB
RHC	1	10	106	TCB
RHC	1	10	340	TCB
RHC	1	15	275	TCB
RHC	1	09	208	TCB
RHC	1	13	064	TCB
RHC	1	12	073	TCB
RHC	1	08	263	TCB
RHC	1	05	066	TCB
RHC	1	18	142	TCB

Table C.1 Continued

Canyon	DU	Dip	Dip Direction	Structure
RHC	1	17	346	TCB
RHC	1	18	150	TCB
RHC	1	09	178	TCB
RHC	1	17	140	TCB
RHC	1	22	177	TCB
RHC	1	24	184	TCB
RHC	1	23	130	TCB
RHC	1	15	125	TCB
RHC	1	12	252	TCB
RHC	1	13	116	TCB
RHC	1	16	240	TCB
RHC	1	15	046	TCB
RHC	1	13	128	TCB
RHC	1	17	189	TCB
RHC	1	09	040	TCB
RHC	1	18	218	TCB
RHC	1	10	346	TCB
RHC	1	18	135	TCB
RHC	1	15	086	TCB
RHC	1	12	187	TCB
RHC	1	19	250	TCB
RHC	1	17	070	TCB
RHC	1	16	052	TCB
RHC	1	11	090	TCB
RHC	1	28	169	TCB
RHC	3	16	215	TCB
RHC	3	06	136	TCB
RHC	3	18	294	TCB
RHC	3	24	317	TCB
RHC	3	20	300	TCB
RHC	3	15	115	TCB
RHC	3	25	280	TCB
RHC	3	11	018	TCB
RHC	3	12	322	TCB
RHC	3	19	279	TCB
RHC	3	13	26	TCB
RHC	3	21	284	TCB
RHC	3	27	270	TCB
RHC	3	10	013	TCB
RHC	3	14	352	TCB
RHC	3	21	308	TCB
RHC	3	23	314	TCB
RHC	3	08	266	TCB
RHC	3	10	278	TCB
RHC	3	09	069	TCB
RHC	3	26	350	TCB
RHC	3	08	170	TCB
RHC	3	15	010	TCB
RHC	3	23	307	TCB
RHC	3	13	98	TCB
RHC	3	19	006	TCB
RHC	3	22	304	TCB
RHC	3	26	308	TCB
RHC	3	22	327	TCB
RHC	3	20	294	TCB
RHC	3	18	286	TCB
RHC	3	20	274	TCB
RHC	3	30	230	TCB
RHC	3	28	326	TCB
RHC	3	18	330	TCB
RHC	3	19	354	TCB
RHC	3	29	346	TCB
RHC	3	17	332	TCB
RHC	3	18	055	TCB
RHC	3	18	006	TCB
RHC	3	16	045	TCB
RHC	3	12	340	TCB
RHC	3	21	288	TCB
RHC	3	33	357	TCB
RHC	3	12	315	TCB
RHC	3	10	123	TCB
RHC	3	4	076	TCB
RHC	3	19	339	TCB
RHC	3	20	308	TCB
RHC	3	06	007	TCB
RHC	3	17	330	TCB
RHC	3	18	54	TCB
RHC	3	13	135	TCB
RHC	3	12	112	TCB
RHC	3	26	025	TCB
RHC	3	12	220	TCB

Table C.1 Continued

Canyon	DU	Dip	Dip Direction	Structure
RHC	3	17	075	TCB
RHC	3	25	020	TCB
RHC	3	24	069	TCB
RHC	3	12	316	TCB
RHC	3	18	060	TCB
RHC	3	16	147	TCB
RHC	3	07	286	TCB
RHC	3	18	276	TCB
RHC	3	28	127	TCB
RHC	3	15	019	TCB
RHC	3	12	310	TCB
RHC	3	20	058	TCB
RHC	3	18	007	TCB
RHC	3	05	023	TCB
RHC	3	19	271	TCB
RHC	3	20	020	TCB
RHC	3	10	313	TCB
RHC	3	11	257	TCB
RHC	3	25	064	TCB
RHC	3	22	072	TCB
RHC	3	18	029	TCB
RHC	3	21	035	TCB
RHC	3	18	076	TCB
RHC	3	23	014	TCB
RHC	3	23	034	TCB
RHC	3	12	312	TCB
RHC	3	10	093	TCB
RHC	3	19	343	TCB
RHC	3	16	324	TCB
RHC	3	20	320	TCB
RHC	3	17	279	TCB
RHC	3	13	015	TCB
RHC	3	15	065	TCB
RHC	3	12	260	TCB
RHC	3	17	254	TCB
RHC	3	20	262	TCB
RHC	3	19	074	TCB
RHC	3	20	176	TCB
RHC	3	06	147	TCB
RHC	3	05	250	TCB
RHC	3	10	153	TCB
RHC	3	18	114	TCB
RHC	3	13	110	TCB
RHC	3	20	092	TCB

Table C.2

Coyote Springs Canyon Measurements

Canyon	DU	Dip	Dip Direction	Structure
CS	1	22	003	TCB
CS	1	15	345	TCB
CS	1	14	054	TCB
CS	1	28	046	TCB
CS	1	10	020	TCB
CS	1	15	050	TCB
CS	1	18	005	TCB
CS	1	12	233	TCB
CS	1	24	346	TCB
CS	1	26	029	TCB
CS	1	30	174	TCB
CS	1	07	276	TCB
CS	1	18	235	TCB
CS	1	10	013	TCB
CS	1	16	330	TCB
CS	1	12	316	TCB
CS	1	13	355	TCB
CS	1	09	346	TCB
CS	1	09	215	TCB
CS	1	16	356	TCB
CS	1	18	034	TCB
CS	1	15	345	TCB
CS	1	17	016	TCB
CS	1	11	303	TCB
CS	1	06	156	TCB
CS	1	11	028	TCB
CS	1	13	325	TCB
CS	1	12	004	TCB
CS	1	15	340	TCB
CS	1	09	321	TCB
CS	1	11	309	TCB
CS	1	21	300	TCB
CS	1	10	057	TCB
CS	1	07	167	TCB
CS	1	10	252	TCB
CS	1	11	287	TCB
CS	1	06	239	TCB
CS	1	15	350	TCB
CS	1	11	345	TCB
CS	1	17	036	TCB
CS	1	16	012	TCB
CS	1	18	339	TCB
CS	1	12	011	TCB
CS	1	20	323	TCB
CS	1	13	040	TCB
CS	1	31	055	TCB
CS	1	17	301	TCB
CS	1	20	037	TCB
CS	1	15	018	TCB
CS	1	19	302	TCB
CS	1	11	316	TCB
CS	1	10	355	TCB
CS	1	19	298	TCB
CS	1	17	356	TCB
CS	1	10	252	TCB
CS	1	06	176	TCB
CS	1	12	106	TCB
CS	1	05	252	TCB
CS	1	16	357	TCB
CS	1	06	308	TCB
CS	1	17	034	TCB
CS	1	17	240	TCB
CS	1	03	126	TCB
CS	1	18	298	TCB
CS	1	19	027	TCB
CS	1	17	345	TCB
CS	1	12	318	TCB
CS	1	16	050	TCB
CS	1	10	026	TCB
CS	1	10	075	TCB
CS	1	20	304	TCB
CS	1	06	242	TCB
CS	1	22	009	TCB
CS	1	07	357	TCB
CS	1	10	008	TCB

Table C.2 Continued

Canyon	DU	Dip	Dip Direction	Structure
CS	1	17	056	TCB
CS	1	20	032	TCB
CS	1	21	106	TCB
CS	1	19	010	TCB
CS	1	26	017	TCB
CS	1	15	349	TCB
CS	1	12	014	TCB
CS	1	19	007	TCB
CS	1	12	260	TCB
CS	1	12	014	TCB
CS	1	13	005	TCB
CS	1	05	010	TCB
CS	1	09	002	TCB
CS	1	22	024	TCB
CS	1	09	011	TCB
CS	1	12	348	TCB
CS	1	12	018	TCB
CS	1	22	015	TCB
CS	1	20	345	TCB
CS	1	16	340	TCB
CS	1	15	046	TCB
CS	1	26	052	TCB
CS	1	14	073	TCB
CS	1	25	060	TCB
CS	3	09	249	TCB
CS	3	16	322	TCB
CS	3	07	184	TCB

Canyon	DU	Dip	Dip Direction	Structure
CS	3	13	045	TCB
CS	3	20	095	TCB
CS	3	19	138	AS
CS	3	09	166	TCB
CS	3	14	063	TCB
CS	3	12	037	TCB
CS	3	22	025	TCB
CS	3	17	132	TCB
CS	3	10	033	TCB
CS	3	16	055	TCB
CS	3	13	140	AS
CS	3	08	095	TCB
CS	3	22	185	TCB
CS	3	08	242	TCB
CS	3	17	092	TCB
CS	3	10	125	TCB
CS	3	08	094	TCB
CS	3	12	070	TCB
CS	3	14	145	TCB
CS	3	13	140	TCB
CS	3	19	109	TCB
CS	3	12	088	AS
CS	3	14	123	TCB
CS	3	09	166	TCB
CS	3	16	248	TCB
CS	3	12	164	TCB
CS	3	15	076	AS

Canyon	DU	Dip	Dip Direction	Structure
CS	3	19	175	TCB
CS	3	04	167	TCB
CS	3	09	305	TCB
CS	3	19	073	TCB
CS	3	05	171	TCB
CS	3	16	230	TCB
CS	3	12	055	AS
CS	3	17	133	TCB
CS	3	20	193	TCB
CS	3	13	354	TCB
CS	3	13	206	TCB
CS	3	04	358	TCB
CS	3	11	015	TCB
CS	3	05	212	TCB
CS	3	09	190	TCB
CS	3	10	214	TCB
CS	3	16	143	TCB
CS	3	11	176	AS
CS	3	14	086	TCB
CS	3	10	009	TCB
CS	3	05	105	TCB
CS	3	11	012	TCB
CS	3	15	244	TCB
CS	3	07	194	TCB
CS	3	12	035	TCB
CS	3	10	053	TCB
CS	3	12	026	TCB

Table C.2 Continued

Canyon	DU	Dip	Dip Direction	Structure
CS	3	10	115	TCB
CS	3	10	062	TCB
CS	3	17	056	TCB
CS	3	16	114	TCB
CS	3	12	036	TCB
CS	3	09	066	TCB
CS	3	08	102	TCB
CS	3	12	147	TCB
CS	3	07	032	TCB
CS	3	10	068	TCB
CS	3	18	103	TCB
CS	3	15	105	TCB
CS	3	18	084	TCB
CS	3	09	032	TCB
CS	3	10	164	AS
CS	3	19	124	TCB
CS	3	16	143	TCB
CS	3	07	137	TCB
CS	3	10	063	TCB
CS	3	11	122	TCB
CS	3	23	168	TCB
CS	3	15	144	TCB
CS	3	12	196	TCB
CS	3	13	030	TCB
CS	3	14	174	TCB
CS	3	06	104	TCB
CS	3	21	100	TCB
CS	3	20	052	TCB
CS	3	09	027	TCB
CS	3	27	104	TCB
CS	3	06	063	TCB
CS	3	18	096	TCB
CS	3	07	046	TCB
CS	3	12	129	TCB
CS	3	15	104	TCB
CS	3	17	090	TCB
CS	3	86	086	TCB
CS	3	12	212	TCB
CS	3	14	189	TCB
CS	3	15	139	TCB
CS	3	15	138	AS
CS	3	22	269	TCB
CS	3	17	200	TCB
CS	3	20	158	TCB
CS	3	19	113	TCB
CS	3	10	23	TCB
CS	3	18	182	TCB
CS	3	12	010	TCB
CS	3	16	040	TCB
CS	3	08	097	TCB
CS	3	13	143	TCB
CS	4	09	064	TCB
CS	4	18	282	TCB
CS	4	08	018	TCB
CS	4	12	222	TCB
CS	4	12	256	TCB
CS	4	14	284	TCB
CS	4	19	224	AS
CS	4	19	252	TCB
CS	4	17	286	TCB
CS	4	08	134	TCB
CS	4	19	064	TCB
CS	4	12	009	TCB
CS	4	13	215	AS
CS	4	08	238	AS
CS	4	22	322	TCB
CS	4	21	018	TCB
CS	4	11	268	TCB
CS	4	25	346	TCB
CS	4	13	028	TCB
CS	4	12	342	TCB
CS	4	18	058	TCB
CS	4	06	224	TCB
CS	4	04	136	TCB
CS	4	12	294	TCB
CS	4	13	272	TCB
CS	4	18	304	TCB
CS	4	13	129	TCB
CS	4	12	012	TCB
CS	4	17	008	TCB
CS	4	22	015	TCB

Table C.2 Continued

Canyon	DU	Dip	Dip Direction	Structure
CS	4	18	324	TCB
CS	4	12	335	TCB
CS	4	18	134	TCB
CS	4	13	166	TCB
CS	4	12	126	TCB
CS	4	14	068	AS
CS	4	17	215	TCB
CS	4	09	184	TCB
CS	4	10	339	TCB
CS	4	18	238	TCB
CS	4	12	074	AS
CS	4	11	208	TCB
CS	4	19	186	TCB
CS	4	12	272	TCB
CS	4	13	168	TCB
CS	4	13	028	TCB
CS	4	09	164	TCB
CS	4	22	158	TCB
CS	4	12	168	TCB
CS	4	10	284	AS
CS	4	15	218	TCB
CS	4	12	254	TCB
CS	4	18	202	AS
CS	4	19	153	TCB
CS	4	09	291	TCB
CS	4	10	202	TCB
CS	4	18	274	TCB

Canyon	DU	Dip	Dip Direction	Structure
CS	4	05	018	AS
CS	4	12	130	TCB
CS	4	08	354	TCB
CS	4	22	106	TCB
CS	4	17	353	TCB
CS	4	12	339	TCB
CS	4	13	064	AS
CS	4	19	032	TCB
CS	4	13	146	TCB
CS	4	10	170	TCB
CS	4	12	212	TCB
CS	4	19	068	TCB
CS	4	14	074	TCB
CS	4	17	009	AS
CS	4	12	012	AS
CS	4	12	094	TCB
CS	4	22	290	TCB
CS	4	21	109	TCB
CS	4	13	306	TCB
CS	4	18	063	TCB
CS	4	18	008	AS
CS	4	10	060	TCB
CS	4	18	029	TCB
CS	4	07	074	TCB
CS	4	12	348	TCB
CS	4	12	326	TCB
CS	4	18	094	TCB

Canyon	DU	Dip	Dip Direction	Structure
CS	4	09	024	TCB
CS	4	15	060	AS
CS	4	19	079	TCB
CS	4	10	113	TCB
CS	4	17	116	TCB
CS	4	06	294	TCB
CS	4	11	029	AS
CS	4	18	007	TCB
CS	4	11	089	TCB
CS	4	16	046	TCB
CS	4	20	090	TCB
CS	4	18	014	TCB
CS	4	10	049	TCB
CS	4	07	048	AS
CS	4	18	065	TCB
CS	4	10	010	TCB
CS	4	20	064	TCB
CS	4	04	192	TCB
CS	4	20	186	TCB
CS	4	03	294	TCB
CS	4	10	008	TCB
CS	4	13	048	TCB
CS	4	07	280	TCB
CS	4	18	150	TCB
CS	4	10	012	TCB
CS	4	18	308	TCB
CS	4	05	295	TCB

Table C.2 Continued

Canyon	DU	Dip	Dip Direction	Structure
CS	4	13	136	TCB
CS	4	17	033	TCB
CS	4	11	034	TCB
CS	4	16	033	AS

Table C.3

Blue Cove Measurements

Canyon	DU	Dip	Dip Direction	Structure
BC	1	18	020	TCB
BC	1	20	208	TCB
BC	1	14	355	TCB
BC	1	10	044	TCB
BC	1	10	006	TCB
BC	1	12	320	TCB
BC	1	09	207	TCB
BC	1	12	010	TCB
BC	1	08	326	TCB
BC	1	12	144	TCB
BC	1	03	098	TCB
BC	1	08	032	TCB
BC	1	07	206	TCB
BC	1	11	304	TCB
BC	1	12	011	TCB
BC	1	12	347	TCB
BC	1	18	335	TCB
BC	1	10	004	TCB
BC	1	12	058	TCB
BC	1	09	318	TCB
BC	2	18	334	IHS
BC	2	15	276	IHS
BC	2	22	316	IHS
BC	2	26	272	IHS
BC	2	19	243	IHS
BC	2	9	248	IHS
BC	2	14	64	IHS
BC	2	11	137	IHS
BC	2	17	144	IHS
BC	2	14	192	IHS
BC	3	18	274	TCB
BC	3	14	244	TCB
BC	3	19	317	TCB
BC	3	19	298	TCB
BC	3	20	352	TCB
BC	3	20	042	TCB
BC	3	18	325	TCB
BC	3	17	004	TCB
BC	3	22	024	TCB
BC	3	10	083	TCB
BC	3	21	030	TCB
BC	3	20	044	TCB
BC	3	10	162	TCB
BC	3	11	002	TCB
BC	3	25	350	TCB
BC	3	27	308	TCB
BC	3	19	039	TCB
BC	3	20	001	TCB
BC	3	10	014	TCB
BC	3	13	015	TCB
BC	3	15	033	TCB
BC	3	21	354	TCB
BC	3	25	326	TCB
BC	3	20	032	TCB
BC	3	24	001	TCB
BC	3	16	005	TCB
BC	3	10	235	TCB
BC	3	13	039	TCB
BC	3	19	066	TCB
BC	3	13	033	TCB
BC	3	19	351	TCB
BC	3	27	340	TCB
BC	3	18	064	TCB
BC	3	15	078	TCB
BC	3	22	010	TCB
BC	3	19	048	TCB
BC	3	13	053	TCB
BC	3	16	304	TCB
BC	3	21	307	TCB
BC	3	16	003	TCB
BC	3	13	274	TCB
BC	3	21	011	TCB
BC	3	12	342	TCB
BC	3	16	292	TCB
BC	3	13	352	TCB

Table C.3 Continued

Canyon	DU	Dip	Dip Direction	Structure
BC	3	15	316	TCB
BC	3	25	023	TCB
BC	3	28	035	TCB
BC	3	20	053	TCB
BC	3	18	066	TCB
BC	3	16	355	TCB
BC	3	12	190	TCB
BC	3	15	314	TCB
BC	3	18	323	TCB
BC	3	22	340	TCB
BC	3	09	059	TCB
BC	3	14	003	TCB
BC	3	19	345	TCB
BC	3	12	315	TCB
BC	3	17	067	TCB
BC	3	15	015	TCB
BC	3	22	028	TCB
BC	3	15	072	TCB
BC	3	22	035	TCB
BC	3	14	328	TCB
BC	3	13	358	TCB
BC	3	21	342	TCB
BC	3	17	045	TCB
BC	3	12	125	TCB
BC	3	17	058	TCB
BC	3	09	080	TCB
BC	3	10	049	TCB

Canyon	DU	Dip	Dip Direction	Structure
BC	3	10	098	TCB
BC	3	15	328	TCB
BC	3	22	312	TCB
BC	3	20	053	TCB
BC	3	09	040	TCB
BC	3	16	010	TCB
BC	3	18	046	TCB
BC	3	20	006	TCB
BC	3	17	313	TCB
BC	3	12	032	TCB
BC	3	09	277	TCB
BC	3	13	202	TCB
BC	3	11	016	TCB
BC	3	26	358	TCB
BC	3	20	044	TCB
BC	3	16	013	TCB
BC	3	25	060	TCB
BC	3	20	349	TCB
BC	3	14	010	TCB
BC	3	18	012	TCB
BC	3	17	196	TCB
BC	3	32	005	TCB
BC	3	06	084	TCB
BC	3	26	009	TCB
BC	3	23	020	TCB
BC	3	19	357	TCB
BC	3	20	060	TCB

Canyon	DU	Dip	Dip Direction	Structure
BC	3	15	145	TCB
BC	4	12	136	TCB
BC	4	16	112	TCB
BC	4	17	336	TCB
BC	4	05	285	TCB
BC	4	13	010	AS
BC	4	12	132	TCB
BC	4	22	135	TCB
BC	4	08	280	TCB
BC	4	19	124	TCB
BC	4	17	078	TCB
BC	4	12	045	TCB
BC	4	06	128	TCB
BC	4	07	026	AS
BC	4	05	167	TCB
BC	4	15	056	TCB
BC	4	09	204	TCB
BC	4	13	004	TCB
BC	4	12	147	TCB
BC	4	05	292	TCB
BC	4	15	248	TCB
BC	4	06	044	AS
BC	4	16	147	TCB
BC	4	12	153	TCB
BC	4	07	052	TCB
BC	4	12	078	TCB
BC	4	11	269	TCB

Table C.3 Continued

Canyon	DU	Dip	Dip Direction	Structure
BC	4	09	193	TCB
BC	4	22	057	TCB
BC	4	15	169	TCB
BC	4	14	059	TCB
BC	4	09	006	TCB
BC	4	08	231	TCB
BC	4	05	290	TCB
BC	4	06	263	TCB
BC	4	14	166	TCB
BC	4	12	050	TCB
BC	4	09	183	TCB
BC	4	04	194	TCB
BC	4	12	145	AS
BC	4	08	008	TCB
BC	4	09	029	TCB
BC	4	12	042	TCB
BC	4	13	082	TCB
BC	4	14	117	TCB
BC	4	09	025	TCB
BC	4	13	153	TCB
BC	4	20	106	TCB
BC	4	11	126	AS
BC	4	23	000	TCB
BC	4	19	126	TCB
BC	4	26	177	TCB
BC	4	13	163	TCB
BC	4	17	194	TCB

Canyon	DU	Dip	Dip Direction	Structure
BC	4	13	103	TCB
BC	4	19	294	TCB
BC	4	15	031	AS
BC	4	26	050	TCB
BC	4	10	206	TCB
BC	4	18	086	TCB
BC	4	07	189	TCB
BC	4	18	264	TCB
BC	4	10	009	TCB
BC	4	08	213	TCB
BC	4	12	252	TCB
BC	4	17	350	AS
BC	4	09	157	TCB
BC	4	05	150	TCB
BC	4	12	288	TCB
BC	4	13	279	TCB
BC	4	09	202	TCB
BC	4	20	206	TCB
BC	4	11	220	AS
BC	4	22	105	TCB
BC	4	17	224	TCB
BC	4	07	314	TCB
BC	4	22	103	TCB
BC	4	19	065	TCB
BC	4	22	082	TCB
BC	4	15	138	TCB
BC	4	17	096	TCB

Canyon	DU	Dip	Dip Direction	Structure
BC	4	10	126	AS
BC	4	07	133	TCB
BC	4	08	359	TCB
BC	4	15	027	TCB
BC	4	29	004	TCB
BC	4	22	296	TCB
BC	4	08	021	AS
BC	4	12	344	TCB
BC	4	17	109	TCB
BC	4	21	329	TCB
BC	4	17	226	TCB
BC	4	11	119	TCB
BC	4	23	138	TCB
BC	4	25	104	TCB
BC	4	09	152	TCB
BC	4	20	340	TCB
BC	4	11	036	TCB
BC	4	12	002	AS
BC	4	17	306	TCB
BC	4	12	283	TCB
BC	4	13	260	TCB
BC	4	17	230	AS
BC	4	13	093	TCB
BC	4	10	090	TCB
BC	4	12	145	TCB
BC	4	12	044	TCB
BC	4	20	346	TCB

Table C.3 Continued

Canyon	DU	Dip	Dip Direction	Structure
BC	4	23	347	TCB
BC	4	12	106	TCB
BC	4	16	325	AS
BC	4	21	354	TCB
BC	4	15	009	TCB
BC	4	16	309	TCB

Table C.4

Ty Hatch Canyon Measurements

Canyon	DU	Dip	Dip Direction	Structure
TH	4	11	116	TCB
TH	4	09	347	TCB
TH	4	22	085	TCB
TH	4	15	014	TCB
TH	4	09	012	TCB
TH	4	09	036	AS
TH	4	13	306	TCB
TH	4	13	054	TCB
TH	4	17	230	TCB
TH	4	10	028	TCB
TH	4	22	098	TCB
TH	4	11	029	AS
TH	4	18	067	TCB
TH	4	20	052	TCB
TH	4	10	044	TCB
TH	4	17	068	TCB
TH	4	07	094	AS
TH	4	11	059	TCB
TH	4	15	009	TCB
TH	4	10	276	TCB
TH	4	18	103	TCB
TH	4	15	028	AS
TH	4	05	251	TCB
TH	4	23	068	TCB
TH	4	09	257	TCB
TH	4	23	023	TCB
TH	4	13	067	AS
TH	4	17	115	TCB
TH	4	20	135	TCB
TH	4	19	043	TCB
TH	4	12	064	TCB
TH	4	20	132	TCB
TH	4	11	004	TCB
TH	4	10	173	TCB
TH	4	18	074	TCB
TH	4	14	033	AS
TH	4	11	222	TCB
TH	4	12	045	TCB
TH	4	14	068	AS
TH	4	08	072	AS
TH	4	15	013	TCB
TH	4	19	007	TCB
TH	4	17	043	TCB
TH	4	18	093	AS
TH	4	22	356	TCB
TH	4	18	348	TCB
TH	4	12	005	AS
TH	4	12	002	TCB
TH	4	11	066	TCB
TH	4	17	096	AS
TH	4	18	345	TCB
TH	4	16	324	TCB
TH	4	15	036	AS
TH	4	12	033	TCB
TH	4	12	034	AS
TH	4	13	020	TCB
TH	4	18	100	TCB
TH	4	16	098	TCB
TH	4	13	023	AS
TH	4	11	254	TCB
TH	4	09	215	TCB
TH	4	06	084	AS
TH	4	13	023	TCB
TH	4	22	096	TCB
TH	4	18	052	TCB
TH	4	16	076	TCB
TH	4	12	001	TCB
TH	4	11	108	TCB
TH	4	10	067	AS
TH	4	7	022	TCB
TH	4	16	148	TCB
TH	4	13	140	TCB
TH	4	9	088	AS
TH	4	19	010	TCB
TH	4	13	076	TCB

Table C.4 Continued

Canyon	DU	Dip	Dip Direction	Structure
TH	4	21	025	TCB
TH	4	18	098	TCB
TH	4	11	085	AS
TH	4	12	076	AS
TH	4	22	176	TCB
TH	4	27	252	TCB
TH	4	9	112	AS
TH	4	12	101	TCB
TH	4	18	123	TCB
TH	4	6	056	TCB
TH	4	8	044	TCB
TH	4	16	098	TCB
TH	4	13	020	TCB
TH	4	12	033	TCB
TH	4	16	002	TCB
TH	4	16	025	AS
TH	4	11	023	TCB
TH	4	10	064	TCB
TH	4	9	280	TCB
TH	4	15	316	TCB
TH	4	29	233	TCB
TH	4	12	154	TCB
TH	4	17	199	TCB
TH	4	14	014	AS
TH	4	18	066	AS

Table C.5
Participants Raw Data

Form #	Group	Gender	Age	Graduation Year	Degree	Experience	Major	Hours Spent Outside	Activities	Reported ft/m	Reported Estimates (ft/m)												Converted Estimates (m)											
											NC-1			SHC-1			NC-2			SHC-2			NC-1			SHC-1			NC-2			SHC-2		
N=63											Left	Center	Right	Left	Center	Right	Left	Center	Right	Left	Center	Right	Left	Center	Right	Left	Center	Right	Left	Center	Right	Left	Center	Right
1	NS	m	22	2010	BS	UG	Geology	17	Snowboarding, Hiking, Backpacking, Mountain Biking, Fishing	ft	10	15	10	30	40	20	25	15	8	45	35	40	3.0	4.6	3.0	9.1	12.2	6.1	7.6	4.6	2.4	13.7	10.7	12.2
2	NS	m	22	2010	MS	GR	Geology	10	Hiking, Fieldwork, Frisbee, Running	m	3	5	2.5	13	18	10	7	9	5	36	22	16	3.0	5.0	2.5	13.0	18.0	10.0	7.0	9.0	5.0	36.0	22.0	16.0
3	NS	m	25	2010	BS	UG	Geology	8	Skiing, Hiking, Camping, Mountain Biking, Sleeping	m	2	5	1	20	40	15	7	3	6	36	36	15	2.0	5.0	1.0	20.0	40.0	15.0	7.0	3.0	6.0	36.0	36.0	15.0
4	NS	f	25	2011	MS	GR	Geology	2	Hiking, Rockhounding, Cross-Country Skiing	ft	9	10	5	20	30	10	15	12	8	15	20	14	2.7	3.0	1.5	6.1	9.1	3.0	4.6	3.7	2.4	4.6	6.1	4.3
5	NS	f	30	2011	MS	GR	Geology	20	Climbing, Running, Hiking	ft	10	15	7	30	50	20	25	20	30	60	45	90	3.0	4.6	2.1	9.1	15.2	6.1	7.6	6.1	9.1	18.3	13.7	27.4
6	S	m	28	2013	PhD	GR	Geology	5	Hiking, Housework, Garden, Skiing, Site-seeing	ft/m	6ft	15ft	6ft	35m	50m	20m	12m	9m	6m	32m	40m	26m	1.8	4.6	1.8	35.0	50.0	20.0	12.0	9.0	6.0	32.0	40.0	26.0
7	S	m	26	2010	MS	GR	Geology	5	Bicycling, Walking, Hiking, Dog Walk	m	2	4	2	9	25	4	6	4	3	15	18	25	2.0	4.0	2.0	9.0	25.0	4.0	6.0	4.0	3.0	15.0	18.0	25.0
8	S	f	60	2011	PhD	GR	Geology	20	Cross Country Skiing, Hiking, Rafting	m	4	8	3	15	13	12	18	30	10	40	100	40	4.0	8.0	3.0	15.0	13.0	12.0	18.0	30.0	10.0	40.0	100.0	40.0
9	S	m	29	2010	PhD	GR	Geology	12	Skiing, Rock Climbing, Walking	m	8	15	6	25	50	15	10	7	6	10	15	12	8.0	15.0	6.0	25.0	50.0	15.0	10.0	7.0	6.0	10.0	15.0	12.0
10	S	f	25	2011	BS	UG	Geology	10	Skiing, Walking, Biking, Rock Climbing	ft	50	100	75	50	100	25	25	75	50	70	100	40	15.2	30.5	22.9	15.2	30.5	7.6	7.6	22.9	15.2	21.3	30.5	12.2
11	NS	m	26	2011	MS	GR	Geophysics	5	Traveling	m	15	30	20	60	75	45	15	6	8	100	160	20	15.0	30.0	20.0	60.0	75.0	45.0	15.0	6.0	8.0	100.0	160.0	20.0
12	NS	f	24	2010	BS	GR	Geology	10	Rock Climbing, Biking, Running	ft	2.5	5	3	40	100	10	20	5	6	40	60	30	0.8	1.5	0.9	12.2	30.5	3.0	6.1	1.5	1.8	12.2	18.3	9.1
13	NS	m	66	1965	PhDF	FAC	Geology	10	Fieldwork, Gardening, Hiking	m	3	5	2	20	30	10	6	11	6	10	10	12	3.0	5.0	2.0	20.0	30.0	10.0	6.0	11.0	6.0	10.0	10.0	12.0
14	NS	m	63	1974	PhDF	FAC	Geology	60	Fieldtrips	m	2	3	4	10	8	5	8	5	4	10	12	6	2.0	3.0	4.0	10.0	8.0	5.0	8.0	5.0	4.0	10.0	12.0	6.0
15	S	m	27	2010	MS	GR	Geology	25	Rock Climbing, Running, Hiking	ft/m	12ft	25ft	10ft	20m	100m	15m	30ft	45ft	30ft	25m	60m	25m	3.7	7.6	3.0	20.0	100.0	15.0	9.1	13.7	9.1	25.0	60.0	25.0
16	NS	f	22	2011	BS	UG	Geology	6	Skiing, Rock Climbing, Mountain Biking	m	10	15	6	100	150	50	15	5	8	300	200	100	10.0	15.0	6.0	100.0	150.0	50.0	15.0	5.0	8.0	300.0	200.0	100.0
17	NS	m	33	2011	PhD	GR	Geography	5	Skiing, Hiking, Motorcycling	m	1	1.5	1	16	30	5	20	2	5	10	30	6	1.0	1.5	1.0	16.0	30.0	5.0	20.0	2.0	5.0	10.0	30.0	6.0
18	S	m	36	2011	MS	GR	Geography/Poli. Sci.	5	Hiking, BMX	ft	70	90	45	100	500	80	80	95	80	75	1000	50	21.3	27.4	13.7	30.5	152.4	24.4	24.4	29.0	24.4	22.9	304.8	15.2
19	S	f	38	2013	PhD	GR	Geography	10	Skiing, Hiking, Biking	ft	180	100	245	1100	1300	750	200	120	250	1500	1800	800	54.9	30.5	74.7	335.3	396.2	228.6	61.0	36.6	76.2	457.2	548.6	243.8
20	S	m	45	2010	MS	GR	Geography	10	Snowboarding, Snowshoeing, Crosscountry Skiing, Hiking, Biking	m	10	20	15	40	80	40	10	20	15	50	80	40	10.0	20.0	15.0	40.0	80.0	40.0	10.0	20.0	15.0	50.0	80.0	40.0
21	S	f	33	2012	PhD	GR	Geography	8	Hiking	m	15	25	20	100	80	30	30	20	15	50	40	30	15.0	25.0	20.0	100.0	80.0	30.0	30.0	20.0	15.0	50.0	40.0	30.0
22	NS	m	26	2011	MS	GR	Geography	10	Walking, Running, Softball, Hiking, Frisbee	m	6	9	5	50	70	40	10	10	13	50	70	40	6.0	9.0	5.0	50.0	70.0	40.0	10.0	10.0	13.0	50.0	70.0	40.0
23	S	f	24	2011	MS	GR	Geography	10	Running, Biking, Hiking, Camping, Rock Climbing	m	20	35	25	70	120	100	6	10	8	35	60	70	20.0	35.0	25.0	70.0	120.0	100.0	6.0	10.0	8.0	35.0	60.0	70.0
24	NS	m	25	2011	BS	UG	Geology	14	Hiking, Camping, Biking, Backpacking	ft/m	11	105	5	6000ft	5000ft	1000ft	40ft	5ft	30ft	2000ft	1000ft	1000ft	11.0	105.0	5.0	1828.8	1524.0	304.8	12.2	1.5	9.1	609.6	304.8	304.8
25	S	m	31	2011	MS	GR	Geography	40	Work, Softball, Hiking, Fishing	ft	14	30	6	80	220	45	40	10	30	15	100	40	4.3	9.1	1.8	24.4	67.1	13.7	12.2	3.0	9.1	4.6	30.5	12.2
26	S	m	27	2010	BS	UG	Business	11	Sports, Reading	ft	20	50	15	100	300	100	30	15	20	120	160	80	6.1	15.2	4.6	30.5	91.5	30.5	9.1	4.6	6.1	36.6	48.8	24.4
27	S	f	19	2013	BS	UG	Theater	10	Dance, Sci Fi	ft	15	30	10	50	25	30	9	25	10	40	35	40	4.6	9.1	3.0	15.2	7.6	9.1	2.7	7.6	3.0	12.2	10.7	12.2
28	NS	m	22	2011	BS	UG	Manufacture Engineering	24	Canoeing/Camping, School	ft	120	130	80	400	700	500	60	11	16	20	200	60	36.6	39.6	24.4	122.0	213.4	152.4	18.3	3.4	4.9	6.1	61.0	18.3
29	NS	m	20	2013	BS	UG	Liberal Arts	20	Magic Cards, Videogames	m	10	20	1	40	60	30	30	20	10	100	60	80	10.0	20.0	1.0	40.0	60.0	30.0	30.0	20.0	10.0	100.0	60.0	80.0
30	S	m	25	2010	MS	GR	Geology	7	Hiking, Walking	ft	12	7	5	30	40	12	17	9	12	100	200	50	3.7	2.1	1.5	9.1	12.2	3.7	5.2	2.7	3.7	30.5	61.0	15.2
31	S	m	23	2011	BS	UG	Geology	10	Hiking, Swimming	m	8	15	4	30	100	15	8	12	7	25	50	20	8.0	15.0	4.0	30.0	100.0	15.0	8.0	12.0	7.0	25.0	50.0	20.0
32	NS	m	29	2014	PhD	GR	Geophysics	4:12	Movie_ Running, Hiking	m	3	3	2	5	10	2	6	4	3	4	6	4	3.0	3.0	2.0	5.0	10.0	2.0	6.0	4.0	3.0	4.0	6.0	4.0
33	S	m	35	2014	PhD	GR	Geology	4	hiking	ft	75	75	30	150	300	100	40	25	25	200	300	150	22.9	22.9	9.1	45.7	91.4	30.5	12.2	7.6	7.6	61.0	91.4	45.7
34	S	m	24	2012	MS	GR	Geology	4:10	Swimming:Cooking	ft	30	30	10	80	350	130	60	10	20	200	150	10	9.1	9.1	3.0	24.4	106.7	39.6	18.3	3.0	6.1	61.0	45.7	3.0
35	NS	m	34	2012	MS	GR	Geology	04:01.0	Biking:Sailing	ft	10	20	5	100	400	100	30	5	10	80	200	50	3.0	6.1	1.5	30.5	121.9	30.5	9.1	1.5	3.0	24.4	61.0	15.2
36	S	m	22	2012	MS	GR	Geology	4:02	Hiking: Soccer	m	3	8	4	12	15	10	10	3	3	15	13	9	3.0	8.0	4.0	12.0	15.0	10.0	10.0	3.0	3.0	15.0	13.0	9.0
37	S	m	24	2012	MS	GR	Geology	6:10+	Running:Reading	m	10	20	12	50	70	40	25	25	20	15	100	15	10.0	20.0	12.0	50.0	70.0	40.0	25.0	25.0	20.0	15.0	100.0	15.0
38	NS	m	22	2012	MS	GR	Geology	10:05	Music:Biking	ft	5	15	4	120	200	50	25	10	8	150	100	150	1.5	4.6	1.2	36.6	61.0	15.2	7.6	3.0	2.4	45.7	30.5	45.7
39	NS	m	23	2012	MS	GR	Geology	14:10	Rock Climbing: Hiking	m	3	5	2	6	7	3	15	3	3	10.3	9	7	3.0	5.0	2.0	6.0	7.0	3.0	15.0	3.0	3.0	10.3	9.0	7.0
40	NS	f	25	2012	MS	GR	Geology	3:11	Surf:Outrigger Canoe Paddle	ft	3	6	3	50	200	15	40	8	10	100	60	25	0.9	1.8	0.9	15.2	61.0	4.6	12.2	2.4	3.0	30.5	18.3	7.6
41	NS	m	27	2012	MS	GR	Geophysics	10:08	Video Games:Reading	ft	15	20	10	40	50	20	20	25	15	50	70	30	4.6	6.1	3.0	12.2	15.2	6.1	6.1	7.6	4.6	15.2	21.3	9.1
42	NS	m	22	2012	MS	GR	Geology	2:03	Ultimate Frisbee:Working Out	ft	20	30	10	40	70	40	25	10	10	20	45	25	6.1	9.1	3.0	12.2	21.3	12.2	7.6	3.0	3.0	6.1	13.7	7.6
43	S	m	23	2014	BS	UG	Education	20:10	Music:Hiking/Climbing	ft	30	75	10	40	500	50	60	70	50	100	500	70	9.1	22.9	3.0	12.2	152.4	15.2	18.3	21.3	15.2	30.5	152.4	21.3
44	NS	m	18	2014	BS	UG	Education	10:08	Sports:Church	ft	6	10	4	12	20	15	8	10	6	20	22	10	1.8	3.0	1.2	3.7	6.1	4.6	2.4	3.0	1.8	6.1	6.7	3.0
45	S	f	20	2011	BS	UG	Environmental Studies	10:10	Biking:Reading	ft	30	60	15	500	300	100	15	10	30	60	150	50	9.1	18.3	4.6	152.4	91.4	30.5	4.6	3.0	9.1	18.3	45.7	15.2
46	S	m	25	2011	BS	UG	Other	6:03	Hiking:Golfing	ft	6	14	7	25	30	20	15	20	10	25	30	20	1.8	4.3	2.1	7.6	9.1	6.1	4.6	6.1	3.0	7.6	9.1	6.1
47	S	m	18	2014	BS	UG	Geology	4:?	Rock Climbing: Hanging Out (its an activity)	ft/m	7m	17m	11m	150ft	350ft	110ft	5m	15m	10m	150ft	300ft	140ft	7.0	17.0	11.0	45.7	106.7	33.5	5.0	15.0	10.0	45.7	91.4	42.7
48	S	m	20	2015	PhD	GR	Geology	10:08	Skiing/Biking	m	3	5	4	15	25	10	5	10	7	30	40	25	3.0	5.0	4.0	15.0	25.0	10.0	5.0	10.0	7.0	30.0	40.0	25.0
49	NS	f	19	2013	BS	UG	Geology	5:08	Biking:Reading	ft	6	10	7	20	35	20	12	15	8	25	40	20	1.8	3.0	2.1	6.1	10.7	6.1	3.7	4.6	2.4	7.6	12.2	6.1
50	NS	m	33	2012	BS	UG	Geophysics	6:21	Fantasy Baseball: Playing with Son	ft	15	17	8	40	55	20	25	35	45	80	120	50	4.6	5.2	2.4	12.2	16.8	6.1	7.6	10.7	13.7	24.4	36.6	15.2
51	S	f	20	2012	BS	UG	Geography	10:06	Skiing:Climbing	ft	25	40	30	200	1000	100	60	20	30	150	350	85	7.6	12.2	9.1	61.0	304.8	30.5	18.3	6.1	9.1	45.7	106.7	25.9
52	NS	m	18	2014	BS	UG	Geology	15:20	Wakeboarding:Snowboarding	ft	25	35	15	60	80	50	60	30	40	200	150	125	7.6	10.7	4.6	18.3	24.4	15.2	18.3	9.1	12.2	61.0	45.7	38.1
53	S	f	30	2013	BS	UG	Geology	60:08:00	Playing with kids/work out	ft	5	10	15	200	300	200	10	5	20	20	40	100	1.5	3.0	4.6	61.0	91.4	61.0	3.0	1.5	6.1	6.1	12.2	30.5
54	S	m	20	2013	BS	UG	Geology	20:10:00	Ski:Climb	ft	40	70	13	200	300	100	45	25	13	85	80	65	12.2	21.3	4.0	61.0	91.4	30.5	13.7	7.6	4.0	25.9	24.4	19.8
55	S	f	49	2014	BS	UG	Geology	5:08	Painting:Drinking Beer	ft	30	60	40	250	600	300	20	30	20	35	40	20	9.1	18.3	12.2	76.2	182.9	91.4	6.1	9.1	6.1	10.7	12.2	6.1
56	S	m	25	2012	BS	UG	Metallurgy	20:04	RC Cars/Poker	ft	50	50	15	125	250	100	50	18	30	50	50	30	15.2	15.2	4.6	38.1	76.2	30.5	15.2	5.5	9.1	15.2	15.2	9.1
57	NS	f	18	2013	BS	UG	Geology	7:04	Workout:Volleyball	ft	12	22	15	120	120	60	20	6	10	65	65	30	3.7	6.7	4.6	36.6	36.6	18.3	6.1	1.8	3.0	19.8	19.8	9.1
58	NS	m	26	2013	BS	UG	Geology	15:04	Video Games:Hockey	ft	50	50	20	120	140	90	35	25	23	75	160	75	15.2	15.2	6.1	36.6	42.7	27.4	10.7	7.6	7.0	22.9	48.8	22.9
59	S	f	21	2012	MS	GR	Other	15:15	Skateboard:Snowboard	ft	15	30	25	120	150	100	20	35	20	110	120	110	4.6	9.1	7.6	36.6	45.7	30.5	6.1	10.7	6.1	33.5	36.6	33.5
60	S	f	19	2012	BS	UG	Geology	20:20	Reading/Playing	ft	100	300	50	1000	2000	500	500	15	700	1000	600	1300	30.5	91.4	15.2	304.8	609.6	152.4	152.4	4.6	213.4	304.8	182.9	396.2
61	S	m	18	2016	BS	UG	Other	10:20	Tabletop Games:Reading	m	12	18	8	55	95	35	10	10	10	35	95	35	12.0	18.0	8.0	55.0	95.0	35.0	10.0	10.0	10.0	35.0	95.0	35.0
62	NS	m	21	2013	BS	UG	Geology	4:04	Soccer:Biking	m	25	45	35	200	100	150	30	60	45	150	120	180	25.0	45.0	35.0	200.0	100.0	150.0	30.0	60.0	45.0	150.0	120.0	180.0
63	NS	m	18	2015	BS	UG	Other	6:06	Sports:Videogames	ft	10	15	8	100	200	80	9	12	17	70	110	35	3.0	4.6	2.4	30.5	61.0	24.4	2.7	3.7	5.2	21.3	33.5	10.7

participant. Table C.6 contains participants estimates, accuracy, and normalized accuracy for each box sorted into the no scaling group (n=27) and the scaling group (n=30). The estimates were converted to meters for comparison (B). The correct height of each box (A) was subtracted from the estimates (B) to calculate the accuracy (B-A) of each estimate. These values were then normalized to the correct answer ({B-A}/A). Table C.6 also contains the confidence (C) of participant's estimates (B) for each panorama (Nelson Canyon or Stone House Canyon) normalized to their own estimates ({C-B}/B). Table C.7 contains the same information as Table C.6 but the participants are sorted into the Geoscience (n=39) and "Other" (n=18) groups discussed in Chapter 2. Table C.8 expresses the same data as Table C.6 and C.7 but participants are sorted into the Undergraduate (n=25) and Graduate (n=32) groups discussed in Chapter 2.

Table C.6

No Scaling vs. Scaling Cues Group

No Scaling Group		Estimates (convereted to meters)(B)											
	N=27	NC-1			SHC-1			NC-2			SHC-2		
Form #	Group	Left	Center	Right	Left	Center	Right	Left	Center	Right	Left	Center	Right
Correct (A)		5.5	8.0	4.5	35.0	60.0	20.0	20.0	6.5	7.0	25.0	35.0	25.0
1	NS	3.0	4.6	3.0	9.1	12.2	6.1	7.6	4.6	2.4	13.7	10.7	12.2
2	NS	3.0	5.0	2.5	13.0	18.0	10.0	7.0	9.0	5.0	36.0	22.0	16.0
3	NS	2.0	5.0	1.0	20.0	40.0	15.0	7.0	3.0	6.0	36.0	36.0	15.0
4	NS	2.7	3.0	1.5	6.1	9.1	3.0	4.6	3.7	2.4	4.6	6.1	4.3
5	NS	3.0	4.6	2.1	9.1	15.2	6.1	7.6	6.1	9.1	18.3	13.7	27.4
11	NS	15.0	30.0	20.0	60.0	75.0	45.0	15.0	6.0	8.0	100.0	160.0	20.0
12	NS	0.8	1.5	0.9	12.2	30.5	3.0	6.1	1.5	1.8	12.2	18.3	9.1
13	NS	3.0	5.0	2.0	20.0	30.0	10.0	6.0	11.0	6.0	10.0	10.0	12.0
14	NS	2.0	3.0	4.0	10.0	8.0	5.0	8.0	5.0	4.0	10.0	12.0	6.0
16	NS	10.0	15.0	6.0	100.0	150.0	50.0	15.0	5.0	8.0	300.0	200.0	100.0
17	NS	1.0	1.5	1.0	16.0	30.0	5.0	20.0	2.0	5.0	10.0	30.0	6.0
22	NS	6.0	9.0	5.0	50.0	70.0	40.0	10.0	10.0	13.0	50.0	70.0	40.0
24	NS	11.0	105.0	5.0	1828.8	1524.0	304.8	12.2	1.5	9.1	609.6	304.8	304.8
28	NS	36.6	39.6	24.4	122.0	213.4	152.4	18.3	3.4	4.9	6.1	61.0	18.3
29	NS	10.0	20.0	1.0	40.0	60.0	30.0	30.0	20.0	10.0	100.0	60.0	80.0
32	NS	3.0	3.0	2.0	5.0	10.0	2.0	6.0	4.0	3.0	4.0	6.0	4.0
35	NS	3.0	6.1	1.5	30.5	121.9	30.5	9.1	1.5	3.0	24.4	61.0	15.2
38	NS	1.5	4.6	1.2	36.6	61.0	15.2	7.6	3.0	2.4	45.7	30.5	45.7
39	NS	3.0	5.0	2.0	6.0	7.0	3.0	15.0	3.0	3.0	10.3	9.0	7.0
40	NS	0.9	1.8	0.9	15.2	61.0	4.6	12.2	2.4	3.0	30.5	18.3	7.6
41	NS	4.6	6.1	3.0	12.2	15.2	6.1	6.1	7.6	4.6	15.2	21.3	9.1
42	NS	6.1	9.1	3.0	12.2	21.3	12.2	7.6	3.0	3.0	6.1	13.7	7.6
44	NS	1.8	3.0	1.2	3.7	6.1	4.6	2.4	3.0	1.8	6.1	6.7	3.0
49	NS	1.8	3.0	2.1	6.1	10.7	6.1	3.7	4.6	2.4	7.6	12.2	6.1
50	NS	4.6	5.2	2.4	12.2	16.8	6.1	7.6	10.7	13.7	24.4	36.6	15.2
52	NS	7.6	10.7	4.6	18.3	24.4	15.2	18.3	9.1	12.2	61.0	45.7	38.1
57	NS	3.7	6.7	4.6	36.6	36.6	18.3	6.1	1.8	3.0	19.8	19.8	9.1
58	NS	15.2	15.2	6.1	36.6	42.7	27.4	10.7	7.6	7.0	22.9	48.8	22.9
62	NS	25.0	45.0	35.0	200.0	100.0	150.0	30.0	60.0	45.0	150.0	120.0	180.0
63	NS	3.0	4.6	2.4	30.5	61.0	24.4	2.7	3.7	5.2	21.3	33.5	10.7

No Scaling Group		Accuracy (Difference From Correct)(B-A)											
	N=27	NC-1			SHC-1			NC-2			SHC-2		
Form #	Group	Left	Center	Right	Left	Center	Right	Left	Center	Right	Left	Center	Right
Correct (A)		5.5	8.0	4.5	35.0	60.0	20.0	20.0	6.5	7.0	25.0	35.0	25.0
1	NS	-2.5	-3.4	-1.5	-25.9	-47.8	-13.9	-12.4	-1.9	-4.6	-11.3	-24.3	-12.8
2	NS	-2.5	-3.0	-2.0	-22.0	-42.0	-10.0	-13.0	2.5	-2.0	11.0	-13.0	-9.0
3	NS	-3.5	-3.0	-3.5	-15.0	-20.0	-5.0	-13.0	-3.5	-1.0	11.0	1.0	-10.0
4	NS	-2.8	-5.0	-3.0	-28.9	-50.9	-17.0	-15.4	-2.8	-4.6	-20.4	-28.9	-20.7
5	NS	-2.5	-3.4	-2.4	-25.9	-44.8	-13.9	-12.4	-0.4	2.1	-6.7	-21.3	2.4
11	NS	9.5	22.0	15.5	25.0	15.0	25.0	-5.0	-0.5	1.0	75.0	125.0	-5.0
12	NS	-4.7	-6.5	-3.6	-22.8	-29.5	-17.0	-13.9	-5.0	-5.2	-12.8	-16.7	-15.9
13	NS	-2.5	-3.0	-2.5	-15.0	-30.0	-10.0	-14.0	4.5	-1.0	-15.0	-25.0	-13.0
14	NS	-3.5	-5.0	-0.5	-25.0	-52.0	-15.0	-12.0	-1.5	-3.0	-15.0	-23.0	-19.0
16	NS	4.5	7.0	1.5	65.0	90.0	30.0	-5.0	-1.5	1.0	275.0	165.0	75.0
17	NS	-4.5	-6.5	-3.5	-19.0	-30.0	-15.0	0.0	-4.5	-2.0	-15.0	-5.0	-19.0
22	NS	0.5	1.0	0.5	15.0	10.0	20.0	-10.0	3.5	6.0	25.0	35.0	15.0
24	NS	5.5	97.0	0.5	1793.8	1464.0	284.8	-7.8	-5.0	2.1	584.6	269.8	279.8
28	NS	31.1	31.6	19.9	87.0	153.4	132.4	-1.7	-3.1	-2.1	-18.9	26.0	-6.7
29	NS	4.5	12.0	-3.5	5.0	0.0	10.0	10.0	13.5	3.0	75.0	25.0	55.0
32	NS	-2.5	-5.0	-2.5	-30.0	-50.0	-18.0	-14.0	-2.5	-4.0	-21.0	-29.0	-21.0
35	NS	-2.5	-1.9	-3.0	-4.5	61.9	10.5	-10.9	-5.0	-4.0	-0.6	26.0	-9.8
38	NS	-4.0	-3.4	-3.3	1.6	1.0	-4.8	-12.4	-3.5	-4.6	20.7	-4.5	20.7
39	NS	-2.5	-3.0	-2.5	-29.0	-53.0	-17.0	-5.0	-3.5	-4.0	-14.7	-26.0	-18.0
40	NS	-4.6	-6.2	-3.6	-19.8	1.0	-15.4	-7.8	-4.1	-4.0	5.5	-16.7	-17.4
41	NS	-0.9	-1.9	-1.5	-22.8	-44.8	-13.9	-13.9	1.1	-2.4	-9.8	-13.7	-15.9
42	NS	0.6	1.1	-1.5	-22.8	-38.7	-7.8	-12.4	-3.5	-4.0	-18.9	-21.3	-17.4
44	NS	-3.7	-5.0	-3.3	-31.3	-53.9	-15.4	-17.6	-3.5	-5.2	-18.9	-28.3	-22.0
49	NS	-3.7	-5.0	-2.4	-28.9	-49.3	-13.9	-16.3	-1.9	-4.6	-17.4	-22.8	-18.9
50	NS	-0.9	-2.8	-2.1	-22.8	-43.2	-13.9	-12.4	4.2	6.7	-0.6	1.6	-9.8
52	NS	2.1	2.7	0.1	-16.7	-35.6	-4.8	-1.7	2.6	5.2	36.0	10.7	13.1
57	NS	-1.8	-1.3	0.1	1.6	-23.4	-1.7	-13.9	-4.7	-4.0	-5.2	-15.2	-15.9
58	NS	9.7	7.2	1.6	1.6	-17.3	7.4	-9.3	1.1	0.0	-2.1	13.8	-2.1
62	NS	19.5	37.0	30.5	165.0	40.0	130.0	10.0	53.5	38.0	125.0	85.0	155.0
63	NS	-2.5	-3.4	-2.1	-4.5	1.0	4.4	-17.3	-2.8	-1.8	-3.7	-1.5	-14.3

No Scaling Group		Normalized Percent Difference From Correct ({B-A}/A)											
	N=27	NC-1			SHC-1			NC-2			SHC-2		
Form #	Group	Left	Center	Right	Left	Center	Right	Left	Center	Right	Left	Center	Right
Correct (A)		5.5	8.0	4.5	35.0	60.0	20.0	20.0	6.5	7.0	25.0	35.0	25.0
1	NS	-0.4	-0.4	-0.3	-0.7	-0.8	-0.7	-0.6	-0.3	-0.7	-0.5	-0.7	-0.5
2	NS	-0.5	-0.4	-0.4	-0.6	-0.7	-0.5	-0.7	0.4	-0.3	0.4	-0.4	-0.4
3	NS	-0.6	-0.4	-0.8	-0.4	-0.3	-0.3	-0.7	-0.5	-0.1	0.4	0.0	-0.4
4	NS	-0.5	-0.6	-0.7	-0.8	-0.8	-0.8	-0.8	-0.4	-0.7	-0.8	-0.8	-0.8
5	NS	-0.4	-0.4	-0.5	-0.7	-0.7	-0.7	-0.6	-0.1	0.3	-0.3	-0.6	0.1
11	NS	1.7	2.8	3.4	0.7	0.3	1.3	-0.3	-0.1	0.1	3.0	3.6	-0.2
12	NS	-0.9	-0.8	-0.8	-0.7	-0.5	-0.8	-0.7	-0.8	-0.7	-0.5	-0.5	-0.6
13	NS	-0.5	-0.4	-0.6	-0.4	-0.5	-0.5	-0.7	0.7	-0.1	-0.6	-0.7	-0.5
14	NS	-0.6	-0.6	-0.1	-0.7	-0.9	-0.8	-0.6	-0.2	-0.4	-0.6	-0.7	-0.8
16	NS	0.8	0.9	0.3	1.9	1.5	1.5	-0.3	-0.2	0.1	11.0	4.7	3.0
17	NS	-0.8	-0.8	-0.8	-0.5	-0.5	-0.8	0.0	-0.7	-0.3	-0.6	-0.1	-0.8
22	NS	0.1	0.1	0.1	0.4	0.2	1.0	-0.5	0.5	0.9	1.0	1.0	0.6
24	NS	1.0	12.1	0.1	51.3	24.4	14.2	-0.4	-0.8	0.3	23.4	7.7	11.2
28	NS	5.7	4.0	4.4	2.5	2.6	6.6	-0.1	-0.5	-0.3	-0.8	0.7	-0.3
29	NS	0.8	1.5	-0.8	0.1	0.0	0.5	0.5	2.1	0.4	3.0	0.7	2.2
32	NS	-0.5	-0.6	-0.6	-0.9	-0.8	-0.9	-0.7	-0.4	-0.6	-0.8	-0.8	-0.8
35	NS	-0.4	-0.2	-0.7	-0.1	1.0	0.5	-0.5	-0.8	-0.6	0.0	0.7	-0.4
38	NS	-0.7	-0.4	-0.7	0.0	0.0	-0.2	-0.6	-0.5	-0.7	0.8	-0.1	0.8
39	NS	-0.5	-0.4	-0.6	-0.8	-0.9	-0.9	-0.3	-0.5	-0.6	-0.6	-0.7	-0.7
40	NS	-0.8	-0.8	-0.8	-0.6	0.0	-0.8	-0.4	-0.6	-0.6	0.2	-0.5	-0.7
41	NS	-0.2	-0.2	-0.3	-0.7	-0.7	-0.7	-0.7	0.2	-0.3	-0.4	-0.4	-0.6
42	NS	0.1	0.1	-0.3	-0.7	-0.6	-0.4	-0.6	-0.5	-0.6	-0.8	-0.6	-0.7
44	NS	-0.7	-0.6	-0.7	-0.9	-0.9	-0.8	-0.9	-0.5	-0.7	-0.8	-0.8	-0.9
49	NS	-0.7	-0.6	-0.5	-0.8	-0.8	-0.7	-0.8	-0.3	-0.7	-0.7	-0.7	-0.8
50	NS	-0.2	-0.4	-0.5	-0.7	-0.7	-0.7	-0.6	0.6	1.0	0.0	0.0	-0.4
52	NS	0.4	0.3	0.0	-0.5	-0.6	-0.2	-0.1	0.4	0.7	1.4	0.3	0.5
57	NS	-0.3	-0.2	0.0	0.0	-0.4	-0.1	-0.7	-0.7	-0.6	-0.2	-0.4	-0.6
58	NS	1.8	0.9	0.4	0.0	-0.3	0.4	-0.5	0.2	0.0	-0.1	0.4	-0.1
62	NS	3.5	4.6	6.8	4.7	0.7	6.5	0.5	8.2	5.4	5.0	2.4	6.2
63	NS	-0.4	-0.4	-0.5	-0.1	0.0	0.2	-0.9	-0.4	-0.3	-0.1	0.0	-0.6

No Scaling Group		Normalized Confidence			
	N=27	N=24			
Form #	Group	NC-1	SHC-1	NC-2	SHC-2
1	NS	3.0	3.0	1.5	1.5
2	NS	2.0	5.0	1.0	4.0
3	NS	0.5	5.0	0.5	5.0
4	NS	0.6	0.6	0.9	0.9
5	NS	4.6	4.6	3.0	3.0
11	NS	11.0	9.0	5.0	20.0
12	NS	0.5	4.6	0.5	3.8
13	NS				
14	NS	2.0	2.0	2.0	2.0
16	NS	50.0	50.0	20.0	20.0
17	NS	3.0	3.0	3.0	3.0
22	NS	20.0	20.0	20.0	20.0
24	NS	20.0	304.9	2.3	152.4
28	NS	9.1	76.2	1.5	6.1
29	NS	5.0	20.0	10.0	40.0
32	NS	2.0	2.0	1.0	1.0
35	NS	1.5	15.2	3.0	3.0
38	NS	30.5	30.5	3.0	30.5
39	NS	1.5	1.5	1.5	1.5
40	NS	3.0	3.0	3.0	3.0
41	NS	3.0	3.0	4.5	4.5
42	NS	1.5	3.8	0.9	1.8
44	NS	0.9	0.9	0.9	0.9
49	NS				
50	NS	3.0	3.0	6.0	6.0
52	NS	91.0	91.0		
57	NS	1.5	4.5	3.0	6.0
58	NS				
62	NS	15.0	15.0	9.0	9.0
63	NS	0.9	10.5	0.6	4.5

Scaling Group		Estimates (convereted to meters)											
	N=30	NC-1			SHC-1			NC-2			SHC-2		
Form #	Group	Left	Center	Right	Left	Center	Right	Left	Center	Right	Left	Center	Right
Correct (A)		5.5	8.0	4.5	35.0	60.0	20.0	20.0	6.5	7.0	25.0	35.0	25.0
6	S	1.8	4.6	1.8	35.0	50.0	20.0	12.0	9.0	6.0	32.0	40.0	26.0
7	S	2.0	4.0	2.0	9.0	25.0	4.0	6.0	4.0	3.0	15.0	18.0	25.0
8	S	4.0	8.0	3.0	15.0	13.0	12.0	18.0	30.0	10.0	40.0	100.0	40.0
9	S	8.0	15.0	6.0	25.0	50.0	15.0	10.0	7.0	6.0	10.0	15.0	12.0
10	S	15.2	30.5	22.9	15.2	30.5	7.6	7.6	22.9	15.2	21.3	30.5	12.2
15	S	3.7	7.6	3.0	20.0	100.0	15.0	9.1	13.7	9.1	25.0	60.0	25.0
18	S	21.3	27.4	13.7	30.5	152.4	24.4	24.4	29.0	24.4	22.9	304.8	15.2
19	S	54.9	30.5	74.7	335.3	396.2	228.6	61.0	36.6	76.2	457.2	548.6	243.8
20	S	10.0	20.0	15.0	40.0	80.0	40.0	10.0	20.0	15.0	50.0	80.0	40.0
21	S	15.0	25.0	20.0	100.0	80.0	30.0	30.0	20.0	15.0	50.0	40.0	30.0
23	S	20.0	35.0	25.0	70.0	120.0	100.0	6.0	10.0	8.0	35.0	60.0	70.0
25	S	4.3	9.1	1.8	24.4	67.1	13.7	12.2	3.0	9.1	4.6	30.5	12.2
26	S	6.1	15.2	4.6	30.5	91.5	30.5	9.1	4.6	6.1	36.6	48.8	24.4
27	S	4.6	9.1	3.0	15.2	7.6	9.1	2.7	7.6	3.0	12.2	10.7	12.2
30	S	3.7	2.1	1.5	9.1	12.2	3.7	5.2	2.7	3.7	30.5	61.0	15.2
31	S	8.0	15.0	4.0	30.0	100.0	15.0	8.0	12.0	7.0	25.0	50.0	20.0
33	S	22.9	22.9	9.1	45.7	91.4	30.5	12.2	7.6	7.6	61.0	91.4	45.7
34	S	9.1	9.1	3.0	24.4	106.7	39.6	18.3	3.0	6.1	61.0	45.7	3.0
36	S	3.0	8.0	4.0	12.0	15.0	10.0	10.0	3.0	3.0	15.0	13.0	9.0
37	S	10.0	20.0	12.0	50.0	70.0	40.0	25.0	25.0	20.0	15.0	100.0	15.0
43	S	9.1	22.9	3.0	12.2	152.4	15.2	18.3	21.3	15.2	30.5	152.4	21.3
45	S	9.1	18.3	4.6	152.4	91.4	30.5	4.6	3.0	9.1	18.3	45.7	15.2
46	S	1.8	4.3	2.1	7.6	9.1	6.1	4.6	6.1	3.0	7.6	9.1	6.1
47	S	7.0	17.0	11.0	45.7	106.7	33.5	5.0	15.0	10.0	45.7	91.4	42.7
48	S	3.0	5.0	4.0	15.0	25.0	10.0	5.0	10.0	7.0	30.0	40.0	25.0
51	S	7.6	12.2	9.1	61.0	304.8	30.5	18.3	6.1	9.1	45.7	106.7	25.91
53	S	1.5	3.0	4.6	61.0	91.4	61.0	3.0	1.5	6.1	6.1	12.2	30.5
54	S	12.2	21.3	4.0	61.0	91.4	30.5	13.7	7.6	4.0	25.9	24.4	19.8
55	S	9.1	18.3	12.2	76.2	182.9	91.4	6.1	9.1	6.1	10.7	12.2	6.1
56	S	15.2	15.2	4.6	38.1	76.2	30.5	15.2	5.5	9.1	15.2	15.2	9.1
59	S	4.6	9.1	7.6	36.6	45.7	30.5	6.1	10.7	6.1	33.5	36.6	33.5
60	S	30.5	91.4	15.2	304.8	609.6	152.4	152.4	4.6	213.4	304.8	182.9	396.2
61	S	12.0	18.0	8.0	55.0	95.0	35.0	10.0	10.0	10.0	35.0	95.0	35.0

Scaling Group		Accuracy (Difference From Correct)											
	N=30	NC-1			SHC-1			NC-2			SHC-2		
Form #	Group	Left	Center	Right	Left	Center	Right	Left	Center	Right	Left	Center	Right
Correct (A)		5.5	8.0	4.5	35.0	60.0	20.0	20.0	6.5	7.0	25.0	35.0	25.0
6	S	-3.7	-3.4	-2.7	0.0	-10.0	0.0	-8.0	2.5	-1.0	7.0	5.0	1.0
7	S	-3.5	-4.0	-2.5	-26.0	-35.0	-16.0	-14.0	-2.5	-4.0	-10.0	-17.0	0.0
8	S	-1.5	0.0	-1.5	-20.0	-47.0	-8.0	-2.0	23.5	3.0	15.0	65.0	15.0
9	S	2.5	7.0	1.5	-10.0	-10.0	-5.0	-10.0	0.5	-1.0	-15.0	-20.0	-13.0
10	S	9.7	22.5	18.4	-19.8	-29.5	-12.4	-12.4	16.4	8.2	-3.7	-4.5	-12.8
15	S	-1.8	-0.4	-1.5	-15.0	40.0	-5.0	-10.9	7.2	2.1	0.0	25.0	0.0
18	S	15.8	19.4	9.2	-4.5	92.4	4.4	4.4	22.5	17.4	-2.1	269.8	-9.8
19	S	49.4	22.5	70.2	300.3	336.2	208.6	41.0	30.1	69.2	432.2	513.6	218.8
20	S	4.5	12.0	10.5	5.0	20.0	20.0	-10.0	13.5	8.0	25.0	45.0	15.0
21	S	9.5	17.0	15.5	65.0	20.0	10.0	10.0	13.5	8.0	25.0	5.0	5.0
23	S	14.5	27.0	20.5	35.0	60.0	80.0	-14.0	3.5	1.0	10.0	25.0	45.0
25	S	-1.2	1.1	-2.7	-10.6	7.1	-6.3	-7.8	-3.5	2.1	-20.4	-4.5	-12.8
26	S	0.6	7.2	0.1	-4.5	31.5	10.5	-10.9	-1.9	-0.9	11.6	13.8	-0.6
27	S	-0.9	1.1	-1.5	-19.8	-52.4	-10.9	-17.3	1.1	-4.0	-12.8	-24.3	-12.8
30	S	-1.8	-5.9	-3.0	-25.9	-47.8	-16.3	-14.8	-3.8	-3.3	5.5	26.0	-9.8
31	S	2.5	7.0	-0.5	-5.0	40.0	-5.0	-12.0	5.5	0.0	0.0	15.0	-5.0
33	S	17.4	14.9	4.6	10.7	31.4	10.5	-7.8	1.1	0.6	36.0	56.4	20.7
34	S	3.6	1.1	-1.5	-10.6	46.7	19.6	-1.7	-3.5	-0.9	36.0	10.7	-22.0
36	S	-2.5	0.0	-0.5	-23.0	-45.0	-10.0	-10.0	-3.5	-4.0	-10.0	-22.0	-16.0
37	S	4.5	12.0	7.5	15.0	10.0	20.0	5.0	18.5	13.0	-10.0	65.0	-10.0
43	S	3.6	14.9	-1.5	-22.8	92.4	-4.8	-1.7	14.8	8.2	5.5	117.4	-3.7
45	S	3.6	10.3	0.1	117.4	31.4	10.5	-15.4	-3.5	2.1	-6.7	10.7	-9.8
46	S	-3.7	-3.7	-2.4	-27.4	-50.9	-13.9	-15.4	-0.4	-4.0	-17.4	-25.9	-18.9
47	S	1.5	9.0	6.5	10.7	46.7	13.5	-15.0	8.5	3.0	20.7	56.4	17.7
48	S	-2.5	-3.0	-0.5	-20.0	-35.0	-10.0	-15.0	3.5	0.0	5.0	5.0	0.0
51	S	2.1	4.2	4.6	26.0	244.8	10.5	-1.7	-0.4	2.1	20.7	71.7	0.9
53	S	-4.0	-5.0	0.1	26.0	31.4	41.0	-17.0	-5.0	-0.9	-18.9	-22.8	5.5
54	S	6.7	13.3	-0.5	26.0	31.4	10.5	-6.3	1.1	-3.0	0.9	-10.6	-5.2
55	S	3.6	10.3	7.7	41.2	122.9	71.4	-13.9	2.6	-0.9	-14.3	-22.8	-18.9
56	S	9.7	7.2	0.1	3.1	16.2	10.5	-4.8	-1.0	2.1	-9.8	-19.8	-15.9
59	S	-0.9	1.1	3.1	1.6	-14.3	10.5	-13.9	4.2	-0.9	8.5	1.6	8.5
60	S	25.0	83.4	10.7	269.8	549.6	132.4	132.4	-1.9	206.4	279.8	147.9	371.2
61	S	6.5	10.0	3.5	20.0	35.0	15.0	-10.0	3.5	3.0	10.0	60.0	10.0

Scaling Group		Normalized Percent Difference From Correct											
	N=30	NC-1			SHC-1			NC-2			SHC-2		
Form #	Group	Left	Center	Right	Left	Center	Right	Left	Center	Right	Left	Center	Right
Correct (A)		5.5	8.0	4.5	35.0	60.0	20.0	20.0	6.5	7.0	25.0	35.0	25.0
6	S	-0.7	-0.4	-0.6	0.0	-0.2	0.0	-0.4	0.4	-0.1	0.3	0.1	0.0
7	S	-0.6	-0.5	-0.6	-0.7	-0.6	-0.8	-0.7	-0.4	-0.6	-0.4	-0.5	0.0
8	S	-0.3	0.0	-0.3	-0.6	-0.8	-0.4	-0.1	3.6	0.4	0.6	1.9	0.6
9	S	0.5	0.9	0.3	-0.3	-0.2	-0.3	-0.5	0.1	-0.1	-0.6	-0.6	-0.5
10	S	1.8	2.8	4.1	-0.6	-0.5	-0.6	-0.6	2.5	1.2	-0.1	-0.1	-0.5
15	S	-0.3	0.0	-0.3	-0.4	0.7	-0.3	-0.5	1.1	0.3	0.0	0.7	0.0
18	S	2.9	2.4	2.0	-0.1	1.5	0.2	0.2	3.5	2.5	-0.1	7.7	-0.4
19	S	9.0	2.8	15.6	8.6	5.6	10.4	2.0	4.6	9.9	17.3	14.7	8.8
20	S	0.8	1.5	2.3	0.1	0.3	1.0	-0.5	2.1	1.1	1.0	1.3	0.6
21	S	1.7	2.1	3.4	1.9	0.3	0.5	0.5	2.1	1.1	1.0	0.1	0.2
23	S	2.6	3.4	4.6	1.0	1.0	4.0	-0.7	0.5	0.1	0.4	0.7	1.8
25	S	-0.2	0.1	-0.6	-0.3	0.1	-0.3	-0.4	-0.5	0.3	-0.8	-0.1	-0.5
26	S	0.1	0.9	0.0	-0.1	0.5	0.5	-0.5	-0.3	-0.1	0.5	0.4	0.0
27	S	-0.2	0.1	-0.3	-0.6	-0.9	-0.5	-0.9	0.2	-0.6	-0.5	-0.7	-0.5
30	S	-0.3	-0.7	-0.7	-0.7	-0.8	-0.8	-0.7	-0.6	-0.5	0.2	0.7	-0.4
31	S	0.5	0.9	-0.1	-0.1	0.7	-0.3	-0.6	0.8	0.0	0.0	0.4	-0.2
33	S	3.2	1.9	1.0	0.3	0.5	0.5	-0.4	0.2	0.1	1.4	1.6	0.8
34	S	0.7	0.1	-0.3	-0.3	0.8	1.0	-0.1	-0.5	-0.1	1.4	0.3	-0.9
36	S	-0.5	0.0	-0.1	-0.7	-0.8	-0.5	-0.5	-0.5	-0.6	-0.4	-0.6	-0.6
37	S	0.8	1.5	1.7	0.4	0.2	1.0	0.3	2.8	1.9	-0.4	1.9	-0.4
43	S	0.7	1.9	-0.3	-0.7	1.5	-0.2	-0.1	2.3	1.2	0.2	3.4	-0.1
45	S	0.7	1.3	0.0	3.4	0.5	0.5	-0.8	-0.5	0.3	-0.3	0.3	-0.4
46	S	-0.7	-0.5	-0.5	-0.8	-0.8	-0.7	-0.8	-0.1	-0.6	-0.7	-0.7	-0.8
47	S	0.3	1.1	1.4	0.3	0.8	0.7	-0.8	1.3	0.4	0.8	1.6	0.7
48	S	-0.5	-0.4	-0.1	-0.6	-0.6	-0.5	-0.8	0.5	0.0	0.2	0.1	0.0
51	S	0.4	0.5	1.0	0.7	4.1	0.5	-0.1	-0.1	0.3	0.8	2.0	0.0
53	S	-0.7	-0.6	0.0	0.7	0.5	2.0	-0.8	-0.8	-0.1	-0.8	-0.7	0.2
54	S	1.2	1.7	-0.1	0.7	0.5	0.5	-0.3	0.2	-0.4	0.0	-0.3	-0.2
55	S	0.7	1.3	1.7	1.2	2.0	3.6	-0.7	0.4	-0.1	-0.6	-0.7	-0.8
56	S	1.8	0.9	0.0	0.1	0.3	0.5	-0.2	-0.2	0.3	-0.4	-0.6	-0.6
59	S	-0.2	0.1	0.7	0.0	-0.2	0.5	-0.7	0.6	-0.1	0.3	0.0	0.3
60	S	4.5	10.4	2.4	7.7	9.2	6.6	6.6	-0.3	29.5	11.2	4.2	14.8
61	S	1.2	1.3	0.8	0.6	0.6	0.8	-0.5	0.5	0.4	0.4	1.7	0.4

Scaling Group		Confidence			
	N=30	N=22			
Form #	Group	NC-1	SHC-1	NC-2	SHC-2
6	S	2.5	3.5	0.7	2.6
7	S	1.5	10.0	1.0	2.5
8	S	10.0	10.0	20.0	20.0
9	S	3.0	3.0	3.0	3.0
10	S	10.0	10.0	10.0	10.0
15	S	3.0	10.0	3.0	10.0
18	S	6.1	6.1	6.1	6.1
19	S	30.5	30.5	18.3	18.3
20	S	5.0	20.0	5.0	20.0
21	S	20.0	20.0	15.0	15.0
23	S	10.0	10.0	10.0	10.0
25	S	1.5	1.5	0.9	0.9
26	S	1.7	10.1	1.3	7.3
27	S	30.5	30.5	12.2	12.2
30	S	3.1	3.1	4.5	4.5
31	S	5.0	5.0	10.0	10.0
33	S	6.1	6.1	15.2	15.2
34	S	1.8	6.1	2.3	9.2
36	S	2.0	2.0	5.0	5.0
37	S	10.0	10.0	15.0	15.0
43	S				
45	S	30.5	30.5	30.5	30.5
46	S	1.5	1.5	1.5	1.5
47	S	15.0	15.0	15.0	15.0
48	S	3.0	6.0	5.0	10.0
51	S	15.2	15.2	20.0	20.0
53	S	30.0	30.0	15.0	15.0
54	S	4.5	4.5	6.0	6.0
55	S				
56	S	3.0	15.0	1.5	6.0
59	S				
60	S	3.0	3.0	30.0	30.0
61	S	20.0	20.0	20.0	20.0

Table C.7

Geoscience vs. "Other" Group

Geoscience	N=39	Estimates (convereted to meters)(B)											
		NC-1			SHC-1			NC-2			SHC-2		
Form #	Group	Left	Center	Right	Left	Center	Right	Left	Center	Right	Left	Center	Right
Correct (A)		5.5	8.0	4.5	35.0	60.0	20.0	20.0	6.5	7.0	25.0	35.0	25.0
1	Geo	3.0	4.6	3.0	9.1	12.2	6.1	7.6	4.6	2.4	13.7	10.7	12.2
2	Geo	3.0	5.0	2.5	13.0	18.0	10.0	7.0	9.0	5.0	36.0	22.0	16.0
3	Geo	2.0	5.0	1.0	20.0	40.0	15.0	7.0	3.0	6.0	36.0	36.0	15.0
4	Geo	2.7	3.0	1.5	6.1	9.1	3.0	4.6	3.7	2.4	4.6	6.1	4.3
5	Geo	3.0	4.6	2.1	9.1	15.2	6.1	7.6	6.1	9.1	18.3	13.7	27.4
6	Geo	1.8	4.6	1.8	35.0	50.0	20.0	12.0	9.0	6.0	32.0	40.0	26.0
7	Geo	2.0	4.0	2.0	9.0	25.0	4.0	6.0	4.0	3.0	15.0	18.0	25.0
8	Geo	4.0	8.0	3.0	15.0	13.0	12.0	18.0	30.0	10.0	40.0	100.0	40.0
9	Geo	8.0	15.0	6.0	25.0	50.0	15.0	10.0	7.0	6.0	10.0	15.0	12.0
10	Geo	15.2	30.5	22.9	15.2	30.5	7.6	7.6	22.9	15.2	21.3	30.5	12.2
11	Geo	15.0	30.0	20.0	60.0	75.0	45.0	15.0	6.0	8.0	100.0	160.0	20.0
12	Geo	0.8	1.5	0.9	12.2	30.5	3.0	6.1	1.5	1.8	12.2	18.3	9.1
13	Geo	3.0	5.0	2.0	20.0	30.0	10.0	6.0	11.0	6.0	10.0	10.0	12.0
14	Geo	2.0	3.0	4.0	10.0	8.0	5.0	8.0	5.0	4.0	10.0	12.0	6.0
15	Geo	3.7	7.6	3.0	20.0	100.0	15.0	9.1	13.7	9.1	25.0	60.0	25.0
16	Geo	10.0	15.0	6.0	100.0	150.0	50.0	15.0	5.0	8.0	300.0	200.0	100.0
24	Geo	11.0	105.0	5.0	1828.8	1524.0	304.8	12.2	1.5	9.1	609.6	304.8	304.8
30	Geo	3.7	2.1	1.5	9.1	12.2	3.7	5.2	2.7	3.7	30.5	61.0	15.2
31	Geo	8.0	15.0	4.0	30.0	100.0	15.0	8.0	12.0	7.0	25.0	50.0	20.0
32	Geo	3.0	3.0	2.0	5.0	10.0	2.0	6.0	4.0	3.0	4.0	6.0	4.0
33	Geo	22.9	22.9	9.1	45.7	91.4	30.5	12.2	7.6	7.6	61.0	91.4	45.7
34	Geo	9.1	9.1	3.0	24.4	106.7	39.6	18.3	3.0	6.1	61.0	45.7	3.0
35	Geo	3.0	6.1	1.5	30.5	121.9	30.5	9.1	1.5	3.0	24.4	61.0	15.2
36	Geo	3.0	8.0	4.0	12.0	15.0	10.0	10.0	3.0	3.0	15.0	13.0	9.0
37	Geo	10.0	20.0	12.0	50.0	70.0	40.0	25.0	25.0	20.0	15.0	100.0	15.0
38	Geo	1.5	4.6	1.2	36.6	61.0	15.2	7.6	3.0	2.4	45.7	30.5	45.7
39	Geo	3.0	5.0	2.0	6.0	7.0	3.0	15.0	3.0	3.0	10.3	9.0	7.0
40	Geo	0.9	1.8	0.9	15.2	61.0	4.6	12.2	2.4	3.0	30.5	18.3	7.6
41	Geo	4.6	6.1	3.0	12.2	15.2	6.1	6.1	7.6	4.6	15.2	21.3	9.1
42	Geo	6.1	9.1	3.0	12.2	21.3	12.2	7.6	3.0	3.0	6.1	13.7	7.6
47	Geo	7.0	17.0	11.0	45.7	106.7	33.5	5.0	15.0	10.0	45.7	91.4	42.7
48	Geo	3.0	5.0	4.0	15.0	25.0	10.0	5.0	10.0	7.0	30.0	40.0	25.0
49	Geo	1.8	3.0	2.1	6.1	10.7	6.1	3.7	4.6	2.4	7.6	12.2	6.1
50	Geo	4.6	5.2	2.4	12.2	16.8	6.1	7.6	10.7	13.7	24.4	36.6	15.2
51	Geo	7.6	12.2	9.1	61.0	304.8	30.5	18.3	6.1	9.1	45.7	106.7	25.9
52	Geo	7.6	10.7	4.6	18.3	24.4	15.2	18.3	9.1	12.2	61.0	45.7	38.1
53	Geo	1.5	3.0	4.6	61.0	91.4	61.0	3.0	1.5	6.1	6.1	12.2	30.5
54	Geo	12.2	21.3	4.0	61.0	91.4	30.5	13.7	7.6	4.0	25.9	24.4	19.8
55	Geo	9.1	18.3	12.2	76.2	182.9	91.4	6.1	9.1	6.1	10.7	12.2	6.1
57	Geo	3.7	6.7	4.6	36.6	36.6	18.3	6.1	1.8	3.0	19.8	19.8	9.1
58	Geo	15.2	15.2	6.1	36.6	42.7	27.4	10.7	7.6	7.0	22.9	48.8	22.9
60	Geo	30.5	91.4	15.2	304.8	609.6	152.4	152.4	4.6	213.4	304.8	182.9	396.2
62	Geo	25.0	45.0	35.0	200.0	100.0	150.0	30.0	60.0	45.0	150.0	120.0	180.0

Form #	Group	Accuracy (Difference From Correct)(B-A)											
		NC-1			SHC-1			NC-2			SHC-2		
		Left	Center	Right	Left	Center	Right	Left	Center	Right	Left	Center	Right
Correct (A)		5.5	8.0	4.5	35.0	60.0	20.0	20.0	6.5	7.0	25.0	35.0	25.0
1	Geo	-2.5	-3.4	-1.5	-25.9	-47.8	-13.9	-12.4	-1.9	-4.6	-11.3	-24.3	-12.8
2	Geo	-2.5	-3.0	-2.0	-22.0	-42.0	-10.0	-13.0	2.5	-2.0	11.0	-13.0	-9.0
3	Geo	-3.5	-3.0	-3.5	-15.0	-20.0	-5.0	-13.0	-3.5	-1.0	11.0	1.0	-10.0
4	Geo	-2.8	-5.0	-3.0	-28.9	-50.9	-17.0	-15.4	-2.8	-4.6	-20.4	-28.9	-20.7
5	Geo	-2.5	-3.4	-2.4	-25.9	-44.8	-13.9	-12.4	-0.4	2.1	-6.7	-21.3	2.4
6	Geo	-3.7	-3.4	-2.7	0.0	-10.0	0.0	-8.0	2.5	-1.0	7.0	5.0	1.0
7	Geo	-3.5	-4.0	-2.5	-26.0	-35.0	-16.0	-14.0	-2.5	-4.0	-10.0	-17.0	0.0
8	Geo	-1.5	0.0	-1.5	-20.0	-47.0	-8.0	-2.0	23.5	3.0	15.0	65.0	15.0
9	Geo	2.5	7.0	1.5	-10.0	-10.0	-5.0	-10.0	0.5	-1.0	-15.0	-20.0	-13.0
10	Geo	9.7	22.5	18.4	-19.8	-29.5	-12.4	-12.4	16.4	8.2	-3.7	-4.5	-12.8
11	Geo	9.5	22.0	15.5	25.0	15.0	25.0	-5.0	-0.5	1.0	75.0	125.0	-5.0
12	Geo	-4.7	-6.5	-3.6	-22.8	-29.5	-17.0	-13.9	-5.0	-5.2	-12.8	-16.7	-15.9
13	Geo	-2.5	-3.0	-2.5	-15.0	-30.0	-10.0	-14.0	4.5	-1.0	-15.0	-25.0	-13.0
14	Geo	-3.5	-5.0	-0.5	-25.0	-52.0	-15.0	-12.0	-1.5	-3.0	-15.0	-23.0	-19.0
15	Geo	-1.8	-0.4	-1.5	-15.0	40.0	-5.0	-10.9	7.2	2.1	0.0	25.0	0.0
16	Geo	4.5	7.0	1.5	65.0	90.0	30.0	-5.0	-1.5	1.0	275.0	165.0	75.0
24	Geo	5.5	97.0	0.5	1793.8	1464.0	284.8	-7.8	-5.0	2.1	584.6	269.8	279.8
30	Geo	-1.8	-5.9	-3.0	-25.9	-47.8	-16.3	-14.8	-3.8	-3.3	5.5	26.0	-9.8
31	Geo	2.5	7.0	-0.5	-5.0	40.0	-5.0	-12.0	5.5	0.0	0.0	15.0	-5.0
32	Geo	-2.5	-5.0	-2.5	-30.0	-50.0	-18.0	-14.0	-2.5	-4.0	-21.0	-29.0	-21.0
33	Geo	17.4	14.9	4.6	10.7	31.4	10.5	-7.8	1.1	0.6	36.0	56.4	20.7
34	Geo	3.6	1.1	-1.5	-10.6	46.7	19.6	-1.7	-3.5	-0.9	36.0	10.7	-22.0
35	Geo	-2.5	-1.9	-3.0	-4.5	61.9	10.5	-10.9	-5.0	-4.0	-0.6	26.0	-9.8
36	Geo	-2.5	0.0	-0.5	-23.0	-45.0	-10.0	-10.0	-3.5	-4.0	-10.0	-22.0	-16.0
37	Geo	4.5	12.0	7.5	15.0	10.0	20.0	5.0	18.5	13.0	-10.0	65.0	-10.0
38	Geo	-4.0	-3.4	-3.3	1.6	1.0	-4.8	-12.4	-3.5	-4.6	20.7	-4.5	20.7
39	Geo	-2.5	-3.0	-2.5	-29.0	-53.0	-17.0	-5.0	-3.5	-4.0	-14.7	-26.0	-18.0
40	Geo	-4.6	-6.2	-3.6	-19.8	1.0	-15.4	-7.8	-4.1	-4.0	5.5	-16.7	-17.4
41	Geo	-0.9	-1.9	-1.5	-22.8	-44.8	-13.9	-13.9	1.1	-2.4	-9.8	-13.7	-15.9
42	Geo	0.6	1.1	-1.5	-22.8	-38.7	-7.8	-12.4	-3.5	-4.0	-18.9	-21.3	-17.4
47	Geo	1.5	9.0	6.5	10.7	46.7	13.5	-15.0	8.5	3.0	20.7	56.4	17.7
48	Geo	-2.5	-3.0	-0.5	-20.0	-35.0	-10.0	-15.0	3.5	0.0	5.0	5.0	0.0
49	Geo	-3.7	-5.0	-2.4	-28.9	-49.3	-13.9	-16.3	-1.9	-4.6	-17.4	-22.8	-18.9
50	Geo	-0.9	-2.8	-2.1	-22.8	-43.2	-13.9	-12.4	4.2	6.7	-0.6	1.6	-9.8
51	Geo	2.1	4.2	4.6	26.0	244.8	10.5	-1.7	-0.4	2.1	20.7	71.7	0.9
52	Geo	2.1	2.7	0.1	-16.7	-35.6	-4.8	-1.7	2.6	5.2	36.0	10.7	13.1
53	Geo	-4.0	-5.0	0.1	26.0	31.4	41.0	-17.0	-5.0	-0.9	-18.9	-22.8	5.5
54	Geo	6.7	13.3	-0.5	26.0	31.4	10.5	-6.3	1.1	-3.0	0.9	-10.6	-5.2
55	Geo	3.6	10.3	7.7	41.2	122.9	71.4	-13.9	2.6	-0.9	-14.3	-22.8	-18.9
57	Geo	-1.8	-1.3	0.1	1.6	-23.4	-1.7	-13.9	-4.7	-4.0	-5.2	-15.2	-15.9
58	Geo	9.7	7.2	1.6	1.6	-17.3	7.4	-9.3	1.1	0.0	-2.1	13.8	-2.1
60	Geo	25.0	83.4	10.7	269.8	549.6	132.4	132.4	-1.9	206.4	279.8	147.9	371.2
62	Geo	19.5	37.0	30.5	165.0	40.0	130.0	10.0	53.5	38.0	125.0	85.0	155.0

Form #	Group	Normalized Percent Difference From Correct ({B-A}/A)											
		NC-1			SHC-1			NC-2			SHC-2		
		Left	Center	Right	Left	Center	Right	Left	Center	Right	Left	Center	Right
Correct (A)		5.5	8.0	4.5	35.0	60.0	20.0	20.0	6.5	7.0	25.0	35.0	25.0
1	Geo	-0.4	-0.4	-0.3	-0.7	-0.8	-0.7	-0.6	-0.3	-0.7	-0.5	-0.7	-0.5
2	Geo	-0.5	-0.4	-0.4	-0.6	-0.7	-0.5	-0.7	0.4	-0.3	0.4	-0.4	-0.4
3	Geo	-0.6	-0.4	-0.8	-0.4	-0.3	-0.3	-0.7	-0.5	-0.1	0.4	0.0	-0.4
4	Geo	-0.5	-0.6	-0.7	-0.8	-0.8	-0.8	-0.8	-0.4	-0.7	-0.8	-0.8	-0.8
5	Geo	-0.4	-0.4	-0.5	-0.7	-0.7	-0.7	-0.6	-0.1	0.3	-0.3	-0.6	0.1
6	Geo	-0.7	-0.4	-0.6	0.0	-0.2	0.0	-0.4	0.4	-0.1	0.3	0.1	0.0
7	Geo	-0.6	-0.5	-0.6	-0.7	-0.6	-0.8	-0.7	-0.4	-0.6	-0.4	-0.5	0.0
8	Geo	-0.3	0.0	-0.3	-0.6	-0.8	-0.4	-0.1	3.6	0.4	0.6	1.9	0.6
9	Geo	0.5	0.9	0.3	-0.3	-0.2	-0.3	-0.5	0.1	-0.1	-0.6	-0.6	-0.5
10	Geo	1.8	2.8	4.1	-0.6	-0.5	-0.6	-0.6	2.5	1.2	-0.1	-0.1	-0.5
11	Geo	1.7	2.8	3.4	0.7	0.3	1.3	-0.3	-0.1	0.1	3.0	3.6	-0.2
12	Geo	-0.9	-0.8	-0.8	-0.7	-0.5	-0.8	-0.7	-0.8	-0.7	-0.5	-0.5	-0.6
13	Geo	-0.5	-0.4	-0.6	-0.4	-0.5	-0.5	-0.7	0.7	-0.1	-0.6	-0.7	-0.5
14	Geo	-0.6	-0.6	-0.1	-0.7	-0.9	-0.8	-0.6	-0.2	-0.4	-0.6	-0.7	-0.8
15	Geo	-0.3	0.0	-0.3	-0.4	0.7	-0.3	-0.5	1.1	0.3	0.0	0.7	0.0
16	Geo	0.8	0.9	0.3	1.9	1.5	1.5	-0.3	-0.2	0.1	11.0	4.7	3.0
24	Geo	1.0	12.1	0.1	51.3	24.4	14.2	-0.4	-0.8	0.3	23.4	7.7	11.2
30	Geo	-0.3	-0.7	-0.7	-0.7	-0.8	-0.8	-0.7	-0.6	-0.5	0.2	0.7	-0.4
31	Geo	0.5	0.9	-0.1	-0.1	0.7	-0.3	-0.6	0.8	0.0	0.0	0.4	-0.2
32	Geo	-0.5	-0.6	-0.6	-0.9	-0.8	-0.9	-0.7	-0.4	-0.6	-0.8	-0.8	-0.8
33	Geo	3.2	1.9	1.0	0.3	0.5	0.5	-0.4	0.2	0.1	1.4	1.6	0.8
34	Geo	0.7	0.1	-0.3	-0.3	0.8	1.0	-0.1	-0.5	-0.1	1.4	0.3	-0.9
35	Geo	-0.4	-0.2	-0.7	-0.1	1.0	0.5	-0.5	-0.8	-0.6	0.0	0.7	-0.4
36	Geo	-0.5	0.0	-0.1	-0.7	-0.8	-0.5	-0.5	-0.5	-0.6	-0.4	-0.6	-0.6
37	Geo	0.8	1.5	1.7	0.4	0.2	1.0	0.3	2.8	1.9	-0.4	1.9	-0.4
38	Geo	-0.7	-0.4	-0.7	0.0	0.0	-0.2	-0.6	-0.5	-0.7	0.8	-0.1	0.8
39	Geo	-0.5	-0.4	-0.6	-0.8	-0.9	-0.9	-0.3	-0.5	-0.6	-0.6	-0.7	-0.7
40	Geo	-0.8	-0.8	-0.8	-0.6	0.0	-0.8	-0.4	-0.6	-0.6	0.2	-0.5	-0.7
41	Geo	-0.2	-0.2	-0.3	-0.7	-0.7	-0.7	-0.7	0.2	-0.3	-0.4	-0.4	-0.6
42	Geo	0.1	0.1	-0.3	-0.7	-0.6	-0.4	-0.6	-0.5	-0.6	-0.8	-0.6	-0.7
47	Geo	0.3	1.1	1.4	0.3	0.8	0.7	-0.8	1.3	0.4	0.8	1.6	0.7
48	Geo	-0.5	-0.4	-0.1	-0.6	-0.6	-0.5	-0.8	0.5	0.0	0.2	0.1	0.0
49	Geo	-0.7	-0.6	-0.5	-0.8	-0.8	-0.7	-0.8	-0.3	-0.7	-0.7	-0.7	-0.8
50	Geo	-0.2	-0.4	-0.5	-0.7	-0.7	-0.7	-0.6	0.6	1.0	0.0	0.0	-0.4
51	Geo	0.4	0.5	1.0	0.7	4.1	0.5	-0.1	-0.1	0.3	0.8	2.0	0.0
52	Geo	0.4	0.3	0.0	-0.5	-0.6	-0.2	-0.1	0.4	0.7	1.4	0.3	0.5
53	Geo	-0.7	-0.6	0.0	0.7	0.5	2.0	-0.8	-0.8	-0.1	-0.8	-0.7	0.2
54	Geo	1.2	1.7	-0.1	0.7	0.5	0.5	-0.3	0.2	-0.4	0.0	-0.3	-0.2
55	Geo	0.7	1.3	1.7	1.2	2.0	3.6	-0.7	0.4	-0.1	-0.6	-0.7	-0.8
57	Geo	-0.3	-0.2	0.0	0.0	-0.4	-0.1	-0.7	-0.7	-0.6	-0.2	-0.4	-0.6
58	Geo	1.8	0.9	0.4	0.0	-0.3	0.4	-0.5	0.2	0.0	-0.1	0.4	-0.1
60	Geo	4.5	10.4	2.4	7.7	9.2	6.6	6.6	-0.3	29.5	11.2	4.2	14.8
62	Geo	3.5	4.6	6.8	4.7	0.7	6.5	0.5	8.2	5.4	5.0	2.4	6.2

Form #	Group	Normalized Confidence			
		N=32			
		NC-1	SHC-1	NC-2	SHC-2
1	Geo	0.9	0.3	0.3	0.1
2	Geo	0.6	0.4	0.1	0.2
3	Geo	0.2	0.2	0.1	0.2
4	Geo	0.3	0.1	0.3	0.2
5	Geo	1.4	0.5	0.4	0.2
6	Geo	0.7	0.1	0.1	0.1
7	Geo	0.6	0.8	0.2	0.1
8	Geo	2.0	0.8	*1.0*	0.3
9	Geo	0.3	0.1	0.4	0.2
10	Geo	0.4	0.6	0.7	0.5
11	Geo	0.5	0.2	0.5	0.2
12	Geo	0.4	0.3	0.1	0.3
13	Geo				
14	Geo	0.7	0.3	0.4	0.2
15	Geo	0.6	0.2	0.3	0.3
16	Geo	4.8	0.5	2.1	0.1
24	Geo	0.5	0.3	0.3	0.4
30	Geo	1.3	0.4	1.2	0.1
31	Geo	0.6	0.1	1.1	0.3
32	Geo	0.8	0.4	0.2	0.2
33	Geo	0.3	0.1	1.7	0.2
34	Geo	0.3	0.1	0.3	0.3
35	Geo	0.4	0.2	0.7	0.1
36	Geo	0.4	0.2	0.9	0.4
37	Geo	0.7	0.2	0.6	0.3
38	Geo	12.5	0.8	0.7	0.8
39	Geo	0.5	0.3	0.2	0.2
40	Geo	2.5	0.1	0.5	0.2
41	Geo	0.7	0.3	0.7	0.3
42	Geo	0.2	0.2	0.2	0.2
47	Geo	1.3	0.2	1.5	0.3
48	Geo	0.8	0.4	0.7	0.3
49	Geo				
50	Geo	0.7	0.3	0.6	0.2
51	Geo	1.6	0.1	1.8	0.3
52	Geo				
53	Geo	9.8	0.4	4.2	0.9
54	Geo	0.4	0.1	0.7	0.3
55	Geo				
57	Geo	0.3	0.1	0.8	0.4
58	Geo				
60	Geo	0.1	0.0	0.2	0.1
62	Geo	0.4	0.1	0.2	0.1

"Other"	N=18	Estimates (convereted to meters)(B)											
		NC-1			SHC-1			NC-2			SHC-2		
Form #	Group	Left	Center	Right	Left	Center	Right	Left	Center	Right	Left	Center	Right
Correct (A)		5.5	8.0	4.5	35.0	60.0	20.0	20.0	6.5	7.0	25.0	35.0	25.0
17	Other	1.0	1.5	1.0	16.0	30.0	5.0	20.0	2.0	5.0	10.0	30.0	6.0
18	Other	21.3	27.4	13.7	30.5	152.4	24.4	24.4	29.0	24.4	22.9	304.8	15.2
19	Other	54.9	30.5	74.7	335.3	396.2	228.6	61.0	36.6	76.2	457.2	548.6	243.8
20	Other	10.0	20.0	15.0	40.0	80.0	40.0	10.0	20.0	15.0	50.0	80.0	40.0
21	Other	15.0	25.0	20.0	100.0	80.0	30.0	30.0	20.0	15.0	50.0	40.0	30.0
22	Other	6.0	9.0	5.0	50.0	70.0	40.0	10.0	10.0	13.0	50.0	70.0	40.0
23	Other	20.0	35.0	25.0	70.0	120.0	100.0	6.0	10.0	8.0	35.0	60.0	70.0
25	Other	4.3	9.1	1.8	24.4	67.1	13.7	12.2	3.0	9.1	4.6	30.5	12.2
26	Other	6.1	15.2	4.6	30.5	91.5	30.5	9.1	4.6	6.1	36.6	48.8	24.4
27	Other	4.6	9.1	3.0	15.2	7.6	9.1	2.7	7.6	3.0	12.2	10.7	12.2
28	Other	36.6	39.6	24.4	122.0	213.4	152.4	18.3	3.4	4.9	6.1	61.0	18.3
29	Other	10.0	20.0	1.0	40.0	60.0	30.0	30.0	20.0	10.0	100.0	60.0	80.0
43	Other	9.1	22.9	3.0	12.2	152.4	15.2	18.3	21.3	15.2	30.5	152.4	21.3
44	Other	1.8	3.0	1.2	3.7	6.1	4.6	2.4	3.0	1.8	6.1	6.7	3.0
45	Other	9.1	18.3	4.6	152.4	91.4	30.5	4.6	3.0	9.1	18.3	45.7	15.2
46	Other	1.8	4.3	2.1	7.6	9.1	6.1	4.6	6.1	3.0	7.6	9.1	6.1
56	Other	15.2	15.2	4.6	38.1	76.2	30.5	15.2	5.5	9.1	15.2	15.2	9.1
59	Other	4.6	9.1	7.6	36.6	45.7	30.5	6.1	10.7	6.1	33.5	36.6	33.5
61	Other	12.0	18.0	8.0	55.0	95.0	35.0	10.0	10.0	10.0	35.0	95.0	35.0
63	Other	3.0	4.6	2.4	30.5	61.0	24.4	2.7	3.7	5.2	21.3	33.5	10.7

Form #	Group	Accuracy (Difference From Correct)(B-A)											
		NC-1			SHC-1			NC-2			SHC-2		
		Left	Center	Right	Left	Center	Right	Left	Center	Right	Left	Center	Right
Correct (A)		5.5	8.0	4.5	35.0	60.0	20.0	20.0	6.5	7.0	25.0	35.0	25.0
17	Other	-4.5	-6.5	-3.5	-19.0	-30.0	-15.0	0.0	-4.5	-2.0	-15.0	-5.0	-19.0
18	Other	15.8	19.4	9.2	-4.5	92.4	4.4	4.4	22.5	17.4	-2.1	269.8	-9.8
19	Other	49.4	22.5	70.2	300.3	336.2	208.6	41.0	30.1	69.2	432.2	513.6	218.8
20	Other	4.5	12.0	10.5	5.0	20.0	20.0	-10.0	13.5	8.0	25.0	45.0	15.0
21	Other	9.5	17.0	15.5	65.0	20.0	10.0	10.0	13.5	8.0	25.0	5.0	5.0
22	Other	0.5	1.0	0.5	15.0	10.0	20.0	-10.0	3.5	6.0	25.0	35.0	15.0
23	Other	14.5	27.0	20.5	35.0	60.0	80.0	-14.0	3.5	1.0	10.0	25.0	45.0
25	Other	-1.2	1.1	-2.7	-10.6	7.1	-6.3	-7.8	-3.5	2.1	-20.4	-4.5	-12.8
26	Other	0.6	7.2	0.1	-4.5	31.5	10.5	-10.9	-1.9	-0.9	11.6	13.8	-0.6
27	Other	-0.9	1.1	-1.5	-19.8	-52.4	-10.9	-17.3	1.1	-4.0	-12.8	-24.3	-12.8
28	Other	31.1	31.6	19.9	87.0	153.4	132.4	-1.7	-3.1	-2.1	-18.9	26.0	-6.7
29	Other	4.5	12.0	-3.5	5.0	0.0	10.0	10.0	13.5	3.0	75.0	25.0	55.0
43	Other	3.6	14.9	-1.5	-22.8	92.4	-4.8	-1.7	14.8	8.2	5.5	117.4	-3.7
44	Other	-3.7	-5.0	-3.3	-31.3	-53.9	-15.4	-17.6	-3.5	-5.2	-18.9	-28.3	-22.0
45	Other	3.6	10.3	0.1	117.4	31.4	10.5	-15.4	-3.5	2.1	-6.7	10.7	-9.8
46	Other	-3.7	-3.7	-2.4	-27.4	-50.9	-13.9	-15.4	-0.4	-4.0	-17.4	-25.9	-18.9
56	Other	9.7	7.2	0.1	3.1	16.2	10.5	-4.8	-1.0	2.1	-9.8	-19.8	-15.9
59	Other	-0.9	1.1	3.1	1.6	-14.3	10.5	-13.9	4.2	-0.9	8.5	1.6	8.5
61	Other	6.5	10.0	3.5	20.0	35.0	15.0	-10.0	3.5	3.0	10.0	60.0	10.0
63	Other	-2.5	-3.4	-2.1	-4.5	1.0	4.4	-17.3	-2.8	-1.8	-3.7	-1.5	-14.3

Form #	Group	Normalized Percent Difference From Correct ({B-A}/A)											
		NC-1			SHC-1			NC-2			SHC-2		
		Left	Center	Right	Left	Center	Right	Left	Center	Right	Left	Center	Right
Correct (A)		5.5	8.0	4.5	35.0	60.0	20.0	20.0	6.5	7.0	25.0	35.0	25.0
17	Other	-0.8	-0.8	-0.8	-0.5	-0.5	-0.8	0.0	-0.7	-0.3	-0.6	-0.1	-0.8
18	Other	2.9	2.4	2.0	-0.1	1.5	0.2	0.2	3.5	2.5	-0.1	7.7	-0.4
19	Other	9.0	2.8	15.6	8.6	5.6	10.4	2.0	4.6	9.9	17.3	14.7	8.8
20	Other	0.8	1.5	2.3	0.1	0.3	1.0	-0.5	2.1	1.1	1.0	1.3	0.6
21	Other	1.7	2.1	3.4	1.9	0.3	0.5	0.5	2.1	1.1	1.0	0.1	0.2
22	Other	0.1	0.1	0.1	0.4	0.2	1.0	-0.5	0.5	0.9	1.0	1.0	0.6
23	Other	2.6	3.4	4.6	1.0	1.0	4.0	-0.7	0.5	0.1	0.4	0.7	1.8
25	Other	-0.2	0.1	-0.6	-0.3	0.1	-0.3	-0.4	-0.5	0.3	-0.8	-0.1	-0.5
26	Other	0.1	0.9	0.0	-0.1	0.5	0.5	-0.5	-0.3	-0.1	0.5	0.4	0.0
27	Other	-0.2	0.1	-0.3	-0.6	-0.9	-0.5	-0.9	0.2	-0.6	-0.5	-0.7	-0.5
28	Other	5.7	4.0	4.4	2.5	2.6	6.6	-0.1	-0.5	-0.3	-0.8	0.7	-0.3
29	Other	0.8	1.5	-0.8	0.1	0.0	0.5	0.5	2.1	0.4	3.0	0.7	2.2
43	Other	0.7	1.9	-0.3	-0.7	1.5	-0.2	-0.1	2.3	1.2	0.2	3.4	-0.1
44	Other	-0.7	-0.6	-0.7	-0.9	-0.9	-0.8	-0.9	-0.5	-0.7	-0.8	-0.8	-0.9
45	Other	0.7	1.3	0.0	3.4	0.5	0.5	-0.8	-0.5	0.3	-0.3	0.3	-0.4
46	Other	-0.7	-0.5	-0.5	-0.8	-0.8	-0.7	-0.8	-0.1	-0.6	-0.7	-0.7	-0.8
56	Other	1.8	0.9	0.0	0.1	0.3	0.5	-0.2	-0.2	0.3	-0.4	-0.6	-0.6
59	Other	-0.2	0.1	0.7	0.0	-0.2	0.5	-0.7	0.6	-0.1	0.3	0.0	0.3
61	Other	1.2	1.3	0.8	0.6	0.6	0.8	-0.5	0.5	0.4	0.4	1.7	0.4
63	Other	-0.4	-0.4	-0.5	-0.1	0.0	0.2	-0.9	-0.4	-0.3	-0.1	0.0	-0.6

Form #	Group	Confidence ({C-B}/B)			
		N=13			
		NC-1	SHC-1	NC-2	SHC-2
17	Other	2.6	0.2	0.3	0.2
18	Other	0.3	0.1	0.2	0.1
19	Other	0.6	0.1	0.3	0.0
20	Other	0.3	0.4	0.3	0.4
21	Other	1.0	0.3	0.7	0.4
22	Other	3.0	0.4	1.8	0.4
23	Other	0.4	0.1	1.3	0.2
25	Other	0.3	0.0	0.1	0.1
26	Other	0.2	0.2	0.2	0.2
27	Other	5.5	2.9	2.7	1.0
28	Other	0.3	0.5	0.2	0.2
29	Other	0.5	0.5	0.5	0.5
43	Other	0.0	0.0	0.0	0.0
44	Other	0.4	0.2	0.4	0.2
45	Other	2.9	0.3	5.5	1.2
46	Other	0.5	0.2	0.3	0.2
56	Other	0.3	0.3	0.2	0.5
59	Other	0.0	0.0	0.0	0.0
61	Other	1.6	0.3	2.0	0.4
63	Other	0.3	0.3	0.2	0.2

Table C.8

Undergradaute vs. Graduate Group

Undergraduate — Estimates (convereted to meters)(B)

Form # (N=25)	Group	NC-1 Left	NC-1 Center	NC-1 Right	SHC-1 Left	SHC-1 Center	SHC-1 Right	NC-2 Left	NC-2 Center	NC-2 Right	SHC-2 Left	SHC-2 Center	SHC-2 Right
Correct (A)		5.5	8.0	4.5	35.0	60.0	20.0	20.0	6.5	7.0	25.0	35.0	25.0
1	B.S.	3.0	4.6	3.0	9.1	12.2	6.1	7.6	4.6	2.4	13.7	10.7	12.2
3	B.S.	2.0	5.0	1.0	20.0	40.0	15.0	7.0	3.0	6.0	36.0	36.0	15.0
10	B.S.	15.2	30.5	22.9	15.2	30.5	7.6	7.6	22.9	15.2	21.3	30.5	12.2
16	B.S.	10.0	15.0	6.0	100.0	150.0	50.0	15.0	5.0	8.0	300.0	200.0	100.0
24	B.S.	11.0	105.0	5.0	1828.8	1524.0	304.8	12.2	1.5	9.1	609.6	304.8	304.8
26	B.S.	6.1	15.2	4.6	30.5	91.5	30.5	9.1	4.6	6.1	36.6	48.8	24.4
27	B.A.	4.6	9.1	3.0	15.2	7.6	9.1	2.7	7.6	3.0	12.2	10.7	12.2
28	B.S.	36.6	39.6	24.4	122.0	213.4	152.4	18.3	3.4	4.9	6.1	61.0	18.3
29	B.A.	10.0	20.0	1.0	40.0	60.0	30.0	30.0	20.0	10.0	100.0	60.0	80.0
31	B.S.	8.0	15.0	4.0	30.0	100.0	15.0	8.0	12.0	7.0	25.0	50.0	20.0
43	B.S.	9.1	22.9	3.0	12.2	152.4	15.2	18.3	21.3	15.2	30.5	152.4	21.3
44	B.S.	1.8	3.0	1.2	3.7	6.1	4.6	2.4	3.0	1.8	6.1	6.7	3.0
45	B.S.	9.1	18.3	4.6	152.4	91.4	30.5	4.6	3.0	9.1	18.3	45.7	15.2
46	B.S.	1.8	4.3	2.1	7.6	9.1	6.1	4.6	6.1	3.0	7.6	9.1	6.1
47	B.S.	7.0	17.0	11.0	45.7	106.7	33.5	5.0	15.0	10.0	45.7	91.4	42.7
49	B.S.	1.8	3.0	2.1	6.1	10.7	6.1	3.7	4.6	2.4	7.6	12.2	6.1
50	B.S.	4.6	5.2	2.4	12.2	16.8	6.1	7.6	10.7	13.7	24.4	36.6	15.2
51	B.S.	7.6	12.2	9.1	61.0	304.8	30.5	18.3	6.1	9.1	45.7	106.7	25.9
52	B.S.	7.6	10.7	4.6	18.3	24.4	15.2	18.3	9.1	12.2	61.0	45.7	38.1
53	B.S.	1.5	3.0	4.6	61.0	91.4	61.0	3.0	1.5	6.1	6.1	12.2	30.5
54	B.S.	12.2	21.3	4.0	61.0	91.4	30.5	13.7	7.6	4.0	25.9	24.4	19.8
55	B.S.	9.1	18.3	12.2	76.2	182.9	91.4	6.1	9.1	6.1	10.7	12.2	6.1
56	B.S.	15.2	15.2	4.6	38.1	76.2	30.5	15.2	5.5	9.1	15.2	15.2	9.1
57	B.S.	3.7	6.7	4.6	36.6	36.6	18.3	6.1	1.8	3.0	19.8	19.8	9.1
58	B.S.	15.2	15.2	6.1	36.6	42.7	27.4	10.7	7.6	7.0	22.9	48.8	22.9
60	B.S.	30.5	91.4	15.2	304.8	609.6	152.4	152.4	4.6	213.4	304.8	182.9	396.2
61	B.S.	12.0	18.0	8.0	55.0	95.0	35.0	10.0	10.0	10.0	35.0	95.0	35.0
62	B.S.	25.0	45.0	35.0	200.0	100.0	150.0	30.0	60.0	45.0	150.0	120.0	180.0
63	B.S.	3.0	4.6	2.4	30.5	61.0	24.4	2.7	3.7	5.2	21.3	33.5	10.7

Undergraduate — Accuracy (Difference From Correct)(B-A)

Form #	Group	NC-1 Left	NC-1 Center	NC-1 Right	SHC-1 Left	SHC-1 Center	SHC-1 Right	NC-2 Left	NC-2 Center	NC-2 Right	SHC-2 Left	SHC-2 Center	SHC-2 Right
Correct (A)		5.5	8.0	4.5	35.0	60.0	20.0	20.0	6.5	7.0	25.0	35.0	25.0
1	B.S.	-2.5	-3.4	-1.5	-25.9	-47.8	-13.9	-12.4	-1.9	-4.6	-11.3	-24.3	-12.8
3	B.S.	-3.5	-3.0	-3.5	-15.0	-20.0	-5.0	-13.0	-3.5	-1.0	11.0	1.0	-10.0
10	B.S.	9.7	22.5	18.4	-19.8	-29.5	-12.4	-12.4	16.4	8.2	-3.7	-4.5	-12.8
16	B.S.	4.5	7.0	1.5	65.0	90.0	30.0	-5.0	-1.5	1.0	275.0	165.0	75.0
24	B.S.	5.5	97.0	0.5	1793.8	1464.0	284.8	-7.8	-5.0	2.1	584.6	269.8	279.8
26	B.S.	0.6	7.2	0.1	-4.5	31.5	10.5	-10.9	-1.9	-0.9	11.6	13.8	-0.6
27	B.A.	-0.9	1.1	-1.5	-19.8	-52.4	-10.9	-17.3	1.1	-4.0	-12.8	-24.3	-12.8
28	B.S.	31.1	31.6	19.9	87.0	153.4	132.4	-1.7	-3.1	-2.1	-18.9	26.0	-6.7
29	B.A.	4.5	12.0	-3.5	5.0	0.0	10.0	10.0	13.5	3.0	75.0	25.0	55.0
31	B.S.	2.5	7.0	-0.5	-5.0	40.0	-5.0	-12.0	5.5	0.0	0.0	15.0	-5.0
43	B.S.	3.6	14.9	-1.5	-22.8	92.4	-4.8	-1.7	14.8	8.2	5.5	117.4	-3.7
44	B.S.	-3.7	-5.0	-3.3	-31.3	-53.9	-15.4	-17.6	-3.5	-5.2	-18.9	-28.3	-22.0
45	B.S.	3.6	10.3	0.1	117.4	31.4	10.5	-15.4	-3.5	2.1	-6.7	10.7	-9.8
46	B.S.	-3.7	-3.7	-2.4	-27.4	-50.9	-13.9	-15.4	-0.4	-4.0	-17.4	-25.9	-18.9
47	B.S.	1.5	9.0	6.5	10.7	46.7	13.5	-15.0	8.5	3.0	20.7	56.4	17.7
49	B.S.	-3.7	-5.0	-2.4	-28.9	-49.3	-13.9	-16.3	-1.9	-4.6	-17.4	-22.8	-18.9
50	B.S.	-0.9	-2.8	-2.1	-22.8	-43.2	-13.9	-12.4	4.2	6.7	-0.6	1.6	-9.8
51	B.S.	2.1	4.2	4.6	26.0	244.8	10.5	-1.7	-0.4	2.1	20.7	71.7	0.9
52	B.S.	2.1	2.7	0.1	-16.7	-35.6	-4.8	-1.7	2.6	5.2	36.0	10.7	13.1
53	B.S.	-4.0	-5.0	0.1	26.0	31.4	41.0	-17.0	-5.0	-0.9	-18.9	-22.8	5.5
54	B.S.	6.7	13.3	-0.5	26.0	31.4	10.5	-6.3	1.1	-3.0	0.9	-10.6	-5.2
55	B.S.	3.6	10.3	7.7	41.2	122.9	71.4	-13.9	2.6	-0.9	-14.3	-22.8	-18.9
56	B.S.	9.7	7.2	0.1	3.1	16.2	10.5	-4.8	-1.0	2.1	-9.8	-19.8	-15.9
57	B.S.	-1.8	-1.3	0.1	1.6	-23.4	-1.7	-13.9	-4.7	-4.0	-5.2	-15.2	-15.9
58	B.S.	9.7	7.2	1.6	1.6	-17.3	7.4	-9.3	1.1	0.0	-2.1	13.8	-2.1
60	B.S.	25.0	83.4	10.7	269.8	549.6	132.4	132.4	-1.9	206.4	279.8	147.9	371.2
61	B.S.	6.5	10.0	3.5	20.0	35.0	15.0	-10.0	3.5	3.0	10.0	60.0	10.0
62	B.S.	19.5	37.0	30.5	165.0	40.0	130.0	10.0	53.5	38.0	125.0	85.0	155.0
63	B.S.	-2.5	-3.4	-2.1	-4.5	1.0	4.4	-17.3	-2.8	-1.8	-3.7	-1.5	-14.3

Undergraduate — Normalized Percent Difference From Correct ({B-A}/A)

Form #	Group	NC-1 Left	NC-1 Center	NC-1 Right	SHC-1 Left	SHC-1 Center	SHC-1 Right	NC-2 Left	NC-2 Center	NC-2 Right	SHC-2 Left	SHC-2 Center	SHC-2 Right
Correct (A)		5.5	8.0	4.5	35.0	60.0	20.0	20.0	6.5	7.0	25.0	35.0	25.0
1	B.S.	-0.4	-0.4	-0.3	-0.7	-0.8	-0.7	-0.6	-0.3	-0.7	-0.5	-0.7	-0.5
3	B.S.	-0.6	-0.4	-0.8	-0.4	-0.3	-0.3	-0.7	-0.5	-0.1	0.4	0.0	-0.4
10	B.S.	1.8	2.8	4.1	-0.6	-0.5	-0.6	-0.6	2.5	1.2	-0.1	-0.1	-0.5
16	B.S.	0.8	0.9	0.3	1.9	1.5	1.5	-0.3	-0.2	0.1	11.0	4.7	3.0
24	B.S.	1.0	12.1	0.1	51.3	24.4	14.2	-0.4	-0.8	0.3	23.4	7.7	11.2
26	B.S.	0.1	0.9	0.0	-0.1	0.5	0.5	-0.5	-0.3	-0.1	0.5	0.4	0.0
27	B.A.	-0.2	0.1	-0.3	-0.6	-0.9	-0.5	-0.9	0.2	-0.6	-0.5	-0.7	-0.5
28	B.S.	5.7	4.0	4.4	2.5	2.6	6.6	-0.1	-0.5	-0.3	-0.8	0.7	-0.3
29	B.A.	0.8	1.5	-0.8	0.1	0.0	0.5	0.5	2.1	0.4	3.0	0.7	2.2
31	B.S.	0.5	0.9	-0.1	-0.1	0.7	-0.3	-0.6	0.8	0.0	0.0	0.4	-0.2
43	B.S.	0.7	1.9	-0.3	-0.7	1.5	-0.2	-0.1	2.3	1.2	0.2	3.4	-0.1
44	B.S.	-0.7	-0.6	-0.7	-0.9	-0.9	-0.8	-0.9	-0.5	-0.7	-0.8	-0.8	-0.9
45	B.S.	0.7	1.3	0.0	3.4	0.5	0.5	-0.8	-0.5	0.3	-0.3	0.3	-0.4
46	B.S.	-0.7	-0.5	-0.5	-0.8	-0.8	-0.7	-0.8	-0.1	-0.6	-0.7	-0.7	-0.8
47	B.S.	0.3	1.1	1.4	0.3	0.8	0.7	-0.8	1.3	0.4	0.8	1.6	0.7
49	B.S.	-0.7	-0.6	-0.5	-0.8	-0.8	-0.7	-0.8	-0.3	-0.7	-0.7	-0.7	-0.8
50	B.S.	-0.2	-0.4	-0.5	-0.7	-0.7	-0.7	-0.6	0.6	1.0	0.0	0.0	-0.4
51	B.S.	0.4	0.5	1.0	0.7	4.1	0.5	-0.1	-0.1	0.3	0.8	2.0	0.0
52	B.S.	0.4	0.3	0.0	-0.5	-0.6	-0.2	-0.1	0.4	0.7	1.4	0.3	0.5
53	B.S.	-0.7	-0.6	0.0	0.7	0.5	2.0	-0.8	-0.8	-0.1	-0.8	-0.7	0.2
54	B.S.	1.2	1.7	-0.1	0.7	0.5	0.5	-0.3	0.2	-0.4	0.0	-0.3	-0.2
55	B.S.	0.7	1.3	1.7	1.2	2.0	3.6	-0.7	0.4	-0.1	-0.6	-0.7	-0.8
56	B.S.	1.8	0.9	0.0	0.1	0.3	0.5	-0.2	-0.2	0.3	-0.4	-0.6	-0.6
57	B.S.	-0.3	-0.2	0.0	0.0	-0.4	-0.1	-0.7	-0.7	-0.6	-0.2	-0.4	-0.6
58	B.S.	1.8	0.9	0.4	0.0	-0.3	0.4	-0.5	0.2	0.0	-0.1	0.4	-0.1
60	B.S.	4.5	10.4	2.4	7.7	9.2	6.6	6.6	-0.3	29.5	11.2	4.2	14.8
61	B.S.	1.2	1.3	0.8	0.6	0.6	0.8	-0.5	0.5	0.4	0.4	1.7	0.4
62	B.S.	3.5	4.6	6.8	4.7	0.7	6.5	0.5	8.2	5.4	5.0	2.4	6.2
63	B.S.	-0.4	-0.4	-0.5	-0.1	0.0	0.2	-0.9	-0.4	-0.3	-0.1	0.0	-0.6

Undergraduate — Normalized Confidence (N=11)

Form #	Group	NC-1	SHC-1	NC-2	SHC-2
1	B.S.	3.0	3.0	1.5	1.5
3	B.S.	0.5	5.0	0.5	5.0
10	B.S.	10.0	10.0	10.0	10.0
16	B.S.	50.0	50.0	20.0	20.0
24	B.S.	20.0	304.9	2.3	152.4
26	B.S.	1.7	10.1	1.3	7.3
27	B.A.	30.5	30.5	12.2	12.2
28	B.S.	9.1	76.2	1.5	6.1
29	B.A.	5.0	20.0	10.0	40.0
31	B.S.	5.0	5.0	10.0	10.0
43	B.S.				
44	B.S.	0.9	0.9	0.9	0.9
45	B.S.	30.5	30.5	30.5	30.5
46	B.S.	1.5	1.5	1.5	1.5
47	B.S.	15.0	15.0	15.0	15.0
49	B.S.				
50	B.S.	3.0	3.0	6.0	6.0
51	B.S.	15.2	15.2	20.0	20.0
52	B.S.	91.0	91.0		
53	B.S.	30.0	30.0	15.0	15.0
54	B.S.	4.5	4.5	6.0	6.0
55	B.S.				
56	B.S.	3.0	15.0	1.5	6.0
57	B.S.	1.5	4.5	3.0	6.0
58	B.S.				
60	B.S.	3.0	3.0	30.0	30.0
61	B.S.	20.0	20.0	20.0	20.0
62	B.S.	15.0	15.0	9.0	9.0
63	B.S.	0.9	10.5	0.6	4.5

Graduate — Estimates (convereted to meters)(B)

Form # (N=32)	Group	NC-1 Left	NC-1 Center	NC-1 Right	SHC-1 Left	SHC-1 Center	SHC-1 Right	NC-2 Left	NC-2 Center	NC-2 Right	SHC-2 Left	SHC-2 Center	SHC-2 Right
Correct (A)		5.5	8.0	4.5	35.0	60.0	20.0	20.0	6.5	7.0	25.0	35.0	25.0
2	MS	3.0	5.0	2.5	13.0	18.0	10.0	7.0	9.0	5.0	36.0	22.0	16.0
4	MS	2.7	3.0	1.5	6.1	9.1	3.0	4.6	3.7	2.4	4.6	6.1	4.3
5	MS	3.0	4.6	2.1	9.1	15.2	6.1	7.6	6.1	9.1	18.3	13.7	27.4
6	PhD	1.8	4.6	1.8	35.0	50.0	20.0	12.0	9.0	6.0	32.0	40.0	26.0
7	MS	2.0	4.0	2.0	9.0	25.0	4.0	6.0	4.0	3.0	15.0	18.0	25.0
8	PhD	4.0	8.0	3.0	15.0	13.0	12.0	18.0	30.0	10.0	40.0	100.0	40.0
9	PhD	8.0	15.0	6.0	25.0	50.0	15.0	10.0	7.0	6.0	10.0	15.0	12.0
11	MS	15.0	30.0	20.0	60.0	75.0	45.0	15.0	6.0	8.0	100.0	160.0	20.0
12	BS	0.8	1.5	0.9	12.2	30.5	3.0	6.1	1.5	1.8	12.2	18.3	9.1
13	PhDF	3.0	5.0	2.0	20.0	30.0	10.0	6.0	11.0	6.0	10.0	10.0	12.0
14	PhDF	2.0	3.0	4.0	10.0	8.0	5.0	8.0	5.0	4.0	10.0	12.0	6.0
15	MS	3.7	7.6	3.0	20.0	100.0	15.0	9.1	13.7	9.1	25.0	60.0	25.0
17	PhD	1.0	1.5	1.0	16.0	30.0	5.0	20.0	2.0	5.0	10.0	30.0	6.0
18	MS	21.3	27.4	13.7	30.5	152.4	24.4	24.4	29.0	24.4	22.9	304.8	15.2
19	PhD	54.9	30.5	74.7	335.3	396.2	228.6	61.0	36.6	76.2	457.2	548.6	243.8
20	MS	10.0	20.0	15.0	40.0	80.0	40.0	10.0	20.0	15.0	50.0	80.0	40.0
21	PhD	15.0	25.0	20.0	100.0	80.0	30.0	30.0	20.0	15.0	50.0	40.0	30.0
22	MS	6.0	9.0	5.0	50.0	70.0	40.0	10.0	10.0	13.0	50.0	70.0	40.0
23	MS	20.0	35.0	25.0	70.0	120.0	100.0	6.0	10.0	8.0	35.0	60.0	70.0
25	MS	4.3	9.1	1.8	24.4	67.1	13.7	12.2	3.0	9.1	4.6	30.5	12.2
30	MS	3.7	2.1	1.5	9.1	12.2	3.7	5.2	2.7	3.7	30.5	61.0	15.2
32	PhD	3.0	3.0	2.0	5.0	10.0	2.0	6.0	4.0	3.0	4.0	6.0	4.0
33	PhD	22.9	22.9	9.1	45.7	91.4	30.5	12.2	7.6	7.6	61.0	91.4	45.7
34	MS	9.1	9.1	3.0	24.4	106.7	39.6	18.3	3.0	6.1	61.0	45.7	3.0
35	MS	3.0	6.1	1.5	30.5	121.9	30.5	9.1	1.5	3.0	24.4	61.0	15.2
36	MS	3.0	8.0	4.0	12.0	15.0	10.0	10.0	3.0	3.0	15.0	13.0	9.0
37	MS	10.0	20.0	12.0	50.0	70.0	40.0	25.0	25.0	20.0	15.0	100.0	15.0
38	MS	1.5	4.6	1.2	36.6	61.0	15.2	7.6	3.0	2.4	45.7	30.5	45.7
39	MS	3.0	5.0	2.0	6.0	7.0	3.0	15.0	3.0	3.0	10.3	9.0	7.0
40	MS	0.9	1.8	0.9	15.2	61.0	4.6	12.2	2.4	3.0	30.5	18.3	7.6
41	MS	4.6	6.1	3.0	12.2	15.2	6.1	6.1	7.6	4.6	15.2	21.3	9.1
42	MS	6.1	9.1	3.0	12.2	21.3	12.2	7.6	3.0	3.0	6.1	13.7	7.6
48	PhD	3.0	5.0	4.0	15.0	25.0	10.0	5.0	10.0	7.0	30.0	40.0	25.0
59	MS	4.6	9.1	7.6	36.6	45.7	30.5	6.1	10.7	6.1	33.5	36.6	33.5

Graduate — Accuracy (Difference From Correct)(B-A)

Form #	Group	NC-1 Left	NC-1 Center	NC-1 Right	SHC-1 Left	SHC-1 Center	SHC-1 Right	NC-2 Left	NC-2 Center	NC-2 Right	SHC-2 Left	SHC-2 Center	SHC-2 Right
Correct (A)		5.5	8.0	4.5	35.0	60.0	20.0	20.0	6.5	7.0	25.0	35.0	25.0
2	MS	-2.5	-3.0	-2.0	-22.0	-42.0	-10.0	-13.0	2.5	-2.0	11.0	-13.0	-9.0
4	MS	-2.8	-5.0	-3.0	-28.9	-50.9	-17.0	-15.4	-2.8	-4.6	-20.4	-28.9	-20.7
5	MS	-2.5	-3.4	-2.4	-25.9	-44.8	-13.9	-12.4	-0.4	2.1	-6.7	-21.3	2.4
6	PhD	-3.7	-3.4	-2.7	0.0	-10.0	0.0	-8.0	2.5	-1.0	7.0	5.0	1.0
7	MS	-3.5	-4.0	-2.5	-26.0	-35.0	-16.0	-14.0	-2.5	-4.0	-10.0	-17.0	0.0
8	PhD	-1.5	0.0	-1.5	-20.0	-47.0	-8.0	-2.0	23.5	3.0	15.0	65.0	15.0
9	PhD	2.5	7.0	1.5	-10.0	-10.0	-5.0	-10.0	0.5	-1.0	-15.0	-20.0	-13.0
11	MS	9.5	22.0	15.5	25.0	15.0	25.0	-5.0	-0.5	1.0	75.0	125.0	-5.0
12	BS	-4.7	-6.5	-3.6	-22.8	-29.5	-17.0	-13.9	-5.0	-5.2	-12.8	-16.7	-15.9
13	PhDF	-2.5	-3.0	-2.5	-15.0	-30.0	-10.0	-14.0	4.5	-1.0	-15.0	-25.0	-13.0
14	PhDF	-3.5	-5.0	-0.5	-25.0	-52.0	-15.0	-12.0	-1.5	-3.0	-15.0	-23.0	-19.0
15	MS	-1.8	-0.4	-1.5	-15.0	40.0	-5.0	-10.9	7.2	2.1	0.0	25.0	0.0
17	PhD	-4.5	-6.5	-3.5	-19.0	-30.0	-15.0	0.0	-4.5	-2.0	-15.0	-5.0	-19.0
18	MS	15.8	19.4	9.2	-4.5	92.4	4.4	4.4	22.5	17.4	-2.1	269.8	-9.8
19	PhD	49.4	22.5	70.2	300.3	336.2	208.6	41.0	30.1	69.2	432.2	513.6	218.8
20	MS	4.5	12.0	10.5	5.0	20.0	20.0	-10.0	13.5	8.0	25.0	45.0	15.0
21	PhD	9.5	17.0	15.5	65.0	20.0	10.0	10.0	13.5	8.0	25.0	5.0	5.0
22	MS	0.5	1.0	0.5	15.0	10.0	20.0	-10.0	3.5	6.0	25.0	35.0	15.0
23	MS	14.5	27.0	20.5	35.0	60.0	80.0	-14.0	3.5	1.0	10.0	25.0	45.0
25	MS	-1.2	1.1	-2.7	-10.6	7.1	-6.3	-7.8	-3.5	2.1	-20.4	-4.5	-12.8
30	MS	-1.8	-5.9	-3.0	-25.9	-47.8	-16.3	-14.8	-3.8	-3.3	5.5	26.0	-9.8
32	PhD	-2.5	-5.0	-2.5	-30.0	-50.0	-18.0	-14.0	-2.5	-4.0	-21.0	-29.0	-21.0
33	PhD	17.4	14.9	4.6	10.7	31.4	10.5	-7.8	1.1	0.6	36.0	56.4	20.7
34	MS	3.6	1.1	-1.5	-10.6	46.7	19.6	-1.7	-3.5	-0.9	36.0	10.7	-22.0
35	MS	-2.5	-1.9	-3.0	-4.5	61.9	10.5	-10.9	-5.0	-4.0	-0.6	26.0	-9.8
36	MS	-2.5	0.0	-0.5	-23.0	-45.0	-10.0	-10.0	-3.5	-4.0	-10.0	-22.0	-16.0
37	MS	4.5	12.0	7.5	15.0	10.0	20.0	5.0	18.5	13.0	-10.0	65.0	-10.0
38	MS	-4.0	-3.4	-3.3	1.6	1.0	-4.8	-12.4	-3.5	-4.6	20.7	-4.5	20.7
39	MS	-2.5	-3.0	-2.5	-29.0	-53.0	-17.0	-5.0	-3.5	-4.0	-14.7	-26.0	-18.0
40	MS	-4.6	-6.2	-3.6	-19.8	1.0	-15.4	-7.8	-4.1	-4.0	5.5	-16.7	-17.4
41	MS	-0.9	-1.9	-1.5	-22.8	-44.8	-13.9	-13.9	1.1	-2.4	-9.8	-13.7	-15.9
42	MS	0.6	1.1	-1.5	-22.8	-38.7	-7.8	-12.4	-3.5	-4.0	-18.9	-21.3	-17.4
48	PhD	-2.5	-3.0	-0.5	-20.0	-35.0	-10.0	-15.0	3.5	0.0	5.0	5.0	0.0
59	MS	-0.9	1.1	3.1	1.6	-14.3	10.5	-13.9	4.2	-0.9	8.5	1.6	8.5

Graduate — Normalized Percent Difference From Correct ({B-A}/A)

Form #	Group	NC-1 Left	NC-1 Center	NC-1 Right	SHC-1 Left	SHC-1 Center	SHC-1 Right	NC-2 Left	NC-2 Center	NC-2 Right	SHC-2 Left	SHC-2 Center	SHC-2 Right
Correct (A)		5.5	8.0	4.5	35.0	60.0	20.0	20.0	6.5	7.0	25.0	35.0	25.0
2	MS	-0.5	-0.4	-0.4	-0.6	-0.7	-0.5	-0.7	0.4	-0.3	0.4	-0.4	-0.4
4	MS	-0.5	-0.6	-0.7	-0.8	-0.8	-0.8	-0.8	-0.4	-0.7	-0.8	-0.8	-0.8
5	MS	-0.4	-0.4	-0.5	-0.7	-0.7	-0.7	-0.6	-0.1	0.3	-0.3	-0.6	0.1
6	PhD	-0.7	-0.4	-0.6	0.0	-0.2	0.0	-0.4	0.4	-0.1	0.3	0.1	0.0
7	MS	-0.6	-0.5	-0.6	-0.7	-0.6	-0.8	-0.7	-0.4	-0.6	-0.4	-0.5	0.0
8	PhD	-0.3	0.0	-0.3	-0.6	-0.8	-0.4	-0.1	3.6	0.4	0.6	1.9	0.6
9	PhD	0.5	0.9	0.3	-0.3	-0.2	-0.3	-0.5	0.1	-0.1	-0.6	-0.6	-0.5
11	MS	1.7	2.8	3.4	0.7	0.3	1.3	-0.3	-0.1	0.1	3.0	3.6	-0.2
12	BS	-0.9	-0.8	-0.8	-0.7	-0.5	-0.8	-0.7	-0.8	-0.7	-0.5	-0.5	-0.6
13	PhDF	-0.5	-0.4	-0.6	-0.4	-0.5	-0.5	-0.7	0.7	-0.1	-0.6	-0.7	-0.5
14	PhDF	-0.6	-0.6	-0.1	-0.7	-0.9	-0.8	-0.6	-0.2	-0.4	-0.6	-0.7	-0.8
15	MS	-0.3	0.0	-0.3	-0.4	0.7	-0.3	-0.5	1.1	0.3	0.0	0.7	0.0
17	PhD	-0.8	-0.8	-0.8	-0.5	-0.5	-0.8	0.0	-0.7	-0.3	-0.6	-0.1	-0.8
18	MS	2.9	2.4	2.0	-0.1	1.5	0.2	0.2	3.5	2.5	-0.1	7.7	-0.4
19	PhD	9.0	2.8	15.6	8.6	5.6	10.4	2.0	4.6	9.9	17.3	14.7	8.8
20	MS	0.8	1.5	2.3	0.1	0.3	1.0	-0.5	2.1	1.1	1.0	1.3	0.6
21	PhD	1.7	2.1	3.4	1.9	0.3	0.5	0.5	2.1	1.1	1.0	0.1	0.2
22	MS	0.1	0.1	0.1	0.4	0.2	1.0	-0.5	0.5	0.9	1.0	1.0	0.6
23	MS	2.6	3.4	4.6	1.0	1.0	4.0	-0.7	0.5	0.1	0.4	0.7	1.8
25	MS	-0.2	0.1	-0.6	-0.3	0.1	-0.3	-0.4	-0.5	0.3	-0.8	-0.1	-0.5
30	MS	-0.3	-0.7	-0.7	-0.7	-0.8	-0.8	-0.7	-0.6	-0.5	0.2	0.7	-0.4
32	PhD	-0.5	-0.6	-0.6	-0.9	-0.8	-0.9	-0.7	-0.4	-0.6	-0.8	-0.8	-0.8
33	PhD	3.2	1.9	1.0	0.3	0.5	0.5	-0.4	0.2	0.1	1.4	1.6	0.8
34	MS	0.7	0.1	-0.3	-0.3	0.8	1.0	-0.1	-0.5	-0.1	1.4	0.3	-0.9
35	MS	-0.4	-0.2	-0.7	-0.1	1.0	0.5	-0.5	-0.8	-0.6	0.0	0.7	-0.4
36	MS	-0.5	0.0	-0.1	-0.7	-0.8	-0.5	-0.5	-0.5	-0.6	-0.4	-0.6	-0.6
37	MS	0.8	1.5	1.7	0.4	0.2	1.0	0.3	2.8	1.9	-0.4	1.9	-0.4
38	MS	-0.7	-0.4	-0.7	0.0	0.0	-0.2	-0.6	-0.5	-0.7	0.8	-0.1	0.8
39	MS	-0.5	-0.4	-0.6	-0.8	-0.9	-0.9	-0.3	-0.5	-0.6	-0.6	-0.7	-0.7
40	MS	-0.8	-0.8	-0.8	-0.6	0.0	-0.8	-0.4	-0.6	-0.6	0.2	-0.5	-0.7
41	MS	-0.2	-0.2	-0.3	-0.7	-0.7	-0.7	-0.7	0.2	-0.3	-0.4	-0.4	-0.6
42	MS	0.1	0.1	-0.3	-0.7	-0.6	-0.4	-0.6	-0.5	-0.6	-0.8	-0.6	-0.7
48	PhD	-0.5	-0.4	-0.1	-0.6	-0.6	-0.5	-0.8	0.5	0.0	0.2	0.1	0.0
59	MS	-0.2	0.1	0.7	0.0	-0.2	0.5	-0.7	0.6	-0.1	0.3	0.0	0.3

Graduate — Confidence ({C-B}/B) (N=30)

Form #	Group	NC-1	SHC-1	NC-2	SHC-2
2	MS	2.0	5.0	1.0	4.0
4	MS	0.6	0.6	0.9	0.9
5	MS	4.6	4.6	3.0	3.0
6	PhD	2.0	3.5	0.7	2.6
7	MS	1.5	10.0	1.0	2.5
8	PhD	10.0	10.0	20.0	20.0
9	PhD	3.0	3.0	3.0	3.0
11	MS	11.0	9.0	5.0	20.0
12	BS	0.5	4.6	0.5	3.8
13	PhDF				
14	PhDF	2.0	2.0	2.0	2.0
15	MS	3.0	10.0	3.0	10.0
17	PhD	3.0	3.0	3.0	3.0
18	MS	6.1	6.1	6.1	6.1
19	PhD	30.5	30.5	18.3	18.3
20	MS	5.0	20.0	5.0	20.0
21	PhD	20.0	20.0	15.0	15.0
22	MS	20.0	20.0	20.0	20.0
23	MS	10.0	10.0	10.0	10.0
25	MS	1.5	1.5	0.9	0.9
30	MS	3.1	3.1	4.5	4.5
32	PhD	2.0	2.0	1.0	1.0
33	PhD	6.1	6.1	15.2	15.2
34	MS	1.8	6.1	2.3	9.2
35	MS	1.5	15.2	3.0	3.0
36	MS	2.0	2.0	5.0	5.0
37	MS	10.0	10.0	15.0	15.0
38	MS	30.5	30.5	3.0	30.5
39	MS	1.5	1.5	1.5	1.5
40	MS	3.0	3.0	3.0	3.0
41	MS	3.0	3.0	4.5	4.5
42	MS	1.5	3.8	0.9	1.8
48	PhD	3.0	6.0	5.0	10.0
59	MS				

REFERENCES

Adams, M.M., and Bhattacharya, J.P., 2005, No change in fluvial style across a sequence boundary, Cretaceous Blackhawk and Castlegate Formations of central Utah, U.S.A.: Journal of Sedimentary Research, v. 75, p. 1038-1051.

AGRC, 2011, Utah GIS Portal: http://gis.utah.gov/ (January 2011).

Allen, J.L., 2009, Transgressive-Regressive Cycles in the John Henry Member, Straight Cliffs Formation southern Utah, USA. [Ph.D. Thesis]: University of Utah, p. 184.

Allen, J. L., and Johnson, C., 2010, Sedimentary facies, paleoenvironments, and relative sea level changes in the John Henry Member, Cretaceous Straight Cliffs Formation, Southern Utah, *in* Carney, S., Tabet, D., and Johnson, C. (eds.), Geology of South Central Utah: UGA Guidebook 39, p. 225-247.

Arnott, R., 1995, The parasequence definition; Are trangressive deposits inadequately addressed?: Journal of Sedimentary Research, v. 65, no. 1b, p. 1-6.

Birkeland, P., 1999, Soils and Geomorphology: New York, NY, Oxford University Press, p. 430.

Bhattacharya, J.P., and Willis, B., 2001, Lowstand deltas in the Frontier Formation, Powder River basin, Wyoming: Implications for sequence stratigraphic models: AAPG Bulletin, v. 85, no. 2, p. 261–294.

Bobb, M., 1991, The Calico Bed, Upper Cretaceous, Southern Utah: A Fluvial Sheet Deposit in the Western Interior Foreland Basin and its Relationship to Eustasy and Tectonics [M.S. Thesis]: University of Colorado, p. 166.

Boggs, S., 2006, Principles of sedimentology and stratigraphy: Upper Saddle River, NJ, Pearson Prentice Hall, 4th edition, p. 662.

Bridge, J., 2003, Rivers and Floodplains; Forms, Processes, and the Sedimentary Record: Malden, MA, Blackwell Publishing, p. 502.

Carmona, N., Buatois, L., Ponce, J., and Mangano, M.G., 2009, Ichnology and sedimentology of a tide-influenced delta, Lower Miocene Chenque Formation,

Patagonia, Argentina: Trace-fossil distribution and response to environmental stresses: Palaeogeography, Palaeoclimatology, Palaeoecology. 273, p. 75-86.

Cattaneo, A., and Steel, R, 2003, Transgressive deposits: A review of their variability: Earth Science Reviews, no. 63, p. 187-228.

Catuneanu, O., 2006, Principles of Sequence Stratigraphy: Amsterdam, Elsevier Press. p. 375.

Catuneanu, O., and Elango, H., 2001, Tectonic control on fluvial styles: the Balfour Formation of the Karoo Basin, South Africa: Sedimentary Geology, v. 140, p. 291-313.

Cheel, R., and Leckie, D., 1993, Hummocky cross stratification: Sedimentology Review, v. 1, Ch.7, p. 103-120.

Christensen, A.E., 2005, Sequence stratigraphy, sedimentology and provenance of the Drip Tank Member, Straight Cliffs Formation, Kaiparowits Plateau, southwestern Utah [M.S. thesis]: New Mexico State University, p. 97.

Cobban, W.A., 1952, Scaphitoid cephalopods of the Colorado group: U.S. Geological Survey Professional Paper 239, p. 42.

Cobban, W. A., Dyman, T. S., Pollock, G. L.. Takahashi, K. I., Davis, L. E., and Riggin, D. B, 2000, Inventory of dominantly marine and brackish-water fossils from late Cretaceous rocks in and near Grand Staircase-Escalante National Monument, Utah, *in* Sprinklel, D. A., Chidsey, T. C., and Anderson P. B. (eds.), Geology of Utah's Parks and Monuments. Utah Geological Association Publication 28, p. 579-589.

Coe, A.L., (ed), 2003, The sedimentary record of sea-level change: Cambridge, Cambridge University Press, p. 287.

Coyan, J., Busch, M., and Reynolds, S., 2010, Using eye trackers to evaluate the effectiveness of signaling to promote the disembedding of geologic features in photographs, *in* Frick, A., Nardi, D., and Ratliff, K., 2010, Spatial Cognition 2010: Doctoral Colloquium, p. 15-19.

Dalrymple, R., and Choi, K., 2007. Morphologic and facies trends through the fluvial–marine transition in tide-dominated depositional systems: A schematic framework for environmental and sequence-stratigraphic interpretation: Earth Science Reviews, v. 81, p.135-174.

Dalrymple, R., Zaitline, B., Boyd, R., 1992, Estuarine Facies Models; Conceptual Basis and Stratigraphic Implications: Journal of Sedimentary Research, v. 62, no. 6, p. 1130-1146.

Decelles, P.G., Lawton, T.F., and Mitra, G., 1995, Thrust timing, growth of structural culminations, and synorogenic sedimentation in the type Sevier orogenic belt, western USA: Geology, v. 23, p. 699-702.

DeepLocal, 2008, Gigapan: http://www.gigapan.org/ (May 2009).

Doelling, H.H., and Graham, R.L., 1972, Kaiparowits Plateau coal field, *in* Doelling, H.H., and Graham, R.L., eds., Southwestern Utah coal fields: Alton, Kaiparowits Plateau, and Kolob-Harmony: Utah Geological and Mineralogical Survey Monograph Series no.1, p. 67–249.

Dott, R.H. and Bourgeois, J., 1982, Hummocky Stratification: Significance of its variable bedding sequences: Geological Society of America Bulletin, v.93, p. 662-680.

Eaton, J.G., 1991, Biostratigraphic framework for the Upper Cretaceous rocks of the Kaiparowits Plateau, southern Utah: GSA Special Paper, v. 260, p. 47–64.

Eaton, J. G., 1995, Cenomanian and Turonian (early Late Cretaceous) multituberculate mammals from southwestern Utah: Journal of Vertebrate Paleontology, v. 15, p. 761–784.

Eaton, J., Cifelli, R., Hutchison, J., Kirkland, J. and Parish, J., 1999, Cretaceous Vertebrate Faunas from the Kaiparowits Plateau, south central Utah: Utah Geological Survey, Miscellaneous Publication 99-1.

Eaton, J.G., Kirkland, J., Hutchinson, J., Denton, R., O'Neill, R., and Parrish, J, 1997, Nonmarine extinction across the Cenomanian-Turonian boundary, southwestern Utah, with a comparison to the Cretaceous-Tertiary extinction event: GSA Bulletin, v. 109, no. 5, p. 560-567.

Eaton, J.G., Laurin, J., Kirkland, J., Tibert, N., Leckie, R., Sageman, B., Goldstrand, P., Moore, D., Straub, A., Cobban, W., and Dalebout, J., 2001, Cretaceous and Early Tertiary Geology of Cedar and Parowan Canyons, Western Markagunt Plateau: Utah. Utah Geological Association Field Trip Road Log, Utah Geological Association Publication 30, p. 337-363.

Ekdale, A. A., 1985, Paleoecology of the Marine Endobenthos. Paleogeography, Paleoclimatology, Paleoecology: v.50, p.63-81.

Emery, D., Myers, K., and Bertram, G.T., 1996, Sequence Stratigraphy: London, Blackwell Publishing Company, p. 297.

Frey, R., 1990, Trace Fossils and Hummocky Cross Stratification, Upper Cretaceous of Utah: Palaios, v.5, p. 203-218.

Frey, R., and Howard, J., 1990, Trace Fossils and Depositional Sequences in a Clastic Shelf Setting, Upper Cretaceous of Utah, Journal of Paleontology, p. 803-820.

Gardner, M., 1995, The Stratigraphic Hierarchy and Tectonic History of the Mid-Cretaceous Foreland Basin of Central Utah: Society of Sedimentary Geology, Special Publication no. 52, p. 283-303.

Gregory, H.E., and Moore, R.C., 1931, The Kaiparowits region, a geographic and geologic reconnaissance of parts of Utah and Arizona: U.S. Geological Survey Professional Paper, v. 164, p. 161.

Gooley, J.T., 2010, Alluvial architecture and predictive modeling of the late Cretaceous John Henry Member, Straight Cliffs Formation, southern Utah. [M.S. Thesis]: University of Utah, p. 366.

Haq, B.U., Hardenbol, J., and Vail, P. R., 1988, Mesozoic and Cenozoic chronostratigraphy and cycles of sea-level change, *in* Wilgus, C.K., Hastings, B.S., Kendall, C.G., Posamentier, H.W., Ross, C.A., and Van Wagoner, J.C., eds., Sea-Level Changes: An intergrated approach: Special Publication of the Society of Economic Paleontologists and Mineralogists, no. 42, p. 72-108.

Heap, A.D., and Nichol, S.L., 1997, The influence of limited accommodation space on stratigraphy of an incised valley succession: Weiti River Estuary, New Zealand, Marine Geology v. 144, p. 229-252.

Heller, P., and Paola, C., 1996, Downstream Changes in Alluvial Architecture: An Exploration of Controls on Channel Stacking Patterns. Journal of Sedimentary Research v. 66, no. 2, p. 297-306.

Hettinger, R.D., 1995, Sedimentological descriptions and geophysical logs of two 300-m cores collected from the Straight Cliffs Formation of the Kaiparowits Plateau, Kane Country, Utah: Open-File Report – U.S.G.S. Report OF 93-0270, p. 50.

Hettinger, R.D., Roberts, L.N.R., and Gognat, T.A., 2000, Investigations of the Distribution and Resources of Coal in the Southern Part of the Piceance Basin, Colorado, Chapter O, *in* Kirschbaum, M. A., Roberts, L.N.R., and Biewick, L.R.H., eds., Geologic Assessment of Coal in the Colorado Plateau: Arizona, Colorado, New Mexico, and Utah, compiled by Colorado Plateau Coal Assessment Group: U.S. Geological Survey Professional Paper 1625-B, Version 1.0, p. O1-O101.

Hettinger, R., Shanley, K.W., and McCabe, P.J., 1993, Detailed Facies Anatomy of Transgressive and Highstand Systems Tracts from the Upper Creataceous of Southern Utah, USA: AAPG Memoir 58, p. 235-257.

Hettinger, R.D., Roberts, L.N.R., Biewick, L.R.H., and Kirschbaum, M.A., 1996, Preliminary investigations of the distribution and resources of coal in the Kaiparowits Plateau, Southern Utah: U.S. Geological Survey, Open Report 96-539, p. 61.

Howard, J., and Reineck, H., 1981, Depositional Facies of High Energy Beach to Offshore Sequence: Comparison with Low Energy Sequence: AAPG Memoir, p. 807-830.

Howell, J., and Flint, S., 1996, A model for high resolution sequence stratigraphy within extensional basins: Geological Society, London, Special Publications, v. 104, p. 129-137.

Hunter, R.E., Clifton, H.E., Phillips, R.L., 1979, Depositional processes, sedimentary structures, and predicted vertical sequences in nearshore systems, south Oregon coast: Journal of Sedimentary Research, v. 49, no. 3, p. 711-726.

Ishikawa, T., and Kastens, K., 2005, Why some students have trouble with maps and other spatial representations: Journal of Geoscience Education, v. 53, no. 2, p. 184-197.

Jones, M., and Taylor, R., 2009, Developing a sense of scale: Looking backward: Journal of Research in Science Teaching, v. 46, no. 4, p. 460-475.

Kastens, K., 2010, Commentary: Object and spatial visualizations in geosciences: Journal of Geoscience Education, v. 58, no. 2, p. 52-57.

Kastens, K., Manduca, C., Cervato, C., Frodeman, R., Goodwin, C., Liben, L., Mogk, D., Spangler, T., Stillings, N., and Titus, S., 2009, How geoscientists think and learn: Eos, v. 90, no. 31, p. 265-272.

Kelly, M., and Riggs. N., 2006, Use of a virtual environment in the geowall to increase student confidence and performance during field mapping: An example from an introductory-level field class: Journal of Geoscience Education, v, 54, no. 2, p. 158-164.

Kraus, M., 1999., Paleosols in Clastic Sedimentary Rocks: their geologic applications: Earth Science Reviews v. 47, p. 41–70.

Kumar, N., and Sanders, J.E., 1976, Characteristics of shoreface storm deposits; modern and ancient examples: Journal of Sedimentary Research, v. 46, no. 1, p. 145-162.

Little, W., 1995, The Influence of Tectonics and Eustasy on Alluvial Architecture, Middle Coniacian Through Campanian Strata of the Kaiparowits Basin, Utah. [Ph.D. Thesis]: University of Colorado, Department of Geological Sciences, p. 328.

Li, W., Bhattacharya, P., Campbell, C., 2010, Temporal evolution of fluvial style in a compound incised-valley, Ferron "Notom Delta," Henry Moutains region, Utah, U.S.A.: Journal of Sedimentary Research, v. 80, p. 529-549.

Liu, S., Nummedal, D., Yin, P., and Luo, H. 2005. Linkage of Sevier thrusting episodes and Late Cretaceous foreland basin megasequences across southern Wyoming (USA): Basin Research, v. 17, p. 487-506.

Liu, L., Spasojevic, S., and Gurnis, M., 2008, Reconstructing Farallon Plate subduction beaneath North America back to the Late Cretaceous: Science, v. 322, p. 934-938.

Mack, G., James, W., and Monger, H., 1993, Classification of Paleosols: Geological Society of America Bulletin, v. 105, p. 129-136.

Massari, F., 1996, Upper-flow-regime stratification types on steep-face, coarse-grained, Gilbert type progradational wedges, Pleistocene, southern Italy: Journal of Sedimentary Research, v. 66, no. 2, p. 364-375.

Miall, A., 1996, The geology of fluvial deposits: Heidelberg, Springer-Verlag Press, p. 582.

Miall, A., 1997, The geology of stratigraphic sequences: Heidelberg, Springer-Verlag Press, p. 439.

Miall, A., 2006, Reconstructing the architecture and sequence stratigraphy of the preserved fluvial record as a tool for reservoir development: A reality check: AAPG Bulletin, v. 90, no. 7, p. 989-1002.

Moran, K., Hilbert-Wolf, H.L., Golder, K., Malenda, H.F., Smith, C.J., Storm, L.P., Simpson, E.L., Wizevich, M.C., and Tindall, S.E., 2010, Attributes of the wood-boring trace fossil Asthenopodichnium in the late Cretaceous Wahweap Formation, Utah, U.S.A.: Palaeogeography, Palaeoclimatology, Palaeoecology, v. 297, Issue 3-4, p. 662-669.

Nummedal, D., and Swift, D. J.P., 1987, Transgressive stratigraphy at sequence-bounding unconformities; some principles derived from Holocene and Cretaceous examples: Special Publication - Society of Economic Paleontologists and Mineralogists, v.41, p.241-260.

Nummedal, D., and Pang, M., 1995, Flexural subsidence and basement tectonics of the Cretaceous Western Interior basin, United States: v. 23, no. 2, p. 173–176.

Obradovich, J.D., 1993, A cretaceous time scale, *in* Caldwell, W.G.E., and Kauffman, E.G., eds., Evolution of the Western Interior Basin: Geological Association of Canada, Special Publication 39, p. 379-396.

O'Byrne, C., and Flint, S., 1995, Sequence, Parasequence, and Intraparasequence Architecture of the Grassy Member, Blackhawk Formation, Book Cliffs, Utah, USA: *in* Wagoner, J.C., and Bertram G.T., 1995, Sequence stratigraphy of

foreland basin deposits: Outcrop and subsurface examples from the Cretaceous of North America. AAPG Memoir 64.

Owen, G., 1996, Anatomy of a water-escape cusp in Upper Proterozoic Torridon Group sandstones, Scotland: Sedimentary Geology, v. 103, p.117–128.

Peterson, F., 1969a, Cretaceous sedimentation and tectonism in the southeastern Kaiparowits region, Utah [Ph.D. Dissertation]: Stanford University, p. 305.

Peterson, F., 1969b, Four New Members of the Upper Cretaceous Straight Cliffs Formation in the Southeastern Kaiparowits Region, Kane County, Utah: Geological Survey Bulletin, 1274- J.

Peterson, F., and Waldrop, H.A., 1965, Jurassic and Cretaceous stratigraphy of southcentralKaiparowits Plateau, Utah, *in* Goode, D. and Robison, R.A., eds., Geology andResources of South-Central Utah: Guidebook of the Geology of Utah 19: UtahGeological Society and Intermountain Association of Petroleum Geologists, p.47–69.

Piburn, M., Reynolds, S., Leedy, D., McAuliffe, C., Birk, J., and Johnson, J., 2002, The hidden earth: Visualization of geologic features and their subsurface geometry: National Association for Research in Science Teaching Annual Meeting, April 7-10, 2002.

Plint, A.G., McCarthy, P., and Faccini, U., 2001, Nonmarine sequence stratigraphy: Updip expressions of sequence boundaries and systems tracts in a high resolution framework, Cenomanian Dunvegan Formation, Alberta foreland basin, Canada: AAPG Bulletin, v. 85, No. 11, p. 1967-2001.

Plint, A.G., and Nummedal, D., 2000, The falling stage systems tract: recognition and importance in sequence stratigraphic analysis, *in* Hunt, D., and Gawthorpe, R.L., Sedimentary Responses to Forced Regressions: Geological Society London, Special Publications 172, p. 1-17.

Posamentier, H.W., Jervey, M.T., and Vail, P.R., 1988, Eustatic controls on clastic deposition conceptual framework: *in* Wilgus, C.K., Hastings, B.S., Kendall, C.G., Posamentier, H.W., Ross, C.A., and Van Wagoner, J.C. (Eds.), Sea Level Changes—An Integrated Approach: SEPM Special Publication, vol. 42, p. 110–124.

Posamentier, H.W., Allen, G.P., James, D.P., and Tesson, M., 1992, Forced Regression in a Sequence Stratigraphic Framework: Concepts, Examples, and Exploration Significance: AAPG Bulletin, v. 76, no.11, p. 1687-1709.

Posamentier, H., and Allen, G.P., 1993, Siliciclastic sequence stratigraphic patterns in foreland ramp-type basins: Geology, v. 21, p. 455-458.

Potter, P.E., 1959, Facies Model Conference: Science, v. 129. p. 1292-1294.

Pratt, W. K., 1978, Digital Image Processing: New York, NY, John Wiley & Sons, p. 720.

Proust, J.N., Mahieux, G., and Tessier, B., 2001, Field and Seismic Images of Sharp-Based Shoreface Deposits: Implications for Sequence Stratigraphic Analysis: Journal of Sedimentary Research, v. 71, no. 6, p. 944-957.

Reesink, A.J.H., and Bridge, J.S., 2007, Influence of superimposed bedforms and flow unsteadiness on formation of cross strata in dunes and unit bars: Sedimentary Geology, v. 202, p. 281–296.

Reynolds, A.D., 1999, Dimensions of Paralic Sandstone Bodies: AAPG Bulletin, v. 83, no. 2, p. 211-229.

Reynolds, S., Johnson, J., Piburn, M., Leedy, D., Coyan, J., and Busch, M., 2005, Visualization in undergraduate geology courses, *in* Glibert, J. 2005. Visualization in Science Education: Dordrecht, The Netherlands, Springer Press, p. 351.

Ryer, T., 1983, Transgressive-Regressive Cycles and the Occurrence of Coal in some Upper Cretaceous Strata of Utah: Geology, v. 11, p. 207-210.

Ryer, T. A., and P. B., Anderson, 2004, Facies of the Ferron Sandstone, east-central Utah, *in* Chidsey, T.C., Adams, R. D., and Morris, T. H., eds., Regional to wellbore analog for fluvial-deltaic reservoir modeling: The Ferron Sandstone of Utah: AAPG Studies in Geology 50, p. 59-78.

Sadler, P.M., 1981, Sediment accumulation rates and the completeness of stratigraphic sections: The Journal of Geology, v. 89, no. 5, p. 569-584.

Scott, G.R., and Cobban, W.A., 1964, Stratigraphy of the Niobrara Formation at Pueblo, Colorado: U.S. Geological Survey Professional Paper, 454-L, p. 1-30.

Shanley, K.W., and McCabe, P.J., 1991, Sequence stratigraphic relationships and facies architecture of Turonian-Campanian strata, Kaiparowits Plateau, South-Central Utah: American Association of Petroleum Geologists Bulletin. v. 73, p. 410-411.

Shanley, K.W., and McCabe, P.J., 1991a, Predicting facies architecture through sequence stratigraphy- an example from the Kaiparowits plateau, Utah: Geology, v.19, p.742-745.

Shanley, K.W., and McCabe, P.J., 1991b, Alluvial architecture in a sequence stratigraphic framework – detailed correlations between marine and nonmarine strata: NUNA Conference on high-resolution sequence stratigraphy, Geological Association of Canada, p. 50-51.

Shanley, K.W., and McCabe, P.J., 1992, Tidal influence in Cretaceous fluvial strata – a key to sequence stratigraphic interpretation: Sedimentology, v. 39, p. 905-930.

Shanley, K.W., and McCabe, P.J., 1993, Alluvial Architecture in a sequence stratigraphic framework – a case history from the Upper Cretaceous of Southern Utah, USA: International Association of Sedimentologists Special Publication, v. 15, p. 21-56.

Shanley, K.W., and McCabe, P.J., 1995, Sequence Stratigraphy of Turonian-Santonian Strata, Kaiparowits Plateau, Southern Utah, USA: Implications for Regional Correlation and Foreland Basin Evolution, *in* Van Wagoner, J.C., and Bertram, G., eds., Sequence Stratigraphy of Foreland Basin Deposits - Outcrop and Subsurface Examples from the Cretaceous of North America: AAPG Memoir 64. p. 103-136.

Stroebel, L., and Zakia, R., 1993, The focal encyclopedia of photography: Woburn, MA, Butterworth-Heinemann Publishing, p. 917.

Swift, D.J.P., 1968, Coastal erosion and transgressive stratigraphy: Journal of Geology, v. 76, p. 444-456.

Taylor, D., and Lovell, R., 1995, High Frequency Stratigraphy and Paleogeography of the Kenilworth Member, Blackhawk Formation, Book Cliffs, Utah, USA, *in* van Wagoner, J.C. and Bertram, G.T., Sequence stratigraphy of foreland basin deposits: Outcrop and subsurface examples from the Cretaceous of North America: AAPG Memoir 64, p. 22-46.

Vail, P.R., Todd, R.G., and Sangree, J.B., 1977, Seismic stratigraphy and global changes in sea level, in Seismic stratigraphy – Applications to hydrocarbon exploration: AAPG Memoir 26, p. 49-212.

Walker, G., and Eyles, C., 1988, Geometry and Facies of Stacked Shallow-Marine Sandier Upward Sequences Dissected by Erosion Surface, Cardium Formation, Willesden Green, Alberta: The American Association of Petroleum Geologists Bulletin, v. 72, no. l2, p. 1469-1494.

Walker, J.D., and Geissman, J.W., compilers, 2009, Geologic Time Scale: Geological Society of America, GSA Today, p. 1.

White, C.A., 1879, Contributions to invertebrate paleontology; Cretaceous fossils of the western states and territories: Report of the U.S. Geological Survey of the Territories, 11th Annual Report, no. 1, p. 273-319.

Vail P. E., Mitchum R.M., and Thompson S., 1977a, Relative changes of sea level from coastal onlap, *in* Payton, C.E., ed., Seismic Stratigraphy-Applications to

Hydrocarbon Exploration: American Association of Petroleum Geologists Memoir, 26, p. 63–82.

van Wagoner, J.C., Mitchum, R.M., Campion, K.M., and Rahmanian, V.D., 1990, Siliciclastic sequence stratigraphy in well logs, cores, and outcrops: concepts for high- resolution correlation of time and facies: AAPG Methods in Exploration Series, No. 7, p. 55.

van Wagoner, J.C., 1991, Sequence Stratigraphy and Facies Architecture of the Desert Member of the Blackhawk Formation and the Castlegate Formation in the Book Cliffs of Eastern Utah and Western Colorado, in van Wagoner, (ed), Sequence stratigraphy applications to shelf sandstone reservoirs: outcrop to subsurface examples : AAPG Field Conference, September 21-28, p. 17 -27.

van Wagoner, J.C., Posamentier, H.W., Mitchum, R.M., Vail, P.R., Sarg, J.F., Loutit, T.S., and Hardenbol, J., 1988, An overview of the fundamentals of sequence stratigraphy and key definitions, *in* Wilgus, C.K., Hastings, B.S., Kendall, C.G.S.C., Posamentier, H.W., Ross, C.A., and Van Wagoner, J.C., eds., Sea-Level Changes: An Integrated Approach: SEPM Special Publication 42, p. 39–45.

Vaninetti, G.E., 1979, Coal stratigraphy of the John Henry Member of the Straight Cliffs Formation, Kaiparowits Plateau, Utah [M.S. thesis]: University of Utah, p. 274.

Zaitlin, B.A., Warren, M.J., Rosenthal, L., and Boyd, R., 2002, Depositional styles in a low accommodation foreland basin setting: An example from the Basal Quartz (lower Cretaceous), southern Alberta: Bulletin of Canadian Petroleum Geology, v. 50, no. 1, p. 31-72.

Zecchin, M., 2007, The architectural variability of small-scale cycles in shelf and ramp clastic systems: The controlling factors: Earth Science Reviews 84, p. 21-55.